Centre for Biological Engineering, Wolfson School Of Mechanical And Manufacturing Engineering, Loughborough University

The influence of spatial scaffold properties on the interaction between cells and embedded growth factors

Thesis submitted to Loughborough University for the degree of Doctor of Philosophy

Jeroen Schmidt

February 2019

Corrections – May 2019

Abstract

While modern-day healthcare continues to improve in terms of available treatments and life expectancy in many countries, increasing costs of providing medical services to aging populations place these systems under increasingly severe pressure. With continuing increases in chronic afflictions and ailments related to old age, more cost-efficient and long-term solutions are needed to meet these challenges.

Regenerative medicine offers the potential for more effective long-term treatments, but is hindered by the high cost of the desired treatments in terms of development and implementation, owing to the complexity of the living materials used for such therapies.

The work described in this thesis focuses on improving the level of control over the local cellular environment in order to reduce the need for costly materials (especially growth factors). Both surface topology and immobilization of growth factors have previously been shown to have an impact, and this research investigates potential interaction between these aspects. Patterning and immobilization of bio-active compounds are combined for the culture of human mesenchymal stem cells on surfaces with differently scaled patterns and concentrations of immobilized TGF-β1.

Initial work focused on the creation of patterned surfaces with feature sizes ranging from 1 to 50 μm. Patterns were successfully produced in Poly (Ethylene Glycol), Polystyrene and Polycaprolactone surfaces using a microparticle-based moulding process.

Further work resulted in the successful immobilization of TGF-β1 onto chemically modified surfaces, chiefly Polycaprolactone. Proteins were successfully immobilized onto Polycaprolactone surfaces at concentrations up to 4 pmol/cm^2, with exact concentrations dependent on the parameters of the immobilization process.

Finally, the developed methods were combined in a hybrid experiment using both patterned surfaces and growth factor immobilization. Results demonstrated a probable link between surface patterning and the effectiveness of immobilized growth factors, although further work is needed to more accurately describe any underlying processes.

Acknowledgements

Completing this project without the assistance and support of those around me would have been a much greater challenge.

First of all, I would like to express my gratitude to my supervisor Rob Thomas for the guidance and regular debates I've experienced during this project. Reviewing my experiments and results together has shown me how much I could still grow in both insight and ambition.

I would also like to thank Marijana Dragosavac for her invaluable assistance in understanding and using the membrane emulsification system.

Finally, my co-workers and friends in the office have not only helped with their own perspectives and knowledge for my project, but have also made my time at the Centre For Biological Engineering a true joy. Andy, Angharad, Ben, Elizabeth, Jon, Katie and Mark, I owe you my thanks for all your support with my cell culture work and the occasional bits of sarcastic humour I needed to keep me going. Andreea and Nick, I could not have completed my functionalization experiments without your help setting up the first few tests. And of course a heart-felt 'thank you' to Jen and Eleri for always being willing to help when I needed yet another reagent, document, or other bit of support for my lab work.

Table of contents

ABSTRACT **2**

ACKNOWLEDGEMENTS **3**

TABLE OF CONTENTS **4**

FIGURES AND TABLES 8

CHAPTER 1: BACKGROUND **11**

1.1. INTRODUCTION 12

1.2. ADVANTAGES OF REGENERATIVE MEDICINE 13

1.2.1. Role of the cellular environment *15*

1.2.2. Challenges in the creation of tissue engineered cartilage *15*

1.3. RESEARCH NOVELTY 16

1.4. HYPOTHESIS AND GOALS 17

1.5. REVIEW OF EXISTING LITERATURE 18

1.5.1. Cell types and differentiation mechanisms *19*

1.5.1.1. General requirements 19

1.5.1.2. Mesenchymal stem cells 19

1.5.1.2.1. Implementation 20

1.5.1.2.2. Growth factors suitable for use with mesenchymal stem cells 21

1.5.1.3. Hematopoietic stem cells 22

1.5.1.3.1. Implementation 23

1.5.1.3.2. Growth factors suitable for use with CD34-positive cells 23

1.5.1.4. Embryonic stem cells 25

1.5.1.5. Induced pluripotent stem cells 25

1.5.1.6. Summary of cell type options 25

1.5.2. Materials for cell culture environments *26*

1.5.2.1. Polymers 26

1.5.2.1.1. Synthetic polymers 27

1.5.2.1.2. Natural materials 31

1.5.2.1.3. Implementation 32

1.5.2.1.4. Summary 32

1.5.2.2. Polymer fabrication techniques 32

1.5.2.2.1. Addition polymerization 33

1.5.2.2.2. Condensation polymerization 34

1.5.2.3. Summary of cell culture material options 35

1.5.3. Options for surface modification and protein immobilization *35*

1.5.3.1. Direct polymer copolymerization 36

1.5.3.1.1. Implementation 36

1.5.3.2. Covalent immobilization 37

1.5.3.2.1. Chemical surface modification for covalent immobilization 38

1.5.3.2.2. Plasma-based surface modification 39
1.5.3.3. Non-covalent immobilization 40
1.5.3.3.1. Biotin-Streptavidin and Biotin-Avidin immobilization 41
1.5.3.4. Summary of surface modification options 41
1.5.4. Structuring techniques for cell culture surfaces 42
1.5.4.1. Phase Separation 42
1.5.4.1.1. Implementation 43
1.5.4.2. Salt Leaching 43
1.5.4.2.1. Implementation 44
1.5.4.3. Photo-lithography and additive manufacturing 44
1.5.4.3.1. Implementation 45
1.5.4.4. Plasma surface etching 46
1.5.4.4.1. Implementation 46
1.5.4.5. Condensation-controlled patterning (Breath Figures) 47
1.5.4.5.1. Application 47
1.5.4.6. Mould-based patterning 49
1.5.4.6.1. Application 49
1.5.4.7. Summary of structuring technique options 50
1.6. SUMMARY OF SELECTED OPTIONS FOR INITIAL EXPERIMENTS 51

CHAPTER 2: CREATION OF MICRO-SCALE PATTERNS ON CELL CULTURE SURFACES 52

2.1. INTRODUCTION 53
2.2. AIM AND GOALS: 55
2.3. MATERIALS AND METHODS: 55
2.3.1. Materials 55
2.3.2. Creation of initial surface patterning 55
2.3.2.1. Results 57
2.3.3. Surface area and microparticle volume reduction 59
2.3.3.1. Results 59
2.3.4. Solvent- and oven-based pattern transfer process development 60
2.3.4.1. Results 61
2.3.5. Application of vacuum during oven-based pattern transfer 63
2.3.5.1. Results 64
2.3.6. Creation of Poly (ethylene glycol) diacrylate pattern surfaces 65
2.3.6.1. Results 66
2.3.7. Contamination risk evaluation in the polymerization process 68
2.3.7.1. Results 69
2.3.8. Increased pattern size and reduction of process risks through the use of silicone moulds 69
2.3.8.1. Results 71
2.3.9. Adaptation of the patterning process for Polycaprolactone and Polystyrene cell culture surfaces 72
2.3.9.1. Results 73

2.4. DISCUSSION 74

CHAPTER 3: CREATION OF MICROPARTICLES FOR PROTEIN IMMOBILIZATION ANALYSIS 76

3.1. INTRODUCTION 77
3.2. AIM AND GOALS 79
3.3. MATERIALS AND METHODS 79
3.3.1. Materials 79
3.3.2. Preparation of membrane emulsification materials 80
3.3.3. Initial membrane emulsification testing 81
3.3.3.1. Results 83
3.3.4. Microparticle fabrication with UV polymerization 84
3.3.4.1. Results 85
3.3.5. Prevention of coalescence prior to particle polymerization 86
3.3.5.1. Results 87
3.3.6. Size analysis of created microparticles 88
3.3.6.1. Results 89
3.3.7. Contrast improvement for microparticle size analysis 90
3.3.7.1. Results 90
3.3.8. Modified suspension liquid for microparticle size analysis 92
3.3.8.1. Results 93
3.3.9. Component preparation and processing for functionalized particles 95
3.3.9.1. Results 96
3.3.10. Common aspects of flow cytometry measurements 98
3.3.11. Initial flow cytometry method testing 100
3.3.11.1. Results 101
3.3.12. Analysis of binding saturation during flow cytometry 102
3.3.12.1. Results 103
3.3.13. Analysis of non-specific binding during flow cytometry 103
3.3.13.1. Results 104
3.3.14. Analysis of time and temperature dependence of fluorophore binding 106
3.3.14.1. Results 107
3.4. DISCUSSION 110

CHAPTER 4: CHEMICAL MODIFICATION OF CELL CULTURE SURFACES 113

4.1. INTRODUCTION 114
4.2. AIM AND GOALS 117
4.3. MATERIALS AND METHODS 118
4.3.1. Materials 118
4.3.2. Initial creation of PEG-based surfaces 118
4.3.3. Cell attachment and culture on modified PEG-based surfaces 119
4.3.3.1. Creation and modification of experimental surfaces 119
4.3.3.2. Cell culture and analysis 120

4.3.3.3. Results 120
4.3.4. Expanded cell attachment analysis 121
4.3.4.1. Creation and modification of experimental surfaces 122
4.3.4.2. Cell culture and analysis 122
4.3.4.3. Results 123
4.3.5. Cell attachment on modified Polystyrene and Polycaprolactone 124
4.3.5.1. Cell attachment on modified Polystyrene and Polycaprolactone 125
4.3.5.2. Results 126
4.3.6. TGF-β1 immobilization on functionalized Polycaprolactone 129
4.3.6.1. Results 131
4.4. DISCUSSION 132

CHAPTER 5: COMBINED PATTERNING AND IMMOBILIZATION FOR CELL CULTURE 134

5.1. INTRODUCTION 135
5.2. AIM AND GOALS 136
5.3. MATERIALS AND METHODS 137
5.3.1. Materials 137
5.3.2. Design of combined patterning-immobilization experiments 137
5.3.3. Creation of patterned surfaces for cell culture 139
5.3.4. Immobilization of TGF-β1 onto prepared surfaces 140
5.3.5. Cell culture on created surfaces 141
5.3.6. Analysis of metabolic activity 142
5.3.7. Analysis of early culture marker expression 143
5.3.8. Analysis of late culture Collagen-II production 144
5.3.9. Statistical analysis of measurement data 145
5.4. RESULTS 145
5.4.1. Metabolic activity during cell culture 146
5.4.2. Early expression of cellular markers CD90 and CD105 151
5.4.3. Cumulative production and deposition of Collagen-II 154
5.5. DISCUSSION 156

CHAPTER 6: DISCUSSION AND CONCLUSION 160

6.1. DISCUSSION 161
6.2. FUTURE WORK 166
6.3. CONCLUSION 170

REFERENCES 171

Figures and tables

Chapter 1 figures:

- Figure 1: Annual average growth rate in per capita health expenditure
- Figure 2: Growth of health spending by healthcare service type

Chapter 2 figures:

- Figure 3: Schematic representation of the pattern creation and copying process
- Figure 4: Imaging of microtome-cut silicone-microparticle hybrid material
- Figure 5: Imaging of silicone-microparticle hybrid materials after acetone treatment and/or cutting with a scalpel
- Figure 6: Imaging of silicone-microparticle hybrid material made without mixing prior to solidification
- Figure 7: Imaging of polystyrene patterns created using the Acetone-based transfer process
- Figure 8: Example of silicone-polystyrene samples using the oven-based transfer process
- Figure 9: Imaging of polystyrene patterns created using the oven-based transfer process
- Figure 10: Imaging of pattern and defects created using the silicone-to-silicone transfer process
- Figure 11: Schematic overview of the two-stage oven transfer process and example of a sample mid-transfer
- Figure 12: Imaging of polystyrene patterns prior to separation, created using the two-stage oven transfer process
- Figure 13: Imaging of created polystyrene patterns after separation, using the two-stage oven transfer process
- Figure 14: Imaging of created Poly (Ethylene Glycol) Diacrylate patterns with 50μm features
- Figure 15: Imaging of created Poly (Ethylene Glycol) Diacrylate patterns with 20μm features
- Figure 16: Imaging of created Poly (Ethylene Glycol) Diacrylate patterns with 1μm features
- Figure 17: Schematic representation and example of the new, flexible mould design
- Figure 18: Sample examples and imaging for patterns created in 96-well plate size
- Figure 19: Schematic representation of defect creation due to particle displacement
- Figure 20: Examples and microscopy imaging of low-quality patterns
- Figure 21: Imaging of Polycaprolactone patterns with 50μm features created using the vacuum oven process

Chapter 3 figures:

- Figure 22: Schematic representation of the membrane emulsification process
- Figure 23: Experimental setup used during the membrane emulsification experiments
- Figure 24: PEGDA+water in kerosene emulsions created with varying emulsification parameters
- Figure 25: Change in emulsion droplet size over time
- Figure 26: Change in emulsion droplet size over time after UV exposure

- Figure 27: Imaging of created particles in the kerosene phase and water phase
- Figure 28: Created emulsions using a larger surface area (multiple small beakers) before and after adding Acetone
- Figure 29: Created emulsions using a larger surface area (large dish) before and after adding Acetone
- Figure 30: Size distributions of the created microparticle suspensions (first experimental procedure)
- Figure 31: Size distribution of dyed microparticles (sample 1 of 3)
- Figure 32: Size distribution of dyed microparticles (sample 2 of 3)
- Figure 33: Size distribution of dyed microparticles (sample 3 of 3)
- Figure 34: Size distribution of dyed microparticles in water (sample 1 of 3)
- Figure 35: Size distribution of dyed microparticles in water (sample 2 of 3)
- Figure 36: Size distribution of dyed microparticles in water (sample 3 of 3)
- Figure 37: Example of microparticle suspension with visible phase separation
- Figure 38: Imaging of the opaque and clear phase of a created microparticle suspension
- Figure 39: Measured events and gated particle population of PEG microparticles.
- Figure 40: Typical fluorescence histogram after selection of the particle population.
- Figure 41: Measured values and model fit for specific and non-specific binding of fluorophore on Streptavidin-functionalized particles
- Figure 42: Variation in fluorescence between different particle types after fluorophore incubation
- Figure 43: FITC and RPE fluorescence 0-3 hours after dilution
- Figure 44: Differences between fluorescence of Streptavidin-functionalized and Streptavidin-free microparticles 0-3 hours after dilution
- Figure 45: AF488 fluorescence of particles stored either cold or at room temperature, 0-3 hours after dilution
- Figure 46: RPE fluorescence of particles stored either cold or at room temperature, 0-3 hours after dilution
- Figure 47: AF488 and RPE fluorescence of particles stored either cold or at room temperature for 1-4 days, 0-3 hours after dilution
- Figure 48: AF488 fluorescence 0-3 hours after 10x-100x dilution

Chapter 4 figures:

- Figure 49: Schematic representation of the selected immobilization process for desired growth factors
- Figure 50: Imaging of cells cultured on PEG-based surfaces, either untreated or with Streptavidin and/or RGD
- Figure 51: Imaging of cell attachment on PEG surfaces with Fibronectin or RGD
- Figure 52: Imaging of cell attachment on Polystyrene, either untreated or treated with Laccase C

- Figure 53: Imaging of cell attachment on Polycaprolactone, either untreated or treated with Laccase C
- Figure 54: Imaging of cell attachment on Sodium Hydroxide-treated Polycaprolactone

Chapter 5 figures:

- Figure 55: microscopy images of created patterns
- Figure 56: Measured Glucose and Lactate concentrations during cell culture in the combined surface patterning/immobilization experiment
- Figure 57: Calculated day-to-day and cumulative Lactate production
- Figure 58: Main effects and interaction plots for measured Lactate at day 3 on surfaces with immobilized TGF- β1
- Figure 59: Main effects and interaction plots for measured Lactate at day 3 on surfaces with soluble TGF- β1
- Figure 60: Pareto charts of the influence of patterning feature size and growth factor concentration on metabolic activity for samples with immobilized TGF- β1
- Figure 61: Pareto charts of the influence of patterning feature size and growth factor concentration on metabolic activity for samples with immobilized TGF- β1
- Figure 62: Measured events and gated population in forward/side scatter plots.
- Figure 63: Main effects plots for CD90 expression at day 2, for both samples with soluble TGF- β1 or immobilized TGF- β1
- Figure 64: Main effects plots for Collagen II deposition on day 14 and 21

Chapter 4 tables:

- Table 1: Calculated immobilization of TGFb1 antibodies on Polycaprolactone

Chapter 5 tables:

- Table 2: Fitting values for a regression model of measured Lactate and Glucose concentrations, patterning scale and TGFb1 concentration
- Table 3: Measured flow cytometry values for cultured samples on days 2 and 4.
- Table 4: Measured fluorescence values for cultured samples on days 14 and 21.

Chapter 1: Background

1.1. Introduction

The modern-day population of Earth is perhaps the healthiest it has ever been, owing to widespread improvements in numerous aspects of society, from food production to environmental safety to both preventative and treatment-based healthcare. However, as the average age steadily increases due to higher life expectancies, healthcare systems are increasingly burdened by the need to care for these aging populations, especially in more developed countries. For most individuals, the majority of all medical expenses occurred over a person's lifetime will take place in the later years of life. Consequently, extended life expectancies have a major impact on total healthcare costs[1–3].

For example, NHS expenses in the UK have steadily risen both in total and per capita, with costs going up by an average of 3.8% per year compared to an average economic growth of 2.2% per year. Similar trends are seen in numerous other countries, as shown in Figure 1.

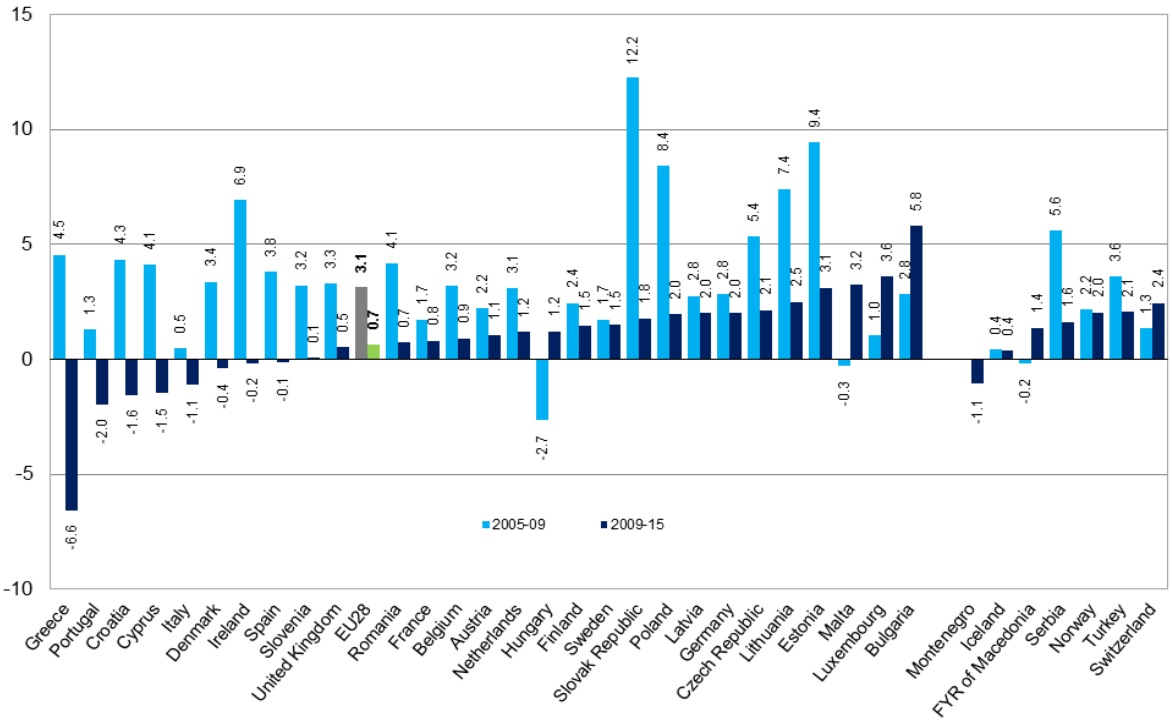

Figure 1: Annual average growth rate in per capita health expenditure, real terms, 2005 to 2015 (or nearest year). Reproduced from Health At A Glance: Europe 2016: State of Health in the EU Cycle[4].

In 2015, numerous western nations spent over 10% of total GDP on healthcare and related services[4]. Further pressure is put on healthcare providers by the problem that a large number of medical needs in older populations are of a chronic or recurring

nature, including Alzheimer's, diabetes, various types of cancer, and degenerative ailments such osteoporosis and arthritis[5]. Long-term care is the fastest-growing source of healthcare expenses, as shown in Figure 2.

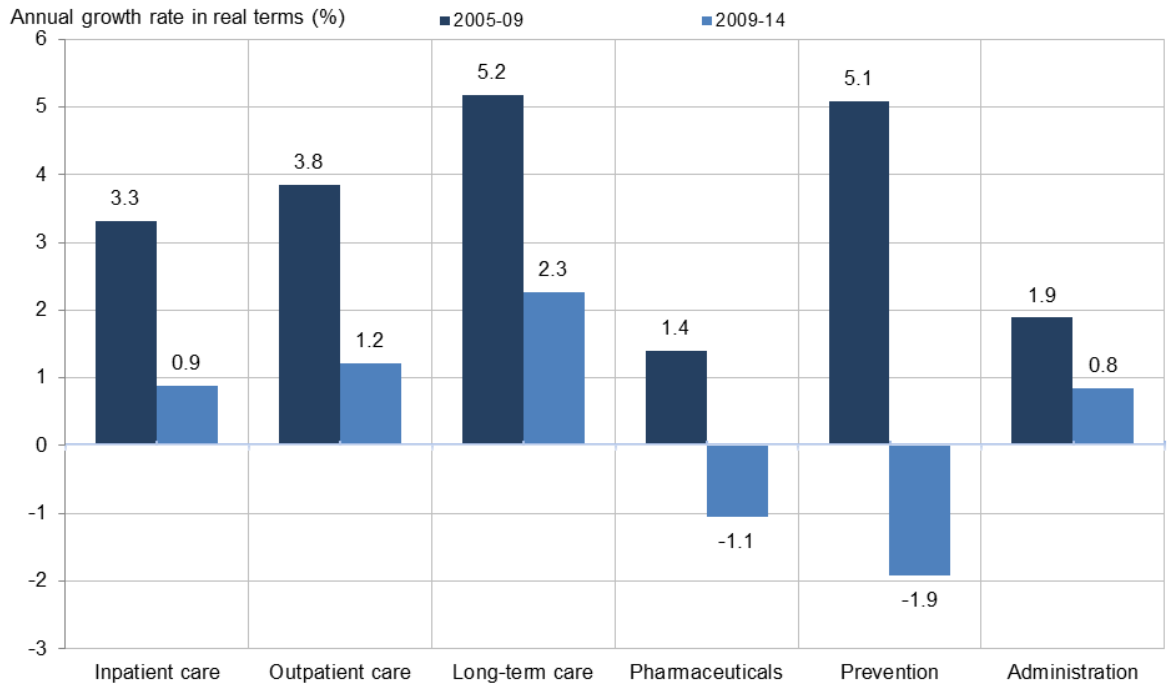

Figure 2: Growth of health spending for selected functions per capita, EU average, 2005-14. Reproduced from Health At A Glance: Europe 2016: State of Health in the EU Cycle[4].

Consequently, the current need for better treatment options is a major priority in healthcare research and development. Reducing costs and increasing efficacy and efficiency of existing treatments has been a long-time focus area in medical research, but does not address the underlying problem where continuing treatment is required for chronic conditions. Regenerative medicine offers a different approach, seeking to provide more effective treatments by actively restoring the damaged or weakened tissues of the patient, restoring long-term function through the use of living materials[6].

1.2. Advantages of Regenerative Medicine

The field of regenerative medicine primarily deals with the use of living materials, including induced or naturally derived stem cells and cell-derived compounds such as extracellular matrix. The main purpose of treatments based on regenerative medicine is to create long-lasting solutions to a patient's problems by creating or re-creating healthy tissues. Examples of regenerative medicine include both cell-based

treatments and the use of artificial materials designed to enhance the body's natural capacity for tissue restoration.

Regenerative medicine is especially promising for the treatment of chronic ailments caused by old age or congenital defects. Theoretically, such therapies need no long-term support like more standard methods; replacing a new-born's faulty aortic valve with a plastic or metallic heart valve will eventually see it wear out, making repeat surgical intervention inevitable. In contrast, a tissue engineered heart valve made of living tissue will grow with the rest of the body while maintaining its function, potentially eliminating the need for further treatment.

Restoration of damaged tissues can be accomplished by the introduction of artificially induced or natural stem cells, such as restoring cardiac function following myocardial infarction[7,8]. Further modification of patient-derived (stem) cells prior to delivery, such as by genetic modification, can provide a means of treatment for ailments such as diabetes, which are not caused by damaged tissue so much as non-functional cells or cellular processes[9]. Artificial degradable scaffolds can be implanted or formed in-situ to provide support for a patient's own healing, in particular for tissues with rapid access to existing stem cells such as blood vessels or heart tissue[10,11]. Finally, some tissues may be re-created ex vivo and implanted whole, allowing for complete replacement of damaged materials and restoring function with only a minimal recovery time, which is especially important for tissues that are required in every-day life such as cartilage and bone.

In summary, stem cells and tissue engineering are a promising source of new treatments for varying illnesses and injuries. However, the development of successful treatments in this area has been hindered by the complexity of the cellular environment and the resulting costs associated with both the use of biological materials and the degree of control necessary to meet regulatory demands[12–16]. Ex vivo culturing of (stem) cells for treatments often requires large amounts of growth factor-enriched medium, suitable surface or scaffold materials with strictly defined properties, or co-culture with different cell types. Creating effective therapies therefore requires that the functional parameters of the culturing system are well understood and precisely controlled, while simultaneously minimizing total costs and use of resources.

1.2.1. Role of the cellular environment

It has previously been established that surface properties can have substantial effects on cellular differentiation, in particular with cell types that are only found in very specific environments such as osteoblasts or nerve cells[17]. For cells to thrive in culture, the local material properties must logically be comparable to that found in their natural environment. The mechanical aspects of the environment, such as the Young's Modulus of the material or (dynamic) loading, are of particular interest for stimulating extracellular matrix production[18]. Similarly, the immobilization of biochemical factors onto solid particles (for suspension culture) or surfaces (for adherent culture) is shown to potentially alter the effectiveness of the factors involved, including increasing the effective dose, preventing negative effects found with equivalent higher doses in solution, reducing the total amounts of factors needed during cell culture and enabling long-term drug effects in tissue engineered scaffolds[19–24]. More broadly, chemical properties such as hydrophobicity and the presence of specific amino acid groups found in extracellular matrix can have a profound effect.

Likewise, the chemical composition of cell culture media has been under continuous investigation for years. While some research focuses on how to better mimic the in-vivo environment through the inclusion of, for example, sera and metabolic by-products from other cultures, the most work takes place in selecting the most effective combination(s) of growth factors, amino acids, and other compounds for particular cell culture methods[25–29].

1.2.2. Challenges in the creation of tissue engineered cartilage

Cartilage is a major focus for regenerative medicine due to the great difficulty of restoring damaged or lost cartilage to full functionality. While cartilage can regrow to some extent, the complexity of its physical structure makes full recovery very difficult. Because the function of cartilage relies on the interplay between osmotic pressure, lubrication and a complex fibrous matrix of arched collagen fibres, even minor defects can create steadily worsening damage. Likewise, this means that most replacements do not have the correct mechanical or structural properties, and further wear and damage are common after medical intervention.

Currently, the main methods to treat damaged cartilage, be it due to trauma such as sports injuries or degenerative ailments such as arthritis, are unable to restore the original cartilage structure. The most straightforward treatment is to remove damaged tissue to create a new, smooth surface within a joint using underlying cartilage. However, this process often leads to complications after further use of the joint, since the new cartilage surface will not have the same mechanical properties due to the reduced thickness and different fibre structures within the tissue. Artificially inducing micro-fractures in the bone underneath damaged cartilage can release stem cells from the underlying bone marrow to induce natural healing, but has shown a lack of reliable long-term effectiveness[30]. Injection of autologous stem cells, either with or without a suitable scaffold, can promote healing in a similar manner[31]. Finally, damaged cartilage may be replaced by autografts, allografts or artificial ex vivo created tissue.

The difficulties inherent in attempting to restore cartilage to its original structure and function make this medical need an important area of research. While artificial cartilage can already be created from various sources of stem cells, challenges remain in creating the correct structure and mechanical properties suitable for long-term use[32,33]. Consequently, insights into how to better control the cellular environment and more effectively direct cells used for the creation of artificial cartilage, such as mesenchymal stem cells and chondrocytes, could lead to immediate advantages in both current research and future treatments.

This project is intended primarily as a proof of concept, and the effects, if any, that are found from combining immobilized growth factors and surface topology may be relevant for multiple different cell or tissue types. The use of chondrocytes for the creation of artificial cartilage will be the initial starting point for further work during this project, but other cell or tissue types may be considered if appropriate.

1.3. Research novelty

A large amount of research is underway to improve various parts of cell-based therapies, but despite the fact this issue has been recognized as a potential factor, limited information is available regarding how the physical environment influences biochemical factors[34]. While some research has been performed that combines

material topology and the immobilization of growth factors[35–37] these studies typically focus on the inclusion of only a small number of environments or growth factor levels.

Because of the inherent complexity of cell-environment interaction and the influence on cellular signalling pathways, looking at a single type of environment may not provide sufficient detail to fully describe the interaction process. Using different types of cellular environments or growth factor concentrations may have different effects on the affected cells. This project will investigate this relationship by focusing on the effect of the topological properties of the substrate and the effective concentration of immobilized growth factors both separately and when combined, using a number of different surface topologies. This should provide novel insights into how these different factors influence each other.

1.4. Project hypothesis

The hypothesis that directs this research is outlined as follows:

- Topological features of cell culture surfaces will influence the effective concentration of growth factors when immobilized on these surfaces. Smaller feature sizes are expected to result in a higher effective concentration.

This project aims to gain additional knowledge regarding the manipulation of cellular pathways through altering cytokine presentation on patterned surfaces. Any positive or negative influences found during this research could allow researchers and industry to enhance their control of cellular proliferation and differentiation processes for use in clinical research and therapies.

Possible benefits that may be revealed by this project include:

- Improved process output due to a reduction in cell loss during culturing (such as those caused by cell death or cells that have to be removed because of faulty differentiation)
- Reduced process costs in existing techniques due to more efficient resource use (particularly growth factors)
- Access to potential new treatment options due to improved or different manipulation of cellular signalling pathways and differentiation

- Potential improvements in bio-active surfaces for both bioreactor culture systems and implant-based treatment designs (both short term degradable scaffolds and longer term semi-permanent implants)

1.5. Review of existing literature

The increasing need for more cost-effective medical treatments indicates that research should not only attempt to develop new treatments, but also improve existing ones for greater efficacy, improved efficiency and reliability, and/or reduced cost. Improving these types of treatments by enhancing control over the process or reducing the required amounts of (costly) resources is then a potentially effective method to reduce or eliminate these therapies' main downsides. This project does not focus on treating a single, specific medical challenge; rather, it is intended to serve as a proof-of-concept, and if beneficial effects are found during the course of this project it is hoped these will be applicable to a broad range of processes in biomedical treatments and research.

However, researching a combination of multiple different aspects of the cellular environment does provide a more complex challenge than more focused research. Consequently, before any actual experimental work can commence it is necessary to identify potential paths forward. For example, it is only feasible to investigate a single cell type during this project. Different cells or tissues have different requirements, and the cell type selection therefore informs most every other decision made during the rest of the project.

Likewise, once a suitable cell type is chosen, numerous different methods of influencing cultured cells are available. The various aspects of interest in the cellular environment need to be matched to different materials, modification strategies and cell culture regimens.

Therefore, a literature review is performed to determine the best choices of cell type, materials and processing techniques for the project, primarily focusing on ease-of-use, adaptation to the currently available infrastructure and research novelty.

1.5.1. Cell types and differentiation mechanisms

1.5.1.1. General requirements

Primarily, all cells used in this project must be capable of short term proliferation and differentiation. While long-term viability is less important for the specifics of this project, cell-lines that remain viable after extended culturing will be more clinically relevant.

Furthermore, the cell line must be clinically relevant (for example, human cell lines are preferable over animal models), and if possible should have a minimum in ethical and procedural considerations associated with it (for example, iPSCs are preferable over embryonic cell lines). Should the cell line be used in the clinic, it may not cause significant adverse effects (such as chronic inflammation or cancer) in any exposed patients.

The growth factors used must create a response in specified cell lines, either individually or when used in combination. At least one growth factor used for a culture situation must be critical for creating the desired response, and this growth factor must be suitable for linking to the polymer construct without experiencing a loss of function. Additional growth factors may be used in suspension as needed.

While a number of growth factors are commercially available and usage can be scaled to fit the needs of the experiment, production costs are still a limiting factor. Any clinically relevant treatment must minimize both use and waste of materials. Finally, there need to be significant safety procedures in place as accidental exposure of the patient to traces of the protein in the product may result in adverse side effects, further limiting the suitability of large-scale use of (multiple) growth factors in therapeutic therapies.

Possible cellular differentiation pathways are provided as combinations of cell types, growth factors and relevant cellular markers for analysis, since the effect of these materials will be highly interdependent and the effects of individual components cannot be translated to different situations.

1.5.1.2. Mesenchymal stem cells

Mesenchymal stem cells are potentially applicable in the creation of material such as cartilage[38,39], bone[40] and fat tissues[41], and are commonly cultured in an adherent

situation due to the similarities with the relevant tissues in vivo and the dependence of these cells on the physical/mechanical environment[42,43], although hydrogels and similar 3D scaffolds are becoming increasingly common. These cells are commercially available in a number of well-defined cell lines. However, if these cells are used in a clinical setting additional safety processes may be necessary to ensure the patient is not exposed to flawed cells in the product, such as cells with tumorigenic potential.

1.5.1.2.1. Implementation

Mesenchymal stem cells are primarily suited for adherent culturing to create tissue engineered 2D and 3D constructs. If a 3D construct is used, care must be taken to ensure medium (including nutrients and biological factors) can reach the entire construct through sufficient porosity or the use of artificial blood vessel-like structures. MSCs have been cultured in non-adherent/suspension situations as well, but this process is relatively less well defined and understood, compared to adherent culturing techniques[44–46].

Analysis of cellular differentiation is typically performed using fluorescent staining, flow cytometry, PCR analysis or by microscopy to quantify the cell morphology and visual characteristics.

Mesenchymal stem cells are frequently used in clinical research; using this type of cells for biological research is relatively easy since several different MSC cell lines are commercially available in addition to primary cell sources. Like all cell culturing methods, MSCs must be cultured in sterile conditions to prevent contamination from bacteria, fungi, and other biological materials.

The use of mesenchymal stem cells is scalable; however, since this cell type is primarily used for adherent cell culturing on surfaces or in scaffolds, the culturing technique may impose limits to the amount of material that can be manufactured at a single time due to effects such as diffusion and cross-tissue variability. Mesenchymal stem cells have the same clinical considerations that apply to every (foreign) cell type that is used for clinical purposes, and strict safety regulations must be in place during every step of the process.

1.5.1.2.2. Growth factors suitable for use with mesenchymal stem cells

1.5.1.2.2.1. TGF-β

In mesenchymal stem cells, TGF-β influences cellular proliferation and differentiation, primarily into chondrogenic cell types[23,24,47–50]. TGF-β is suitable for presentation in solution or controlled release[51] and for immobilization on the culturing surface through various methods, including UV-copolymerization after binding with a photo-reactive linker[20,23,24], the use of streptavidin-biotin linking methods, or non-covalent adsorption onto a surface[22].

TGF-β can be controlled by adjusting its (effective) concentration, either in solution or bound to a substrate. It may also be possible to modify its effect through covalent bonding with other proteins or molecules, or by combining it with other growth factors[52] but this may also risk a loss of function and unknown side effects; thereby limiting clinical applicability.

Implementation

The effectiveness of this method will depend in part on the methods used to immobilize this protein and culture cells on the polymer construct, as not all modification strategies may be suitable. TGF-β can influence cells both through exterior contact and following phagocytosis, allowing for strategies involving both (non-) covalent binding and proteins in solution [53–56]. This not only allows for strategies involving both (non-) covalent binding and proteins in solution, but may introduce additional differences in effectiveness between these approaches.

1.5.1.2.2.2. FGF-2

Fibroblast Growth Factor 2 influences cellular proliferation and differentiation by promoting pluripotent lineages. FGF-2 on its own has a limited effect on differentiation in affected cells; rather it maintains proliferation and differentiation potential by keeping cells in an undifferentiated state for longer periods of time [57–59]. However, FGF-2 has also shown enhanced chondrogenic differentiation in cultured cells, especially if compared with TGF-β[60,61]. FGF-2 can stimulate both chondrogenesis and osteogenesis[62], and can be used to support cell proliferation on otherwise suboptimal surfaces[22].

However, the complexity of the FGF-2 induced effects also leads to significant challenges during experiments. The broad impact of FGF-2 can lead to off-target effects and make interpretation of experimental data more difficult than when using biochemical factors with more limited effects.

Implementation

The addition of FGF-2 during cell culture has multiple simultaneous effects; consequently experiments with FGF-2 should analyse proliferation, cellular differentiation, and extracellular matrix production over time to gain a complete picture of differences between experimental groups. However, the fact that the effect of FGF-2 can involve multiple different processes (proliferation, differentiation, synergistic effects with other growth factors), using this growth factor may make future experiments needlessly complex for little additional insight.

FGF-2 can be provided in solution or immobilized by various methods such as non-specific adsorption.

1.5.1.2.2.3. Analysis

Determining the presence of growth factors in a material or solution can be achieved using various methods. Fluorescent or radio-isotope labelling of the protein itself may be possible, but may not be suitable for all situations. Quantitative analysis of immobilized growth factor may be accomplished by analysing the change in concentrations of the growth factor solution during the immobilization process, or by adding specific antibodies with fluorescent or catalytic conjugates and measuring concentrations indirectly. Chondrogenic differentiation of MSCs can be analysed using the expression of Sox9 and cellular markers CD44, CD90, and CD105. During chondrogenic differentiation, these markers will undergo a permanent reduction in expression levels[39]. Finally, production of extracellular matrix, including Collagen II and Collagen X, provides further insight into the behaviour of affected cells[63–66].

1.5.1.3. Hematopoietic stem cells

Hematopoietic stem cells are precursors for the various blood-related tissues in the body, including Megakaryocytes[67], Erythroblasts[68], Lymphocytes[69], and platelets[70], and can be isolated from bone marrow or primary blood using techniques such as magnetic bead isolation to select cells with positive CD34 expression. CD34 positive

cells form a heterogeneous population that express a specific expression marker rather than a single population, and further isolation of cell types can be accomplished by screening for additional cell surface markers[71,72].

1.5.1.3.1. Implementation

Hematopoietic stem cells are an excellent option for suspension culture. The consistent need for appropriate donor blood in medical interventions, such as those relating to major trauma or cancer treatment, makes the ex vivo creation of a reliable supply of unifversally applicable donor a potentially important medical advancement. Likewise, maintaining, replacing or strengthening the populations of a patient's immune system-related blood cells can be relevant in the treatments of afflictions such as leukaemia.

Hematopoietic cells are usually cultured in suspension, making this cell line more easily scalable than cell types that require adherent cultures. Hematopoietic stem cells or the containing tissue (specifically blood) are commercially available from various sources. However, adherent culture-based systems are also shown to be viable[73,74]. The main limitation of culturing hematopoietic stem cells is the cost of the culture media, relevant growth factors and other necessary additions to the cellular environment.

Analysis of created hematopoietic cell lines typically involves measurement of cellular marker expression, though depending on the desired cell type other analysis methods may also be employed (such as enucleation testing for red blood cell maturation).

1.5.1.3.2. Growth factors suitable for use with CD34-positive cells

Many of the growth factors that are currently under investigation for stimulating differentiation of hematopoietic stem cells are frequently used in combinations to provide specific effects. Therefore, rather than looking at each of these growth factor individually, this section instead focuses on the relevant combinations discussed in the literature.

1.5.1.3.2.1. Megakaryocyte differentiation

Megakaryocyte differentiation is primarily induced by combinations of Interleukin-3 (IL-3), Stem Cell Factor (SCF, Steel factor) and Thrombopoietin (TPO).

TPO directs hematopoietic stem cells to differentiation into Megakaryocytes[75], especially when supplemented with SCF[76]. However, some work as also shown that TPO in isolation may increase proliferation without inducing differentiation[77]. The addition of IL-3 to TPO-containing cultures further supports Megakaryocyte differentiation[67,68,78,79], indicating that hematopoietic differentiation may be best managed with combinations of growth factors instead of single additions.

If Low Density Lipoproteins are added to an SCF and IL-3 containing culture, this results in greater differentiation towards Mast Cells[80].

1.5.1.3.2.2. Erythroid differentiation

Erythroid differentiation is primarily induced by combinations of Erythropoietin (EPO), Interleukin-3 (IL-3) and Stem Cell Factor (SCF, Steel factor).

EPO both supports progenitor survival and induces erythroid differentiation[81], while SCP further supports proliferation. EPO combined with IL-3 also supports differentiation and proliferation without addition of SCP[82]. Differentiation with these growth factors is shown to also deplete the progenitor population, resulting in limited total production[83], although further additions to the culture medium can alleviate this issue.

1.5.1.3.2.3. Implementation

Many of the growth factors suggested above can be provided in both soluble and immobilized form. However, the need to combine multiple different growth factors for use with hematopoietic stem cells substantially increases the complexity and risks involved in these processes. Furthermore, the substantial overlap in necessary growth factors for different differentiation lineages shows that even minor differences can have immediate and far-reaching consequences for cellular behaviour. As this project's main goal is focused on interactions with (modified) surfaces, the use of these cell types may provide only limited insight. While initial culture can include adherent conditions, the subsequent suspended nature of the cells in question mean that any cell-surface interactions will remain extremely limited. Therefore, hematopoietic stem cells will not be considered further for this project.

1.5.1.4. Embryonic stem cells

Embryonic stem cells are a cell type that possesses broader differentiation characteristics than stem cells harvested from specific adult tissues[84,85]. These cells are usually harvested from embryos that were created for in vitro fertilization but were not implanted. Because of their origin, there are considerable moral and ethical considerations in their use for medical treatments and research. While they can (in theory) be used to form any tissue in the body, it is not possible to acquire embryonic stem cells from a patient and the creation of patient-specific tissues is therefore not possible.

Because this project does not require the broad differentiation potential offered by these cells, and because of the additional difficulties with using these cells, embryonic stem cells are not considered for this project.

1.5.1.5. Induced pluripotent stem cells

IPSCs are artificially prepared stem cells created from non-stem cells. This type of cell provides a promising new method to create new tissues for therapeutic purposes, combining the regenerative potential of embryonic stem cells with the option to create these cells using a patient's own tissues[86]. However, questions remain regarding potential health risks and the best methods to prepare these cells[87,88]. Consequently, the (potential) advantages of this type of stem cell do not outweigh the added complexity and risk of complications, and IPSCs are not considered for this project.

1.5.1.6. Summary of cell type options

Various different cell types are available for research involving cell culture, but not all cell types are equally suitable for this project. Because this project focuses primarily on the interaction of cultured cells with (modified) surfaces, the optimal choice will be a cell type suitable for adherent cell culture. Although both Mesenchymal Stem Cells and Hematopoietic Stem Cells can meet this requirement, Mesenchymal Stem Cells are the most immediately suitable cell type. Therefore, all future experiments during this project will use Mesenchymal Stem Cells as the starting point. Other cell types will only be considered if unforeseen problems are encountered that warrant changing to a different type.

1.5.2. Materials for cell culture environments

The most common materials used in tissue engineering processes are ceramics and polymers, depending on the tissues of interest. Ceramics are typically used to create solid or porous substrates, primarily for adherent cell culture involving bone and bone-related tissues (such as bone marrow). Studies into ceramic materials primarily focus on controlling pore size, crystallinity, degradation and mechanical properties. As this project will initially focus on the culture of cells for softer tissues, ceramics are not considered as a primary material for use during this project. Hybrid materials that include ceramics (such as hydrogels with ceramic particles) will not be investigated to avoid impractically high complexity of the final cell culture material[89].

In contrast to ceramics, polymers offer a more varied environment for adherent and embedded cell culture. Depending on the polymer type and production method, polymers can be created as solid surfaces, hydrogels, and fibrous matrices, making this material type suitable for more numerous applications but also requiring care in selecting the correct polymer properties for any particular purpose.
Scientific research on polymers for cell culture primarily focuses on replacing extracellular matrix of softer tissues such as cartilage, muscle and spinal cord tissue, be it using degradable or (semi-) permanent structures. For this project, polymers are the main material of interest, and will be covered in more detail.

Finally, surfaces constructed of metals, such as titanium, are researched as replacements for bone structures, most commonly to counter osteoporosis or damage due to trauma[90–92]. Due to the much greater processing requirements and more limited options for modification, metals are not considered during this project.

1.5.2.1. Polymers

Polymers form long, interconnected molecular networks with highly variable behaviour depending on the chemical structure of the materials, the volume fractions of used components, crosslinking density and numerous other details of their construction. They are commonly used for tissue engineering and regenerative medicine, and a number of necessary properties have been identified over the years[93,94]. First, any polymer used as an environment for cell culture must be non-toxic both during use and, if applicable, after degradation. Additionally, while long-term biocompatibility is not always necessary for in vitro experiments, using

materials with poor biocompatibility may cause complications when used in vivo due to rejection, inflammation, allergic reactions or other biological processes.
The material properties of the polymers of interest must be matched to the desired tissue; many cell and tissue types require elastic moduli, porosity or surface charge to remain within specific bounds for optimal cell growth and function.
For this project, polymers must also degrade slowly or be non-degradable so as to maintain their topography, and be suitable for patterning with one or more patterning techniques as described below. Finally, the polymer surface must be suitable for the immobilization of growth factors, either by direct incorporation of suitable functional groups in the polymer chains or by introducing such groups through chemical modification after creation of the polymer construct.

1.5.2.1.1. Synthetic polymers

Synthetic polymers have the advantage of being chemically defined, with physical and chemical properties selected by the user before creation or purchase. Synthetic polymers can be made pure or from a mixture of multiple monomer types, allowing for the creation of materials with highly customizable behaviours. However, this broad selection of possible structures also means the user must select the correct properties, more-so than for the use of naturally occurring polymers.
Unlike natural polymers, synthetic polymers may be created from components with substantial toxicity or other health risks, such as irritants or carcinogenic compounds. Long-term cell culture on polymers created from toxic components may need additional washing and quality control to ensure no unsafe levels of unpolymerized components remain.
Finally, without the need to collect tissue from living individuals or animals, synthetic polymers are significantly easier to prepare than natural materials, thus providing an additional advantage given the increasingly high demand for cost reductions in medical therapies.

1.5.2.1.1.1. Effects of hydrophobicity

The hydrophobicity of the chosen material has a direct influence on the behaviour of both the cells in culture and the scaffold material itself. Materials with a low hydrophobicity, such as Poly (Ethylene Glycol), Poly (L-Lactic Acid) or Poly (Lactic-Co-Glycolic Acid) derived polymers, are frequently used in the form of hydrogels. The hydrophilic nature of such polymers causes the material to attract water, thereby

causing swelling of the scaffold. In addition, hydrophilic scaffolds typically show low protein adsorption and low cellular adhesion due to a lack of available adhesion peptides on the scaffold material [95–97].However, some indications show that protein adsorption will further increase if hydrophilicity increases too much[98]. Hydrogels are most often used with added cell attachment groups such as RGD or Laminin and/or with the cells of interest already embedded within.

Hydrophobic segments in most proteins allow materials with higher hydrophobicity, such as Polystyrene and Polyethylene, to bind more proteins onto their surface. With increased adhesion sites available on the scaffold material, cellular adhesion and spreading will typically be greater than that for hydrophilic surfaces. However, since hydrophobic materials will *non-selectively* adsorb proteins out of solution, the surface of these materials will become both biologically active and poorly defined compared to materials that do not bind proteins. Furthermore, strongly hydrophobic materials have been shown to interfere with cell attachment and spreading, indicating that such surfaces may still need to be modified to ensure optimal culture conditions[98,99].

1.5.2.1.1.2. Copolymers

The use of copolymers can allow development of materials with more varied properties. Alternating monomer units within the polymer will influence hydrophobicity, cellular adhesion, crystallinity, can introduce additional reactive groups to the polymer surface and may alter degradation, thermal and mechanical properties and surface tension[100]. Block-copolymers in particular can also create spatially dependent variations in the polymer's properties, allowing for localized addition or modification of functional groups, manipulation of cell phenotype, attachment on various material surfaces or directed cell migration[101–106], though more complex polymer structures are also seeing use[107]. The vastly increased range of possibilities in terms of material properties for copolymers comes at the cost of a substantial increase in complexity for the creation of the material. Not only must suitable blends of monomers be selected, the choices made for monomer concentrations, polymerization processes, and other aspects of the polymer's creation and modification will have far-reaching consequences for the final material. Due to the inherent complexity of this type of approach, copolymers will not be considered for use during this project.

1.5.2.1.1.3. Degradation

Synthetic polymers can be either degradable or non-degradable, with degradation occurring through processes such as hydrolysis, enzyme digestion or photosensitive, thermal or chemical reactivity of the polymer chains. Degradable materials are typically used in situations where cultured cells (or infiltrating host cells, if used in vivo) are expected to produce extracellular matrix (ECM) to replace the lost scaffold, including many materials designed for in-vivo therapies. Additionally, the degradation properties of the polymer can influence the behavior of cultured cells by enabling a time-dependent change in material properties or long-term release of bioactive molecules from the polymers[108–112].

1.5.2.1.1.4. Identified options for synthetic polymers

Polystyrene

Polystyrene is commonly used in cell culture experiments, and is a common 'default' material for the various well plate designs used in biomedical research.

Numerous cell types will readily attach and grow on Polystyrene surfaces, including hMSCs, reducing the need for modifications to allow for successful cell culture experiments. However, the higher hydrophobicity of Polystyrene compared to other polymer options means that proteins will readily adsorb out of solution.

The high chemical stability of Polystyrene means harsher modification treatments like metal chlorides[113], anhydrides[114], plasma[115,116] or similarly reactive species[117] are necessary before cell culture surfaces can be further functionalized.

Poly (Ethylene Glycol)

PEG is a hydrophilic polymer most commonly employed as a hydrogel, though its uses also include crosslinking of proteins and modification of chemicals to reduce biological response (known as 'pegilation').

Depending on the volume fraction of PEG used to create a cell culture scaffold, the resulting material may be suitable as a semi-solid 2D surface for adherent culture or as a porous gel serving as a 3D environment[118]. 3D Hydrogels can be later seeded with cells, though inclusion of cells prior to polymerization of the PEG monomers is also a possibility[119–123].

Using higher volume fractions of PEG, stiffer and more solid gels are created, which will retain their topology if patterned using techniques such as photolithography[124,125].

PEG scaffolds are not innately degradable, though the exact method used to polymerize the material and/or create crosslinks may introduce chemical groups allowing for degradation over time[108,109].

A major advantage of PEG as a material for cell culture is that it is easily modified with various bioactive compounds. Inclusion of growth factors, enzymes, and other materials of interest can be achieved both using copolymerization using functionalized proteins and after completion of the scaffold[126]. Access to thiolation, monoacrylate functionalization and PEGilation processes allows for substantial functionalization without the need to introduce major chemical differences in the polymer scaffold itself[23,24,127,128].

Because PEG is innately hydrophilic, it shows less protein adsorption than more hydrophobic materials. However, the material consequently also provides a less favourable surface for cellular attachment, necessitating functionalization with compounds such as Laminin[118], Fibrin[129] and especially RGD peptides[95,96,130,13197,126,132,133].

Polycaprolactone

Polycaprolactone is a hydrophobic polymer suitable for adherent cell culture, in particular for osteogenic lineages[134,135]. Polycaprolactone degrades in physiological conditions through hydrolysis of ester groups within the polymer chains. However, this process takes a substantial amount of time and partially depends on modifications and exposure to stresses and/or more extreme pH levels[136–141]. Consequently, degradation is not expected to be a major issue for the planned experimental work.

In contrast, deliberately inducing hydrolysis in Polycaprolactone allows for an easy initial modification with functional groups which can then be used for further immobilization of proteins[135,142,143].

Polycaprolactone is most often used for solid materials rather than hydrogels, though porous materials can be created using various methods such as electrospinning and solvent-based mixtures[142,144–146].

While cell attachment and culture on Polycaprolactone is possible without modification, the material is not ideal for such experiments[147]. Modification with beneficial proteins such as RGD peptides or fibrin, or alteration of surface chemistry with plasma treatment may improve culture of different cell types by enhancing proliferation, migration, or differentiation[134,135,143,148].

Other materials

Polyethylene, Poly (lactic acid), Polyacrylamide, and Poly (lactic-co-glycolic-acid) will not be considered for this project. While cell culture on these materials has been reported in literature, they each presented risks in regards to patterning, degradation, chemical modification or material cost that were deemed too great for this project[19,102,149,150].

1.5.2.1.2. Natural materials

Naturally derived scaffolds such as those composed of collagen, fibrin and alginate provide a cellular environment that more accurately mimics the extracellular matrix found in vivo. Cell adhesion and viability tend to be much less problematic with natural materials than with synthetic polymers; however, these materials are also less well-defined than synthetic polymers in terms of bio-activity due to bio-active components that are present in the material. The mechanical and biological properties of such scaffolds depend significantly on the origin (if harvested in vivo) or the cells used to create the extracellular matrix (if created in vitro)[151,152].

Natural materials are commonly hydrophilic and degradable nature by either hydrolysis or enzymatic digestion[153]. This makes natural scaffolds well-suited for the creation of temporary 3D hydrogels, but limits the usefulness for long-term use without replacement of extracellular matrix by cultured (or native) cells.

Alternatively, naturally derived materials may be added to a synthetic polymer support in order to provide greater cell-matrix interaction and improve cell survival[150,154], and some naturally-derived polymers such as Hyaluronic Acid can be synthesized. Due to the need for a precisely controlled environment in planned experiments, natural materials will not be used as the (primary) material for creation of cell culture environments during this project.

1.5.2.1.3. Implementation

Polymers can be used for cell culture-related techniques in a number of different ways. Due to the variety of different options available, possible methods for using polymer-based materials are covered in sections 2.3.2 (polymer fabrication techniques) and 2.4 (surface modification and protein immobilization) instead of summarized here.

1.5.2.1.4. Summary

Various different materials are available for use in cell and tissue culture techniques, with different properties and associated advantages and disadvantages.
This project requires material that is well-defined, chemically modifiable, and which allows for cell culture without significant degradation during the course of the experiments. In addition, non-specific protein adsorption should be minimized where possible. Based on these requirements, synthetic polymers are the most immediately suitable material type.
To ensure these requirements are met, the material initially used for creation of cell culture surfaces is Poly (Ethylene Glycol), with additional cellular adhesion- and cytokine-related surface modifications added to ensure a healthy cell culture environment.
To create these surfaces, Poly (Ethylene Glycol) Diacrylate, or PEGDA, is selected as the initial monomer. PEGDA can be polymerized from its liquid state into solid PEG using UV-based methods, which will allow for the creation of patterned surfaces from a patterned substrate without the need to modify surface topology of solid polymer scaffolds.

1.5.2.2. Polymer fabrication techniques

At this point, it is not yet clear if the desired cell culture surfaces will be created and/or patterned by modification of an existing material or by creating the new material in the desired shape. Synthetic polymers may possibly be created in the desired patterned topology, though natural polymers will mostly remain limited to (re-)shaping after acquisition. Therefore, a brief investigation into potential polymerization methods for synthetic polymers may shed additional insight into possible routes forward. Methods to modify polymer topology after polymerization are not covered here and will be found later in this chapter.

Synthetic polymers are typically created from a mixture of monomers, either a single type or, in the case of copolymers, two or more different types. Monomers are polymerized using various different techniques, some of which may be of use during this project both for polymerizing the desired cell culture material in the right shape and for directly incorporating covalently bound bioactive proteins.

Techniques using catalysts will have a more reliable crosslinking throughout the material but may also require measures to remove waste products once the reaction is complete. Techniques relying on heat may cause damage to any proteins included in the material prior to polymerization.

Analysis of the cross-linking of polymers is typically performed using mechanical testing (compression or tensile testing) for mechanical properties such as elasticity or material stiffness, as well as techniques to analyse chemical bonds present in the construct such as spectroscopy (infrared, X-ray) and NMR analysis[155–157].

Directly polymerizing the desired surfaces is potentially suitable for creating or strengthening polymer constructs in micro-beads, although there is a risk of forming cross-links between polymer segments belonging to different beads. However, good results may be found if the chosen process is used on a sufficiently diluted suspension or emulsion of particles/droplets, or when the mixture contains additional measures to prevent bead-to-bead contact such as surfactants.

1.5.2.2.1. Addition polymerization

Addition polymerization directly binds existing monomers without the creation of unbound molecules or waste products. Addition polymerization is most often some form of free radical polymerization, and typically creates non-degradable polymers (unless the monomer components themselves are already degradable).

Free radical polymerization uses radical-producing end groups or additions to the monomer mixture to initiate crosslinking. This technique is typically used with either reactive groups on monomers or with initiating compounds, either of which may be spontaneously reactive due to chemical instability or which may form radicals when subjected to specific wavelengths of light (most commonly ultraviolet radiation) or heat. Thermal polymerization reactions are typically controlled through temperature

and/or heating time, and some methods can be made reversible by cooling the material[158].

Polymers that are suitable for radical polymerization often include carbon-carbon double/triple bonds such as those in acrylate groups[159] or radical-stabilizing phenyl groups along the polymer chain such as those found in styrene/polystyrene[49,160].

If this process is used on an existing polymer such as a hydrogel, this may result in (usually isotropic) shrinking of the construct as the additional crosslinking causes the polymer network to contract.

Exposing photo-sensitive polymer constructs to UV light will create cross-links due to the emergence of reactive radicals within the polymer chains. Using additional photo-initiators can improve the process but is not required for all polymer types. Photo-initiators can be used for polymers that are otherwise not UV-sensitive, as the photo-initiator is the compound that provides the initial free radicals necessary for the cross-linking process. UV polymerization is primarily controlled by the duration and intensity of the UV exposure and the concentration of reactive groups in the monomer solution. Additionally, adding different polymer components or UV-initiators can provide improved process control, for example by adding components that will terminate the polymer chain reaction and correspondingly reduce the total amount of crosslinking with equivalent exposure[161]. UV polymerization is very suitable for creating or reinforcing 2D surfaces, as the level of control over the UV exposure is greatest at the exterior of the construct. It is also suitable for creating or reinforcing 3D scaffolds, but the depth of penetration of the UV light may be a limiting factor. For thick scaffolds, it may be difficult or impossible to get a comparable amount of cross-linking across the entire construct since the effect will be strongest at the surface.

Polymerization with spontaneous radical production does not have the geometric limitations of photo-initiated reactions but typically requires a high degree or control over added initiators or the addition of additional control compounds such as used in RAFT polymerization[158].

1.5.2.2.2. Condensation polymerization

In condensation polymerization, the monomers used to create the polymer chains must have reactive end groups capable of polymerizing with the removal of a small

molecule (such as water). If a single monomer is used to create the chain it may be necessary to include two different reactive end groups.
Chemical equilibrium ensures that a portion of the monomer chains polymerizes until the rates of the polymerization and degradation reactions cancel out. When the environment of the mixture is adjusted such that the small molecule created by polymerization is continually removed from the environment, such as by evaporation, chemical equilibrium drives the reaction towards the fully polymerized state.

If the material is expected to be used without degradation in an aqueous environment, the condensing product must not be water. On the other hand, Polymers created using a water-based condensation reaction consequently make for excellent candidates for degradable scaffolds as these are guaranteed to be degradable in physiological conditions. However, since this project requires long-term stability of created surface geometries, these types of polymers will not be considered.

Alternatively, more stable water-based polymers can be created using catalysts or enzymes to make use of polymerization reactions with otherwise very slow reaction rates [162,163]. Stable polymers can also be created by condensing small molecules not found in the intended cell culture environment, such as volatile liquids/gasses [105,164,165].

1.5.2.3. Summary of cell culture material options

A number of different techniques are available for the creation of new polymer materials. Most techniques rely on creating a high-energy environment or adding additional chemicals to initiate the polymerization. Techniques that require external stimuli (photo-polymerization, thermal polymerization) have more easily controlled reactions. This project will use photo-polymerizable PEG-diacrylate based polymers for the additional control provided over the crosslinking process.

1.5.3. Options for surface modification and protein immobilization

Finally, a method must be selected for the immobilization of growth factors and, potentially, other biologically active compounds on the created surfaces. While non-specific binding can be used to bind proteins, this project's focus on determining the interaction between immobilized growth factors and surface topography means that

large amounts of non-specifically bound protein may introduce unwanted effects and, consequently, additional noise, bias or measurement errors.
Furthermore, the desired immobilization method must meet a number of requirements. Most importantly, the used techniques must bind growth factors in such a way that their functionality remains intact, and the growth factor itself is presented to cells on the surface of the construct. Due to a likely need for lengthy cell culture experiments to verify effects, the method to link the growth factors may not substantially degrade over time or otherwise release growth factors into solution (if non-covalent binding is used).

1.5.3.1. Direct polymer copolymerization

By conjugating one or more reactive functional groups to the growth factors that need to be added to the material, it is possible to directly integrate these growth factors when the material is polymerized.
Photo-polymerization requires additional steps to be performed during the synthesis of the construct and growth factor; however these steps are not significantly more difficult or equipment-dependent than those required for the photo-polymerization process itself. The main challenges are that larger amounts of growth factor that need to be used even for 2D surfaces (as the entire 3D structure will contain immobilized proteins) and it is necessary to use a polymerization method that does not damage the growth factor itself.

1.5.3.1.1. Implementation

To link the growth factors to the polymer scaffold during the polymerization process, a photo-reactive end group that is compatible with the monomer mix components is attached to the growth factor. During the polymerization process, the growth factor will be linked to the forming polymer chains much like the chains are linked to each other, for example with a thiol-acrylate link[23,24].
Embedding the growth factors into a polymer surface or 3D scaffold requires the addition of the growth factor during the polymerization process. The growth factor will be present throughout the resulting material, but this consequently also requires that the polymerization process doesn't cause severe degradation of the proteins involved.
Using photo-polymerization to embed growth factors in a polymer structure around micro-beads has the same problems as creating a polymer structure around the

micro-beads in the first place; only if the polymerization can be limited to within a short distance of the micro-beads will this method be useful.
This method allows very limited control over growth factor embedding and presentation; only the concentrations of the different compounds can be controlled. Spatial distribution of the growth factors throughout the construct is therefore difficult to control, although it may be possible to create a layered structure by exposing a small amount of material at a time using a process such as additive manufacturing. Analysis of copolymerized growth factors may require advanced measurement techniques such as NMR or IR Spectroscopy, or destroying the material itself to analyse its components. However, using fluorescence marked growth factors or suitable fluorescent antibodies may allow users to evaluate growth factor concentrations at the surface of the material (or deeper inside if used in a hydrogel). Using photo-polymerization to embed growth factors has the same limits regarding scalability as the use of photo-polymerization itself. Large-scale 3D constructs may be limited in size due to restrictions of the polymerization process, such as the penetration depth of the UV light into the polymer/growth factor solution.
Unless a highly porous 3D structure is used, many growth factors will be bound within the construct instead of being presented at the exterior. Due to the inefficient use of growth factors, materials made using this technique will have a higher manufacturing cost than those made with more efficient techniques.

1.5.3.2. Covalent immobilization

The process to covalently bind proteins is similar to direct copolymerization as described above. However, the proteins of interest are not bound directly into the material during creation. Instead, for covalent immobilization proteins are added at a later stage and chemically reacted with the cell culture surface using methods such as thiolation or carbodiimide crosslinkers. Covalent immobilization of proteins onto cell culture surfaces consequently relies on the presence (or creation) of reactive surface groups, such as esters or primary amines.

This technique is suitable for numerous types of materials, and has previously been used in hydrogels, polymer scaffolds and ceramics[23,24,128,166].

The exact details of the process will depend on the choice of material; however proteins are typically bound through the creation of covalent bonds on primary

amines or carboxylic acids, or through the introduction of new reactive groups. Protein immobilization often includes crosslinkers, and research has shown that crosslinker length can have an impact on the structure and effectiveness of bound proteins[167].

Rather than describe all the possible methods for covalent immobilization here, relevant modification strategies may be found in the sections for specific cell culture materials.

1.5.3.2.1. Chemical surface modification for covalent immobilization

The most common method for covalently binding organic materials such as carbohydrates or proteins is the use of carboxylic acid or (primary) amine groups, owing to the numerous chemical reactions that can be used with these groups. Carbodiimide- and succinimide-based crosslinkers, ester condensations and aldehydes can all be used to create covalent bonds without the need for complex chemical reactions or mixtures[127]. Many surface materials can be functionalized with such groups through oxidation, with processes ranging from washing in acids or bases of varying pH to using catalysts or enzymes such as Ammonium Persulfate, Laccase, or Sodium Periodate[127,168].

Another approach for covalent binding of proteins is to focus on using the chemical properties of specific amino acids. The addition of thiol-reactive groups to a material or crosslinker chain allows for covalent binding of proteins by targeting free cysteine residues, typically creating disulphide or sulfone bonds between the protein and the reactive group[23,24,127]. The rarity of cysteine compared to other amino acids in many proteins allows for a more controlled linking method and potentially immobilization of only specific proteins in solution. Likewise, varying pH levels of a solution allows for the selective activation of specific amino acids, further increasing options for targeted reactions.

The greatest advantage of using chemical modification of surfaces to allow for covalent immobilization is that most cell culture surfaces can be treated in bulk, including the interiors of porous scaffolds, without the need for complex processes or equipment. However, chemical modification is substantially less suitable for the creation of gradients – adding gradients to such a treatment often requires inclusions

of additional effects such as catalyst diffusion, varying electrical charges or modified surface submersion times[169–171].

1.5.3.2.2. Plasma-based surface modification

Surface modification using plasma-based techniques has substantial overlap with plasma surface etching described previously in this chapter. The primary difference between these two techniques is the level of plasma exposure applied to the surface in question. While plasma surface etching directs a stream of plasma with enough power to damage and entirely remove existing material, this process uses far lower energies and plasma volumes.

On contact, the highly energetic plasma interacts with the molecular structures in the exposed material, disrupting molecular bonds and creating temporary highly reactive groups such as radicals. Depending on the choice of plasma, these groups may then react with the plasma itself (for example using Oxygen or Carbon Dioxide plasma for the creation of Oxygen-containing functional groups), or they may simply decay and leave modified surface chemistries based on the original material chemistry (for example when using noble gases like Helium or Neon). However, this process can also be used for depositing more complex materials, including amino acid groups and newly-created polymer chains[90,172,173].

1.5.3.2.2.1. Implementation

A number of considerations must be taken into account for the use of plasma-based chemical modifications. Most importantly, the material must not be significantly damaged by the plasma jet under the selected exposure. In addition, the material must also remain intact in near-vacuum conditions, meaning this process is primarily suitable for solid materials while presenting substantial difficulties for use on microspheres, hydrogels or 3D scaffolds where the plasma can't effectively enter the material.

However, with the correct plasma source and material chemistry, this technique offers a high degree of control over the type and amount of modification. Variations in the energy of the plasma jet, the components of the plasma and the functional groups (if any) that are present on the material surface at the start of the procedure will all have an impact on the final chemistry presented at the material surface and the larger-scale effects on the treated material[172,174].

Consequently, this method will create different functional groups on the surface of a material, allowing for the immobilization of growth factors using different covalent binding reactions[175,176].

Plasma surface treatment is relatively scalable and has been previously used for samples including fibrous matrices[177], cell culture plates[178] and feedstock used for the creation of surgical implants[179]; however, the size of the plasma chamber will be a limiting factor for the surface area that can be modified at any given time.

1.5.3.3. Non-covalent immobilization

In contrast to covalent binding of proteins, non-covalent binding is always of a temporary nature. Any bound proteins will be released into the liquid environment over time, though depending on the exact method of immobilization this process may proceed at various rates; non-specific adsorption will release more quickly than specific non-covalent binding methods such as those involving complementary DNA or RNA chains or the Biotin-Streptavidin link.

Non-covalent binding of proteins will occur on every surface regardless of material, with the deposition rate, strength of binding and equilibrium surface concentrations depending on the chemical properties of the material in question. Surfaces can be chemically modified to increase or decrease the adsorption of proteins out of solution. In particular, the hydrophobicity of a material is of key importance[98]. Most proteins are amphiphilic, with both hydrophilic and hydrophobic segments, and one of the most important processes for protein adsorption is the binding of the hydrophobic segments of a protein to hydrophobic surfaces – though this process can also cause potential loss of function due to changed protein folding.

'Traditional' non-covalent binding is non-specific: any protein with hydrophobic segments can be adsorbed out of solution. This, combined with the temporary nature of the immobilization, makes this type of approach unsuitable for the planned work in this project.

However, non-covalent binding can also be used to bind proteins of interest using highly specific protein-protein interactions such as those seen in the binding of complementary DNA or RNA chains or the binding of Biotin to Avidin or Streptavidin[180].

1.5.3.3.1. Biotin-Streptavidin and Biotin-Avidin immobilization

The biotin-streptavidin immobilization technique is a particular method that is commonly used. As the name implies, it relies on the non-covalent binding between the proteins biotin and either Streptavidin or Avidin to attach other bioactive compounds to a selected surface or scaffold[128,159]. Streptavidin tends towards a slightly stronger non-covalent binding of biotin. Typically Streptavidin are covalently bound to the surface of the material that needs to be enhanced while Biotin is linked to proteins as Biotin's smaller size is less likely to influence protein function. The reverse process is also possible, but is typically applied to link smaller materials[173]. The biotin-protein complex can then be placed in contact with the surface to create a non-covalent and resilient but reversible bond between the two segments. It is also possible to use the Streptavidin complex to create a Biotin-Streptavidin-Biotin chain[181].

The Biotin-Streptavidin immobilization is effective for 2D surfaces, and has been used by other groups to create functionalized pores in polymer films[182]. The biotin-streptavidin immobilization is also suitable for creating functional micro-beads[183]. Finally, the biotin- streptavidin immobilization can also be used to enhance 3D scaffolds. However, the permeability of the structure must be considered (non-porous structures might only bind the growth factors on surface pores).

The addition of growth factors to a surface using the biotin-streptavidin link is primarily controlled by the concentrations of the used solutions. The use of additional control mechanisms such as hydrophilic/hydrophobic groups in the polymer is possible, but these will need to be included in the process used to create the polymer construct.

The effectiveness of surface immobilization may be analysed using fluorescent microscopy, using either fluorescently marked biotin or streptavidin, depending on which connection needs to be confirmed. Fluorescent markers for the linked protein may also be used, if applicable.

1.5.3.4. Summary of surface modification options

A number of different strategies are available for immobilizing proteins onto cell culture surfaces, including methods to prepare these surfaces for such efforts through chemical modification.

As this project requires a high specificity without causing potential damage to the cell culture surfaces, the initial choices for immobilizing proteins will be the use of carbodiimide crosslinkers, potentially with further protein-protein non-specific binding. Other techniques may be considered depending on the choice of materials and results of completed experiments.

1.5.4. Structuring techniques for cell culture surfaces

Surfaces with highly defined topologies will be evaluated to identify the presence or absence of any topology-biochemistry relationships. Surfaces with randomized size and shape of features and topology are more easily created, especially in bulk, by techniques such as phase separation and additive manufacturing[184]. Their relatively easy production and correspondingly lower cost makes these materials more clinically relevant, as such surfaces are used more frequently than more well-defined but less affordable options.

However, the use of surfaces with ordered patterns will provide a more controlled experimental environment, providing potential advantages during pre-clinical work. The surfaces used during this project will focus on the influence of pore size and three-dimensional pore anisotropy on growth factor presentation. Consequently, structuring and patterning techniques should ideally be able to provide a defined and highly regular topology to the material structure at multiple scales, ideally in the range of 0.1-100µm. The applied topology must be similar across the entire construct, with a minimum in shape and size deviation between different pores.

1.5.4.1. Phase Separation

For phase separation, two liquid components are mixed into a single solution. Altering the liquid's environment, such as by increasing or decreasing temperature or allowing elimination of one or more components by evaporation or chemical reaction, then causes the two liquids to change phase to a solid material at different times. The material that turns solid thus forms a porous scaffold containing the remaining liquid. Phase Separation is also called Gas Foaming if one of the materials changes to a gas phase to create bubbles rather than liquid pockets. If the mixture instead separates into a (semi-) solid and a gaseous phase, the process is also often called gas foaming[185].

1.5.4.1.1. Implementation

Phase separation relies on adjusting the environmental parameters of a polymer mixture in such a way that the mixture spontaneously separates into two immiscible components. The most common methods involves the use of a mixture that is miscible at high temperatures but separates at low temperatures, but other techniques such as pressure differences, freeze drying, and other sources of solvent evaporation are also possible[133,186–188]. Phase separation can be used to create both 2D surfaces and 3D scaffolds, but is not directly applicable to the creation of patterned microparticles within the mixture. However, if the (unseparated) mixture is present as a suspension in a second immiscible liquid, it may be possible to apply phase separation to these droplets to create patterned particles.

This process is particularly useful for creating highly porous 3D scaffolds that allow cell infiltration of the scaffold, including scaffolds for tissue regeneration of bone or cartilage[17,185,189]. Scaffolds can be created in bulk or formed into smaller, more precisely controlled shapes through controlled deposition and polymerization[190].

The phase separation of the mixture can be controlled by modifying the different materials and solvents used during this process. Depending on the cells that will be seeded onto or within the scaffold, different pore sizes may be required[191]. While the size and porosity of the resulting material can be controlled fairly well, the exact topology of the material is not readily controlled and will show significant variation, though additional materials such as micro- and nano-particles can be included in the mixture(s) for multi-scale properties and altered mechanical properties[185,192].

Because of the higher variation in topology caused by this process, phase separation will not be considered for use during this project.

1.5.4.2. Salt Leaching

Salt leaching creates porous scaffolds by mixing solid salt crystals into a salt-saturated mixture of monomers to be polymerized. When the monomer solution is polymerized, for example by heating or exposure to UV light, the resulting scaffold only fills the spaces not occupied by the salt crystals. Once the polymerization process is completed, the salt can be removed, for example by using a suitable solvent, leaving only the completed porous polymer scaffold.

1.5.4.2.1. Implementation

Salt leaching functions by polymerizing a salt-saturated monomer or oligomer solution containing salt crystals of pre-defined size at a desired volume fraction[129,193]. After polymerization, the salt crystals are dissolved and flushed out of the finished construct using a solvent. The resulting polymer structure contains pores with the shape, size and position of the removed salt crystals, allowing for the creation of pore sizes from 200 µm to as small as <20µm[151,193–195].

Salt leaching is suitable for creating a patterned 2D surfaces and 3D scaffolds, and any volume of polymerized material will have a patterned surface at the solution-atmosphere interface provided the used monomer mixture does not result in full submersion of the salt crystals used during the process. Patterned surfaces at the solution-container interface may have a patterned surface depending on whether or not the salt crystals remain in contact with the container surface prior and during polymerization. For 3D scaffolds sufficiently high pore connectivity may be required to flush all the salt crystals from the finished product, especially in larger scaffolds. However, despite the presence of solid salts within a polymer blend, appropriate volume fractions may still allow for the use of techniques relying on the mixture's liquid behaviour, such as electrospinning[194,196].

Salt leaching is otherwise easily scalable; the process is identical for creating small or large surface areas and volumes, with the only difference being the resources, equipment and time required. The main limit of this process is the possible presence of remaining salt particles in the scaffold due to discontinuous pores (only applicable to 3D scaffolds, depending on chosen volume fractions).

The rough pore size and shape can be controlled by filtering the salt crystals prior to salt leaching. However, more precise control over the shape distribution of the salt crystals will be required for the creation of highly defined patterns such as those desired for this project. Depending on the availability of such materials salt leaching may be considered or rejected for further work during this project.

1.5.4.3. Photo-lithography and additive manufacturing

Additive manufacturing is a process wherein two- or three-dimensional structures are created from a feedstock of solid or liquid materials such as metal[197], ceramic particles[198] or (unpolymerized) plastics or hydrogels[199–201]. Materials are fused

together one layer at a time, typically using heat- or UV-induced polymerization, heat sintering, or cooling of molten materials.

The most simplistic method using additive manufacturing is the creation of a single layer, possibly on top of an existing structure. The most commonly used technique for such structures is photolithograpy, wherein the necessary structures are created by polymerizing a photosensitive monomer mixture with spatially-dependent exposure to UV light[125,186,202].

1.5.4.3.1. Implementation

Additive manufacturing techniques are applicable to 2D surfaces, with the primary limitation being the resolution limit of the manufacturing equipment. The process for creating a 3D scaffold is very similar to that for creating a 2D surface, except it requires repeatedly adding additional layers and/or structures over time. Possible techniques include laser sintering of powders, ink-jet style chemical printing of plastics and hydrogels, and UV-based polymerization of monomer solutions. After a layer has been completed, a new layer of the necessary material (either a deposit of powder such as metals and ceramics, or a liquid polymer layer) is added on top of the existing structure and the process repeats. Variations in the process between layers can result in spatially-dependent changes in the properties of the final structure[199,203].

Additive manufacturing is not applicable for the creation of micro-bead covers, although micro-beads may themselves be incorporated into any created designs[204–206]. Depending on the process, growth factors or living cells can be incorporated in the created material[199,207]. In these cases, fabrication parameters must be such that manufacturing the product does not damage the growth factors or cells due to, for example, excessive heat.

The amount of control over the process will be highly dependent on the exact specifications of the equipment used during this process, as well as the chosen material. However, typically a high degree of control over the 3D shape and porosity can be attained, with the primary limit being the resolution of the manufacturing equipment, the used digital designs and the limits of the source material (such as minimum size of sintered particles)[197,208,209]. Additive manufacturing is typically used to create larger scale structures with macro features in the range of µm-mm, and pore size is limited by the resolution of the used equipment. Pores of <150 µm have

been shown to be possible, though larger pores may be necessary for cell migration through a material[210]. The creation of smaller pores will depend primarily on the used material (diameter of the micro/nanoparticles used during the additive manufacturing process), though such materials have also been created previously[206].
Analysis and quality control of the manufactured constructs may be performed using various microscopy techniques including bright field, fluorescent and polarized light microscopy; for small sized patterns methods such as scanning electron microscopy or atomic force microscopy may be required to distinguish the smallest details.

A downside to this process is that additive manufacturing techniques are not readily scalable, since the equipment necessary for these processes typically has a number of limitations regarding the volume of created constructs. Additionally, producing large numbers of constructs may require multiple instances of any piece of equipment when time limitations of the manufacturing process restrict higher production rates. Additive manufacturing techniques are not typically found in clinical/sterile environments; to ensure the product is safe for clinical use additional measures may be necessary to prevent contamination by micro-organisms, be it during manufacture or by including sterilization steps following surface creation.

1.5.4.4. Plasma surface etching

The chosen polymer must not become toxic during etching and must be able to remain intact in a near-vacuum. The plasma used to etch the surface of the polymer construct either does not alter the surface properties of the polymer, or alters them based on desired parameters. Finally, the plasma jet must be sufficiently narrow and sufficiently accurate that small-scale topology can be created.

1.5.4.4.1. Implementation

With this technique, the surface of a material is etched using a stream of highly energetic plasma particles (different plasma compositions are possible, including Neon, Argon etc.). The high physical (velocity/temperature) and chemical (radical components) energy of the plasma jet causes material on the surface to ablate, leaving empty space[172,174]. Alternatively, a lower energy plasma jet can deposit material onto the surface, although the types of materials that can be deposited have some strict requirements[174].

Creation of a 2D surface is the default use of this technique. Plasma surface modification is not directly applicable to micro beads or 3D scaffolds, only the exposed surface is affected. The unexposed side of any micro-beads and the internal parts of a scaffold remains unaffected.

This technique primarily depends on the type of plasma used, the temperature/charge and exposure time, and the properties of the polymer, each of which can be strictly controlled. The possible scales of the patterning created using this technique will depend on the used equipment and, to a lesser extent, on the chosen material. Nonetheless, patterning of >1 μm have been created before on Titanium wafers[172].

The analysis of the surface after exposure to the plasma jet will typically involve optical, fluorescent, electron or atomic force microscopy, depending on the scale of the created patterns and the desired information.

Plasma surface modification is scalable to a certain limit; this process is dependent on the controlled exposure of the construct to the plasma jet(s) and any surfaces to be modified will consequently have a maximum size. This technique has already been analysed for use in multiple biomedical applications such as surface sterilization and biocompatibility enhancement, and proper use should not result in any clinical risks[90].

1.5.4.5. Condensation-controlled patterning (Breath Figures)

Using water condensation to create ordered patterns, also called the 'breath figures' method, is a promising technique that relies on maintaining a high degree of control over the size and shape of liquid droplets at a specific temperature, humidity and chemical environment. The breath figures technique has some similarities to the phase separation method described above, but alters the final structure of the polymer with condensed liquid droplets in a regular pattern. These droplets force the solid phase of a polymer/volatile solvent mixture into a specific shape during solvent evaporation[211], creating more controlled pores than the semi-random effect seen in normal phase separation.

1.5.4.5.1. Application

A layer made of a blend of one or more polymers and a volatile solvent is used to form the scaffold material. An air flow with specified flow and (high) humidity is directed onto the surface of the polymer blend at a specific angle, resulting in

condensation of the water in the air due to temperature changes as it hits the cooler polymers. With the right environmental parameters, condensation setup[212] and polymer blend properties[103,213], droplets formed on the surface will form a honeycomb-shaped pattern. During this process, the solvent containing the polymer(s) will evaporate, causing phase separation of the polymer blend to occur. The solidifying polymer is shaped into the final construct pattern by the water droplets. Once the solvent has evaporated completely, the water droplets may be removed with various drying methods, and the resulting polymer surface will remain, containing the required pore pattern.

This process is most commonly used to create a 2D patterned surface, although a 3D scaffold can also be constructed using the breath figures method. Production of a 3D scaffold requires that water droplets sink into the polymer blend to provide additional space for new droplets to form[212]. Therefore, the environmental parameters and the properties of the polymer blend must adhere to more strict requirements. The breath figures approach is not applicable to creating patterned surfaces of micro-beads, as one of the requirements for this method is the presence of a flat polymer solution surface.

However, despite this process' limitations, it can provide excellent control over pore size (typically creating pores of 0.25-25 µm), shape and pattern, depending on the specifics of the technique that is used. It is also possible to add functional groups to the surface of the polymer material, both evenly distributed or with local variations depending on the polymer blend properties[182,212].
The breath figures approach is also relatively scalable; the process primarily requires a well-controlled air flow and solvent evaporation at each point of the polymer solution. The creation of large surfaces may yield variations in the surface topology from spot to spot if control of the process environment is insufficient. Also, the creation of large 3D structures may be difficult since larger polymer layers may restrict the evaporation of the solvent. There may therefore be a limit to the number of stacked layers that can be created using this method. The breath figures approach does not cause any clinical risks not covered by the used materials, provided any potentially dangerous solvent is thoroughly removed from the final product.
The breath figures approach requires does not require a lot of specialized equipment, but effectively combining the necessary components (air flow, temperature, etc.) may

present some challenges. Likewise, while the principles of the process are quite simple, the large number of controllable parameters may require significant testing to find the optimal settings for a specific project.

1.5.4.6. Mould-based patterning

The last major patterning process is to create patterned surfaces using a previously-created pattern as a mould. Depending on the method used to create the solid material intended for cell culture, as well as said material's properties, directly creating the material in the final, intended shape may be an option. This process is the most straight-forward out of all patterning methods, but requires that a suitable pattern can be created out of a solid or semi-solid material prior to solidification of the final material.

1.5.4.6.1. Application

The critical step in using a mould-based patterning process is the creation of a suitable pattern prior to deposition of the material to be patterned. Moulds can be used to create numerous different patterns, depending on the original mould shape, but include convex and concave shapes based on particles, or straight shapes such as pillars and grooves based on photolithography[214–216].

However, for this project both a high regularity of the pattern and a low requirement for advanced equipment and training is a priority. As such, a promising option is the use of particle-based moulds. A regular honeycomb-style pattern will automatically form when a supply of spherical particles is allowed to settle under gravity, making particle-based moulds a potentially highly reliable and easy to implement process for this project.

Most commonly, these types of pattern are created by the addition of a suitable amount of microparticles, such as paraffin[154,217], sugar[218], silica[219] or polymers such as polystyrene[220], to a liquid solution before solidification. Once the liquid solution is solidified using methods such as UV-induced polymerization, cooling, or similar processes, the spheres are removed by heating, the use of solvents or other techniques. The resulting material then contains pores formed by the space that was originally occupied by the beads.

This process creates a 3D scaffold by default, the number of pore layers is directly dependent on the amount of particles used and the volume of the final construct; a small volume of beads can theoretically create a patterned 2D surface instead of a

3D scaffold. Creating a 3D scaffold requires that the microspheres can be dissolved inside the material without damaging the surrounding material, and a minimum porosity/microparticle connectivity may be required. If particles embedded within the material can't be removed, the process effectively creates a 2D pattern instead.
The amount of control that can be applied to mould-based techniques is directly dependent on how precise the shape and size of the mould particles can be controlled, and therefore depends primarily on the chosen mould material and preparation technique.
Microsphere-based moulds will create pores that are entirely dependent on the size of the microspheres, with potential sizes in the order of millimetre to sub-micrometre[154,214,218–220].
The use of microsphere-based moulds is very scalable; the only requirement is that both the beads and polymer solution can completely fill the desired volume. Flaws in the volume filling such as air bubbles will result in structural irregularities in the final construct. A particular risk is the potential for toxic materials to remain in the final product; to ensure safety of the patient it may be necessary to use non-toxic materials during one or more steps of the process.
Using microsphere moulds is a relatively simple technique, but different amounts of laboratory or chemistry experience may be required to reliably create patterns or microspheres of the correct shape and size.

1.5.4.7. Summary of structuring technique options

Various different techniques may be used for patterning materials prior to cell culture, from semi-random structures based on spontaneous material changes to directly crafted shapes. However, most high-precision patterning methods require substantial investments in advanced equipment and appropriate infrastructure, making them impractical for use in this project.

Since this project is meant as a proof-of-concept and more complex surface designs are unlikely to add relevant information, this project will only employ simple but accurately created patterns. Initially, this project will focus on using microparticle-based moulds to create suitable patterns, with phase separation and additive manufacturing as potential replacements depending on initial results.

1.6. Summary of selected options for initial experiments

A large number of different options exist for the experiments planned during later parts of this project. It is not possible to choose all parameters definitively at this early stage; only initial selections are made.

For experimental work, this project will initially focus on the use of Mesenchymal Stem Cells, induced into chondrogenesis by exposure to TGF-β1. Cell culture environments will consist of Poly (Ethylene Glycol) based materials with covalently bound proteins (either directly bound growth factors or Biotin/Streptavidin for non-covalent binding). Surface patterning will be created using moulds based on dry microparticles of uniform size.

Depending on the results of this project, recommendations for randomized surfaces may also be included. This project may also proceed to multiple growth factors for immobilization, dependent on the final selections of material type, cell lineage and differentiation target, and other relevant considerations such as results of early experimental work.

Chapter 2: Creation of micro-scale patterns on cell culture surfaces

2.1. Introduction

This project seeks to investigate the interaction between surface topology and growth factor presentation. One requirement of this project is to reliably create well-defined micro-scale patterning on the cell culture surfaces.

Due to the numerous possible interaction mechanisms between cells and surfaces and the potential for properties to be beneficial or detrimental depending on feature size, it is necessary to select the desired feature sizes carefully[221].

In this project, the main focus is on the interplay between surface geometry and the effectiveness of biologically active proteins immobilized on these surfaces. Ideally, the chosen method will allow for the creation of feature sizes around the size of the cells cultured on the surface, as these scales will likely show good variation between small and large feature sizes. Scales at cell size or above will primarily influence the curvature of the cell membrane and may have effects linked to macro-scale cell morphology and the cytoskeletal system. Conversely, scales at or below cell size are more likely to show possible effects due to direct distortion of the cell membrane and mechanical influences on membrane-bound proteins such as integrins[222].
While nanoscale features have been shown to influence cellular behaviour[89,223,224], these scales will not be investigated during this project.

Various different types of patterning are possible, depending on the type of technique used to create or modify the desired cell culture surfaces. Most common processes, such as electrospinning or phase separation, result in random surface topologies with only limited control over the surface features[185,191,202,225]. Top-down techniques such as masked UV polymerization and etching techniques can allow for a higher degree of control over the created geometry, but these are typically used to create pillars, pits or grooves and provide limited means for curved or 3D features [172,215,216,224,226].

Other research focuses on increasing the roughness or porosity of created surfaces without creating a specific pattern, either by modifying existing surface roughness or by creating a surface out of individual grains of material, most commonly ceramics or metals, of the desired size(s) that are then fused together[186,188,222,227,228]. Combining polymers with embedded fragments provides an additional option for creating more

complex materials and surfaces[188,229]. However, while these methods allow for a more easy creation of surfaces with varying feature sizes or gradients, the random nature of the process means that ordered patterns are typically not possible. The choice of method is especially important considering that varying levels of randomness in the pattern orientation may themselves have an impact on cellular behaviour[17,223].
Because this project focuses primarily on the interaction between surface features and immobilized proteins, introducing additional effects due to randomness of the pattern is not a priority. All processes are developed with the goal of creating patterns with uniformly ordered structures, with no random elements other than unavoidable defects.

In summary, creating highly variable or advanced surfaces is both unnecessary and counterproductive; methods that require complex processes or equipment will cost additional time to develop and use, but they are unlikely to offer any additional insights and may even interfere with the project's main focus.

Instead, a simple method that provides the necessary patterning in a reliable way would be more suitable, both to avoid extensive troubleshooting and to reduce the number of variables that may influence the experimental results.

A comparatively uncommon method for creating patterned surfaces is to use three dimensional moulds to directly shape the surface[186,214].

While this type of process does not allow for easy modifications to change feature shapes, using moulds to create the necessary patterns is expected to be the most time-efficient way to achieve the necessary progress for the project.

This part of the project focuses on the creation of these surfaces, based on using polystyrene microspheres of varying sizes to create a mould, which is then used to mass-produce suitable cell culture surfaces similar to work done by other groups[154,217–219]. Findings of the experiments detailed below will be used to optimize the process and the quality of the surface patterns used during the later stages of the project.

2.2. Aim and goals:

This part of the project will aim to create mass-producible patterned surfaces in three polymer types. To achieve this, the following aspects are focused on:

- The development of a repeatable method for creating micrometre-scale patterning on surfaces made from Poly (Ethylene Glycol), Polystyrene and Polycaprolactone
- The analysis of pattern quality and defects due to the process steps as well as environmental factors
- Modifications to environmental parameters during creation and replication of patterned surfaces
- Mass-production of patterns for use in cell culture experiments in 96- and 24-well plates

2.3. Materials and methods:

2.3.1. Materials

Polystyrene microparticles were acquired from Phosphorex Inc. USA. Mold Star 15 Slow silicone was acquired from Bentley Advanced Materials, UK. All other materials are acquired from Sigma-Aldrich Company Ltd, UK.

2.3.2. Creation of initial surface patterning

Based on literature reviewed during chapter 1, the method investigated for the creation of micro-scale patterns is the use of positive and negative microparticle-based moulds to imprint the pattern into materials suitable for cell culturing.

The primary pattern is created from plain polystyrene microparticles embedded in a mixture of a commercially available silicone, and

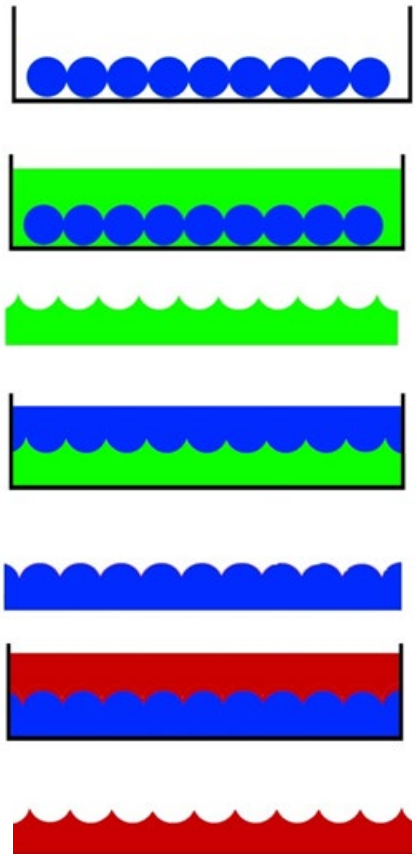

Figure 3: Schematic representation of the pattern creation and copying process. The polystyrene microparticles (blue) are mixed into uncured silicone (green) in a glass petri dish. The silicone is then cured and used to create a polystyrene negative mould (blue) and this mould is used to create multiple PEGDA cell culture surface material (red).

transferred to other materials after creation as shown schematically in Figure 3. The initial process development will only be applied to microparticles with a mean diameter of 50 μm.

5 mg of microspheres is mixed with silicone at approximately 3:1 to 4:1 volume ratio to ensure packing of the microspheres. While some defects in the pattern are to be expected, sufficient microparticles need to be packed together to ensure a cut through the material will expose the microparticles along the entire revealed surface within the cut, requiring the total amount of silicone in this mixture to be minimized. The initial process is tested using solid polystyrene microspheres with a 50 μm diameter. 0.5g of the selected microspheres is mixed with silicone at a 4:1 volume. The resulting mixture is spread into a glass petri dish with a surface area of approx. 9cm^2, creating a layer with a final thickness of approx. 2.75 mm. Only a limited area is used to create the initial patterned surface to ensure homogeneity of the microparticle layer, enable the use of different pattern sizes in a single wells plate, and reduce the use of high-value resources.
The silicone mixture is allowed to cure for 2 hours, after which an additional 2 g of uncured silicone mix is added to improve structural resilience and ease-of-use of the material through the creation of a thicker ‘top’ layer over the microparticles. This added volume is not mixed with the existing microparticle-silicone mixture to ensure all the microparticles are present at the bottom layer of the material. After addition of the extra silicone, the entire mixture is allowed to cure overnight.

Once the microparticle-silicone composite is finished, the pattern within the material must be exposed. Two options are used to access the microparticle volume. The first method is by cutting through the mixed volume to expose the microparticles using a standard scalpel at room temperature. In the second method, a glass shard microtome is used to cut through the material following cooling to sub-zero temperatures by pressurized carbon-dioxide. These options are used to determine if the elastic nature of the silicone might prevent a good cut through the material, and if freezing the mixture can allow for a more precise cut.
Once the initial cut is created, the surface is washed with Acetone to dissolve any remaining polystyrene microparticles and fragments. This will remove the original microparticles while retaining the pattern created in the silicone, allowing for

evaluation of the surfaces prior to further experiments to transfer the created patterns.

Samples processed using the room-temperature scalpel process, are analysed at four stages to determine the influence of the Acetone on the silicone matrix. The material is imaged before and after exposure to Acetone without first exposing the microparticles to determine macro-scale degradation, warping, or other forms of damage. The creation of the pattern was investigated by imaging the surface after making a cut but before exposure to Acetone (surface including microparticles) and after exposure to Acetone (silicone surface only).

2.3.2.1. Results

A micro-scale pattern was successfully created using the polystyrene microparticles and silicone mixture. The microparticles embedded in the silicone are packed into an orderly structure due to gravity, with silicone located throughout the gaps between the particles. This creates a functional micrometre-scale pattern at any plane inside of the material as seen in Figures 4a, 4b, 5c and 5d. However, some limitations of this process were identified.

First, it is necessary to create a horizontal cut through the created material to expose the microparticles. The chosen surface area (approx. 9 cm^2) proved too large to effectively process in this manner. To create suitable surfaces for analysis, the original surface was cut into smaller fragments to ease manual handling and processing before the microspheres were exposed. Consequently, all images are created from the same initial microparticle-silicone sample.

Using a carbon-dioxide cooled glass shard microtome, the composite material created from the silicone and microparticles showed that while the pattern was present, significant defects were present in the material. The most likely explanations are that the cooling of the material damages the microparticles or silicone, or that the brittleness of the cooled silicone causes the force applied during the cutting process to damage the material.

Microscopy images of the material after the cooled cut can be seen in Figure 4.
By comparison, creating a cut with a (disposable) scalpel at room temperature on a pattern created using identical methods proved more effective. Microscopy images at

each step of the analysis process for the silicone-microparticle material following a room temperature cut are shown in Figure 5.

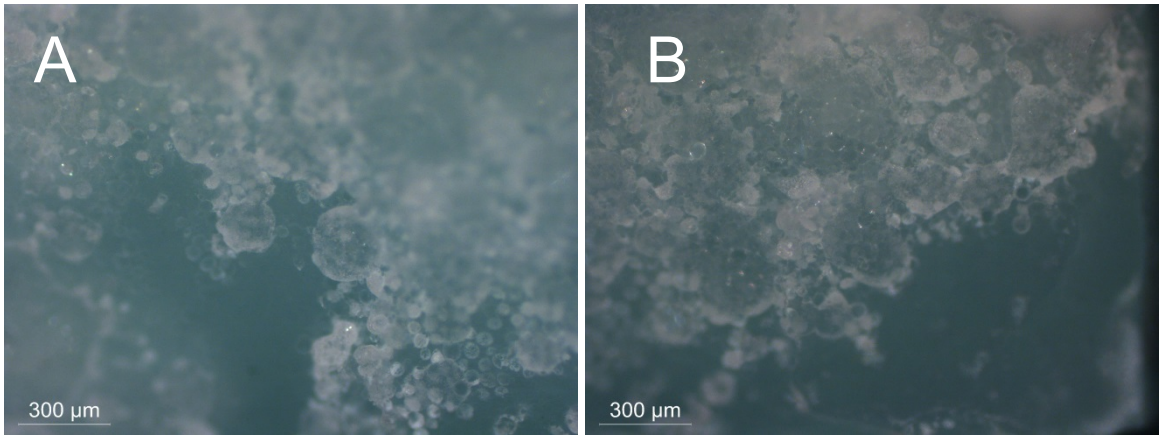

Figure 4: Microscopy images of the mixed silicone + polystyrene microparticle material after cutting with a cooled glass microtome blade and soaking the material in Acetone. The original microparticles (diameter of the particles is 50 µm) are visible as small white spheres, while defects in the composite show as large, white clumps of material such as in the center of image A. Gaps in the micro-scale pattern are visible as the larger, dark areas in the center-left area of image A and the lower right area of image B. Image A and B represent different locations on a single sample.

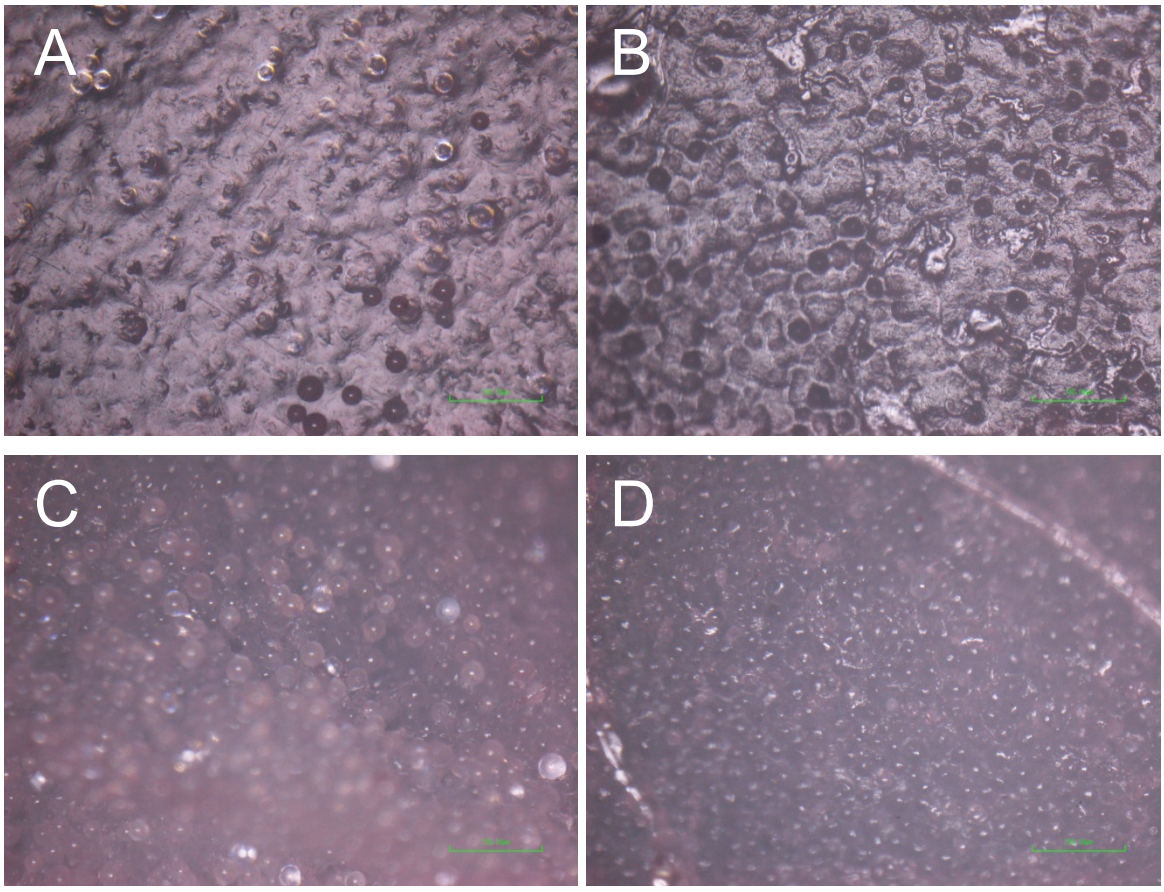

Figure 5: Microscopy images of the surface of the mixed silicone + polystyrene microparticle material. Images show the surface without modifications (A), after treatment with Acetone (B), after creating a cut through the material (C) and after creating a cut and treatment with Acetone (D). The scale bar in all images is 200 µm; microparticle diameter is 50 µm. Figures A, B, C, and D all represent the same sample at different stages of processing, but locations cannot be guaranteed to be the same.

2.3.3. Surface area and microparticle volume reduction

The current method for the creation of microscale patterns in silicone provides accurate patterns, as seen in Figures 5C and 5D. However, the total volume of microparticles used to create these patterns is comparatively large: only the particles located at the plane exposed using the cut actually contribute to the final pattern.
To improve the process and increase the number of surfaces that can be created using each batch of microparticles, a new method was tested. #
The process for creating patterned surfaces as described previously is repeated, with the modification that the microparticles are used without first mixing them with silicone.
Dry 50 µm diameter microparticles are spread over a square 4 mm^2 surface in a custom-made glass and silicone mould, to a thickness of approx. 2mm. Uncured silicone is prepared as before, and is carefully poured onto the microparticles without mixing the components together. The silicone is allowed to flow into the microparticle layer under the influence of gravity, after which the mixture is allowed to cure overnight.
After curing, the solid silicone material is removed and the created surface is analysed using microscopy without creating a cut as was necessary in the previous method.

2.3.3.1. Results

Using the modified procedure, a patterned silicone surface was successfully created. However, inspection using microscopy showed that the created pattern was noticeably lower quality than those produced using the previous method. Significant defects in both the size and shape of the individual features are present in the newly created pattern, as can be seen in Figure 6.
The most likely cause of these defects is air trapped within the system, which cannot escape once the silicone fully covers the surface. At this point the silicone does not fully cover the microparticles and as such the features in the created pattern are not an exact match to shapes of the original microparticles. Therefore, later experiments will continue to mix microparticles into silicone before curing.

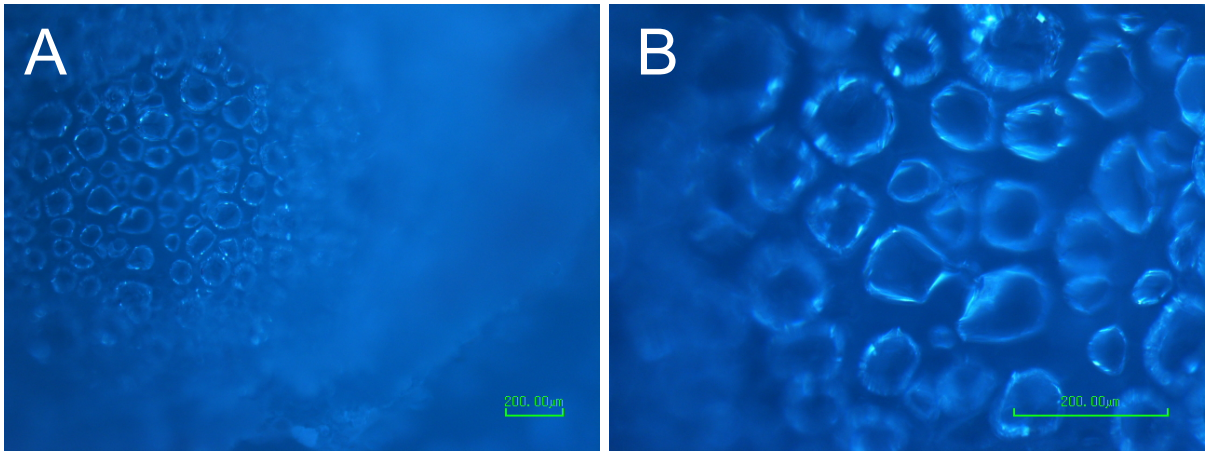

Figure 6: Microscopy images of the silicone pattern showing overall structure (A) and details at higher magnification (B). Both images are the same sample surface, initially created using unmixed microparticles covered with silicone. Both scale bars are 200 µm.

2.3.4. Solvent- and oven-based pattern transfer process development

The currently developed method allows for the creation of silicone surfaces with micrometre-scale patterning. To create more robust, multiple-use patterns, the created silicone patterns need to be transferred to a different material to avoid degradation and potential release of the polystyrene microparticles embedded within the material.

Therefore, various methods are investigated for transferring the pattern, into solid polystyrene (using solvent and oven-based methods), or into silicone.

For the solvent-based polystyrene method, polystyrene pellets are dissolved in acetone at 0.25 g/mL in a ducted fume hood, to a total volume of 10 mL (2.5 g polystyrene). The mixture is poured onto the previously created silicone pattern, and additional Acetone is manually added to the material every 5 minutes for a total of 1 hour to keep the polystyrene fully dissolved until any remaining air bubbles are eliminated from the acetone-surface interface. Once the mixture is allowed to fully cover the pattern without leaving any air bubbles, the acetone present in the solution is left to evaporate over 3-7 days. After solidifying, the polystyrene is collected and evaluated using optical microscopy.

For the oven-based polystyrene method, the patterned surface is covered with polystyrene pellets and heated to 200 degrees Celsius in an oven. Temperature is maintained for 15 minutes, allowing the polystyrene to melt and flow into the features of the pattern.

Once the polystyrene has fully melted and covered the silicone, the material is removed from the oven and allowed to cool. The silicone and polystyrene are gently separated to avoid damage to the pattern, and the polystyrene is imaged using optical microscopy.

For the silicone-to-silicone method, the piece of silicone containing the original pattern is coated in uncured silicone mix which is allowed to cure overnight. After curing, a small incision is made at the interface between the two silicone pieces to facilitate separation, after which the two silicone segments are gently pulled apart to reveal the new pattern. The new pattern is analysed using optical microscopy.

2.3.4.1. Results

The solvent-based process for transferring the created patterns to solid polystyrene was not successful. While the surface of the polystyrene solidified as expected, a significant amount of acetone remained within the deeper parts of the material. As a consequence, the evaporation of this Acetone caused a very porous structure in the material. Acetone in the deeper layers of the material (approx. 5mm and deeper) did not evaporate even after 7 days, preventing the polystyrene from fully solidifying.

The poor material properties of the created material made analysis highly unreliable, but microscopy analysis of the material was performed on a sample that was recovered intact from the procedure. This sample indicated a pattern was successfully created. See Figure 7 for an example. However, the sample surface was significantly deformed from the expected semi-flat surface that was expected. Based on the fact that a number of the polystyrene microspheres were still present during this process, it is assumed that the pattern found in this sample is a result of these particles being preserved when exposed to Acetone rather than the creation of a single, solid pattern.

The deformation and poor properties of the material makes the created patterns unsuitable for use in later stages of the project regardless of the quality of the patterning that is created. With the additional risk of the pores created by the Acetone interfering with the created patterns, this method will not be used for later work.

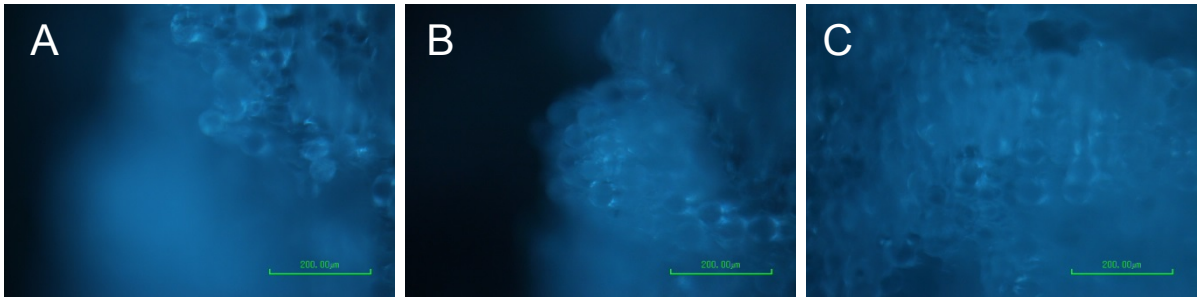

Figure 7: examples of patterning created in polystyrene using the Acetone-based method with 50 µm diameter microparticles. All images are taken from different locations of a single sample pattern. While some patterning is clearly visible, the surface of the material no longer has an even surface with features, as indicated by the large areas of the image that are out of focus, especially in images A and B. All scale bars are 200 µm.

The original pattern created using the polystyrene microparticles was successfully copied into a polystyrene mould using the oven-based method. Some defects in the polystyrene pattern are still present. Visual inspection of the polystyrene mould indicated a large number of air bubbles within the polystyrene. An example of the silicone-polystyrene setup, including air bubbles after use of the oven, is shown in Figure 8.

It is thought the presence of air between the silicone pattern and the polystyrene pellets causes air bubbles to be trapped between the two materials. These bubbles prevent molten polystyrene from occupying this space, resulting in flat area defects in the copied pattern. To improve the quality of the process, these air bubbles will need to be removed. Microscopy images of polystyrene with a copied pattern, including defects, are shown in Figure 9.

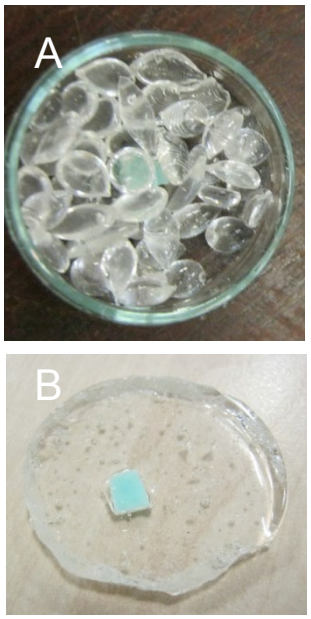

Figure 8: patterned silicone (green) with polystyrene (transparent) before (A) and after (B) the oven-based melting process. The glass petri dish has a diameter of 3cm.

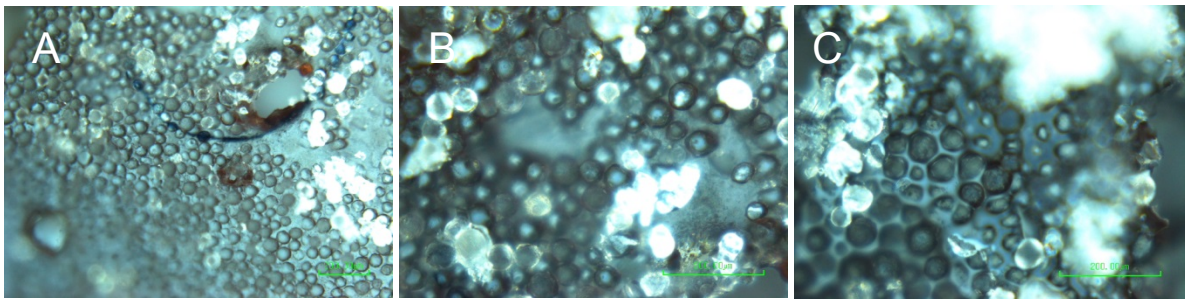

Figure 9: patterned polystyrene following the oven-based pattern transfer method. Some defects are present (including smooth, un-patterned areas and clumps of trapped particles such as on the right side of image A and the centre of image B, but at substantially reduced level compared to earlier silicone methods. The scale bar is 200 µm, original microparticle diameter is 50 µm. Images A, B and C are different locations on a single sample pattern.

The original silicone and microparticle pattern was successfully copied into a second piece of silicone to form a negative of the original pattern. However, large defects in the copied pattern are visible. While the two silicone pieces can be separated successfully after curing, the two pieces still stick to each other with sufficient strength to cause damage to the pattern.

The copied pattern is considered too damaged for use in later stages of the project, and no direct silicone to silicone pattern transfers will be used. However, alternate materials and techniques may still be considered for the transfer of the created patterns.

Microscopy images of the pattern transferred into silicone are shown in Figure 10.

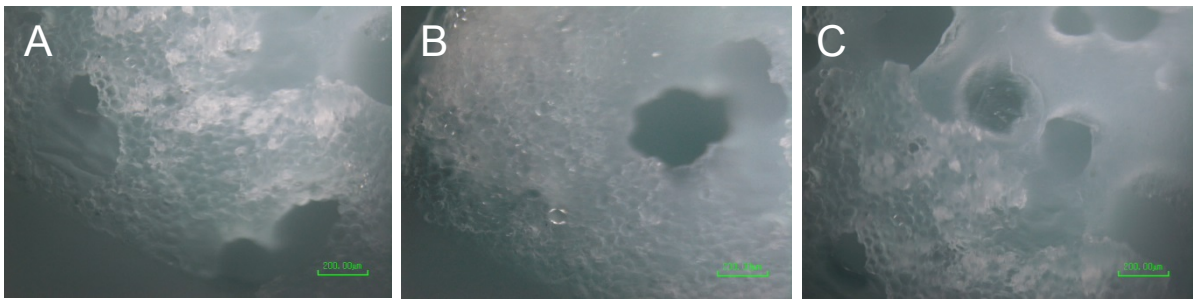

Figure 10: Microscopy images of the patterns copied from silicone to silicone. The copied pattern is clearly visible alongside defects. Dark gaps such as those in the lower right corner of image A and the centre of image B indicate the presence of holes, likely caused by air bubbles. Smooth areas such as the centre right of image C show a lack of patterning where the new silicone was not in contact with the existing pattern. All images are taken at different locations of a single sample pattern. The scale bar is 200 µm; original microparticle diameter is 50 µm.

2.3.5. Application of vacuum during oven-based pattern transfer

Further improvements to the patterning and transfer process allow for the creation of larger numbers of patterned polystyrene surfaces, however defects due to trapped air remain a problem. To prevent formation of air bubbles between the silicone and polystyrene, a vacuum oven (Technico TEC-240-010S) is used to remove all air from the system before the polystyrene is heated. The microparticles themselves are not removed prior to this process, both to prevent any defects due to traces of solvent remaining at the pattern interface, and because any particles present at the surface will melt and fuse with the added polystyrene.

The oven-based process used to transfer the pattern into polystyrene is repeated, with the change that the entire setup is placed under vacuum (<100 mBar remaining pressure). The vacuum oven heats the polystyrene to 200 degrees Celsius for 15

minutes (two hours total time including warm-up) to ensure the polystyrene becomes sufficiently liquid to flow into the silicone pattern.

The process is applied to microparticles with a diameter of 50 µm as before, as well as microparticles with a diameter of 20 µm to gain further insight into potential risks of defects due to smaller feature sizes, such as the polystyrene not properly filling the smaller patterns.

Because the polystyrene flows over the silicone surface, even upwards against gravity, the resulting pattern consists of a very thin layer of polystyrene. To create a thicker polystyrene construct without introducing defects in the pattern, this method is combined with heating in a standard furnace to add additional bulk to the polystyrene layer. This way, the pattern retains the intended quality from using the vacuum oven, while also having the resilience of the original oven-based method.

The created pattern is moved from the vacuum oven straight into a furnace (Carbolite BWF 1100 Muffle Furnace). Additional polystyrene is added to provide sufficient material, and the entire setup is heated to 200 degrees Celsius for 15 minutes.

After cooling the material the polystyrene and silicone segments are separated. The original silicone piece can be re-used to create additional polystyrene moulds, while the new patterned polystyrene is used for the future steps in the process. A schematic overview of the process is shown in Figure 11.

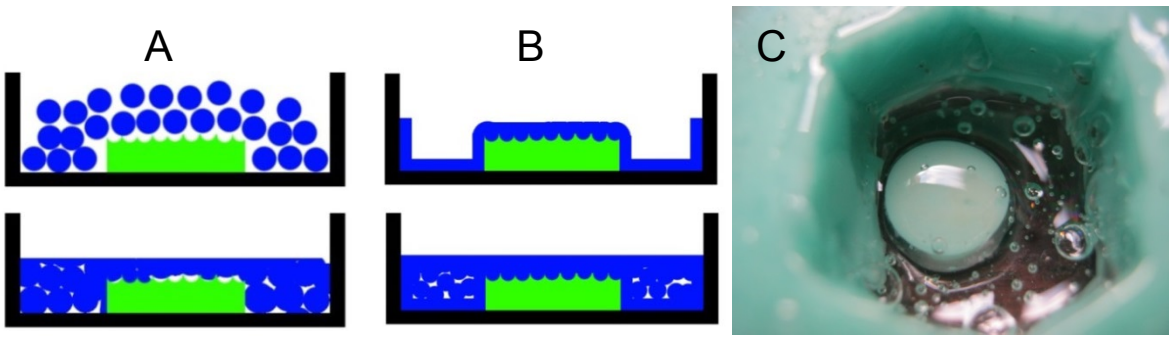

Figure 11: Schematic representation of the single oven process with surface defects (A), the vacuum-based process without surface defects but with possible air bubbles in the bulk of the material (B), and an example of the polystyrene pattern prior to the second stage of the process (C).

2.3.5.1. Results

The initial microparticle-silicone surface was successfully copied to a solid polystyrene material using both 50 and 20 µm patterns. The copied pattern showed

no indications of damage, defects or air bubbles like the surfaces created without applying a vacuum. Microscopy images of the copied 50 µm pattern after the vacuum process are shown in Figure 12. The created patterns following polystyrene reinforcement in the furnace and removal from the silicone are shown in Figure 13. Some fragments of the microparticle-silicone mixture remained on the pattern surface, indicating potential degradation of the original pattern and release of the embedded microparticles. For future experiments, all surfaces will be washed before further use.

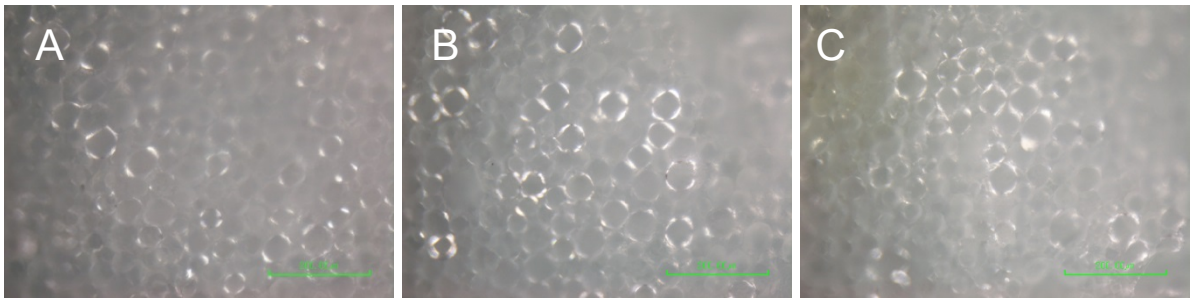

Figure 12: Microscopy images of the polystyrene pattern. Note that these images are taken while the polystyrene and the silicone materials are still in contact; the polystyrene itself is transparent. Images A, B and C are taken from three different samples. The scale bar in all images is 200 µm.

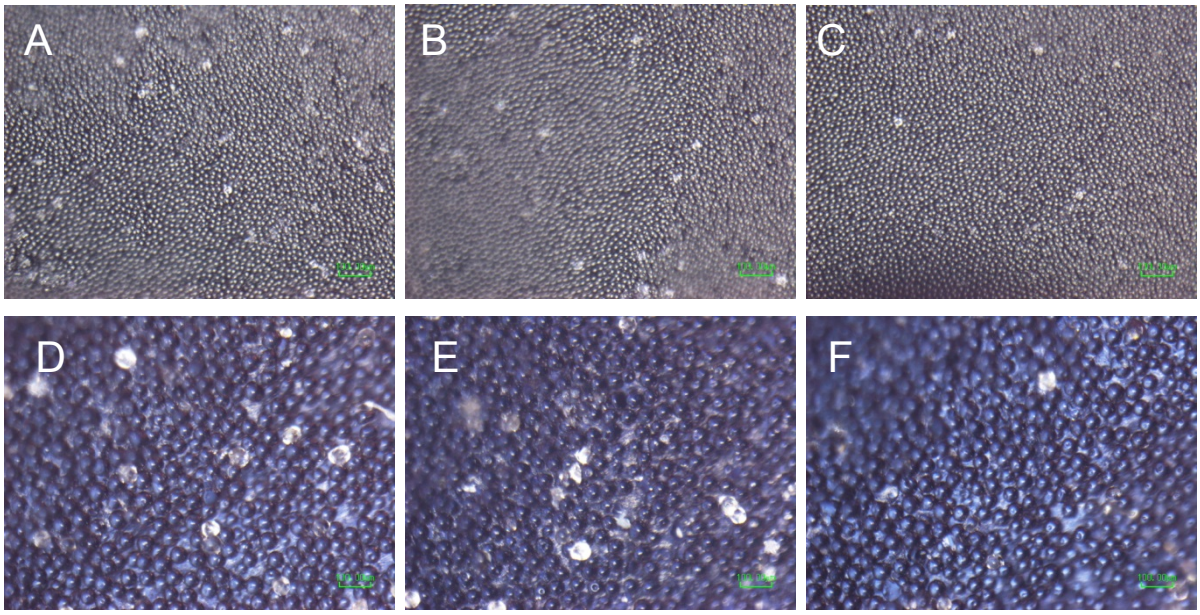

Figure 13: microscopy images of patterned polystyrene created from microparticles with a diameter of 20 µm (A, B, C) and 50 µm (D, E, F) using the vacuum oven. The white fragments are remnants of the microparticle-silicone material. Images A, B, C, D, E and F are taken from six different samples. All scale bars are 100 µm.

2.3.6. Creation of Poly (ethylene glycol) diacrylate pattern surfaces

Patterned polystyrene and silicone surface moulds have been successfully created using the vacuum oven-based method. As the planned cell culture experiments will take place on Poly (ethylene glycol) for its expected advantages in terms of non-

specific adsorption and protein immobilization, the next step is to transfer these created patterns from the existing moulds onto new Poly (ethylene glycol) patterns.

New patterned polystyrene surfaces are created with feature sizes of 1 μm, similar to the process described previously. Previously created polystyrene surfaces with features of 20 and 50 μm are re-used for this experiment. Surfaces are thoroughly cleaned using water and industrial methylated spirit to remove any remaining microparticle-silicone fragments that may be present on the surface.

A 75% w/w Poly Ethylene Glycol (PEGDA) in water mixture is prepared, with 2% w/v DMPA as a photo-initiator. The mixture is vortexed for 10 seconds and the DMPA is allowed to fully dissolve into the water and PEGDA at room temperature for 30 minutes while protected from external light.

The prepared PEGDA mixture is slowly poured onto the created patterned polystyrene surfaces. The polystyrene moulds are gently tapped to remove any air bubbles that may be trapped at the interface between the polystyrene and PEGDA. The PEGDA is only added to a layer of at most 2 mm thick to ensure sufficient UV penetration through the material.

Once the PEGDA is in place, the liquid is polymerized to create the new pattern. A portable UV lamp was used to expose the liquid to 254 mm UV light for 60 minutes, at an exposure level of approx. 100 μW/cm^2.

Upon polymerization, the material will form a cell culture surface composed primarily of crosslinked Poly Ethylene Glycol, with a minor portion of the material composed of the crosslinking chains. When the PEGDA is fully polymerized, the new pattern is removed from the polystyrene mould and analysed using optical microscopy.

2.3.6.1. Results

Patterned surfaces were successfully created using Poly (ethylene glycol) diacrylate. 50 μm and 20 μm scale patterns were created without major defects in the pattern, as shown in Figure 14. However, 20 μm patterns do show an increased chance for pattern defects as shown in Figure 15.

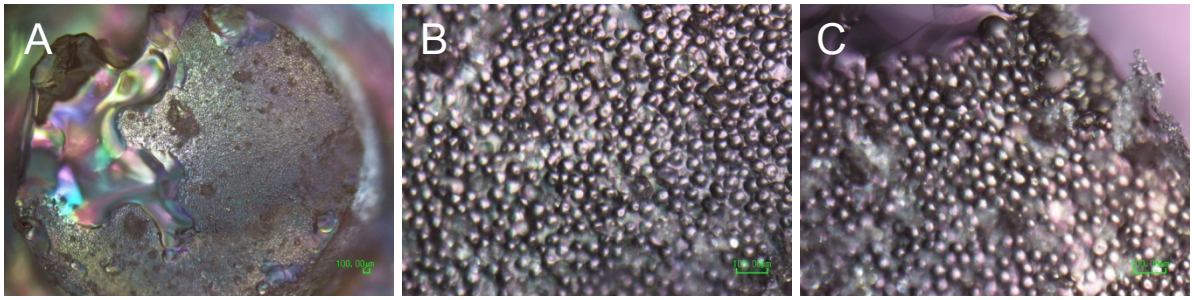

Figure 14: patterned surfaces created in PEGDA after UV exposure. Original microparticle size is 50 µm. The upper left of image A shows how part of the material has broken off, images B and C show the created pattern at higher magnification. All images show the same sample pattern. All scale bars are 100 µm.

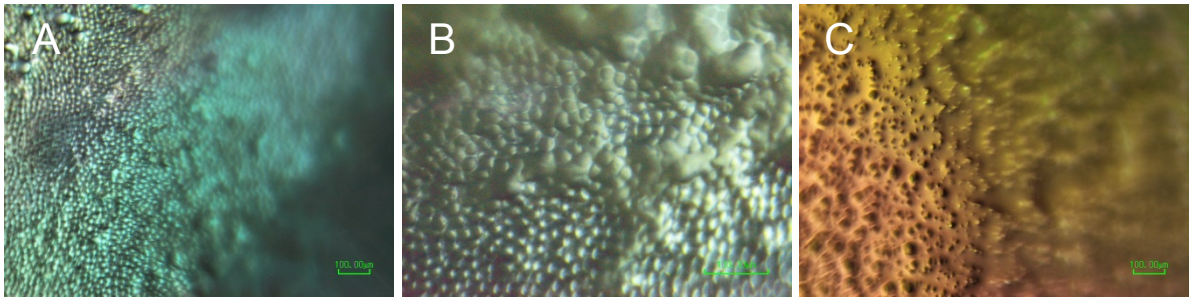

Figure 15: patterned surfaces created in PEGDA after UV exposure. Original microparticle size is 20 µm. Image A shows a high-quality pattern. Image B shows the same pattern, zoomed in to show a handful of defects in more detail. Image C shows a low-quality pattern (too smooth surface without suitable patterning). Images A, B and C are taken from three different patterns. All scale bars are 100 µm.

1 µm scale patterns were created but a significant fraction of the resulting surface showed defects in the pattern as see in Figure 16. Furthermore, the size of the features in the 1 µm pattern is too small to effectively analyse with the current optical microscopy method. The 1 µm patterns will be considered unsuitable until further analysis is performed.

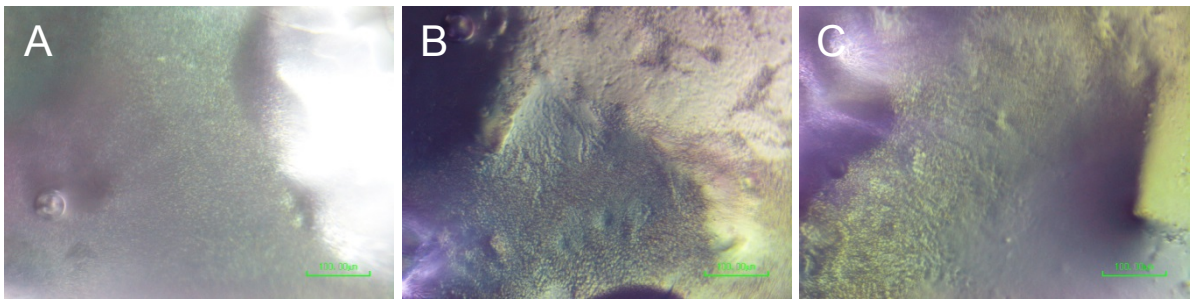

Figure 16: patterned surfaces created in PEGDA after UV exposure. Original microparticle size is 1 µm. Some patterning can be seen such as in the lower centre of image B, but large areas of smooth, un-patterned material are also present, visible as smooth, white-ish areas such as in the top right of image B. Images A, B and C are taken from three different patterns. All scale bars are 100 µm.

Finally, separating the PEGDA surface from the polystyrene mould proved difficult due to the design of the polystyrene mould. At times, the PEGDA would fracture, resulting in the loss of part of the pattern as can be seen in Figure 14a. This is

primarily due to the rigid nature of the polystyrene mould used to create the new pattern, but improvements to the mould may be possible.

2.3.7. Contamination risk evaluation in the polymerization process

The current method for creating patterned PEGDA based surfaces shows good results in terms of creating the necessary pattern structure. However, the final goal of this process is to create a patterned surface suitable for cell culture. Infections and contaminations are a significant risk to cell culture experiments. The UV light used to polymerize the PEGDA monomers has a sterilizing effect[230], but it is not known if this effect sufficiently reduces contamination risk for is sufficient to fully sterilize the used materials.

Therefore, it is necessary to determine if additional sterilization is required before the current PEGDA surfaces are suitable for cell culture. A new series of PEGDA based surfaces is created using the same materials and process explained previously, with some modifications to the process.

First, a 75% w/w PEGDA in water solution is prepared and left opened. An air flow is directed straight onto the solution using the fume hood, such that the solution is exposed to significantly more micro-organisms than during normal processing in the lab.

After one hour, 2% w/v DMPA is mixed into the solution, and the unpolymerized mixture is added to a number of wells in a 96 well plate.
The well plate with the unpolymerized mixture is placed in a sterilized air-tight container. The container is sealed, and the PEGDA is polymerized by UV exposure as described before.

All further handling of the PEG-based surfaces takes place in Biological Safety Cabinets that have been sterilized before use, and the outside of the (sealed) container is sterilized when it is placed in the cabinet.

Nutrient broth is prepared and sterilized by autoclaving. The sterile broth is added to the PEG-based surfaces as a culture media, and the 96 well plate is placed in an incubator for one week such that any potential infections have the opportunity to grow.

After one week, the well plate is removed from the incubator and inspected for any signs of infection using microscopy.

2.3.7.1. Results

No signs of infection were found in the well plates after incubation. Microscopy inspection showed no microbial or fungal contaminations. Furthermore, neither the culture media nor the PEG-based surfaces themselves showed any sign of contamination in the form of colour changes or smell.

For future experiments, it is assumed that the UV exposure combined with the processing methods currently used sufficiently reduces the contamination risks of the cell culture environment for further experiments. No modifications to the current methods are implemented, but all experiments will be regularly checked to identify any contamination. If contamination is found in future experiments, additional steps may be taken to further reduce risk of contamination.

2.3.8. Increased pattern size and reduction of process risks through the use of silicone moulds

During the previous experiments a number of potential problems were identified. It was determined that while the patterning created on PEG surfaces can be successfully transferred, collecting the rigid patterns from the moulds posed significant problems.

The current shape of the polystyrene mould requires a significant amount of force to release the PEG surface. Combined with the lack of easy leverage points, applying this force may cause damage to the PEG surface.

To solve this problem and make the process more suitable for use with other material types, a new system of mould designs is implemented to improve the ease of access to the patterned materials, be they Polystyrene, PEG, or other materials used during later parts of the project.

As a proof-of-concept, a negative mould of a 96 well late is made by filling the well plate with play-dough clay (Hasbro, Inc.), using plastic film to allow for easier extraction from the well plate. The clay form is taken out of the well plate, and silicone mix (similar to that used for creating the initial micro-scale patterns) is

poured onto the material. After curing overnight, the newly created silicone form can substitute for the rigid materials used before. An overview of the new design is given in Figure 17.

The vacuum-based process to copy the micro-scale patterns from silicone into polystyrene is performed as described previously, but the process is adjusted to include the new ‘plate’. The microparticle-silicone patterns are placed inside the plate and polystyrene pellets are added into the well. The entire setup is placed in a vacuum oven and heated to 200 degrees Celsius while under a <100 mBar vacuum, for two hours total.

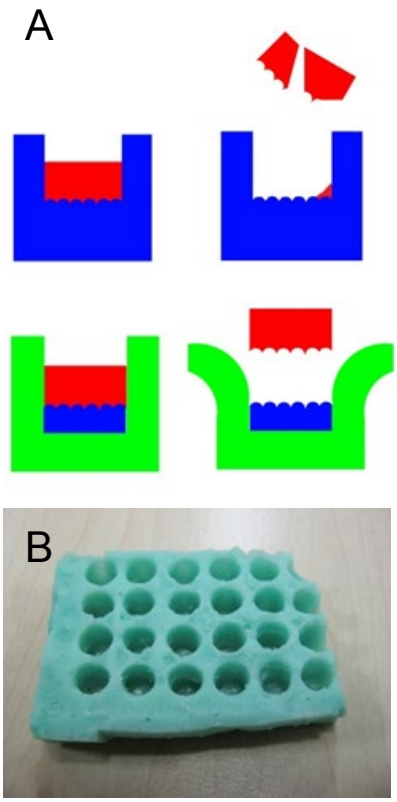

Figure 17: schematic representation of the use of the new silicone moulds compared to previous solid polystyrene moulds (A) and example of a created silicone mould (B)

Once the initial vacuum-sealed layer is completed, additional polystyrene is added under atmospheric conditions to improve the strength of the created polystyrene pattern. Additional polystyrene pellets are added to the mould, and the material is treated at 200 degrees Celsius for 15 minutes before being allowed to cool to room temperature over approximately an hour.

After cooling, removal of the polystyrene patterns is tested and created patterns are analysed with optical microscopy to identify any damage to the material.

In addition to the above changes, alternate surface sizes are also tested. The initial process was developed using 96-well plates in part to reduce to total amount of materials needed to create a specific pattern. While this is suitable for testing the process and evaluating the created patterns, it does cause problems with later parts of the project where cell culture is included. As the total surface area of each material is a major limitation for the amount of cells that can be cultured in a single sample, the use of larger surface areas for each pattern will allow for larger numbers of cells. This in turn will increase the cells in each sample that are available for analysis, allowing for more robust measurements.

Therefore, the patterning and vacuum-based transfer processes are tested for use with 24-well plates in order to identify any new problems related to the larger surface area, using the same steps described previously.

2.3.8.1. Results

Patterned Polystyrene moulds were successfully created with the new silicone based process, with reduced risk of damage due to manual handling. No adverse consequences were encountered during any part of the process while creating 15 new patterns in 96-well plate size, as shown in Figure 18.

Figure 18: Created 96-well plate sized polystyrene patterns prior to separation (A), after separation (B) and a created 50 µm pattern under microscope view (C). The scale bar in image C is 100 µm.

Larger-scale patterns were successfully created in a 24-well plate. However, the pattern itself was not created as a flat surface. Due to the larger surface area, the additional silicone poured into the well caused defects by displacing the already present microparticle-silicone mixture as shown in Figure 19.

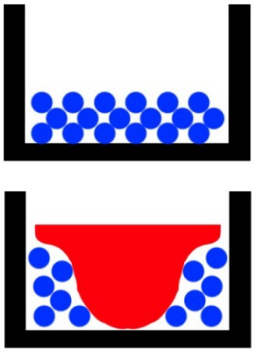

Figure 19: schematic representation of defects caused by displacement of particles during the addition of uncured silicone.

To prevent uneven spacing of the microparticles, an excess of particles is mixed into the initial amount of silicone, leaving a small amount of air trapped both within the mixture and between the mixture and the bottom of the well plate. Pouring additional silicone into a 96-well plate does not leave enough room for major horizontal flow patterns in the silicone, but such flow is possible in a 24-well plate.

Consequently, as shown in Figure 20, a pattern is created on an uneven surface, with the final geometry depending on the displacement of the original microparticle-silicone mixture and the movement of air pockets trapped within the well. Although the surface itself does show a high-quality pattern, the larger scale geometry means

these surfaces are not suitable for the planned work beyond proof of concept experiments.

Figure 20: Examples of a larger created silicone pattern with defect caused by an air bubble (A), a larger silicone pattern created using microparticle-silicone mix to form the surface (B), and a created (uneven) 50 µm pattern under microscope view (C), showing a functional but uneven pattern. The scale bar in image C is 100 µm.

Further experiments using this procedure will require modifications to ensure an even distribution of the microparticle-silicone mixture. Manually packing the pattern before the addition of more silicone, increasing the total volume of the mixture used to create each pattern, adding the extra silicone in such a way to minimize disruption of the existing layers, applying a vacuum to prevent air bubble formation, and allowing the silicone to partially cure before adding more uncured silicone will all be considered.

However, the current (flawed) patterns created during these experiments will still be used to further develop later stages in the project, as this geometry may be useful in identifying process flaws that might not be readily visible on an evenly distributed pattern.

2.3.9. Adaptation of the patterning process for Polycaprolactone and Polystyrene cell culture surfaces

Based on further experiments with Poly (Ethylene Glycol) based materials (see chapter 3 for details), the use of alternative materials for the patterned cell culture surfaces was required.

Reviewing published literature for alternatives, (see chapter 1 for details), Polycaprolactone and Polystyrene were selected as additional cell culture materials to explore further options suitable for the project. The process used for creating the Polystyrene patterns described previously in section 2.3.5 can be used to create the required patterned cell culture surfaces without the need for extensive modifications.

However, additional experiments are needed to test the use of Polycaprolactone, with the process adapted from that used to treat Polystyrene.

Polycaprolactone (Mn ≈ 80,000, Sigma Aldrich) pellets are added to a previously created 50 µm pattern silicone mould. The material is heated to 150°C under vacuum for a total of 1.5 hours, in order to ensure the polymer fully melts into the desired pattern. The material is allowed to cool down without removal from the silicone mould before further analysis, to prevent warping of the created pattern.

To maintain sterility of the material for use in cell culture experiments, the created patterns are sterilized using an autoclave, and evaluated after sterilization for pattern integrity and the presence of defects.

2.3.9.1. Results

Polycaprolactone was successfully patterned using the vacuum oven process initially developed for use with Polystyrene and silicone. Example patterns are shown in Figure 21.

Some potential problems were identified during the process. Unlike Polystyrene, the Polycaprolactone used during the process remains highly viscous at higher temperatures. Consequently, Polycaprolactone has a substantially greater risk of entrapped air bubbles and defects. As such, the main priority during the process is to ensure the entire surface is covered by Polycaprolactone before the atmospheric pressure is restored. This way, the air pressure on the material will make it deform onto the pattern without air being allowed in between the surfaces to cause defects. Once there is an air-tight seal between the Polycaprolactone and silicone, additional Polycaprolactone can be added

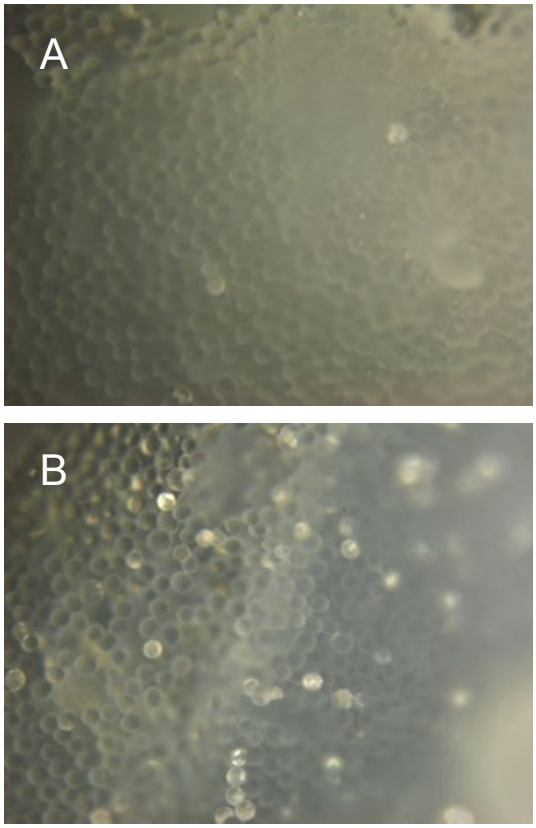

Figure 21: examples of 50 µm Polycaprolactone patterns created under vacuum from a patterned silicone mould. Image A and B are taken from two different samples.

to the well (optionally by applying additional pressure) without risking the pattern.

Autoclaving Polycaprolactone proved effective, without damaging the created patterns. However, because the autoclave temperature is higher than the melting temperature of the material, the surfaces can only be sterilized this way before they are removed from the silicone pattern. Furthermore, care must be taken that water condensation can't pool in any of the wells, since this may cause large-scale defects in the material. The materials must be covered, possibly with foil, to prevent water damage from pooling while still allowing the steam to reach the material.

For future experiments, the material will be sterilized without the use of an autoclave, relying instead on the applied heat and vacuum in the vacuum oven.

2.4. Discussion

A method for the creation of Poly (Ethylene Glycol)-based surfaces with micrometre-scale features from the initial PEGDA monomer solution was developed in this chapter. The process proved to be suitably robust, with patterning being created successfully even in sub-optimal conditions as seen in 2.3.6 and 2.3.8. The process itself is comparatively simple, allowing for straight-forward scale-up or modification to expand the process.

Polystyrene microparticles were chosen for their robust characteristics and comparatively straight-forward processing. Using the same material for both the microparticles and the first copied pattern reduces the risks of contamination, and while Acetone proved unsuitable for use during these experiments, melting the Polystyrene allowed for effective pattern transfer without the need to remove exposed particles from the pattern surface. The use of other materials without major risk of contamination with Polystyrene becomes possible after at least one polymer surface has been created.

The patterning created using the developed method is comparatively simple, a uniformly convex shape. While the creation of anisotropic features may be possible by applying strain onto the created patterns during transfer to a new material, this process is otherwise difficult to modify for different types of features.

Other research commonly employs more advanced features such as pillars or struts[215,216], grooves[224], or more angular pockets[226]. Complex interactions between the surface topology and cultured cells, such as combinations of smaller and large feature sizes, surface gradients or localized depositions of growth factors on the surface are beyond the scope of this project. Instead, the currently developed technique is aimed at creating a robust proof-of-concept for enhancing the effectiveness of immobilized proteins, focusing on practical implementation over investigation of any underlying cellular processes.

Currently, the largest risk during the patterning process is the creation of the initial pattern by embedding microparticles in silicone. All other surfaces can be mass-produced by repeatedly copying the pattern, but the first pattern can only be created once.

As a consequence, the steps in the process that rely on copying the existing patterns into solid silicone still have a small risk of introducing defects from an imperfect surface interface, trapped air bubbles, etc. This does not appear to be a major problem at this point in the project, but it may result in difficulties when smaller feature sizes are being created. For further experiments, adding the uncured silicone mixture in a vacuum may be considered.

Finally, one of the main limitations of the developed process is the reliance on adherent cell culture. Current research increasingly focuses on 3D cell culture to create functionalized hydrogels and injectable scaffolds for therapies[231,232], limiting the usefulness of this method for developing improvements to clinically relevant methods. However, there is also an increasing amount of research focusing on the use of suspended micro-carriers to combine the benefits of both adherent and suspension-based cell culture[233]. Any insights into surface topology gained from this work would be highly relevant to these types of processes, although some work may be necessary to translate the advantages (if any) of the experiments during this project to work with micro-carriers rather than surfaces.

Chapter 3: Creation of microparticles for protein immobilization analysis

3.1. Introduction

This project focuses on the interaction between patterned cell culture surfaces and immobilized growth factors on these surfaces in the context of cell culture. Consequently, quantifying the amount of growth factors available to the cells in culture would improve the understanding of the cellular environment and enable a more precise evaluation of protein influence. To this end, it is necessary to determine how much growth factor is present at the surface and how much is immobilized at inaccessible sites deeper in the material. In this chapter a method for quantifying protein immobilization onto Poly (Ethylene Glycol) microparticles using Flow Cytometry was tested.

Analysing solid surfaces with immobilized proteins presents a number of unique challenges; depending on surface characteristics conventional cell culture techniques and analysis methods may not be suitable. Many analysis techniques used in biomedical research rely on measuring protein solutions (such as infrared or UV spectroscopy, NMR or mass spectrometry) or liquid suspensions (such as flow cytometry or bead-based ELISA assays), none of which can be used on solid surfaces. Certain optical techniques can be modified to operate on surface-bound proteins instead of solutions, though such methods do require precise controls to allow for qualitative instead of quantitative measurements[234]. The quality of references and controls has a profound impact on such methods[235], and more accurate methods may require equipment or chemicals which were deemed too difficult to acquire for this project. For example, proteins labelled with radioactive isotopes could be used for direct quantitative measurement while avoiding measurement errors due to covalently bound fluorescent markers, but would also require a substantial investment in training and use of equipment not currently available to Loughborough University's Center For Biological Engineering, as well as the purchase of these radiological compounds.

A further issue is that published research into immobilized proteins frequently only describes the total concentration of protein in the material[20,95,97,133,236–238]. While such descriptions can be useful for cell culture experiments where the cells are dispersed throughout the material (such as in cell-seeded hydrogels), without looking at the

actual proteins that are made available on the surface of the material this information is difficult to use for comparisons to surface-bound proteins.
Rather than focusing on these methods and attempt to measure protein absorption on the surfaces directly, a different approach was chosen.
This chapter focuses on the creation and analysis of microparticles meant as an alternative for the cell culture surfaces to be used during later parts of the project.

These particles can be analysed with Flow Cytometry such that, when combined with the particles' size and chemical properties, they should give a quantifiable measure of proteins per surface area on the created surface. A particle-based approach is expected to be more robust than surface-based measurements such as ELISA due to eliminating biases caused by complex surface topology; surfaces with complex topology and/or unknown roughness will require an estimation of total surface area compared to sample surface area that is not currently available for this project's samples.

Various methods for the creation of polymer microparticles are available, with the most common methods using microfluidics- or emulsion-based processes[123,239–243].

Membrane emulsification was chosen as the process for this project, due to the greater ease at setting up the necessary equipment compared to microfluidics. In addition, membrane emulsification is already under investigation at Loughborough University, allowing for easier access to instruction and experimental support.

Most literature focusing on functionalized particles aims at creating such particles as temporary carriers, meant to release bound proteins through diffusion or degradation of the polymer[111,244–247]. Other work focuses on creating porous microparticles for various purposes including internalized and surface cell culture[239,248–251].

Consequently, little data is available on using microparticles for permanent protein immobilization. While this lack of comparisons may make interpretation more difficult, this is not considered sufficiently problematic to require a different method and may indeed be a net positive due to the novelty value.

In this chapter, the initial process for creating microparticles in the 5-20 µm range is developed and adjusted for use with UV-based polymerization. Following the

successful creation of microparticles, particles that include covalently bound Streptavidin are created.

Following the creation of the Streptavidin-functionalized particles, biotinylated markers are used to enable the analysis of these particles using Flow Cytometry, and the process is evaluated and adjusted to deal with possible measurement errors including non-specific binding and temperature dependence.

3.2. Aim and goals

The aim of this part of the project is to measure the amount of protein that can be (specifically) bound onto a cell culture surface of a defined total area. In order to acquire this information through the analysis of functionalized microparticles, the following goals need to be reached:

- Create Poly (Ethylene Glycol)-based microparticles of approximately 5-10 µm diameter
- Functionalize these particles with Streptavidin to ensure these particles have similar potential for immobilizing relevant proteins as the planned cell culture surfaces
- Determine specific (Biotin-Streptavidin) binding and non-specific (adsorption onto the particle's polymer surface) binding of biotinylated proteins
- Determine the ratio of accessible Streptavidin at the surface of the created particles compared to the total Streptavidin content

3.3. Materials and methods

3.3.1. Materials

Poly (ethylene glycol) diacrylate, 2,2-Dimethoxy-2-phenylacetophenone and Acrylate Poly(Ethylene Glycol)-N-hydroxysuccinimide were purchased from JenKem Technologies Co. Ltd.

Biocytin-Alexa Fluor 488 and biotin-R-Phycoerythrin) were purchased from Thermo Fischer Scientific, Inc.

Quantum Alexa Fluor 488 MESF and Quantum R-Phycoerythrin MESF were purchased from Stratetch Scientific, Ltd.

Water-soluble blue food dye was purchased from TESCO Stores, Ltd.

Unless otherwise specified, all other chemicals were purchased from Sigma Aldrich, Inc.

The membrane emulsification setup used is a Micropore Technologies Ltd (Derbys, UK) Dispersion Cell, equipped with a hydrophobic steel disk membrane with uniformly placed 10 μm diameter pores. Exact shear stress and rpm values were not calculated for these experiments, but are estimated at 200-600 rpm[252,253].

The UV lamp used is a 3UV (8W) handheld lamp from UPV, LLC. The lamp is set to the 254nm wavelength for all experiments.

3.3.2. Preparation of membrane emulsification materials

To create the necessary micrometre-scale particles, a membrane emulsification system is used, wherein a dispersed phase is added dropwise into a continuous phase while stirred to ensure a uniform size distribution of droplets. Before experimental work with membrane emulsification begins, the necessary components of the mixture must be prepared.

The continuous phase is kerosene with 2% v/v Span80 as a surfactant. The continuous phase is created prior to experiments by adding the Span80 into kerosene and stirring the mixture overnight to ensure the two components are fully mixed prior to the start of the membrane emulsification process.

For the initial emulsion tests, the dispersed phase is a solution of 75% w/w PEGDA in water. The dispersed phase is created prior to experiments by adding 25% w/w water to PEGDA, vortexing the mixture for 1 minute and leaving the mixture for at least one hour before the start of the membrane emulsification process to eliminate any air bubbles.

For membrane emulsification experiments with the purpose of creating solid microparticles, 2% w/w DMPA is added to the mixture described for the emulsion tests while keeping all other parameters equal.

For membrane emulsification experiments with the purpose of creating dyed microparticles, an additional 10% v/v food dye is added to the mixture described above for the solid microparticles while keeping all other parameters equal.

The membrane emulsification setup used is a Micropore Technologies Ltd (Derbys, UK) Dispersion Cell, equipped with a hydrophobic steel disk membrane with uniformly placed 10 µm diameter pores. Exact shear stress and rpm values were not calculated for these experiments.

3.3.3. Initial membrane emulsification testing

For the planned flow cytometry measurements, the size of the created particles will have a direct impact on the total amount of fluorophores each particle can bind. Consequently, while the exact diameter of the particles does not have a specific requirement, a narrow size distribution will allow for substantially easier analysis than a broad distribution.

Before creating actual microparticles, the process is performed with varying flow rates and stirring speeds to test the reliability of the process for creating emulsions with sufficiently narrow size distributions. Unlike later steps in the process, the emulsions are not yet polymerized using UV.

Emulsions and microparticles are created using a membrane emulsification setup. Briefly, membrane emulsification works by mixing two immiscible liquids together as one of the liquids is pumped through a porous membrane. The shear from mixing that is applied to the liquid as it flows through the membrane causes the liquid stream to disperse into an emulsion with a homogeneous size distribution.

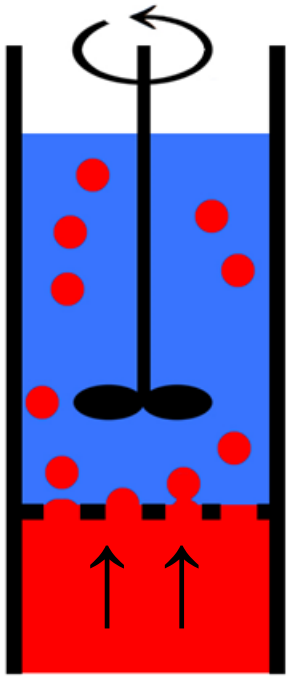

Figure 22: Schematic representation of a membrane emulsification system. The continuous phase (kerosine and Span80) is in blue, the dispersed phase (water, PEGDA and optionally DMPA and coloring) is in red.

Initial parameters for the membrane emulsification are a flow rate of 0.5, and 1 ml/min for the dispersed phase, and a stirring voltage of 12 and 16 Volt. Tests with 5 and 15 mL/min flow rate were also attempted,

but these rates resulted in emulsions with droplet size and density that were judged to be too large to be suitable for further work, and these test runs were therefore not analysed in more detail.

The created emulsions are analysed with a top-down microscope immediately after the end of the emulsification process (< 30s) to provide additional information on the size distribution of the droplets. Exact values for stirring rate, shear stress on droplets or fluid transfer per membrane pore are not calculated as these details are not considered necessary for the project.

Finally, an emulsion created with 16V stirring and 1 ml/min flow rate was analysed at multiple time points to determine the change in droplet size over time. A top-down microscope is used to image the created emulsion immediately after the end of the membrane emulsification process (< 30s), as well as at 2 and 5 minutes afterwards, to compare droplet size, distribution, and coalescence.

A schematic representation of the membrane emulsification process is shown in Figure 22. The membrane emulsification cell and processing equipment are shown in Figure 23.

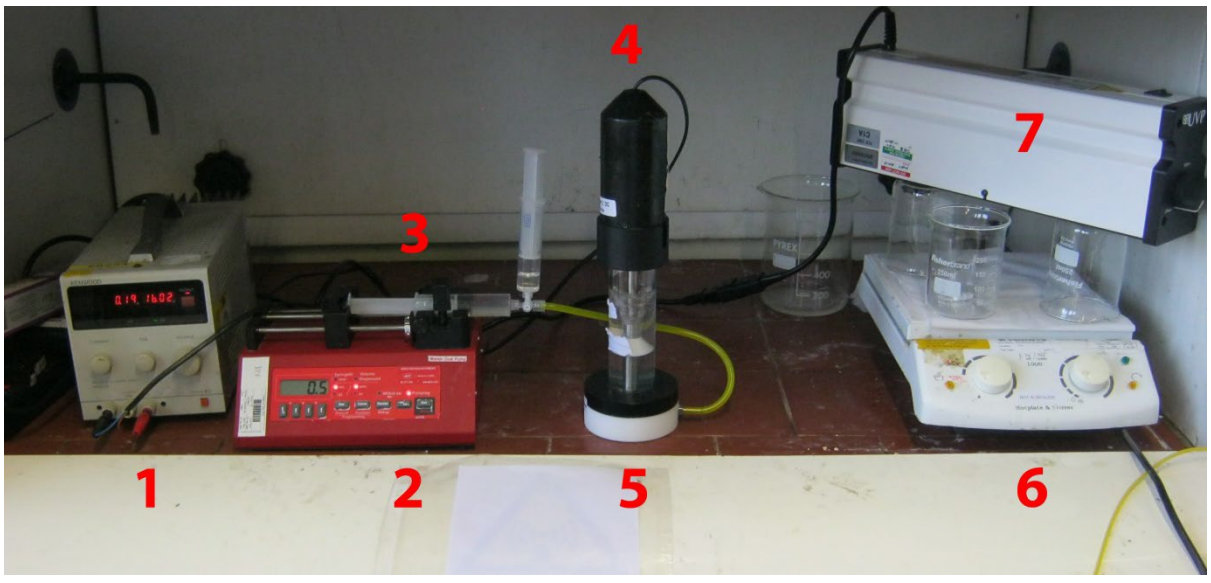

Figure 23: The experimental setup used during the membrane emulsification experiments. Parts are as follows: 1) Power source for the stirrer 2) Pump for the dispersed phase 3) syringe and tubing containing the dispersed phase prior to the experiment 4) stirrer part of the membrane emulsification cell 5) container and membrane of the membrane emulsification cell 6) stir plate used to stir emulsions during UV exposure 7) UV lamp used to polymerize created emulsions

3.3.3.1. Results

The initial membrane emulsification process successfully created an emulsion of PEGDA and water in kerosene. Varying the flow rate with a constant stirring speed resulted in significantly differing emulsions with droplet sizes of approx. 10-200 µm were created, as can be seen in Figure 24.

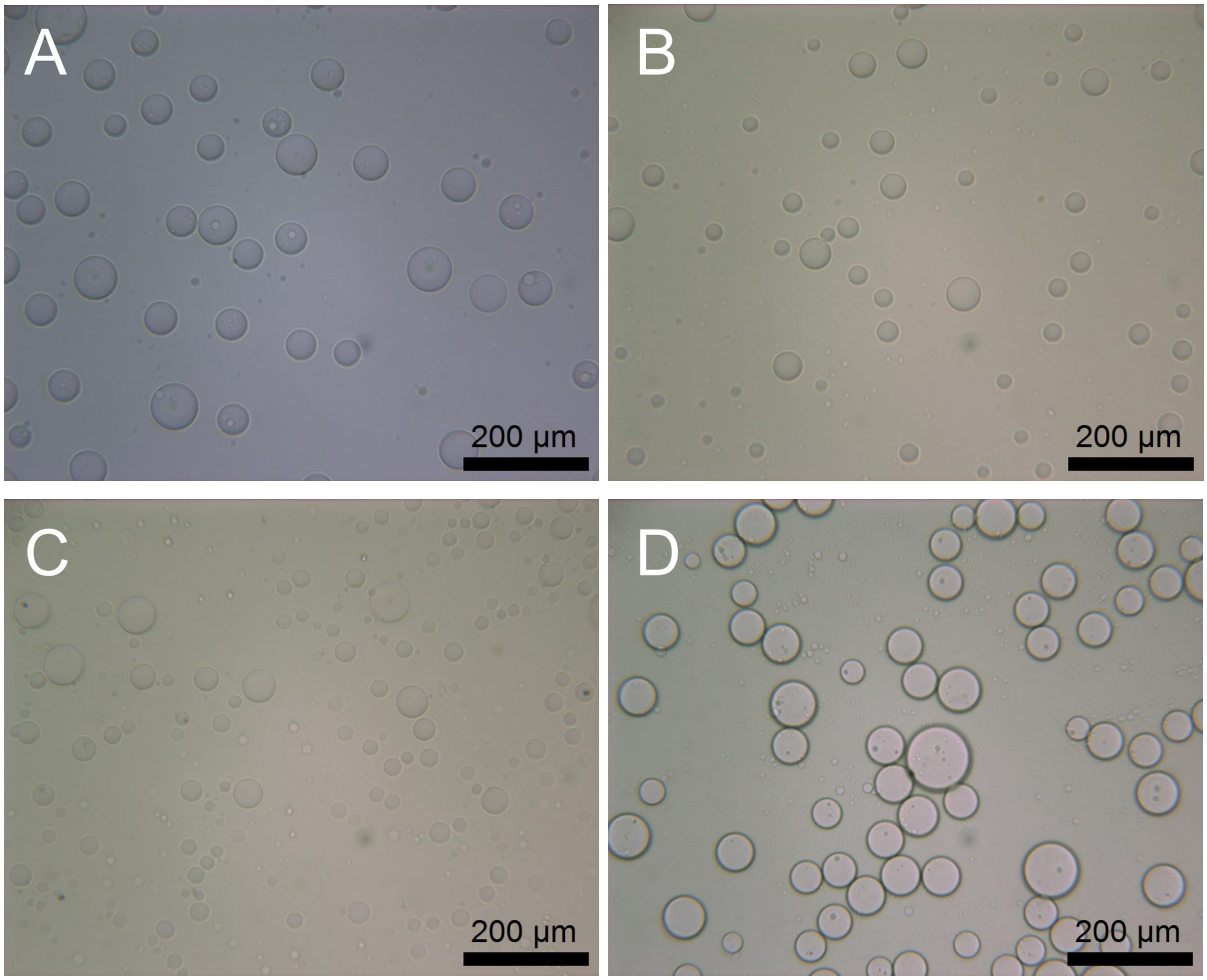

Figure 24: PEGDA+water emulsions in kerosene, created with settings: 12V stirring voltage and 0.5 ml/min flow speed (A), 12V stirring voltage and 1 ml/min flow speed (B), 16V stirring voltage and 0.5 ml/min flow speed (C) and 16V stirring voltage and 1 ml/min flow speed (D).

The emulsion that is measured at multiple time points indicates that coalescence occurs over several minutes once the emulsion is allowed to settle. Coalescence does occur during the membrane emulsification process itself, but only in limited amounts as a large number of small droplets were still present in the emulsion right after the process is completed. The coalescence of the emulsion droplets can be seen in Figure 25. Settling time was minimized for all later experiments to reduce the effects of coalescence.

Based on these measurements, it is determined that the membrane emulsification setup can be used to create an emulsion with a sufficiently reliable size distribution for use in later experiments.

3.3.4. Microparticle fabrication with UV polymerization

Initial tests of the membrane emulsification method allowed for the creation of a water-in-oil emulsion. However, to create usable microparticles, the created droplets must be polymerized while in the emulsion to create solid particles.

For this experiment, the droplet emulsion is created using the same methods described above. In addition to the membrane emulsification setup, a UV lamp is used to expose the created emulsions and polymerize the dispersed phase.

Initial membrane emulsification settings are a flow rate of 0.5 ml/min and a stirring voltage of 16V. After emulsification, the emulsion is transferred to a 250 mL beaker and exposed to UV light (254nm wavelength at approx. 100-500 uW/cm^2, depending on depth) for 15 minutes to polymerize the resulting particles.

Initial analysis of the created microparticles is performed by imaging the particles under an optical

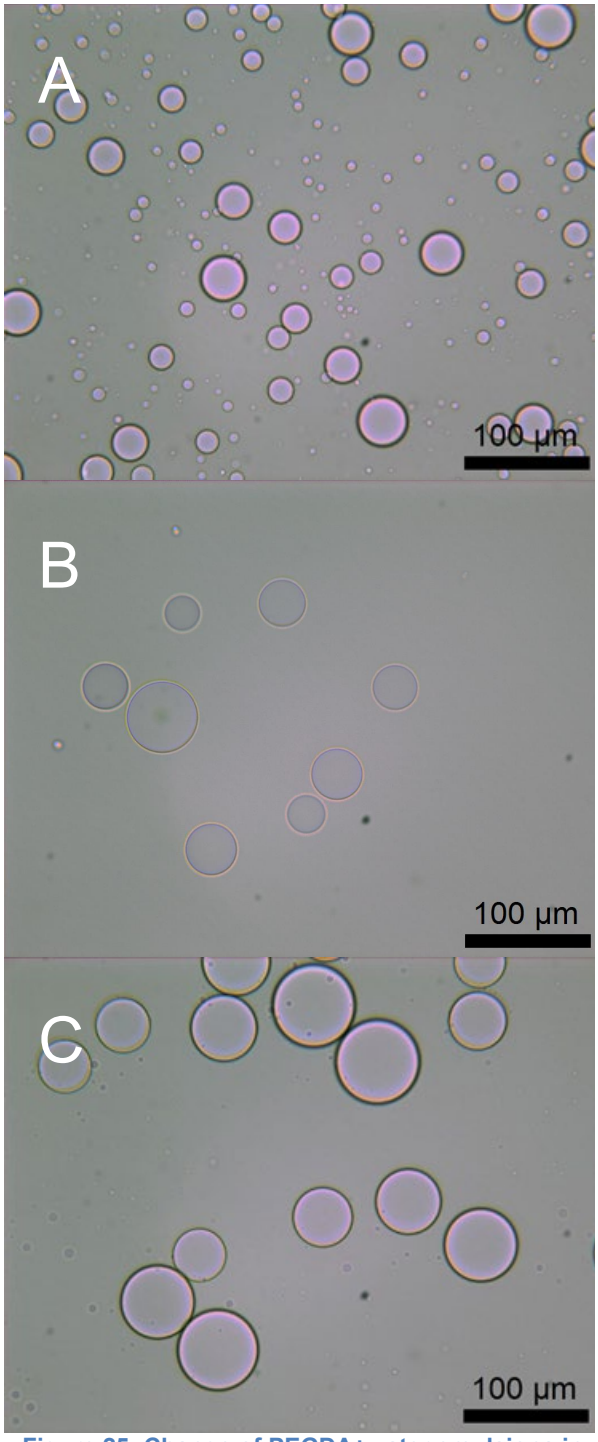

Figure 25: Change of PEGDA+water emulsions in kerosene over time, created with 16V stirring speed and 1ml/min flow rate. All images are the same sample, taken at 0 minutes (A), 2 minutes (B) and 5 minutes after stirring ends (C).

microscope.

3.3.4.1. Results

The initial process for creating microparticles proved to be unreliable. While some particles were created, coalescence still occurred in the final suspension. As can be seen in Figure 26, the size distribution of the droplets in the processed emulsion quickly shifts to fewer, larger droplets. This indicates a portion of the dispersed phase has not fully polymerized and is still present as a liquid. Furthermore, during the experimental analysis it was observed that the suspension of water/PEGDA in kerosene will eventually settle into a two-phase system, with the kerosene on top and an unpolymerised mixture of water and PEGDA underneath. Polymerized microparticles are present in both the kerosene and the unpolymerized mixture, but the majority of the particles are found in the heavier PEGDA/water mixture as can be seen in Figure 27.

All created microparticles are diluted in water for storage, to ensure no further crosslinking of the particles and suspension liquid will occur.

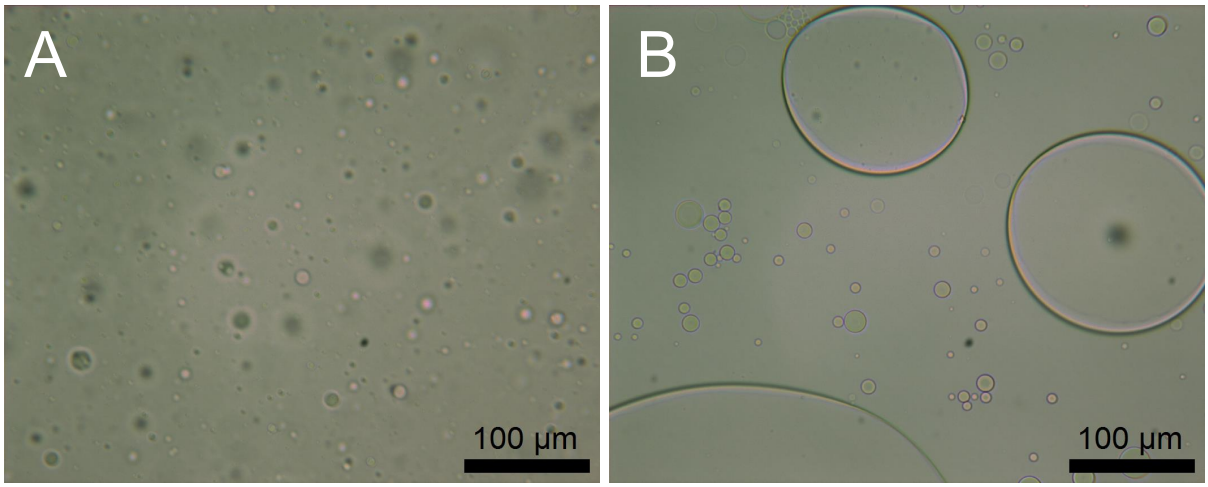

Figure 26: Microscopy images of a single created microparticle suspension immediately after UV exposure (A) and five minutes after the UV exposure (B).

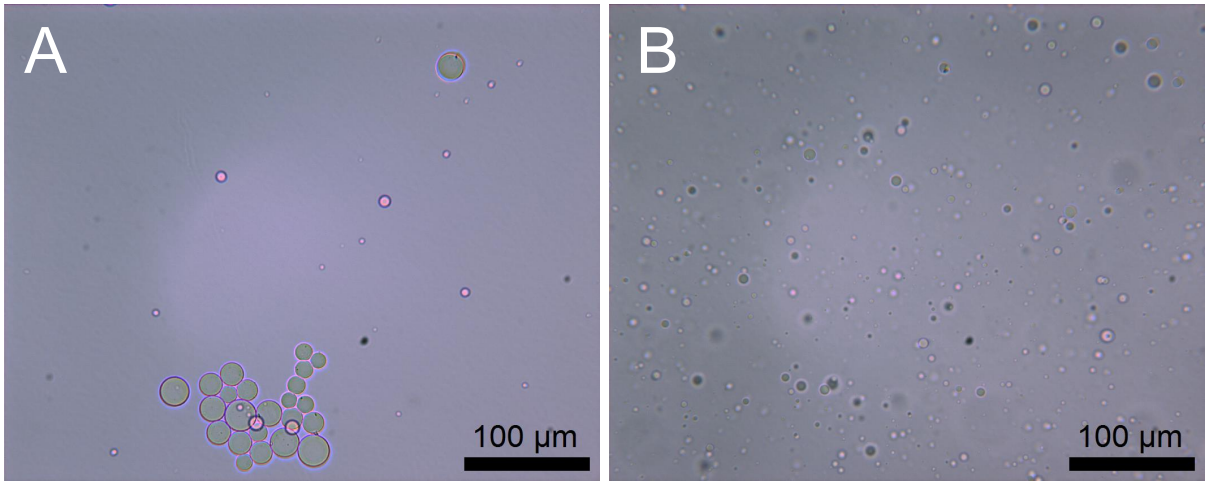

Figure 27: Microscopy images of the kerosene part of a settled emulsion (A) and PEGDA+water part of a settled emulsion (B). Microparticles are present in both liquids, visible as small dots, though the majority is found in the un-polymerized PEGDA+water solution. Both images are collected from the same initial sample suspension.

3.3.5. Prevention of coalescence prior to particle polymerization

In the previously developed method, microparticles were successfully created but the total yield of the process was still lower than anticipated due to unpolymerized PEGDA remaining after UV exposure.

To counter the very limited polymerization of the particles, the process is modified to increase the total UV exposure of the emulsion before coalescence occurs.

The UV exposure time is increased to 45 minutes. To prevent coalescence from occurring during the UV exposure of the emulsion, the liquid is slowly stirred using a magnetic stirring rod and plate (approx. 3Hz stirring speed) to prevent settling and phase separation of the two emulsion mixtures.

Furthermore, to improve the UV exposure of the particles without increasing the necessary time of exposure, the total surface area of the emulsions exposed to UV light was increased. Rather than using the previous method, the emulsion created with membrane emulsification is transferred into three beakers (approx. 5cm diameter each), or into a larger dish (approx. 20 cm diameter) prior to UV exposure to provide a larger total surface area.

All other aspects of the membrane emulsification process were kept identical to those of the previous experiment.

Finally, to determine the stability of the created particles, a small amount of Acetone is added to the suspension to briefly disrupt the surface tensions of any droplets or

semi-liquid particles. During this process, the suspensions are visualized under a microscope to spot any coalescence or disruption of the particles or droplets.

3.3.5.1. Results

Using the two different setups for increased surface area resulted in few differences between the two situations as can be seen in Figures 28 and 29. Both situations show a majority of small, non-coalesced particles with a smaller number of larger coalesced droplets.

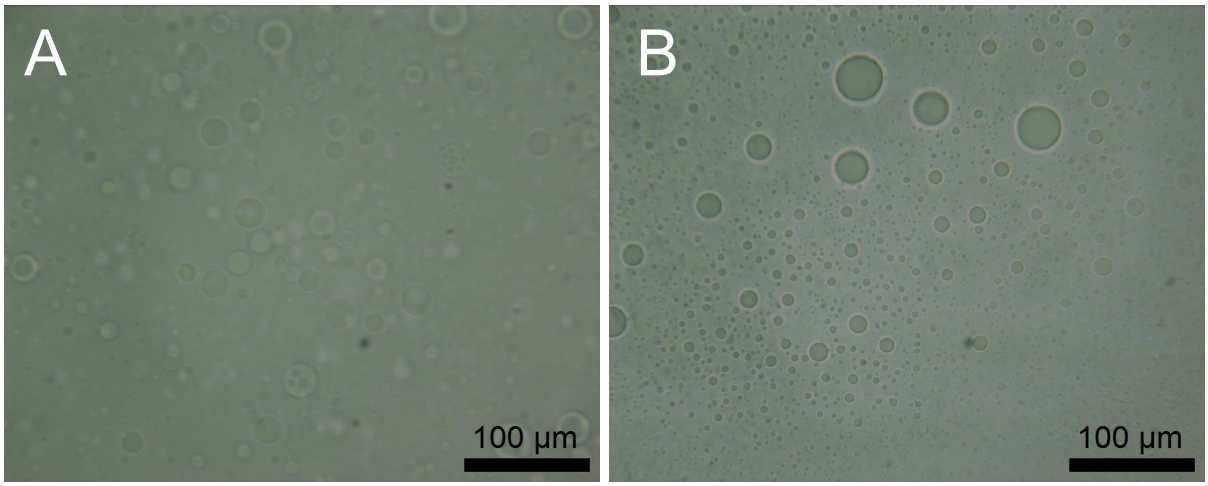

Figure 28: Microscopy images of emulsions created using multiple smaller beakers and stirring during 45 minutes of UV exposure, before (A) and after adding Acetone (B). Both images are the same sample.

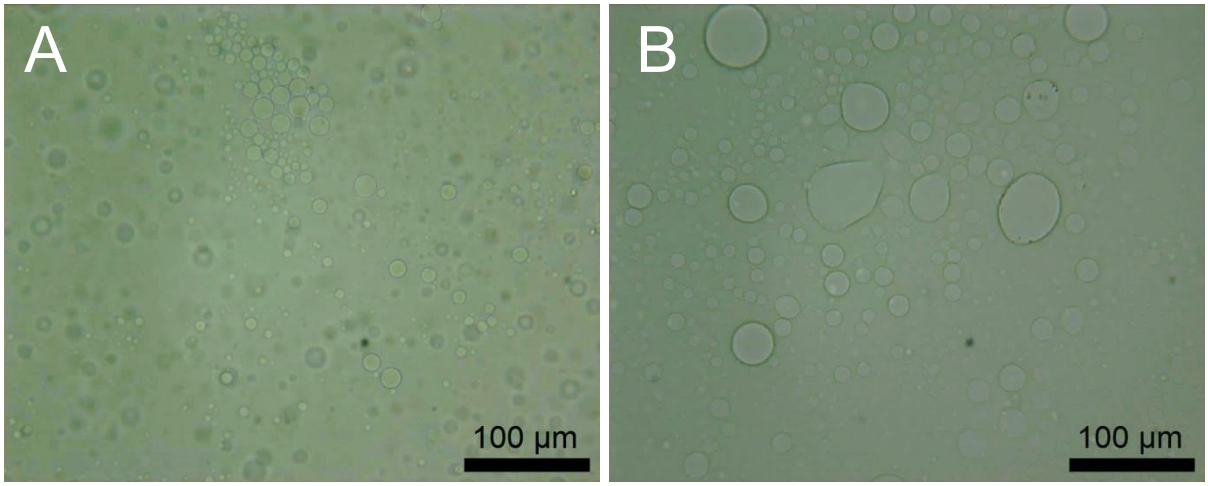

Figure 29: Microscopy images of emulsions created using the larger dish and stirring during 45 minutes of UV exposure, before (A) and after adding Acetone (B) to disrupt droplet formation. Both images are the same sample.

Stability of the particles in both situations was analysed by addition of Acetone to the particle suspension. The addition of Acetone caused significant disruption of the particles depending on the used method of UV exposure. Particles created by using

the smaller beakers showed some coalescence but mostly remained stable during the Acetone exposure.

Particles created using the larger dish instead showed significant coalescence with a large portion of the particles merging into larger droplets. Therefore, particles created using this method were not fully solidified despite the larger surface area that was exposed to UV at any given time.

Due to the poor polymerization of the particles using the larger dish approach, it is assumed that only part of the larger dish was sufficiently exposed to UV light to cause polymerization of the droplets. This, combined with less effective stirring, then leads to only part of the emulsion being polymerized and other parts remaining liquid.

In later experiments, only the smaller beakers are used during UV exposure to ensure stirring allows even exposure and polymerization of droplets.

The increased UV exposure did not result in complete polymerization of all PEGDA in the dispersed phase. Like in the previous method, the suspension or emulsion will separate out into a two-phase system with both microparticles and unpolymerized PEGDA in the heavier second phase. However, particle production was improved and during the process, sufficient droplets are polymerized and turned into microparticles for future use.
While the presence of unpolymerized PEGDA is not considered a major problem, further improvements to the process may be investigated to increase particle yield.

3.3.6. Size analysis of created microparticles

With the newly developed process, microparticles can be reliably produced with a narrow size distribution as determined by optical microscopy. The next step is analysis of the created particle suspensions for a quantified size distribution, using a Coulter LS130 particle sizer.

The created microparticle suspensions are added dropwise to the measurement chamber with the dilution liquid, until the Coulter registers an obscuration value of 7-13%. Once the obscuration has an acceptable value, the measurements are started. Each measurement lasts 60 seconds, with a wait time of 30 seconds between measurements. All measurements are performed in triplicate to reduce the influence of measurement errors and noise.

To prevent possible measurement errors caused by differing refraction index of the dilution liquid, the initial measurements use a 75% PEGDA in water mixture similar to the unpolymerized emulsion for the dilution liquid during the measurement. The refractive index of this mixture is determined to be 1.4452 using a Leica Abbe Mark II refractometer.

Measurement data is graphed for further analysis using Matlab (The Mathworks, Inc.).

3.3.6.1. Results

The size distribution measurements showed a very large amount of noise. The obscuration values measured by the Coulter fluctuated wildly, and many measurements could not be completed due to extremely low obscuration values (1-5%).

It is now thought that the low contrast between the particles and the suspension liquid caused by the very similar materials (polymerized vs. unpolymerized PEGDA) prevents the Coulter from gaining correct data. As can be seen in Figure 30, there were little to no overlapping features between the measurements.

Based on these results, it is assumed that any particle sizes measured in these experiments are noise from air bubbles.

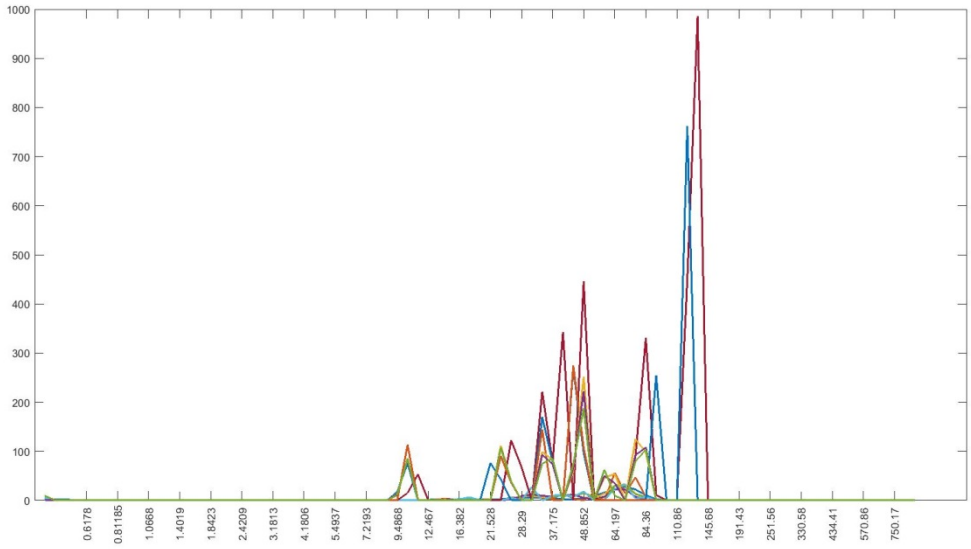

Figure 30: Measured size distributions of multiple samples (each sample measured in triplicate) using the first experimental procedure. The X-axis indicates the size of the particles (the axis is exponential from 0 to 900 µm). The Y-axis shows the relative volume fraction of the particles at the indicated size range.

3.3.7. Contrast improvement for microparticle size analysis

Due to the high similarity in contrast between the solid microparticles and the unpolymerized dilution liquid, additional contrast needs to be introduced to the suspension before accurate measurements of the size distribution can be taken. New particles are created using the previously described methods, but using a dispersed phase that contains an additional 10% blue food dye.

The dilution liquid is the same as used previously; a 75% w/w PEGDA in water solution with no added dye.
When the particle suspension is diluted during the preparation for the analysis, the liquid will become more transparent due to the dilution while the particles are less severely altered and will therefore contain a higher proportion of dye.

All size measurements are performed using the following settings: 120 seconds for each measurement with all measurements performed in triplicate (tree different samples taken from each emulsion to be tested), with a target sample obscuration of 7-13%.

3.3.7.1. Results

Using dyed microparticles, more accurate measurements of the particle size distribution were acquired. Size distributions for three separate samples are shown in Figures 31-33. Results are an excellent match, showing good consistency in the size distribution between samples. While some differences between these measurements are visible, in particular the more skewed size distribution in sample 1 as compared to samples 2 and 3, this is not considered a major problem.

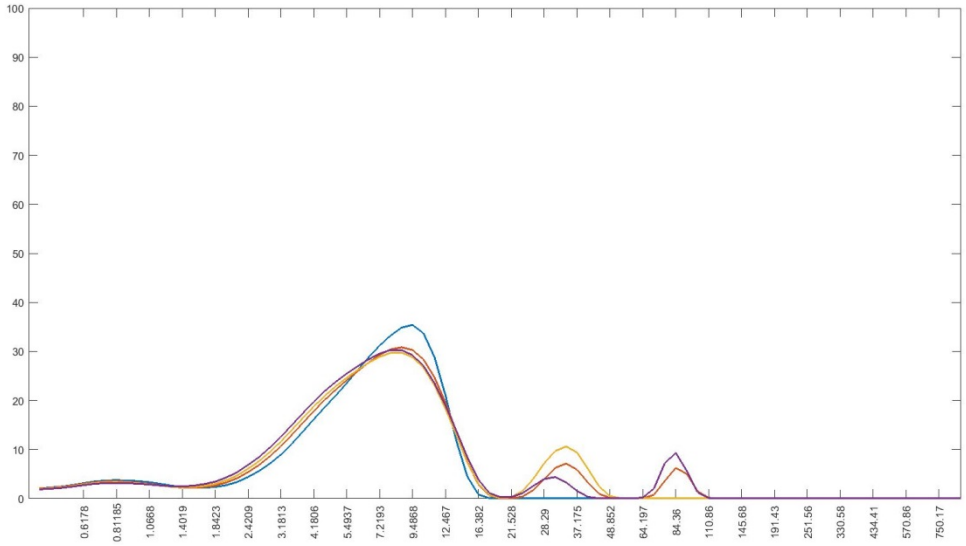

Figure 31: Size distribution of sample 1, using repeat measurements of a single sample volume. The X-axis indicates the size of the particles (the axis is exponential from 0 to 900 µm) The Y-axis shows the relative volume fraction of the particles at the indicated size range. Some measurement errors from air bubbles are visible as extra peaks to the right of the main peak.

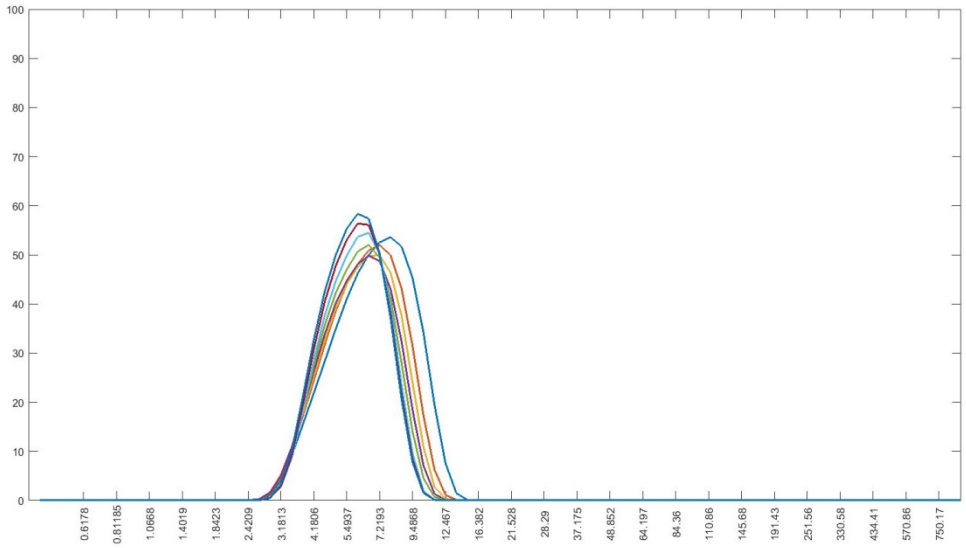

Figure 32: Size distribution of sample 2, using repeat measurements of a single sample volume (different sample than shown in Figure 31). The X-axis indicates the size of the particles (the axis is exponential from 0 to 900 µm) The Y-axis shows the relative volume fraction of the particles at the indicated size range.

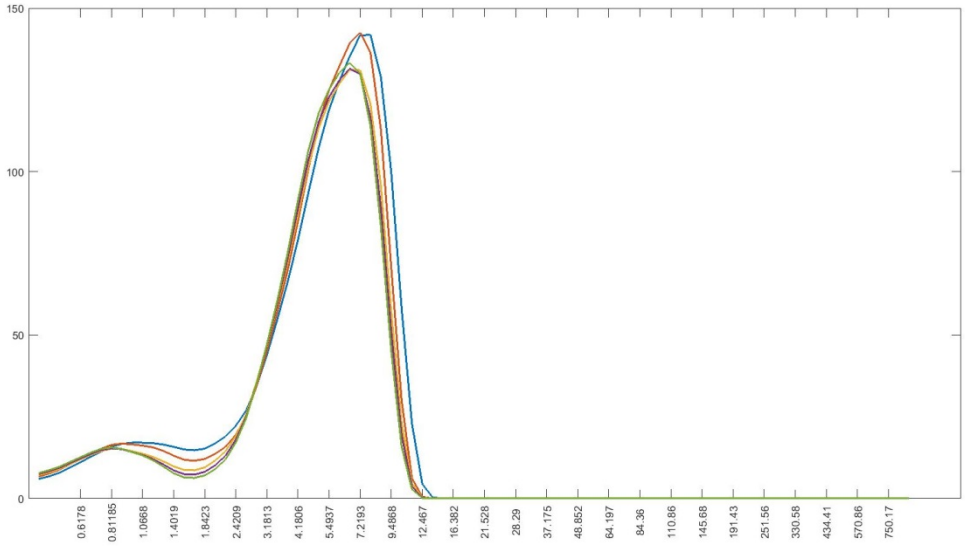

Figure 33: Size distribution of sample 3, using repeat measurements of a single sample volume (different sample than shown in Figures 31 and 32). The X-axis indicates the size of the particles (the axis is exponential from 0 to 900 µm) The Y-axis shows the relative volume fraction of the particles at the indicated size range. Some measurement noise is visible at very small sizes.

3.3.8. Modified suspension liquid for microparticle size analysis

Accurate size measurements for the created microparticles have been acquired. However, since the created microparticles are eventually expected to include immobilized proteins, including the food dye to improve contrast between the particles and the surrounding liquid is not a suitable modification to the process for later stages of the project.

Instead, as a final modification to the process, the analysis of the particles is performed while using water instead of the un-polymerised 75% w/w PEGDA solution as a dilution liquid.

For the analysis the refractive index is set to 1.3330, but some minor errors may be introduced by this change as the refractive index will no longer be exactly correct due to the small volume of unpolymerized PEGDA still present in the particle suspension. The measurements with the modified dilution liquid are compared to earlier measurements to determine if the dilution liquid causes unacceptable deviations in the particle size measurements.

A new series of microparticles is created using the method described for the previous experiment, except no dye is added to the dispersed phase.

All size measurements are performed using the following settings: 180 seconds for each measurement with all measurements performed in triplicate, target sample obscuration of 7-13%.

3.3.8.1. Results

Diluting the particle suspensions in water did not introduce major errors in the measurements of the size distributions. As can be seen in Figures 34-36, each measurement has peaks at the same approximate location as were found in the previous experiments, though some additional peaks are also present due to air bubbles.

One result visible in these experiments is that unlike the measurements using 75% PEGDA for dilution, these measurements indicate a second peak just to the right of the main peak, distorting the size distribution slightly (especially visible in Figures 35 and 36). The location of this distortion at approx. twice the particle diameter of that of the main peak indicates the most likely cause is aggregation of two particles which are then measured as a single event. It is not known if this occurs only using the water-based dilution or if this also occurs in the 75% PEGDA-based dilution and this has not been found due to random chance.

The particle size is not distributed in a Normal Distribution, as determined by the use of one-sample Kolmogorov-Smirnov tests on the acquired data.

Based on both these results and the results of the previous experiments, the process is considered ready to create microparticles with an approximate diameter of 4-5 μm for the purpose of functionalization and protein immobilization analysis.

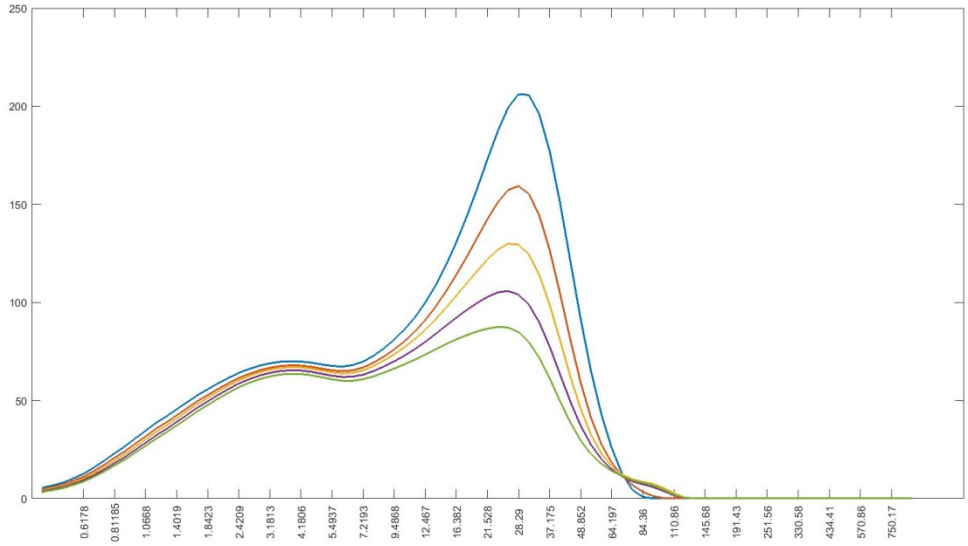

Figure 34: Size distribution of sample 1, using measurements of a multiple sample volumes. The X-axis indicates the size of the particles (the axis is exponential from 0 to 900 µm). The Y-axis shows the relative volume fraction of the particles at the indicated size range. In this sample, large measurement errors due to air bubbles can be seen in the peaks on the right.

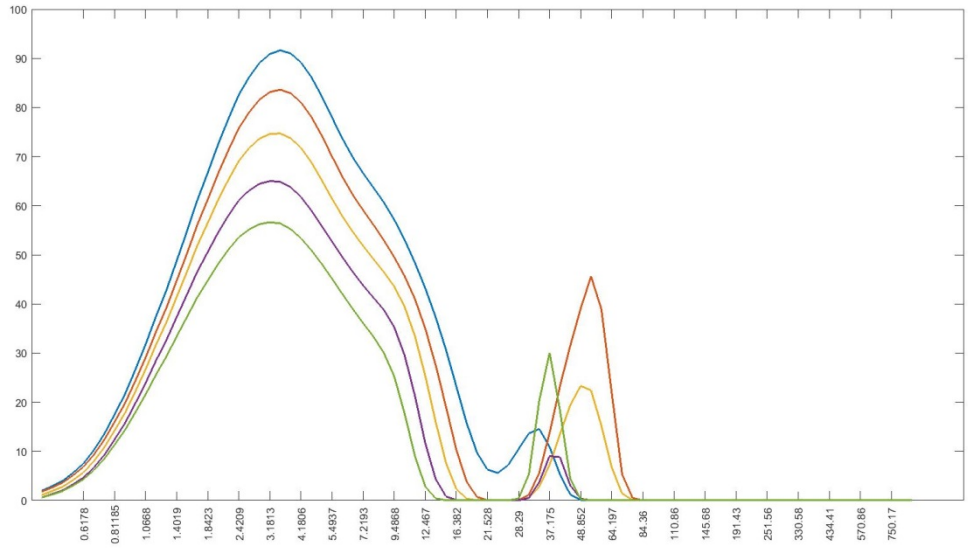

Figure 35: Size distribution of sample 2, using measurements of multiple sample volumes. The X-axis indicates the size of the particles (the axis is exponential from 0 to 900 µm). The Y-axis shows the relative volume fraction of the particles at the indicated size range. Measurement errors due to particle aggregation can be seen as a distortion on the right side of the left peaks, and errors due to air bubbles can be seen in the peaks on the right.

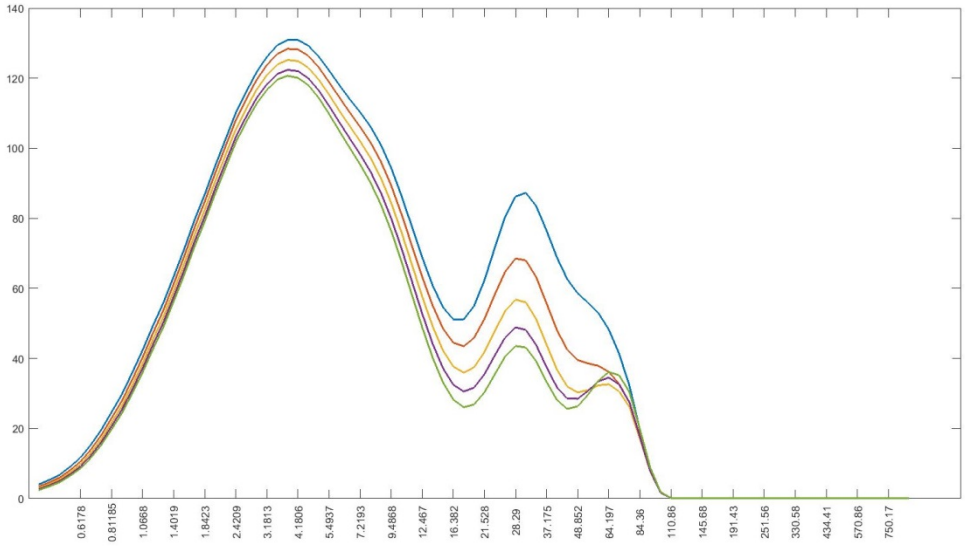

Figure 36: Size distribution of sample 3, using measurements of multiple sample volumes. The X-axis indicates the size of the particles (the axis is exponential from 0 to 900 µm). The Y-axis shows the relative volume fraction of the particles at the indicated size range. Like in sample 2, measurement errors due to particle aggregation can be seen as a distortion on the right side of the left peaks, and errors due to air bubbles can be seen in the peaks on the right.

3.3.9. Component preparation and processing for functionalized particles

Now that the process to create suitable microparticles is complete, the next step is to immobilize suitable proteins onto these particles for further analysis. In this section, particles are functionalized with Streptavidin so that biotinylated proteins can be immobilized onto the particle surfaces.

Streptavidin is linked to Acrylate Poly(Ethylene Glycol)-N-Hydroxysuccinimide by mixing the components at a ratio of 1:35 (1 mg Streptavidin = 16.66 nmol, 3 mg Acrylate-PEG-NHS = 600 nmol), based on work by Hempel[254] to ensure crosslinking of every Streptavidin molecule. The mixture is stirred overnight at 4-7°C.

The continuous phase consists of kerosene with 2% Span80 as a surfactant.

To create the dispersed phase, 75% w/w PEGDA in water with 2% w/w DMPA is used as the primary mixture. Depending on the required concentrations of proteins in the microparticles, varying amounts of the previously created Acrylate-PEG-Streptavidin solution are added. The total water content is adjusted to compensate, ensuring that the final PEGDA concentration is maintained at 75% w/w.

The highest Streptavidin concentrations used in the creation of the particles is 0.5 mg/mL (8.33 nmol/ml), making the concentration in the actual particles an approximate 2.08 nmol/ml. Additional functionalized particles are created from a dilution series of the Streptavidin solution, to a concentration 2, 4, 8, 16, 32, 64, 128, 256 or 512 times lower (down to ≈0.004 nmol/ml). Particles are labelled based on the concentration of Streptavidin, from 'Type 1' at the highest concentration to 'Type 10' with a 512 time dilution. 'Type N' particles are particles created without Streptavidin.

Combined with the size measurements described earlier (approximate diameter of 4µm, volume of 33.5 μm^3), this means that theoretically the mean number of Streptavidin molecules per microparticle is 42,000 for the highest concentration. Only one concentration of particles is created at a time, varying concentrations are not mixed.

Once the polymerization mixture is completed, the microparticle suspension is created the previously described process. The microparticle suspension is exposed to UV light (254 nm wavelength) at approx. 500-1000 uW/cm^2 for 45 minutes to polymerize the resulting particles. The microparticle suspension is continually stirred at low intensity to ensure even exposure of the particles.

After completion of the process, the particle suspensions are stored at 4-7°C until further processing and analysis.

3.3.9.1. Results

Particle suspensions were successfully created for particles of Type 1-3, Type 5-10 and Type N, with estimated Streptavidin content ranging from ≈0.004 nmol/ml to ≈ 2.08 nmol/ml. No particles were created of Type 4 (≈ 0.26 nmol/ml Streptavidin), as the Streptavidin solution for this sample was lost during processing due to accidental spilling. Recreating the necessary starting solution of Streptavidin was not feasible in a practical timeframe, and further experiments were performed without this sample type.

Figure 37: Newly created microparticle suspension, with a visible separation into two phases.

One notable difference between the newly created suspensions and those seen in previous experiments was that

the newly created microparticles will separate into two different phases after removal of the remaining kerosene. The majority of the suspension remains the mostly-clear liquid seen in previous experiments, but a noticeable portion forms into an opaque, foam-like phase that floats on top of the remaining liquid. See Figure 37 for an example.

Both liquid phases are analysed using microscopy to verify the presence of microparticles. As shown in Figure 38, the created microparticles are predominantly found in the clear phase similar to previous experiments. Because the opaque phase still contains substantial amounts of kerosene and surfactant (seen in the form of larger bubbles) in addition to the microparticle suspension, all samples are taken exclusively from the clear phases in all following experiments.

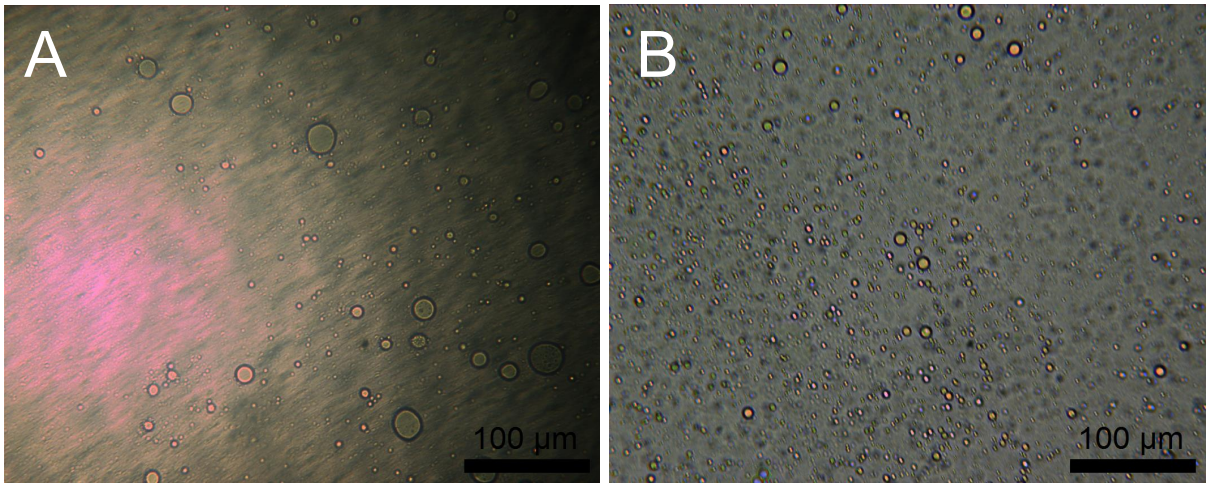

Figure 38: microscopy images of the opaque (A) and clear (B) phase of a single suspension. Microparticles are present in both liquids, seen as the small spheres (<10µm).

All samples created this two-phase system, though the exact cause remains unknown. One possible cause for the formation of the opaque foam is that the Streptavidin in the solution is adsorbed on the water/oil interface. This behaviour is a known risk especially for amphiphilic proteins, though information for Streptavidin specifically could not be found. Because of the complexity of the adsorption process, which may depend on the liquids used, the surfactant, protein rigidity and folding mechanisms[255–259], it is unlikely the problem can be solved in a sufficiently timely manner. Furthermore, the differences between Streptavidin-containing and Streptavidin-free particles in later measurements indicate that at least a portion of the Streptaivin does remain in the created particles. While foam presents a potential problem with loss of protein during the emulsification step and further improvements

would be necessary for a more efficient process, the created particles are expected to be sufficient for the current proof-of-concept plans. Therefore, the foam and possible methods of preventing its formation were not analysed further.

3.3.10. Common aspects of flow cytometry measurements

Following the creation of particles with varying concentrations of Streptavidin, these particles need to be analysed. Although various details of the following experiments vary from experiment to experiment, in particular sample preparation, most of the flow cytometry measurements itself were performed using the same standard methodology. This process is described here, with any further deviations from this method noted in the sections for each individual experiment as appropriate.

Prepared samples are stored protected from direct light by covering the samples with foil. All samples are analysed using a FACSCanto II Flow Cytometer (BD Biosciences). Prior to loading in the flow cytometer, each sample is briefly vortexed to ensure an even suspension of particles and to prevent clumping and subsequent measurement of doublets. Each sample is measured at the slowest acquisition speed to preserve sample volumes in case repeat measurements are necessary, and event limits are set at 100,000 events total. A 200V forward scatter (FSC-A) threshold is implemented to exclude debris.

Once measurements are complete, measurement data is exported and further analysed using FlowJo (FlowJo LLC, USA).

In FlowJo, particle populations are selected based on the forward and side scatter values for events (FSC-A and SSC-A) so that deformed particles can be excluded. All measurements showed a clear particle population with a tight distribution of forward and side scatter values, with a lengthy trail of poorer quality particles with high side scatter values (indicating non-spherical shape). Typical scatter data for the total measurement and the selected particle population are shown Figure 39.

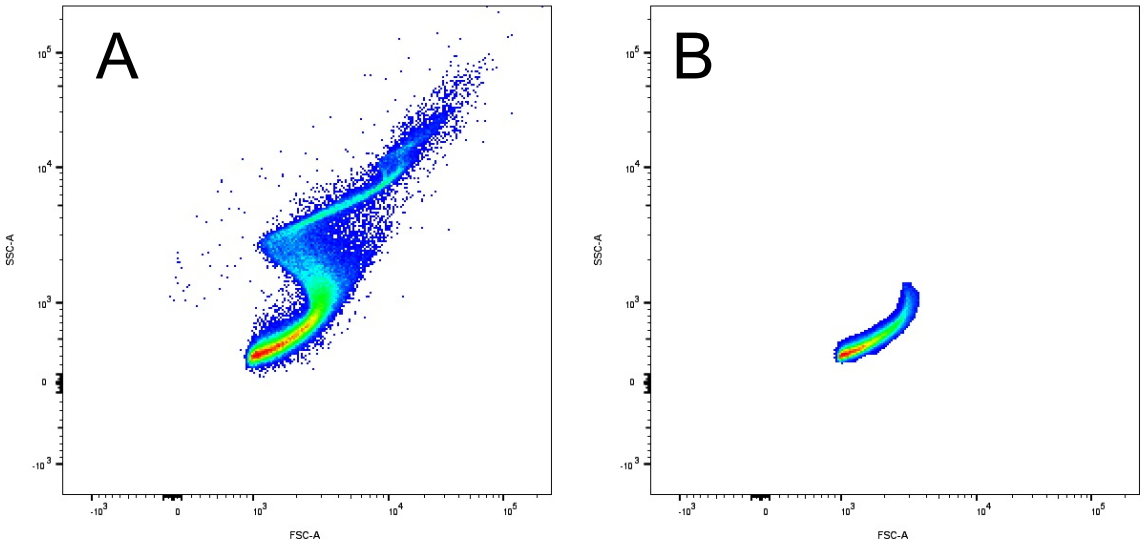

Figure 39: examples of forward scatter (FSC-A, horizontal axis) and side scatter (SSC-A, vertical axis) plots of the all measured events (A) and the selected particle population (B) of a typical flow cytometry measurement using created PEG microparticles.

New population selections are defined for each experiment to account for modified measurement parameters and potential day-to-day differences, but within experiments identical population criteria are used for all measured samples.

Following population selection, additional thresholds are applied to the fluorescence intensity (FITC-H and/or PE-H) to exclude non-fluorescent events caused by air bubbles as a consequence of the vortexing prior to the measurement, as shown in Figure 40.

Once the particles are selected, the geometric mean of the fluorescence intensities of interest (FITC-H, PE-H or both) is calculated for the remaining population.

The measured fluorescence values are then converted into estimates of the total number of fluorophores on each particle using the QuickCal calculation process provided by Bangs Laboratories,

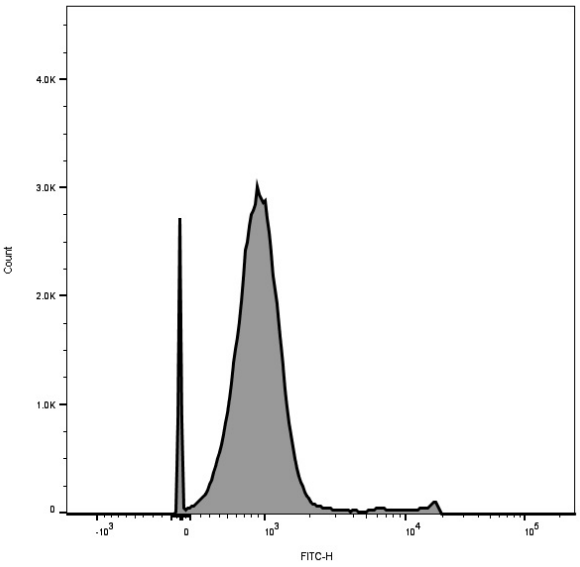

Figure 40: example of a typical fluorescence histogram after selection of the particle population. Note the peak at zero fluorescence caused by small numbers of bubbles remaining in the suspension following vortexing.

Inc. The QuickCal excel files are configured using measured fluorescence intensities of Quantum MESF particles analysed prior to the particle measurements (using identical flow cytometer settings).

The calculated fluorescence or MESF values of the particles are then used for analysis as described in further detail for each experiment.

3.3.11. Initial flow cytometry method testing

The first flow cytometry experiment is intended to determine if the functionalized particles created with the membrane emulsification process can be analysed using the selected method. While samples are incubated with biotinylated fluorophores to create a fluorescent signal, the actual fluorescence results acquired from this experiment are of secondary concern. Instead, the main focus is detecting any major problems that need to be solved before the particles can be analysed during later experiments. In particular, particle counts, preparation requirements and measurement settings are investigated.

Ten samples are created by incubating Type 1 particles (estimated 2.08 nmol/ml Streptavidin) in various concentrations of biocytin-Alexa Fluor 488 for two hours and fifteen minutes. Concentrations are based on the expected Streptavidin content of particles, calculated by assuming equally distributed Streptavidin throughout the entire PEG solution (during membrane emulsification) and solidified particles (during flow cytometry).

Fluorophore is added to the particle suspension at a 32:1 molar concentration for the brightest staining, with particles using lower concentrations receiving 16:1, 8:1, 4:1, 2:1, 1:1, 1:2, 1:4, 1:8 or 1:16 ratios of fluorophore to estimated Streptavidin content.

As a control group, particles that have not been incubated with fluorophore are also analysed using the same measurement settings.

Because the density of the microparticles is nearly equal to that of the suspension liquid, collection or concentration of the microparticles by centrifugation is not possible. No washing step is included in order to minimize the irreversible dilution of the particles prior to measurements.

The particles are analysed using a FacsCANTO II Flow Cytometer (BD Biosciences). Particles are diluted 1:40 in Phosphate Buffered Saline before the measurements. Signal thresholds for forward scatter, side scatter and FITC fluorescence are set at 200V to eliminate signal noise caused by possible bubbles, (fluorescent) debris and other small-scale artefacts in the particle suspension.

Fluorescence signals are quantified using Quantum Alexa Fluor 488 MESF reference particles using the QuickCal system provided by Bangs Laboratories, Inc.

After measurements are completed, data is collected and analysed using FlowJo (Flowjo LLC) and Microsoft Excel. Unless specified otherwise, all shown fluorescence values are the calculated geometric mean of each measurement.

First, sample measurements are gated to select only the desired (spherical) particles by eliminating particles with higher side scatter values, manually selected from the forward scatter-side scatter plot in FlowJo. All samples use identical population selections.

The selected population is then analysed by comparing the fluorescence intensity, calculated as the geometric mean of the FITC signal in each sample population. Finally, measured fluorescence values are converted to absolute MESF values to estimate total fluorophores per particle, using the fluorescence values of the MESF reference particles in the QuickCal conversion method offered by Bangs Laboratories, Inc.

3.3.11.1. Results

Created particles were successfully analysed with the flow cytometry method described above.

Measured data show a clear connection between the initial fluorophore concentration and the calculated fluorescence of the particles. A linear fit of: $F_s = 27.99R_s + 104.4$ with F_s the fluorescence of the given sample and R_s the ratio of Fluorophore to Streptavidin of each sample, provides a fit of the results with an R-squared of 0.9022, with both measurements and model fit shown in Figure 41.

While this model provides a good fit, the found value of only 104.4 as the fluorescence due to specific binding indicates that a large portion of the Streptavidin did not bind fluorophores. Furthermore, no plateau was observed at higher ratios, indicating that even with a 32-fold excess of fluorophore no saturation of the particles occurred and non-specific binding and adsorption can still increase.

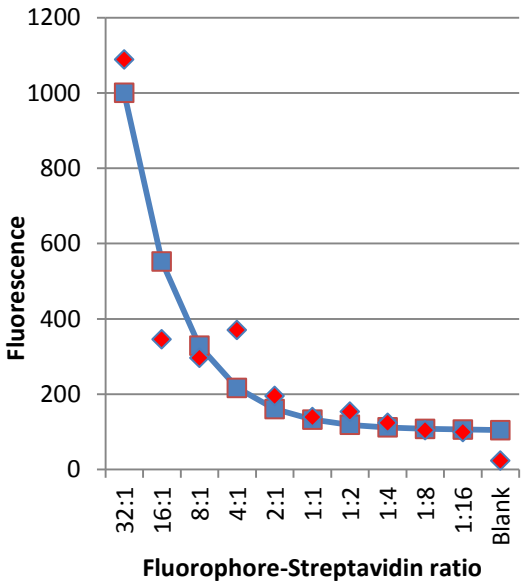

Figure 41: Fluorescence (MESF) values for the created dilution series and model fit F_S. Note the non-linearity of the X-axis.

Comparison to the non-fluorescent control indicates that the particles do bind more fluorophores with Streptavidin present; however the comparatively similar levels of fluorescence mean that an accurate quantification of the total fluorescence per Streptavidin molecule is not possible without further investigation of the binding process.

A potential explanation for this result is that the biocytin-Alexa Fluor 488 used during this experiment was not fully bound to the available Streptavidin. Streptavidin molecules on the surface will bind fluorophores first, and it is possible that the concentration gradient between the inside of the particles and the suspension liquid is insufficient to cause enough diffusion of the fluorophore into the particles. This effect will be especially pronounced for the lower concentrations due to the comparatively larger influence of non-specific binding. As such, determining the amount of non-specific binding is a priority for further experiments.

3.3.12. Analysis of binding saturation during flow cytometry

Initial testing of the flow cytometry method was promising, but results remained highly dependent on the concentration of fluorophores used during incubation. It is unclear if the used microparticles were fully functionalized during the previous experiment or if free Streptavidin remains, and how much non-specific binding takes place on the particles. To this end, additional experiments are run with increased ratios of biotinylated fluorophores to Streptavidin in order to determine non-specific binding and saturation.

For this experiment, the fluorescent marking process described above is repeated with a biotinylated fluorophore concentration of 32:1 excess compared to the total Streptavidin content of Type 1 particles (estimated 2.08 nmol/ml Streptavidin). Only one type of fluorophore is used for any sample, fluorophores are not mixed. All other particle types are incubated using an identical fluorophore concentration, to eliminate differences due to varying non-specific binding. Samples are created for all particle types after incubating with the same concentration (64:1 excess for Type 2, 128:1 excess for Type 3, etc.). All measurements are performed in triplicate.

Further processing and analysis are otherwise identical to the previous experiment.

Fluorescence signals are quantified using Quantum Alexa Fluor 488 MESF reference particles as described before.

3.3.12.1. Results

Particles of each type except Type 4 were incubated with the same concentration of fluorophore to determine potential saturation of Streptavidin on particles. The resulting measurements indicate a nearly constant fluorescence between particles, as shown in Figure 42.

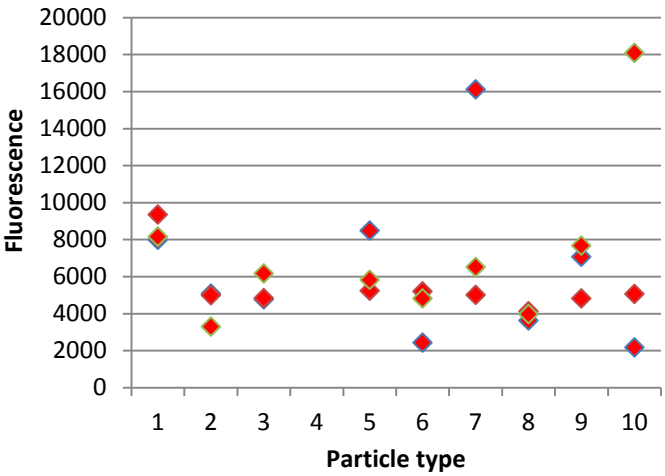

Figure 42: Fluorescence values for the different particle types after incubation with the same fluorophore concentration.

Consequently, the fluorophore binding of each particle appears to be independent of the Streptavidin content on each particle type. Non-specific binding occurs at a sufficient level to eclipse the signal from any biotin-Streptavidin binding that occurs in the samples. For further experiments, work will focus on not just adding varying amounts of fluorophore to the particles of interest but also on removing non-specifically bound fluorophores after incubation.

3.3.13. Analysis of non-specific binding during flow cytometry

Previous experiments showed sufficiently great non-specific binding that estimation of the specific binding through the Biotin-Streptavidin link was impossible. Therefore, a different approach is tested for determining the non-specific binding onto the

microparticles. While the Streptavidin-biotin bond is difficult to break, non-specific binding is easily disrupted and will vary depending on the fluorophore concentration in the surrounding medium. By measuring a single sample of functionalized particles over an extended period of time after sudden dilution, additional insight may be gained into how the fluorophore binding changes for that sample.

Biotinylated R-Phycoerythrin is used as an additional fluorophore and possible alternative for Alexa Fluor 488. The higher molecular weight of the chosen R-Phycoerythrin fluorophore (≈240 kDa compared to the previously used Alexa Fluor's ≈1 kDa) may provide additional clues to potential binding issues involving steric hindrance of the Streptavidin in the particles.

Type 1 particles (estimated 2.08 nmol/ml Streptavidin) and non-Streptavidin functionalized particles are incubated at room temperature with a 40:1 excess of either biotinylated Alexa Fluor 488 or biotinylated R-Phycoerythrin for one week prior to measurements.

For the flow cytometry measurement, the final samples are created by diluting the existing microparticle suspension in Phosphate Buffered Saline at a ratio of 1:10, 1:20, 1:40 and 1:80. Sample measurement takes place immediately after dilution (start within 1 minute). All samples are stored protected from light at 4-7°C, and measured again at 1, 2 and 3 hours after dilution. Final measurements are performed after 20 days to determine the equilibrium for the particle fluorescence.

Thresholds for the Flow Cytometry are 200V for the forward scatter, side scatter, FITC and PE signals. Fluorescence signals are quantified using Quantum Alexa Fluor 488 MESF reference particles or Quantum R-Phycoerythrin MESF reference particles, as appropriate.

3.3.13.1. Results

The fluorescence of the measured particles shows a strong dependence on both the presence of Streptavidin on the particles and the dilution of the particles prior to measurements, as seen in Figure 43. For particles stained with biocytin-Alexa Fluor 488, fluorescence intensity shows the expected progression with the Streptavidin containing particles having the highest fluorescence at the lowest dilution and signal strength dropping as dilutions are increased or Streptavidin is absent.

Particles stained with biotinylated R-Phycoerythrin show a different result however, with samples showing wildly varying fluorescence both between concentrations and over time. In particular, several of the samples show fluorescence intensities increasing over time, a change that should not occur as a consequence of the sample dilution prior to the first measurement.

Consequently, the R-Phycoerythrin measurements indicate the presence of an unknown effect on the fluorescence that may depend on the molecular weight difference between Alexa Fluor 488 and R-Phycoerythrin.

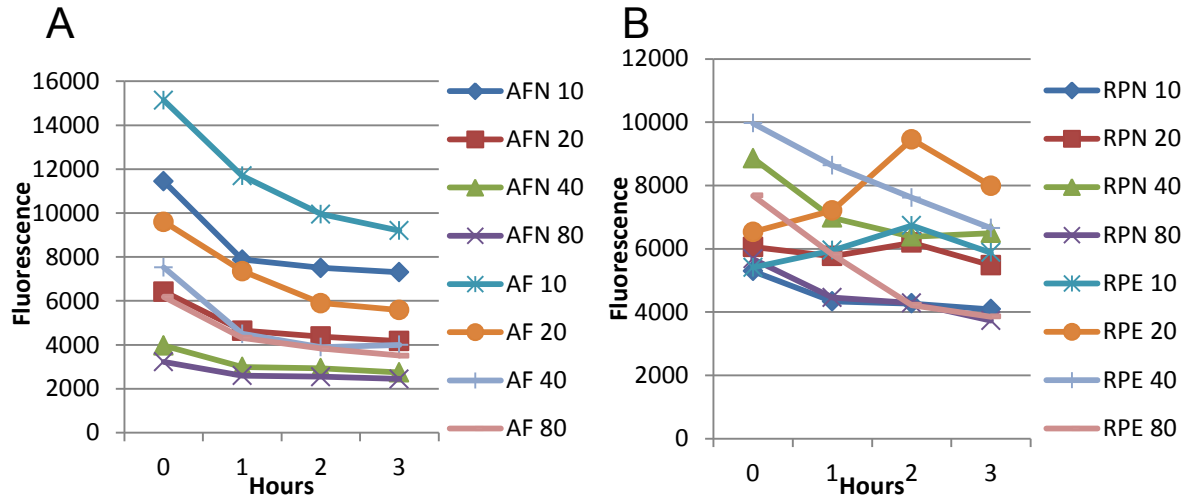

Figure 43: Fluorescence intensities 0, 1, 2, and 3 hours after 10-80x dilution for Alexa Fluor 488 (A), and R-Phycoerythrin samples (B). Streptavidin-containing particles are AF and RPE respectively; Streptavidin-free particles are AFN and RPN respectively. All measurements are performed as N=1.

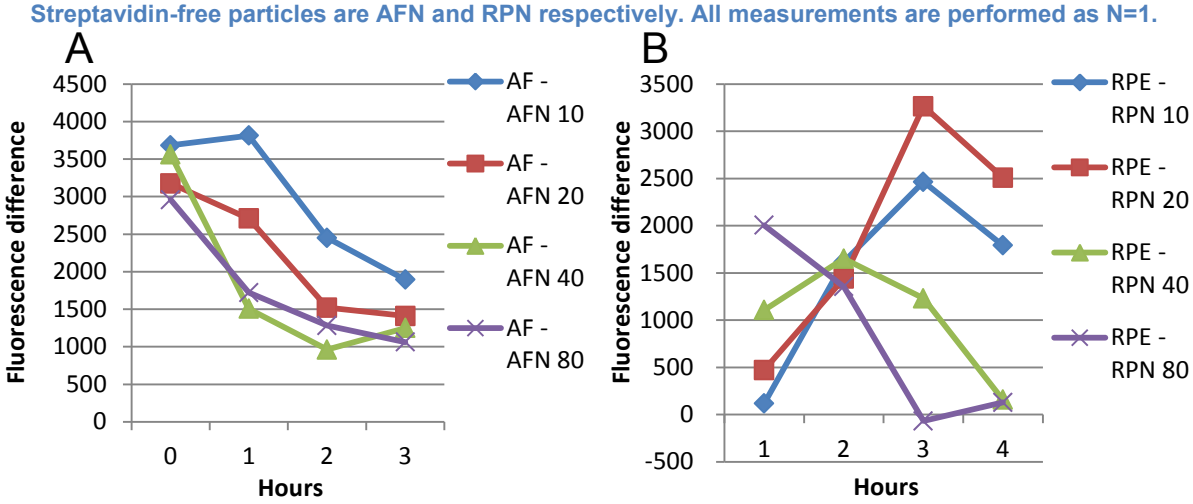

Figure 44: difference in fluorescence values between Streptavidin containing particles and Streptavidin-free particles at 0, 1, 2 and 3 hours after 10-80x dilution for Alexa Fluor 488 (A) and R-Phycoerythrin (B). Streptavidin-containing particles are AF and RPE respectively; Streptavidin-free particles are AFN and RPN respectively. All measurements are performed as N=1.

Differences between Streptavidin and non-Streptavidin particles approach equilibrium for Alexa Fluor F488, indicating a possible value for the specific binding

as seen in Figure 44. Assuming a 10 nm thick layer accessible to solution[95], the expected volume of available binding sites on particles with a diameter of 4 µm is ≈ 0.5 μm^3. With a 2.08 nmol/mL Streptavidin concentration, this would result in approximately ≈ 626.5 total molecules available on the surface.

In comparison, fluorescence values for Alexa Fluor 488 approach an average of approx. 1500 units of fluorophore per particle. Consequently, with these assumptions even a best-case scenario would indicate that more than half of the current signal is caused by non-specific binding.

In published literature, Hern et al also noted that for their choice of peptide and spacer, only 10% of the available sites might be available to cells due to steric hindrance[95]. This provides further support for the difference seen between Alexa Fluor binding and R-Phycoerythrin binding, and suggests that the binding dynamics are sufficiently unfavourable that the fluorophores undergo only limited binding to the presented Streptavidin. Therefore, adjustments may be necessary to ensure sufficient binding of fluorophores.

3.3.14. Analysis of time and temperature dependence of fluorophore binding

The differences between the binding of Alexa Fluor 488 and R-Phycoerythrin found in the previous experiment suggest an effect due to differing molecular weights and steric hindrance. The most likely parameter to be influenced due to this difference is the binding speed and affinity of the two fluorophores. Based on this, it is thought the storage conditions for the fluorophore and particles may negatively impact the binding dynamics. If the fluorophore only partially binds to the particles, this will cause a reduction in the signal strength.

A new experiment is run to compare how much influence storage conditions during incubation affect the fluorescence of the particles. Furthermore, additional time will be allowed for binding to occur, in order to acquire a stronger signal.

Type 1 particles (0.433 nmol/ml Streptavidin following dilution) are compared with non-functionalized particles using two different storage temperatures. Biocytin-Alexa Fluor 488 or biotin-R-Phycoerythrin is added to the particles, with the total amount in both situations equal to that needed for a ratio of 10:1 fluorophore to Streptavidin for

the functionalized particles (4.33 nmol/ml). After addition of the relevant fluorophore, the mixtures are stored at different temperatures. One mixture of each type of fluorophore is stored at room temperature (20° C) and one mixture of each type of fluorophore is stored in the fridge (4-7° C) similar to previous experiments.

Flow cytometry measurements are performed to determine the fluorescence of the particles after 1, 2, 3 or 4 days in storage.

Before the first measurements on any specific day, samples are prepared for analysis as quickly as possible to minimize potential changes over time between sample preparation and measurement. All measurements begin within 1 minute after the initial sample preparation and removal from their storage temperature (for samples stored at low temperature).

Samples are diluted in PBS immediately prior to the first measurement (measurement starts within one minute from mixing) at two concentrations: one set of samples is diluted 1:10, one set of samples is diluted 1:100. Each prepared sample is measured at 0, 1, 2 and 3 hours after initial preparation. Samples are stored at room temperature between measurements.

Thresholds are used to prevent measuring possible bubbles, (fluorescent) debris and other small-scale artefacts in the particle suspension. Thresholds used are 200V for forward scatter and 200V side scatter minima. No thresholds are used for fluorescence.

Voltages used are 10V for forward scatter, 250V for side scatter, 500V for FITC and 500V for PE. Fluorescence signals are quantified using Quantum Alexa Fluor 488 MESF reference particles and Quantum R-Phycoerythrin MESF reference particles.

3.3.14.1. Results

Particles were measured and analysed on four separate days, with four time points on each day and different storage conditions depending on the sample.

Streptavidin-free particles that were stained with Alexa Fluor 488 and stored in the fridge could not be measured for day 4, and the sample for Streptavidin-free particles that were stained with Alexa Fluor 488 and stored at room temperature was lost during the measurement. These samples are not included in the analysis.

Alexa Fluor 488 did not show major differences between room temperature and fridge storage for any of the sample parameters. However, numerous samples show a drop in fluorescence over time after dilution. This may indicate that a significant portion of the measured fluorescence is caused by reversible (i.e. non-specific) binding of fluorophores. This is further supported by the higher fluorescence of the 1:10 dilution samples compared to the 1:100 dilution samples. This difference, seen even on the earliest time points immediately after dilution, further indicates there are two different types of loosely-bound fluorophore: one that rapidly disperses into the surrounding liquid (causing the difference between 1:10 dilution and 1:100 dilution at time=0), and a further amount of fluorophores that slowly disperses into the liquid (causing the gradual drop of fluorescence over time seen in the measurements). See Figure 45 for examples.

Possible explanations include varying binding mechanics for the fluorophores depending on presentation and steric hindrance, as well as fluorophores that may be bound deeper within the particles. However, the underlying mechanics are not investigated further.

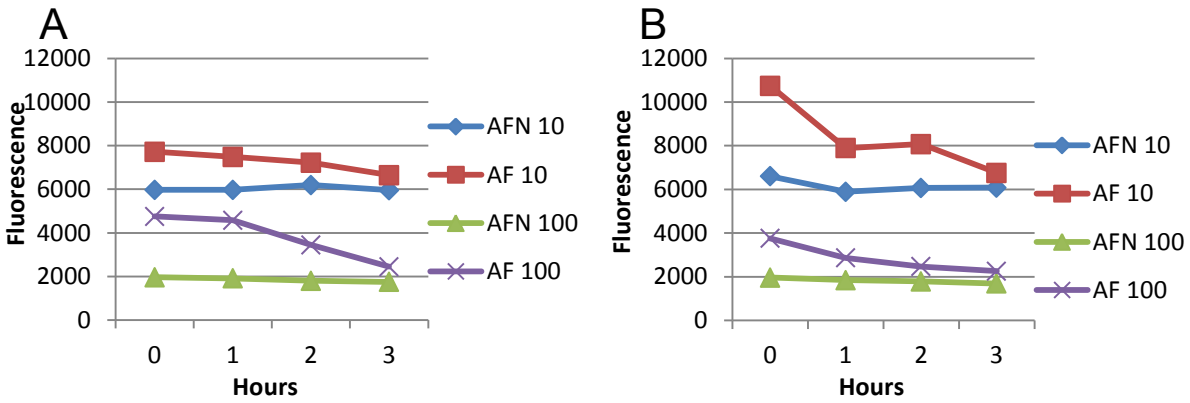

Figure 45: Fluorescence intensities 0, 1, 2, and 3 hours after 10-100x dilution for Alexa Fluor 488 stained particles stored cold (A), and at room temperature (B) on day 3. Streptavidin-containing particles are AF, Streptavidin-free particles are AFN. All measurements are performed as N=1.

R-Phycoerythrin stained particles showed similar behaviour for most sample types, but with a smaller difference between Streptavidin-containing and Streptavidin-free particles, as shown in Figure 46. R-Phycoerythrin stained particles, measured after 1:100 dilution in PBS, showed much higher fluorescence values than expected, but this is thought to be an outlier. Possible causes are accidental incubation with a higher-than-intended concentration of R-Phycoerythrin prior to incubation and storage, though this was not confirmed. The samples are otherwise comparable to

those incubated with Alexa Fluor 488, indicating that the molecular weight of the fluorophore is not a problem for binding onto the surface of the particles.

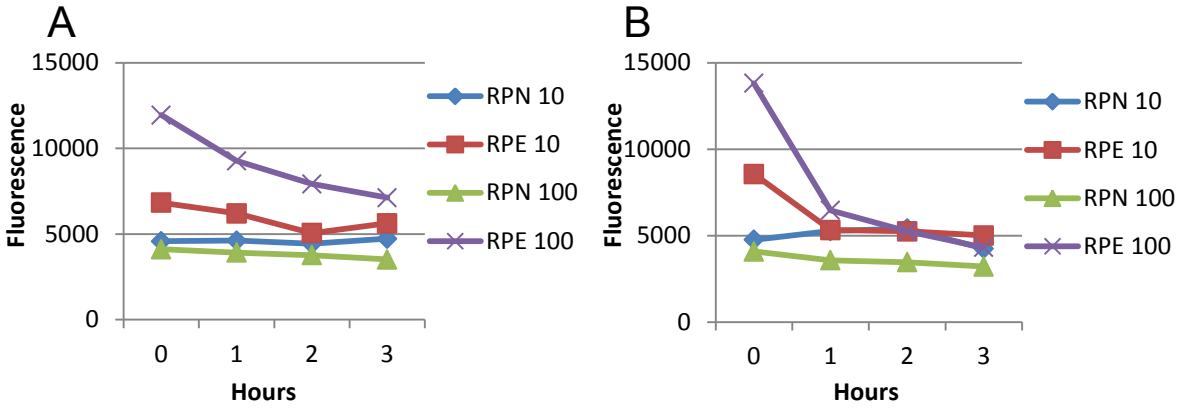

Figure 46: Fluorescence intensities 0, 1, 2, and 3 hours after 10-100x dilution for R-Phycoerythrin stained particles stored cold (A), and at room temperature (B) on day 3. Streptavidin-containing particles are RPE, Streptavidin-free particles are RPN. All measurements are performed as N=1.

Minor differences were seen between different days, but overall the behaviour was very similar. Particles stained with fluorophores all showed a near constant fluorescence levels, with only minor reductions in fluorescence on days 2, 3 and 4, as shown in Figure 47. Dilution of the particles appears to have only limited effect on most samples, with fluorescence remaining largely constant in most samples. The main exceptions are the samples of Streptavidin-containing particles that were stained with R-Phycoerythrin and diluted 1:100 prior to measurements, which showed a reduction in fluorescence of as much as 50%. However, the 1:10 dilution samples showed very little change in comparison. This may indicate that R-Phycoerythrin in particular may have a high non-specific binding to available Streptavidin and not to the remainder of the PEGDA material, but more robust measurements would be needed to determine this with any confidence.

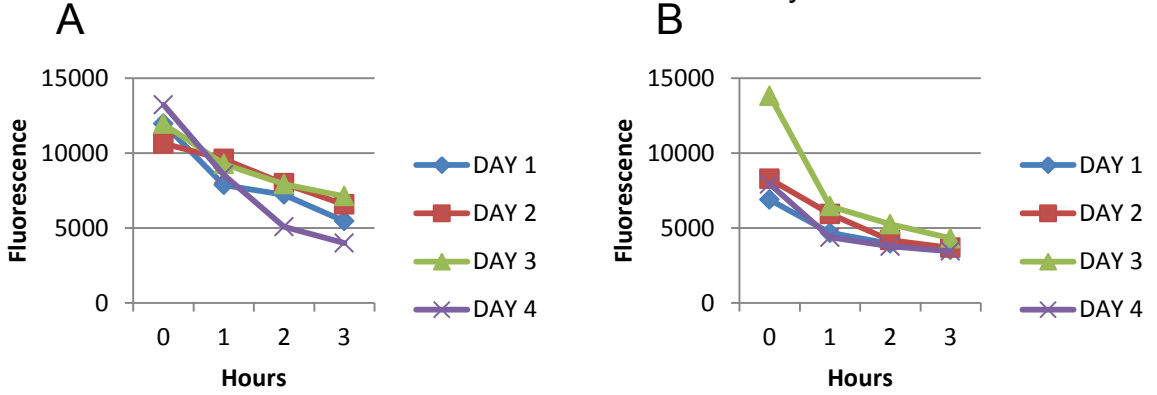

Figure 47: Fluorescence over time for Streptavidin-containing particles stained with R-Phycoerythrin, after 1:100 dilution following cold storage (A) and room temperature storage (B). All measurements are performed as N=1.

However, a major problem with these results is that while the samples do provide some useful information, the results are unsuitable for determining the actual non-specific binding of the measured particles. While each sample could potentially be used to calculate how much non-specific binding occurs, variation between the samples is too great to acquire a single, dependable value. There are not enough measurements to determine an accurate level of noise between measurements, but there is a high level of variation seen in samples such as the fridge-stored Alexa Fluor 488 particles on day 1 or the room temperature R-Phycoerythrin particles on day 4, as seen in Figure 48. This indicates that errors due to noise or undocumented variations in the process are likely severe enough to prevent these measurements from providing sufficiently high quality data for accurately measuring the binding of proteins to Streptavidin on the particles.

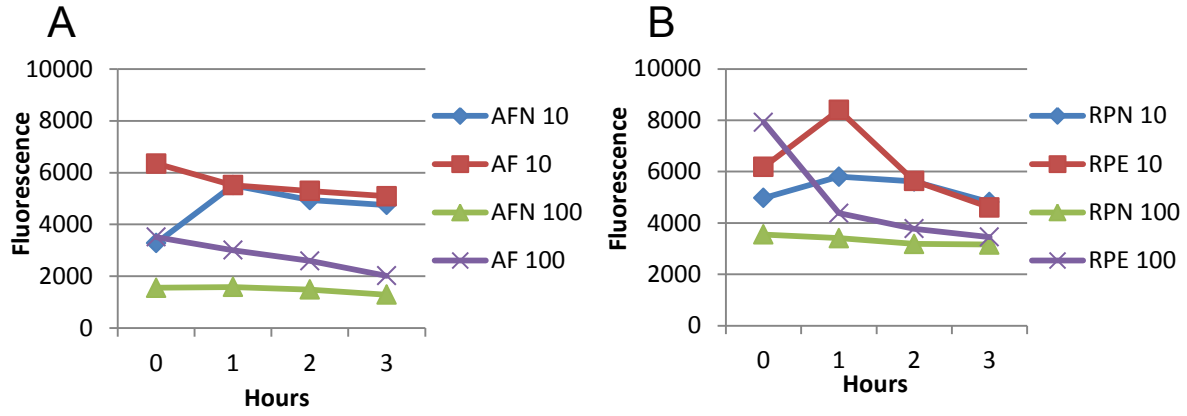

Figure 48: Fluorescence over time for particles stained with Alexa Fluor 488, after 1:10 or 1:100 dilution following cold storage on day 1 (left), and particles stained with R-Phycoerythrin, after 1:10 or 1:100 dilution following room temperature storage on day 4 (right). Note the fluorescence intensity increasing from hour 0 to hour 1, despite the recent dilution, for AF 10, RPE 10 and RPN 10. All measurements are performed as N=1.

3.4. Discussion

A membrane emulsification process was used to create solid Poly (Ethylene Glycol) Diacrylate microparticles.

Using the modified UV exposure methods, the microparticles created with the membrane emulsification setup are suitable for further analysis. A portion of the PEGDA/water mixture is not polymerized, but the particles are solid and can be safely stored for longer periods of time if the suspension liquid is diluted with water right after the particles are created.

The Flow Cytometry measurements encountered a substantial number of problems, especially variations between measurements from particular samples and difficulties in determining the non-specific binding of proteins. While the experiments do suggest that specific binding occurs, variation was severe enough that no accurate levels of this binding could be determined.

The most likely cause of the problems identified during these experiments is that the UV exposure necessary to polymerize the PEGDA into solid particles is much higher than that used for creating hydrogels particles in literature[120,243,245,248,260,261], though times of up to an hour have been reported for non-functionalized particles[262]. The currently used UV exposure may be high enough to cause Streptavidin degradation; consequently the Streptavidin may no longer be able to properly bind biotinylated proteins such as the used fluorophores. Because the Flow Cytometry method used to determine the amount of available Streptavidin is directly reliant on the functionality of the immobilized Streptavidin, it is not possible to identify differences between particles with damaged or missing Streptavidin.

Additional problems may arise from the use of the membrane emulsification process itself; the interaction between Streptavidin and the continuous phase (both kerosene and Span80) is not known in detail. It is therefore possible that the surfactant or the interface between the continuous and dispersed phases may disrupt Streptavidin folding or leech Streptavidin-containing polymer chains out of the solution that forms the eventual solidified microparticles. The appearance of a two-phase separation in Streptavidin-containing solutions that did not occur in Streptavidin-free particles further supports the idea that there may be deeper problems with the membrane emulsification process. While a reduction in (functional) Streptavidin content is not a critical failure on its own, it does compound further problems encountered during the flow cytometry measurements.

In retrospect, the use of microfluidics instead of membrane emulsification for the creation of the PEGDA particles may have been a better choice. While microfluidics would have required a larger amount of time and effort to establish a suitable process, it would also have been easier to ensure an even exposure of the created droplets to the UV used to polymerize the material or modifications to exposure

times[243,261]. Diameter variation might likewise be reduced[242], though varying dimensions do not necessarily hinder further analysis.

Different choices for the continuous phase, surfactant and other parameters of the process may have provided better results. However, the time restraints imposed by this project mean that more extensive optimization simply wasn't feasible.

For future work, the use of alternative polymerization methods may prove more successful, and other analysis methods such as NMR or directly labelling Streptavidin with fluorescent or radioactive markers might be useful to determine the presence of Streptavidin in the created particles. These alternatives are not further investigated during this project due to time constraints.

While the concept of a microparticle-based analysis method as a surrogate for surface measurements remains sound, the challenges encountered during this chapter suggest the experiments performed during this chapter may have been chosen in the wrong order. An initial verification of protein immobilization, even if merely qualitative, may have been a faster and easier route to identifying the problems encountered here than immediately moving to quantitative measurements using flow cytometry. Because of time constrains and the continuing difficulties encountered during these experiments, the decision was made to cease further work on quantifying the available Streptavidin in the created material and move to qualitative analyses and cell culture work instead.

Chapter 4: Chemical modification of cell culture surfaces

4.1. Introduction

While the functionalization and patterning of the materials for cell culture are a major part of this project, it is still necessary to confirm if the designed materials are suitable for cell culture, and whether the desired proteins can be effectively immobilized prior to cell culture.

Numerous different materials are used for cell culture, depending on the requirements of the cells in question, the chosen process, and other limitations or demands of the culture system. Initially, a Poly (Ethylene Glycol) based material was selected for further experiments as shown in chapter 1. However, the results and problems from subsequent experimental work with PEG-based microparticles (see chapter 3) indicated that there may be insurmountable difficulties with the current process for using PEG-based surface chemistry for the immobilization of growth factors. Therefore, a review of alternatives materials may be necessary.

Specifically, while the particles themselves worked fairly well for the flow cytometry measurements, difficulties with specific and non-specific binding on the created particles suggest that the underlying problems are caused by the choice of material and chemical modification strategy. Because the immobilization of proteins onto the selected surfaces is critical for further cell work, the choice was made to focus on quantitative surface modification and cell culture tests rather than continue work on quantifying immobilization prior to cell culture experiments.

The main requirements for the material are that it is possible to mould it into specific shapes, ideally through melting or in-situ polymerization, that it is possible to covalently bind proteins onto the material surface using one or more crosslinking processes, and that the material itself should have a low non-specific adsorption of proteins. However, it may not be possible to create a ‘perfect’ surface material; improvements for cell culture or attachment may come at the cost of reduced protein immobilization or an increase in non-specific binding and subsequently increased noise in any measured effects on cell culture. Currently, non-specific adsorption is considered a lower priority: the main goal at this time is to create a material suitable for cell culture that can be modified with covalently bound proteins.

PEG-based materials have relatively low hydrophobicity, and will adsorb fewer proteins out of solution than more hydrophobic alternatives[234] when used for cell culture experiments. This was deemed a sufficiently advantageous property to warrant further use despite the expected need for further modification of surfaces to allow for cell attachment. However, although PEG-based surfaces are expected to provide advantages in terms of non-specific binding of proteins, sufficiently extensive modification with cell attachment proteins may lead to a needlessly complex process that eliminates the main advantage of using PEG over other, less hydrophilic proteins.

Further work with PEG diacrylate showed substantial difficulties in immobilizing the necessary proteins onto the surface, as seen in chapter 3. As such, rather than attempting to gain an exact value of immobilized protein concentrations, the choice is now made to test for cell culture suitability of PEG and other materials before further quantifying protein immobilization.

Poly (Ethylene Glycol) is still the most advantageous candidate in terms of controlled surface presentation, due to a reduced non-specific protein adsorption. However, PEG is less suitable without further modification, and the necessary processes for functionalizing the surface are more complex than those for Polystyrene or Polycaprolactone. The need to combine radical-based chemical cross-linkers, UV exposure and, ideally, a two-stage process to use the Streptavidin-Biotin non-covalent link means that this process has an increased number of potential failure points.

In contrast, Polystyrene has the advantage of being substantially more beneficial in terms of cellular attachment; treated Polystyrene is a common material for commercially available well plates. However, protein adsorption is high due to the material's hydrophobic nature, and the chemical stability of the material prevents easy covalent binding of proteins, as required for this project, without harsh or dangerous processes. While methods such as plasma treatment[115,263,264], exposure to energetic radiation such as UV or Microwaves[117,265], or harsh pH are possible, more direct chemical modification will require highly reactive species such as radical oxygen or anhydrides[113,114,116].

Polycaprolactone is another polymer that may be a suitable candidate. Active groups suitable for immobilization of proteins can be introduced by hydrolysis in Sodium Hydroxide solutions[135,143], and cell attachment occurs on Polycaprolactone even with the introduction of additional hydrophilic groups[135,147]. MSCs can be cultured on this material both with and without further surface modification[134,142]. Polycaprolactone is also more advantageous compared to Polystyrene due to its lower hydrophobicity, which results in a slower adsorption of proteins out of solution.

Polyacrylamide, Polyethylene, Polyurethanes, Poly (lactic-co-glycolic-acid) and Hyaluronic Acid were all considered as alternative materials, but were discarded due to expected difficulties with surface creation and patterning, material degradation, chemical modification or overall suitability for cell culture.

Based on the material requirements, PEG remains the primary candidate for further work. Polycaprolactone and Polystyrene will be included as secondary choices, should the need for higher hydrophobicity and higher adsorption of proteins be considered an acceptable trade-off for improved cell attachment and proliferation.

Briefly, the following types of immobilization processes are considered suitable for use during this project.

Non-covalent adsorption is the most straightforward process, wherein materials adsorb proteins out of solution without the need for chemical immobilization. Hydrophobic materials adsorb more proteins due to the stronger binding with hydrophobic segments found in most biologically active proteins[234]. While this process requires no prior treatments, it is considered unsuitable due to the length of planned cell culture experiments and the need for a strong, specific binding of selected proteins.

Covalent binding of proteins is performed using various different chemical reactions, such as using amine- or carboxylic acid-reactive crosslinkers to create stable amide bonds, or using photo-reactive crosslinkers[127,128,266]. Covalent binding can include crosslinkers with longer chains to prevent protein denaturation, but this process still retains higher risks due to the need for direct attachment to the proteins of interest, especially if additional reactive groups need to be introduced (such as with thiolation for disulphide linking)[23,24].

Non-covalent, specific protein immobilization can be achieved with a two-stage process, first binding protein combinations with a high specific binding such as complementary DNA or RNA sequences (most commonly for biosensors or assays)[267–269] or Biotin combined with Avidin or Streptavidin[165,173,181,270]. This requires covalent binding of sequences or binding proteins, but afterwards allows for easy binding of multiple different proteins (such as proteins with covalently bound biotin or DNA/RNA sequences) using a single process. This approach maintains a high degree of specificity, but allows proteins to be conjugated with smaller and safer binding chains, reducing the risk of denaturation and loss of function. A process based on the Biotin-Streptavidin binding process was used during chapter 3, and is included in the evaluations during this chapter.

In this chapter, the use of PEG, Polycaprolactone, Polystyrene and a number of material modification strategies including the original PEG-based method, are evaluated for cell culture suitability and effectiveness of protein immobilization. This information will be used to define the final treatment process applied for the combined patterning/protein immobilization experiments.

Methods and results are described throughout this chapter due to the iterative nature of the experimental work.

4.2. Aim and goals

This part of the project aims to verify the suitability of specific material surfaces for long-term culture following functionalization. To do so, this chapter will focus on the following goals:

- Determining the suitability of modified Poly (Ethylene Glycol), Polycaprolactone and Polystyrene surfaces for cell culture by verifying cell attachment and proliferation on selected surfaces
- Verify if the selected covalent or non-covalent protein immobilization techniques can be used to create surfaces with controllable concentrations of immobilized growth factors
- Selecting the most suitable cell culture material and modification method for later cell culture experiments by comparing growth factor immobilization and cell attachment

4.3. Materials and methods

4.3.1. Materials

Acrylate-PEG-NHS and Biotin-PEG-NHS were acquired from Jenkem Technology, USA.

RoosterBio hMSC high performance media kit was acquired from RoosterBio, USA.

TrypLE, Trypsin, Sodium Hydroxide, Hydrochloric Acid, Fibronectin, StemPro culture media, Glutamax, MES buffered saline, 1-ethyl-3-(3-dimethylaminopropyl) carbodiimide hydrochloride (EDC) and N-hydroxysuccinimide (NHS) were acquired from Fisher Scientific Ltd, UK.

Polycaprolactone, Polystyrene, Poly (ethylene glycol) diacrylate, 2,2-dimethoxy-2-phenylacetophenone, Streptavidin, RGD and TGF-β1 were acquired from Sigma Aldrich Company Ltd, UK.

Fluorescent antibodies and isotypes were acquired from BD Biosciences, UK.

4.3.2. Initial creation of PEG-based surfaces

Before analysis can begin, the PEG-based surfaces of interest must first be created, using a process similar to that described in chapters 2 and 3. A schematic overview of the process outlined in this section is shown in Figure 49.

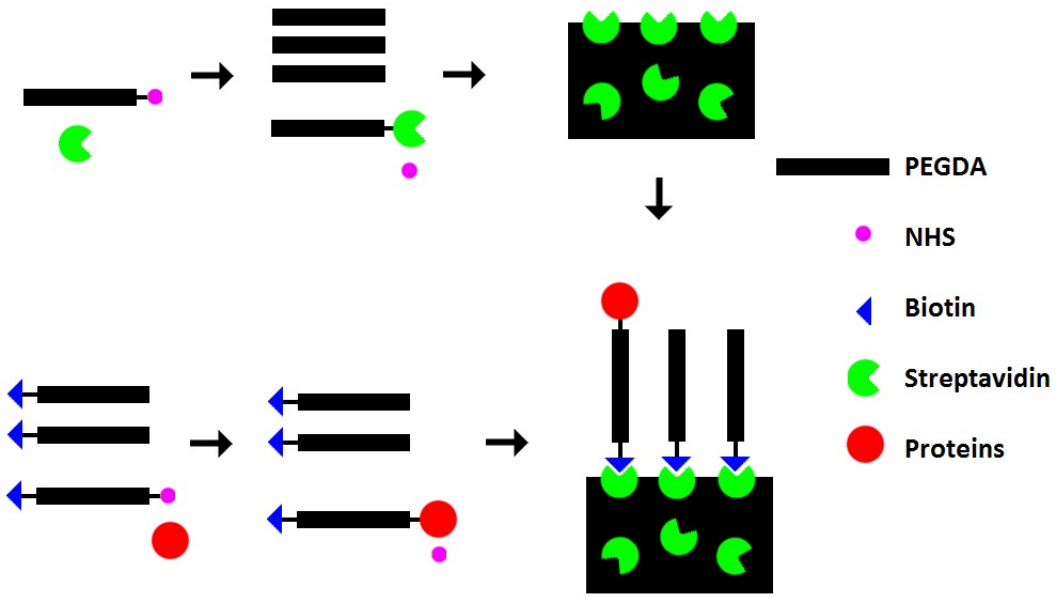

Figure 49: Schematic overview of the cytokine immobilization process, starting from individual components (dimensions not to scale).

Similar to previous methods (see chapters 2 and 3), PEG solutions were created from a mixture of 75% w/w PEG-diacrylate (PEGDA, Mn ≈ 575) with 1 mM Acryl-PEG-N-hydroxysuccinimide (Acryl-PEG-NHS, Mn ≈ 2000) and 1 v/v% 2,2-dimethoxy-2-phenylacetophenone (DMPA) as photo-initiator[95,119,124,236,271]. Cell culture surfaces are initially created in 96-well plates.

After mixing, the material is polymerized by UV-exposure (312 nm wavelength at 10 mW/cm^2 for 45 minutes[24,95,272]) and washed with sterile PBS to remove any unbound components that remain in the material.

4.3.3. Cell attachment and culture on modified PEG-based surfaces

Since Poly (Ethylene Glycol) Diacrylate (PEG)-based surfaces are not suitable for cell culture without modification[95,119,237,273,274], it is necessary to evaluate the effectiveness of including additional cell attachment proteins on the material surface. Therefore, the created surfaces are tested in a cell culture experiment to determine attachment and viability of cultured cells.

Human mesenchymal stem cells (Rooster Bio Inc.) are cultured from passage P+2 in serum-free media to determine the effectiveness of the selected materials. While MSC culture commonly includes the use of fetal bovine serum, serum-free culture environments have been shown to provide increased performance in MSCs[275–279]. The medium used for this experiment consists of StemPro MSC serum free media with added Glutamax as per manufacturer's instructions (2 mM concentration).

Initially, four experimental groups are compared:

- PEG-based surfaces with no treatment after UV-induced polymerization
- PEG-based surfaces with added Streptavidin
- PEG-based surfaces with added Streptavidin and Biotin-PEG-RGD
- Untreated tissue culture plastic (control group)

The PEG-based surfaces are otherwise identical prior to treatment and culture, and are created as flat surfaces without any added patterning or surface features.

4.3.3.1. Creation and modification of experimental surfaces

Streptavidin was prepared for immobilization by mixing the Acrylate-PEG-N-NHS linker with Streptavidin at a 4:1 molar ratio, to a total concentration of 3 mg/mL Streptavidin. The protein and linker are allowed to bind overnight under gentle

agitation at 4-7°C. Any remaining NHS groups are assumed to have hydrolysed at the conclusion of the process.

For Streptavidin-containing experimental groups, Acrylate-PEG-Streptavidin was added to the unpolymerized PEG-Diacrylate solution prior to polymerization described in 4.3.2., to a total concentration 60µg/mL Streptavidin.

RGD was prepared for immobilization by mixing the Biotin-PEG-NHS linker with RGD at a 2:1 molar ratio, to a total concentration of 2mg/mL RGD and allowing the protein and linker to bind overnight at 4-7°C. Any remaining NHS groups are assumed to have hydrolysed at the conclusion of the process.

Biotin-PEG-RGD was diluted 1:15 and added to the appropriate created and functionalized cell culture surfaces at a total volume of 32 µL per well, then allowed to incubate overnight. After incubation, surfaces are washed with sterile PBS.

Four 24-well well plates are created, with total numbers of 9 wells each of PEG, PEG + Streptavidin and PEG + Streptavidin + RGD.

4.3.3.2. Cell culture and analysis

Human Mesenchymal Stem Cells are seeded from P+2 at a density of 5000 cells/cm^2, and cultured in StemPro culture medium (84 mL StemPro media + 15 mL StemPro supplement + 1 mL Glutamax for 2mM concentration). Following cell culture, cells are analysed on day 1 using a Nucleocounter NC-250 (Chemometec, Denmark), and days 3, 6 and 8 using optical microscopy.

For Nucleocounter analysis, cells were detached by incubating with TrypLE (32 µL per well, 10 minutes at 37°C), and cells were counted after pooling collected cells from three wells.

For microscopy analysis, wells are imaged directly without staining or further treatment of cells. All wells are kept for further analysis on later days, and no measurements are sacrificial.

4.3.3.3. Results

NucleoCounter analysis of the collected samples on day 1 showed very low cell counts (<1*10^4 cells total), including measurements on the control group. This indicates a failure to collect sufficient (viable) cells from the cell culture surfaces.

Microscopy analysis on days 3, 6 and 8 showed that while cells seeded on the control surface could attach and proliferate normally, those seeded on the PEG-based surfaces did not. Cells seeded on PEG surfaces, whether functionalized or not, showed severely reduced attachment and a rounded phenotype. This result was expected for untreated PEG surfaces, however a greater amount of cell attachment was expected for the Streptavidin-functionalized and especially the Streptavidin + RGD-functionalized surfaces. This indicates a possible failure in the immobilization of Streptavidin, Biotin-PEG-RGD, or both. Results for day 8 are shown in Figure 50.

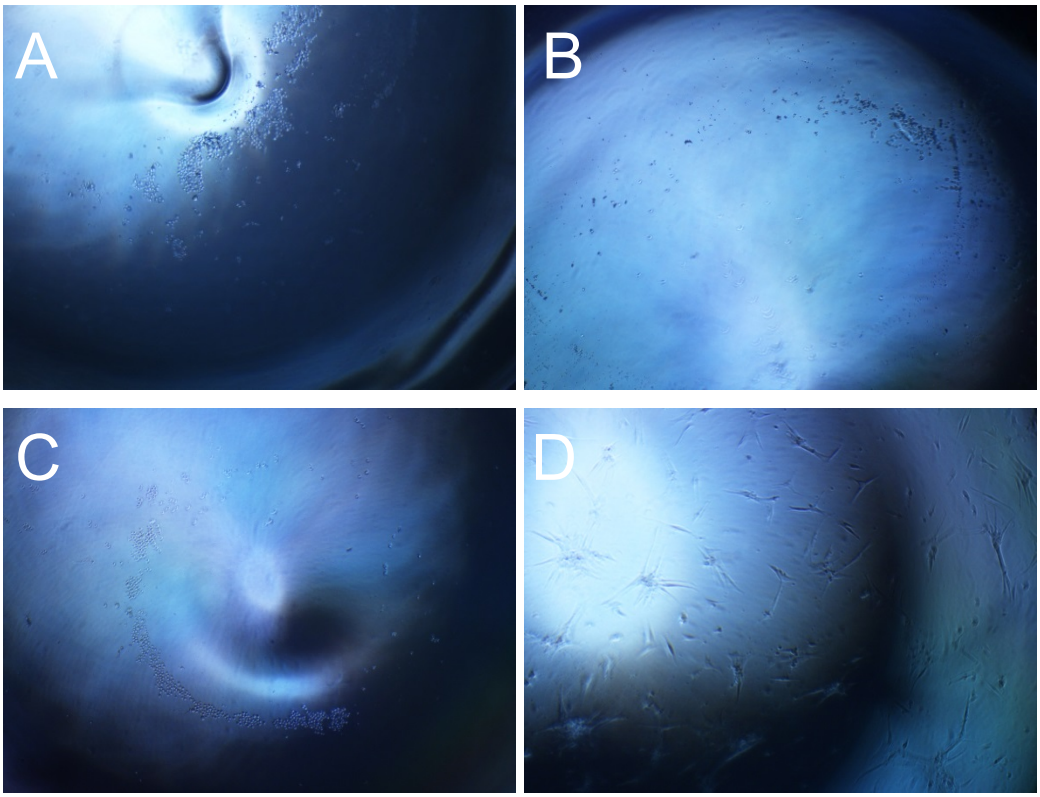

Figure 50: Representative microscopy images for the untreated PEG surfaces (A), Streptavidin-functionalized PEG surfaces (B), Streptavidin+RGD functionalized PEG surfaces (C) and control group (D) at day 8. Note the low seeding density, particularly notable in the contrast between the large, empty spaces in images A, B and C and the small amount of cells (seen as small, round dots).

4.3.4. Expanded cell attachment analysis

The lack of cell attachment during the first experiment casts doubts on the suitability of the Streptavidin-based immobilization of RGD. To determine if cell attachment during the first experiment failed as a consequence of using RGD as the cell attachment protein, or because the proteins themselves were not properly immobilized, the experiment is repeated with the addition of Fibronectin as a comparison.

While Fibronectin was initially not used due to the increased risk of undesired interactions with the cells (including allowing increased adsorption of proteins out of solution), the increased molecular size and availability of cell attachment regions on Fibronectin ensures this material serves as a more powerful cell attachment protein than RGD. As such, Fibronectin will be used as a substitute for RGD, to both serve as a control group and to determine if the previous failure is more likely to be caused by the Streptavidin binding process or the RGD binding process.

Five experimental groups are included in this experiment:

- Untreated PEG
- PEG with added Streptavidin
- PEG with added Streptavidin and Biotin-PEG-RGD
- PEG with added Streptavidin and Biotin-PEG-Fibronectin
- Untreated tissue culture plastic (control group)

4.3.4.1. Creation and modification of experimental surfaces

New polymer surfaces are created for the coming experiments. The processes for creating the 24-well sized untreated PEG surfaces, as well as the addition of Streptavidin and Biotin-PEG-RGD were identical to the methods previously described in this chapter. Biotin-PEG-Fibronectin was created by mixing 0.5 mg Fibronectin with 0.11 mg Biotin-PEG-NHS, for a 1:100 molar ratio and a 0.5 mg/ml concentration of Fibronectin. The solution is allowed to react for 45 minutes at 4-7°C, and is used immediately afterwards for surface functionalization.

Once the Biotin-PEG-Fibronectin is prepared, 50 µL of the solution is added to the appropriate Streptavidin-functionalized PEG surfaces. Surfaces in the other four experimental groups receive 50 µL of PBS to prevent any additional differences due to this step in the process. The well plates are incubated at 37°C for six hours.

4.3.4.2. Cell culture and analysis

In addition to the surface modification, three different media types are investigated due to potential relevance of adsorption of proteins out of solution in the Fibronectin-containing wells.

- RoosterBio medium: RoosterBio serum-free hMSC culture medium prepared as per manufacturer instructions (Roosterbio, Inc.)

- Serum-free medium: 84% v/v Gibco StemPro serum free hMSC culture medium +15% v/v Supplement + 1% v/v Glutamax (ThermoFisher Scientific)
- Serum medium: 75.6% v/v Gibco StemPro serum free hMSC culture medium +13.5% v/v Supplement + 0.9% v/v Glutamax + 10% v/v Fetal Bovine Serum (ThermoFisher Scientific)

Cells are seeded onto surfaces as described before, and each surface + medium combination is cultured in five 96-well plate wells at 37°C and 5% CO_2. Cell cultures are analysed with optical microscopy at days 2, 4 and 6.

Culture media is fully replaced every three days.

4.3.4.3. Results

A number of important differences were seen in the attachment tests performed during this experiment.

Cells showed proper attachment and proliferation on tissue culture plastic as expected. However, no attachment occurred on untreated PEG, functionalized PEG surfaces with Streptavidin, or surfaces further improved with RGD or Fibronectin. The culture medium used had no detectable effect on cell attachment.

Representative cell culture results for day 2 are shown in Figure 51.

Long-term analysis of the cell cultures was not possible due to bacterial contamination of the samples.

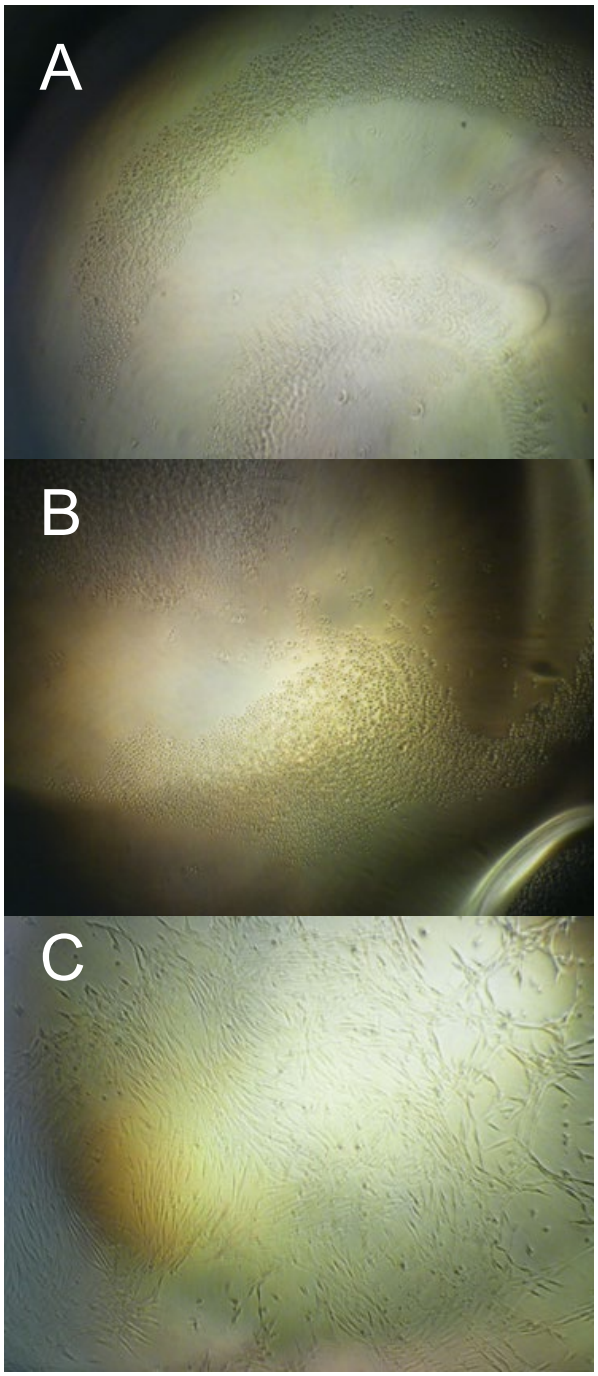

Figure 51: Microscopy imaging of cell attachment on day 2 for culture in serum-free medium, on surfaces with Fibronectin (A), RGD (B) and tissue culture plastic (C). Note the rounded shape of cells in image A and B, indicating poor attachment and cell viability.

However, the total lack of attachment on PEG-based surfaces, even with Fibronectin, indicates that the functionalization process was not sufficient to enable cell culture on PEG.

The most likely cause for the failure of the surface treatment process is the comparatively high UV exposure time needed to fully polymerize the PEG (up to 45 minutes, compared to <5 minutes in literature[95,97,126,133,237]. This is not a major problem for purely PEG-based surfaces; however, inclusion of Acrylate-PEG-Streptavidin during this process exposes the Streptavidin itself to the UV as well. It is unclear how much Streptavidin degradation occurs due to UV exposure, but sufficient degradation of the Streptavidin would prevent immobilization of biotinylated proteins, including the RGD and Fibronectin used during this experiment.

4.3.5. Cell attachment on modified Polystyrene and Polycaprolactone

Previous experiments showed a persistent lack of success in the creation of modified PEG-based cell culture surfaces. Further analysis of the developed process is possible, for example by measuring the exact concentrations of immobilized proteins on the surface. However, the choice was made to reduce the risk of further failures by using Polycaprolactone and Polystyrene instead of PEG for future experiments. New modification techniques are investigated to acquire a suitable cell culture material.

Based on further review of relevant literature, the first surface modification process chosen is the treatment of Polycaprolactone with a Sodium Hydroxide solution, based on published work by Drevelle, Sun and Yeo[135,143,280]. Short-term exposure to the Sodium Hydroxide solution results in degradation of the ester groups in Polycaprolactone, creating new oxygen-rich functional groups at the surface of the polymer, which can be used for further immobilization processes. Long-term exposure will not be tested as this can result in not only surface chemistry alterations, but also significant degradation of the material at macro-scale levels[148].

The second process chosen for this experiment is the treatment of Polycaprolactone and Polystyrene with a solution of Laccase C. The Laccase acts as a catalyst for the creation of reactive oxygen species from molecular oxygen, which in turn react with the polymers for the creation of new functional groups. The greater reactivity of the created oxygen species is expected to cause more rapid modification of surface

chemistry, as well as more rapid degradation of the polymer. However, the higher health and processing risks that must be considered for the use of Laccase solutions means that Sodium Hydroxide treatment remains the preferred method.

Regardless of the method, the created functional groups (carboxylic acids, alcohols, aldehydes) on the Polycaprolactone and Polystyrene surfaces may then be used for immobilization of various proteins, but this step is not performed during this experiment and all surfaces are only chemically treated with no additional proteins.

This experiment focuses on the suitability of treated and untreated Polycaprolactone and Polystyrene for adherent cell culture of human Mesenchymal Stem Cells.

4.3.5.1. Cell attachment on modified Polystyrene and Polycaprolactone

The following experimental groups are included in the experiment:

- Untreated Polycaprolactone as a control group
- Untreated Polystyrene as a control group
- Polycaprolactone surfaces treated with 0.5M NaOH, for a duration of 1, 2 or 4 hours of exposure.
- Polycaprolactone surfaces treated with 0.25 u/mL Laccase C, for a duration of 2 hours of exposure.
- Polystyrene surfaces treated with 0.25 u/mL Laccase C, for a duration of 2 hours of exposure.

Note: Laccase concentrations are provided as ‘unit per mL’ and not the molar concentration, to account for potential differences in enzymatic activity between different batches and suppliers.

Initial surfaces are created using the vacuum oven-based process described in chapter 2. Surfaces are kept sterile and, where appropriate, treated with Sodium Hydroxide or Laccase C in a biological safety cabinet to prevent contamination.

After treatment, MSCs are seeded onto the surfaces at a density of 20,000 cells/cm^2 in RoosterBio media as described before, and cultured at 37°C and 5% CO_2 for 24 hours to allow for attachment.

Following attachment, cells are stained with a 1%w/v Toluidine Blue solution for 10 minutes. Cell attachment and morphology on the different surface types is evaluated using optical microscopy. Cell attachment and health will primarily be evaluated based on morphology, spread, and cell density per surface area. No additional cell culture is performed past the initial 24 hours.

4.3.5.2. Results

After 24 hours of incubation time, most of the selected surface materials showed cell attachment. The main differences between materials are found in the ratio between fully attached and spread out cells, and the amount of cells that remain in a rounded morphology, indicating limited attachment and health.

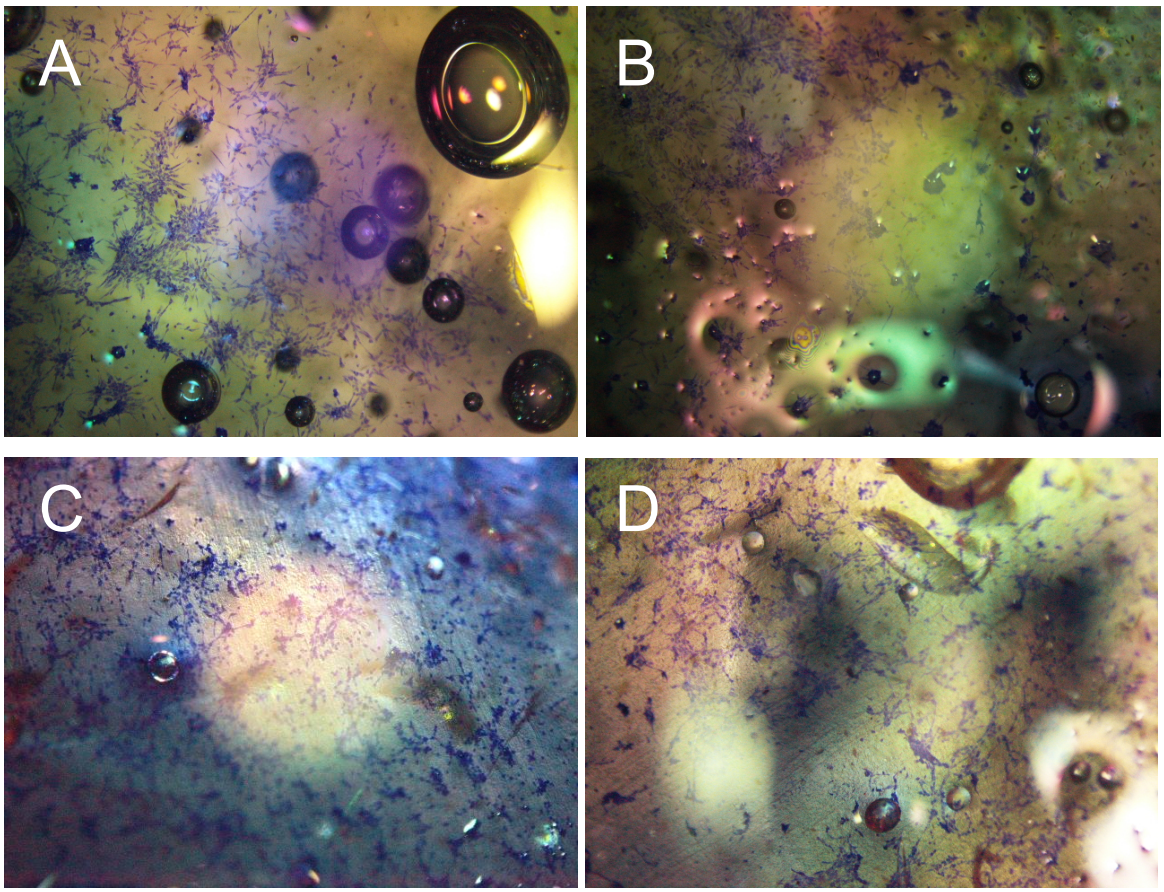

Figure 52: hMSC attachment on surfaces made of untreated Polystyrene (A, B) and Laccase-treated Polystyrene (C, D). Note: due to light reflections from the material interfering with analysis, image brightness was modified for clearer visualization. No other alterations to the images are made.

Both untreated and Laccase-treated Polystyrene showed excellent attachment, as was expected due to the higher hydrophobicity of the starting material. Almost all cells are fully attached and showing the desired, spread out morphology. This shows the Polystyrene-based surfaces allow for good cell culture environments, though

increased influence of protein adsorption still makes these surfaces a secondary choice. Representative surfaces for both Polystyrene types are shown in Figure 52.

Untreated Polycaprolactone and Laccase-treated Polycaprolactone show attachment from the seeded cells, but also show a number of cells with a rounded morphology. These surfaces therefore allow for cell attachment, but may be reconsidered for further use due to potential difficulties with long-term cell viability and expected non-specific binding of proteins and other components out of the culture medium. Representative surfaces for untreated and Laccase-treated Polycaprolactone are shown in Figure 53.

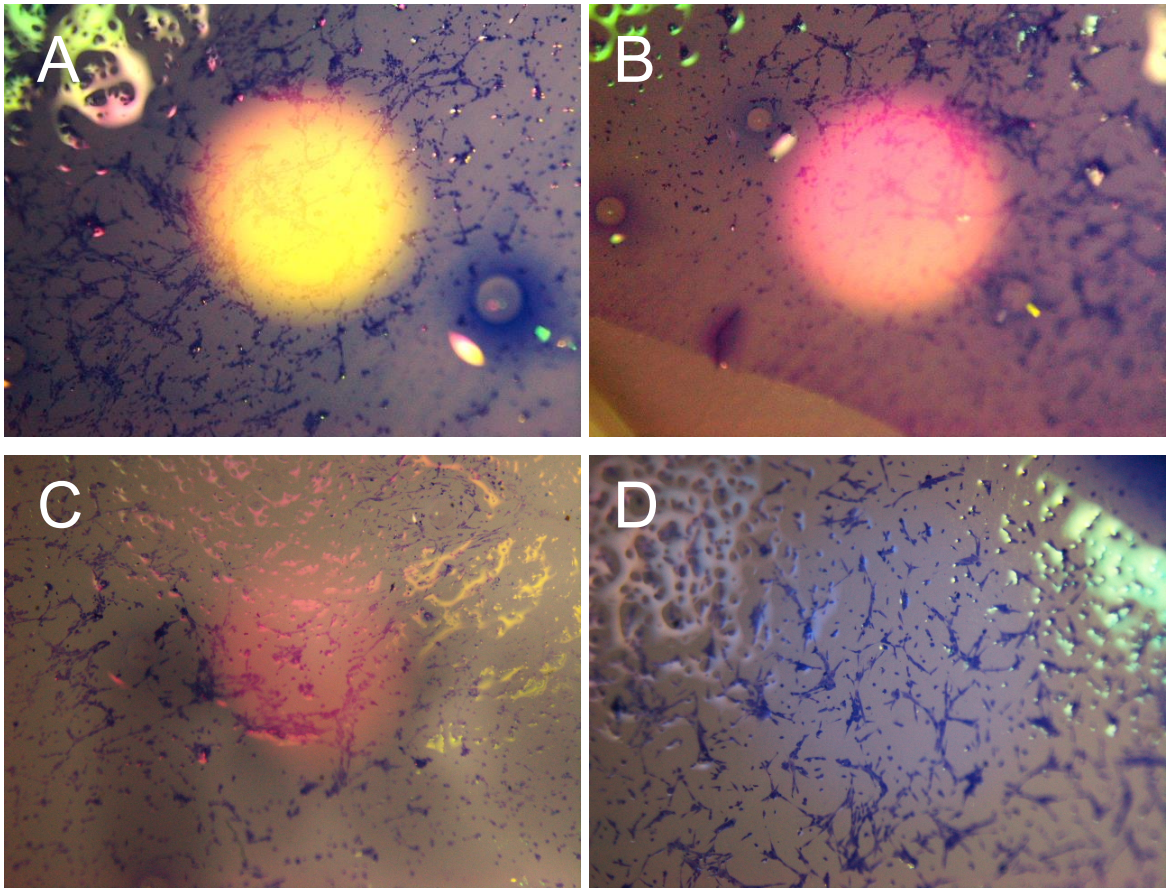

Figure 53: hMSC attachment on surfaces made of untreated Polycaprolactone (A, B) and Laccase-treated Polycaprolactone (C, D). Note: due to light reflections from the material interfering with analysis, image brightness was modified for clearer visualization. No other alterations to the images are made.

Polycaprolactone surfaces that were treated with Sodium Hydroxide showed different levels of cell attachment depending on the total treatment time. Treating the surface for one or two hours resulted in good cell attachment comparable to untreated Polycaprolactone. The surfaces treated for four hours showed fewer cells with the desired attachment and morphology, with the majority of cells having either

failed to attach or showing a rounded morphology. Treatments of four hours or longer are therefore not considered suitable and will not be used for any further work. One- and two-hour treatments do allow for suitable cell attachment, providing results comparable to the two-hour Laccase treatment. Representative surfaces for all three Sodium Hydroxide-treated Polycaprolactone materials are shown in Figure 54.

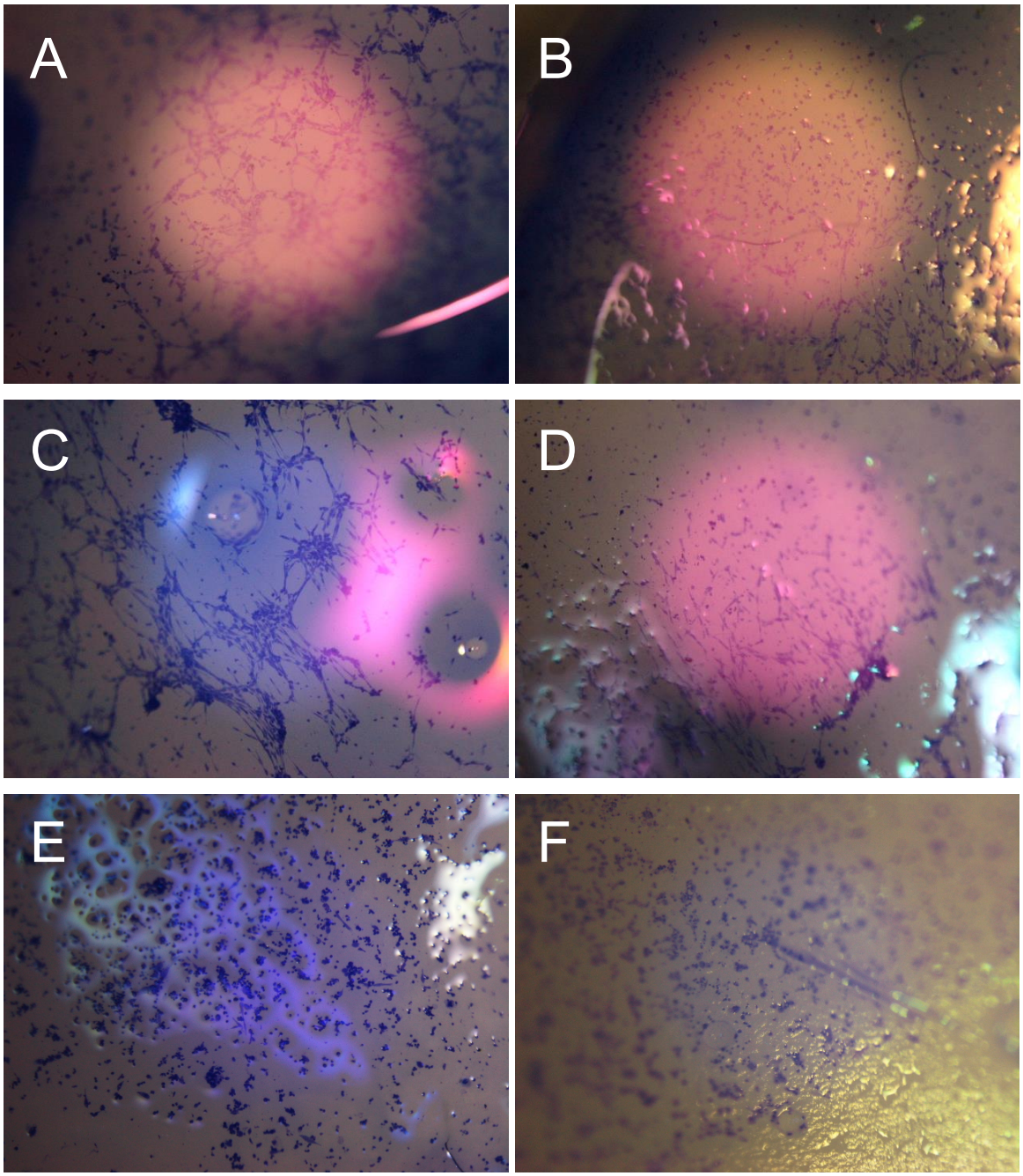

Figure 54: hMSC attachment on surfaces made of Polycaprolactone treated with Sodium Hydroxide for 1 hour (A, B), 2 hours (C, D), and 4 hours (E, F). Note: due to light reflections from the material interfering with analysis, image brightness was modified for clearer visualization. No other alterations to the images are made.

While it was not possible to acquire quantitative measurements for cell attachment for this experiment, it does provide sufficient information to continue with further cell culture experiments. Both Polystyrene and Polycaprolactone can be modified without eliminating the capacity for cell attachment on the surface.

Based on these results, both the 2-hour Laccase treatment and the 1-hour or 2-hour Sodium Hydroxide treatments on Polycaprolactone are considered suitable for surface modifications. For later experiments, Polycaprolactone incorporating a 2-hour treatment with Sodium Hydroxide will be used to ensure sufficient functional groups. 1-hour Sodium Hydroxide treatment may be considered if further problems are encountered in later experiments; Laccase treatment will not be included due to the higher costs and risks involved in the use of the required Laccase solutions.

4.3.6. TGF-β1 immobilization on functionalized Polycaprolactone

It is now possible to create cell culture surfaces with the necessary groups for (covalent) binding of proteins. Before cell culture experiments using these surfaces can begin, it is necessary to verify both the immobilization of such proteins and whether it is possible to create varying surface concentrations through alterations of the treatment process.

Based on literature, soluble TGF-β1 concentration ranging from approximately 0.01 nM to 1 nM during cell culture [20,24,47,281] can induce both differentiation and upregulated production of extracellular matrix in hMSCs. To ensure a similar concentration of total growth factors per well using immobilized TGF-β1, the peak surface concentration should be 0.5 pmol TGF-β1 per square cm, or 25 ng/cm^2 (total surface area is 2 cm^2 per well).

The following experimental groups are included in the experiment:

- Untreated Polycaprolactone as a control group
- Untreated Polystyrene as a control group
- Polycaprolactone surfaces treated with 0.5M NaOH, for a duration of 1, 2 or 4 hours of exposure.
- Polycaprolactone surfaces treated with 0.25 u/mL Laccase C, for a duration of 2 hours of exposure.

- Polystyrene surfaces treated with 0.25 u/mL Laccase C, for a duration of 2 hours of exposure.

Sterile flat Polycaprolactone and Polystyrene surfaces were created in a vacuum oven, using the process described in chapter 2. Briefly, polymer pellets were placed in a silicone mould based on the shape of a 24-well plate and melted at a temperature of 175°C for 30 minutes. Samples were then placed in a sterile, sealed autoclave bag and kept at 175°C for a further 60 minutes to ensure sterility.

After samples have cooled down, they are transferred to sterile storage for later use.

Created samples are functionalized as described before. All surfaces are washed with PBS between steps of the functionalization process.

Polycaprolactone samples are treated with 0.25 u/mL Laccase for 2 hours, or with 0.5M Sodium Hydroxide solution for 1, 2 or 4 hours. Polystyrene surfaces are treated only with 0.25 u/mL Laccase for 2 hours. Functionalized surfaces are then treated with a solution of 0.380 mg/mL EDC (1-ethyl-3-(3-dimethylaminopropyl)carbodiimide hydrochloride) and 0.575 mg/mL NHS (N-Hydroxysuccinimide) in MES buffered saline (0.1M, 0.9% sodium chloride, pH 4.7) for 15 minutes.

Finally, all surfaces are washed and treated for two hours with TGF-β1 solutions in PBS of 0.4 µg/mL, 0.2 µg/mL, or TGF-β1-free PBS as a control group.
After treatment, non-specific binding is blocked by addition of 1.5 mg/mL Bovine Serum Albumin for 15 minutes, followed by washing in sterile PBS.

TGF-β1 immobilization is verified by incubating all samples with fluorescent antibodies (Alexa Fluor 488-conjugated anti-TGF-β1) at manufacturer's recommended concentration for 30 minutes. Samples are washed with PBS, and fluorescence intensity is measured using a FLUOStar Omega plate reader. Fluorescence is compared to a dilution series of Alexa Fluor (0.165 nMol – 1.29 pMol per well) to calculate the total amount of immobilized TGF-β1 antibody in each well. All individual measurements are performed as N=1, with no replicates.

4.3.6.1. Results

Calculation of the amount of immobilized TGF-β1 antibody showed a number of important differences between the materials used in this experiment. The calculated antibody values for the different materials are shown in Table 1.

	0.4 µg/mL TGF-β1	0.2 µg/mL TGF-β1	No added TGF-β1
PS Untreated	3.65	4.01	4.43
PCL Untreated	4.18	2.94	3.69
PS + Laccase	2.21	0.80	1.47
PCL + Laccase	2.10	1.52	1.15
PCL + 1h NaOH	2.41	1.28	1.68
PCL + 2h NaOH	2.26	1.90	1.65
PCL + 4h NaOH	2.15	1.92	1.05

Table 1: calculated TGF-β1 antibody immobilization onto surfaces, in pMol per well.

Polystyrene showed higher fluorescence than Polycaprolactone, but this was largely independent of the concentration of TGF-β1 used to treat the surfaces. This result, especially the high value for the TGF-β1-free surface, indicates that most of the signal is caused by nonspecific binding of the fluorescent antibody, though differing optical properties of the material compared to Polycaprolactone may also play a part in the comparatively higher values.

Laccase treatment of Polystyrene substantially reduced antibody binding, further supporting this interpretation as the reduced hydrophobicity of the Polystyrene would reduce nonspecific binding. This also indicates that any added capacity for specific binding through the EDC + NHS crosslinking process is responsible for a smaller portion of the signal than nonspecific binding. More long-term treatment of the surface could further clarify this effect, but such measurements were not performed.

Untreated Polycaprolactone showed a substantially higher fluorescence than treated Polycaprolactone, which is again in line with the expectations regarding a higher hydrophobicity resulting in increased specific and non-specific binding. The fluorescence of Sodium Hydroxide-treated and Laccase-treated Polycaprolactone surfaces exposed to 0.4 µg/mL TGF-β1 are consistently higher than surfaces treated with 0.2 µg/mL TGF-β1, which in turn show a higher signal than TGF- β1-free surfaces. This indicates that despite measurement issues a repeatable difference in the amount of immobilized protein could be established. Resulting immobilizations are similar enough that each method is likely equally suitable, offering little advantage or disadvantage of selecting one over the other. However, Laccase- and 4-hour Sodium Hydroxide-treated surfaces show a reduced fluorescence without TGF-β1, suggesting a further reduced non-specific binding and a higher level of hydrolysis on the treated surfaces. The consistent differences in the measured

immobilization based on used TGF-β1 concentrations suggest both the Sodium Hydroxide-based treatment and the Laccase C-based treatment would provide good control over surface properties for future experiments.

However, the measurements do show substantial variation in fluorescence that can't be attributed to the surface chemistry and proteins. In particular, several of the 0.2 µg/mL TGF-β1 samples show a lower fluorescence than samples without TGF-β1, especially in the untreated and Laccase-treated experimental groups. Consequently, the exact values of measurements may be unreliable and only larger trends should be used to inform decisions regarding future experiments. It is unclear what caused these effects, though a potential explanation may be that small differences in the geometry of the samples resulted in differing reflection or refraction, which may have an impact on the measured fluorescence intensity.

4.4. Discussion

The work performed in this chapter showed substantial difficulties in creating functional cell culture surfaces as originally designed in chapter 2. The immobilization of proteins for mediation of cell attachment on the surface failed to support cell attachment and further culture both for the inclusion of RGD sequences and Fibronectin.

Although the exact cause of the failed immobilization is not known, the fact that neither modification was successful suggests that the problem lies in the original immobilization process, failing to bind functioning Streptavidin. The failure to bind this protein despite successes reported in literature may be due to the need for a more rigid structure and, consequently, a higher PEG-to-water ratio in the created material compared to the hydrogels created by Zhu, Hern and Nuttelman that were used as the initial starting point for the experiment designs[95,133,282]. Additionally, the longer UV exposure necessary for full polymerization compared to that for such gels may likewise have caused a negative impact on protein immobilization through a more substantial degradation of Streptavidin.

After modifying the experimental design to include different materials, a method for immobilizing bioactive proteins onto the cell culture surfaces was successfully developed. Modified Polycaprolactone surfaces were shown to provide variable

protein immobilization under controlled conditions, suitable for the remainder of the experiments planned for this project. The calculated amounts of immobilized protein, while only approximations, will allow for the creation of multiple different concentrations of immobilized protein during later experiments.

The use of Polycaprolactone also provides a minor benefit in that patterns may be created without the need for on-site polymerization.

In retrospect, determining a rough estimate of immobilization effectiveness would have been more effective than immediately attempting to quantify the proteins in terms of surface area. This perhaps illustrates the importance of not staying overly reliant on results in literature, and to perform smaller scale verification of a process before proceeding to full-scale experiments and improvements.

Despite these setbacks, a suitable cell culture surface was developed. Based on the experimental results shown in this chapter, Polycaprolactone surfaces provide a good balance of desired properties. Polycaprolactone allows for cell attachment and proliferation both with and without functionalization, while at the same time enabling a controlled level of immobilization of relevant growth factors following induced hydrolysis and Carbodiimide crosslinking. Furthermore, while treated surfaces do show some non-specific binding, they result in lower such binding than seen with Polystyrene-based materials. These results, when compared to the use of Poly (Ethylene Glycol) or Polystyrene, show a clear advantage for the use of Polycaprolactone.

Therefore, Polycaprolactone-based surfaces will be used for the remainder of the experimental work in this project. As longer treatment with Sodium Hydroxide shows little improvement past 2 hours, future cell culture experiments will initially use Polycaprolactone surfaces treated with 2h of Sodium Hydroxide exposure similar to the process described by Drevelle and Yeo[135,280].

Chapter 5: combined patterning and immobilization for cell culture

5.1. Introduction

With the completion of the experiments described in the previous chapter, it is now possible to perform a cell culture experiment incorporating both patterned cell culture surfaces and immobilized growth factors.

In this chapter, the patterning process developed and described in chapter 2 is combined with the material modification and protein immobilization developed in chapters 3 and 4.

Due to the complexity of the cellular environment and the numerous methods of manipulation and analysis possible for cell culture of human Mesenchymal Stem Cells, it is necessary to decide which aspects to cover and which to ignore. Given that the goal of this project is not aimed at solving a specific medical challenge but has focused primarily on chondrogenesis as its proof of concept, the final experiments must be placed in this context.

As such, the experimental work described in this chapter will focus primarily on inducing differentiation and matrix production in human Mesenchymal Stem Cells using the different patterning sizes and protein immobilization concentrations analysed during previous chapters. As before, culture surface patterning will include feature sizes around the approximate cell size as this range is thought to be the most promising for creating synergistic effects and identifying further underlying mechanisms after the experiments have concluded.

Analysing the rate and growth factor requirements of cellular differentiation will show whether patterning and/or immobilization of growth factors can be used during early stages of cell culture, while total matrix production can provide insight into potential long-term advantages or disadvantages. In particular, the need for cultured chondrocytes to not only show the correct phenotype but also produce suitable extracellular matrix for viable tissue engineering procedures (such as the creation of artificial cartilage) means that overall Collagen production should provide critical insight into whether cultured cells mature into a fully functional chondrocyte phenotype.

Both surface topology and cytoskeletal alterations have already been implicated in altered behaviour of focal adhesion sites in adherent culture of mesenchymal stem

cells[18,222], as well as having a direct impact on cell differentiation[283,284]. Together, these findings strongly suggest that alterations of cell morphology and adhesion characteristics may have further effects not only on the sensitivity of cultured cells to exposed growth factors, but specifically to growth factors at the contact between cells and the underlying substrate.

Feature sizes are selected primarily to provide a wide range of potential effects. While most published work focuses on either regular patterning of sub-cellular feature sizes (<1µm)[215,224], larger-scale features have also shown substantial influence[216]. As such, the selected feature sizes are chosen to allow analysis of both these approaches, with the range of used feature sizes centred on (approximate) cellular size and extending towards both sub-cellular scale and scales substantially larger than the cultured cells. Sub-micron feature sizes and features larger than 100µm will not be considered during this project due to practical limitations.

Likewise, the selected TGF-β1 concentrations used during these experiments are chosen to provide a sufficiently wide range of concentrations to identify potential saturation effects, based primarily on previous work by Fisher, Hume, McCall and Mann[20,23,24,281]. TGF-β1 concentration ranges outside of the 0.02 - 0.2 pmol/cm^2 or equivalent soluble concentrations may be considered depending time constraints.

Beyond the process developed in previous chapters, the introduction of new techniques is minimized to avoid adding additional complexity to the planned experiments. The main exception to this is the analysis of the cultured cells, which is more thorough than that used during previous experiments. Cultured cells will be analysed using Flow Cytometry to determine early marker expression, fluorescent staining of deposited Collagen II to evaluate extracellular matrix production, and metabolic activity during cell culture is quantified.

5.2. Aim and goals

This part of the project will attempt to test the hypothesis suggested in chapter 1 of this thesis:

- Topological features of cell culture surfaces will influence the effective concentration of immobilized growth factors, with smaller feature sizes resulting in a higher effective concentration

In order to test this hypothesis, the following goals are set for this part of the project:

- Determine the influence of pattern size (topology) on the differentiation of hMSCs and the extracellular matrix production of differentiated cells
- Determine the effectiveness of immobilized growth factor TGF-β1 compared to providing this growth factor in solution
- Identify, where applicable, synergistic or antagonistic effects of combining patterned cell culture surfaces and the use of immobilized or soluble growth factors

5.3. Materials and methods

5.3.1. Materials

The experimental work described in this chapter used microparticles acquired from Polysciences Europe GmbH, Germany, rather than Phosphorex Inc. USA (the previous supplier).

Mold Star 15 Slow silicone was acquired from Bentley Advanced Materials, UK.

RoosterBio hMSC high performance media kit was acquired from RoosterBio, USA.

Polycaprolactone, NHS, TGF-β1, Anti- Collagen II conjugated Rabbit IgG and FITC-conjugated anti-Rabbit IgG were acquired from Sigma-Aldrich Company Ltd, UK.

EDC, MES buffered saline and Rabbit IgG were acquired from Fisher Scientific Ltd, UK.

FITC-conjugated anti-CD90, PE-conjugated anti-CD105 and their isotype controls were acquired from BD Biosciences, UK.

5.3.2. Design of combined patterning-immobilization experiments

The final experiment of this project was developed as a paired two-level factorial design with center-point, one for the cultures on surfaces created with immobilized TGF-β1 and one for cultures with TGF-β1 in solution.

Although additional options were initially considered for both pattern scales and concentrations of TGF-β1, only three options are included during these experiments:

two corner points each for pattern feature size and concentration, respectively. Expanding the number of different environments used during the coming experiment could provide additional information, but would also result in greatly increased workload to create and modify the necessary surfaces prior to cell culture and analysis.

The two-level factorial design will only provide a preliminary description of any relationships between patterning, growth factor concentrations and cell behaviour, but it can still be used to estimate a linear model between these parameters as well as identify potential non-linear effects such as exponential or logarithmic relationships even if such relationships cannot be precisely parameterized using the current experimental design. This approach is the most efficient for addressing the original hypothesis as stated in chapter 1, while providing further support for additional experiments that may be considered in the future.

Both corner points and centre points in this experiment are initially planned to be performed with two replicates for metabolic analysis, marker expression analysis, and Collagen production analysis. Each replicate consists of a single well. However, do note that this planned design was not kept for the marker expression and Collagen production aspects during the experimental run due to adverse results (see section 5.4.2 and 5.4.3 for more details).

As before, surface feature sizes were selected to provide features ranging from smaller than cell size (of Mesenchymal Stem Cells) to larger than cell size. The surface topologies used during cell culture are pattern sizes of 49.1 µm diameter for larger-than-cell-size features, 1.93 µm diameter for sub-cellular sized features, or 18.8 µm diameter for center-points of approximately equal size to cultured cells. Used TGF-β1 concentrations for the experiments with immobilized TGF-β1 are 0.2 pmol/cm^2, 0.02 pmol/cm^2, or 0.1 pmol/cm^2 for center-points, while used TGF-β1 concentrations for the experiments with soluble TGF-β1 are 0.4 pmol/mL, 0.04 pmol/mL, or 0.2 pmol/mL for center-points. Flat surface materials and TGF-β1-free culture conditions are included as controls but are not part of the main experimental analysis.

To distribute labour more evenly, half the selected samples are seeded, cultured and analysed at a one day offset compared to the other half. All center-point samples are

cultured in duplicate, one each starting during initial culture and one starting at the offset. This will enable detection of potential bias due to the later cultures having received one additional day of preparatory culture prior to seeding at T=0.

Combined, the following sample types are included in the experiment:

Immobilized TGF-β1 samples:

- 0.2 pmol/cm^2 + 49.1μm pattern
- 0.2 pmol/cm^2 + 1.93 μm pattern
- 0.02 pmol/cm^2 + 49.1 μm pattern
- 0.02 pmol/cm^2 + 1.93 μm pattern
- 0.1 pmol/cm^2 + 18.8 μm pattern (centerpoint, standard culture time)
- 0.1 pmol/cm^2 + 18.8 μm pattern (centerpoint, offset culture time)

Soluble TGF-β1 samples:

- 0.4 pmol/mL + 49.1μm pattern
- 0.4 pmol/mL + 1.93 μm pattern
- 0.04 pmol/mL + 49.1 μm pattern
- 0.04 pmol/mL + 1.93 μm pattern
- 0.2 pmol/mL + 18.8 μm pattern (centerpoint, standard culture time)
- 0.2 pmol/mL + 18.8 μm pattern (centerpoint, offset culture time)

Control samples:

- TGF-β1-free + 18.8 μm pattern
- TGF-β1-free + flat surface
- 0.1 pmol/cm^2 + flat surface
- 0.2 pmol/mL + flat surface

5.3.3. Creation of patterned surfaces for cell culture

Patterned cell culture surfaces were created using the process developed and described in chapter 2.

Silicone micrometre-scale patterns were created from commercially available microparticles with diameters of 49.1±1.34 μm, 18.8±1.20 μm or 1.93±0.05 μm.

Microparticle solutions were placed in 24 well plate wells and dried at 90°C for up to three days to create a dry powder composed of regularly stacked microparticles. The dry particles were then carefully covered with uncured silicone mix, created per manufacturer's instructions, while ensuring the particle layer receives only the minimum amount of disruption by adding only small volumes of silicone at a time. A vacuum is applied to degas the silicone mixture and to remove any air bubbles that might remain, after which the silicone mix was allowed to cure overnight. Once cured, the created silicone surfaces have a topology of regular patterns with feature sizes equal to the dimensions of the used microparticles.

The silicone patterns were then copied into solid Polystyrene. The silicone surfaces were removed from the well plates, and Polystyrene pellets were added and heated to 175°C for 1 hour under vacuum. After fully melting, the Polystyrene is allowed to cool, and the Polystyrene and silicone are carefully separated.

The process for creating silicone patterns was then repeated using the polystyrene patterns, rather than the original microparticles, as the base mould to create a total of ten silicone patterns of each pattern size.

Finally, these silicone patterns were used to create Polycaprolactone patterns by adding Polycaprolactone pellets and heating to 175°C for 30 minutes under vacuum. The created surfaces were placed in a sealed, paper autoclave sterilization bag and kept at 175°C and atmospheric pressure for an additional 60 minutes to ensure sterility. A total of 40 Polycaprolactone surfaces were created for each pattern size, as well as an additional 40 'flat' surfaces without any microparticle-based pattern that are intended for use as control groups.

Created Polycaprolactone surfaces were allowed to cool and were stored sterile at 4-7°C until further processing. Examples of created surfaces are shown in Figure 55.

5.3.4. Immobilization of TGF-β1 onto prepared surfaces

With the creation of the patterned surfaces for cell culture, the next step is to add the desired immobilized growth factors. TGF-β1 immobilization is based on the hydrolysis and crosslinking process developed and described in chapter 4.

All previously created Polycaprolactone surfaces are treated by submersion in filter-sterilized 0.5M Sodium Hydroxide solution for 2 hours. This process is used to add

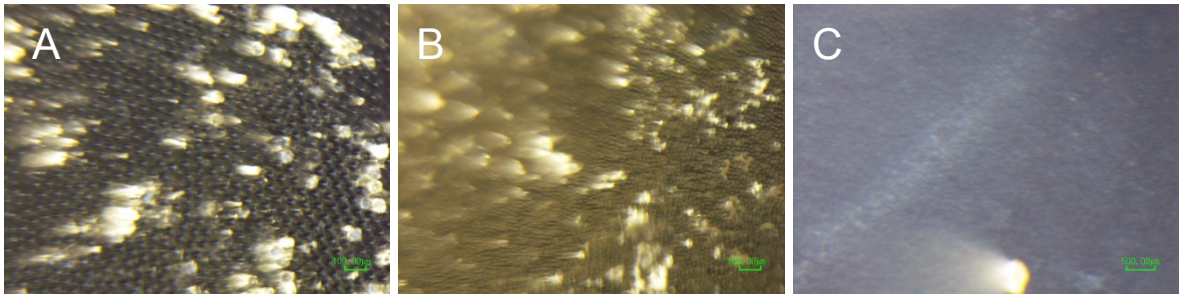

Figure 55: examples of three created patterns used during the experiment with feature sizes of 49.1µm (A), 18.8µm (B) and 1.93µm (C). Scale bars are 100µm in the left and middle image, and 20µm in the right image.

functional oxygen groups to the surface by hydrolysis of the ester groups in the Polycaprolactone polymer chains.

Treated samples are then washed with sterile PBS, and placed in 24-well plate wells. Each sample is treated with 1.5 mL per well of a solution of a 0.380 mg/mL EDC (1-ethyl-3-(3-dimethylaminopropyl) carbodiimide hydrochloride) and 0.575 mg/mL NHS (N-Hydroxysuccinimide) in MES buffered saline (0.1M, 0.9% sodium chloride, pH 4.7) for 15 minutes.

Immediately after, all surfaces assigned to groups with immobilized TGF-β1 are washed in sterile PBS and treated for 2 hours with the appropriate sterile solutions of TGF-β1 in PBS. TGF-β1 solutions used are 1.5 mL per well at 26 ng/mL, 13 ng/mL and 2.6 ng/mL, which based on the results of the work from chapter 4 will create surface concentrations of approximately 0.2 pMol/cm2, 0.1 pMol/cm2 and 0.02 pMol/cm^2 respectively. Surfaces assigned to groups with soluble TGF-β1 are washed and kept in sterile PBS for 2 hours.

After immobilization of TGF-β1, samples are washed in sterile PBS and stored at 4-7°C until the start of the cell culture.

Samples without immobilized TGF-β1 receive the same treatments using sterile PBS without any added EDC, NHS or TGF-β1.

5.3.5. Cell culture on created surfaces

Following the creation and functionalization of the polymer surfaces, the next experimental step is the addition of cells for long-term cell culture on these materials.

All media used for cell culture (TGF-β1 free, low, medium and high concentration media) is prepared before cell culture begins, with unused media stored in the fridge at 4-7°C until use.

Prior to experiments, hMSCs were taken out of nitrogen storage, thawed, and cultured for one week at an initial density of 5000 cells/cm^2 to ensure cells no longer suffer any potential lingering negative effects of cryopreservation. At the time of seeding, cells were at passage P+3. Two separate flasks are used for initial culture to account for the staggered experimental work, as described in the section on experimental design.

Cells are seeded onto the prepared surfaces at an initial concentration of 20,000 cells per well (10,000 cells/cm^2). Cells are added to the surface in a single drop (30 µL at 6.6*10^5 cells per mL, calculated using a Nucleocounter cell counter) in order to prevent cells from spilling over the side of the treated samples and attaching on the bottom of the well plate well.

Cells are allowed to attach for 3 hours at 37°C based on Mobasseri and Rana[285,286] after which an additional 1.5 mL of cell culture medium is carefully added to each well.

Cell culture takes place at 37°C, 5% CO_2 and 90% humidity, and the culture medium is changed every 3 days. Because the size and shape of the samples prevents implementation of a complete medium change, a partial medium change of 500 µL per well is used instead.

All spent media collected during the media change is stored frozen at -20°C for later analysis of metabolic activity.

Cells are cultured in separate well plates for each intended measurement time point. With the exception of media collection, all measurements are sacrificial and remove the entire well plate from culture. Wells are sacrificed for analysis at day 2, day 4, day 14 and day 21.

5.3.6. Analysis of metabolic activity

Media collected every three days during the cell culture is analysed for metabolic activity using a Cedex Bio HT Analyzer (Roche Diagnostics GmbH). Previously

frozen samples are thawed, vortexed and centrifuged at 1000g for 5 minutes prior to analysis. Tests are performed in a randomized order to prevent time-based measurement biases. Samples are tested for Glucose and Lactate concentrations with two replicates based on the original experimental design (i.e. one measurement per well).

5.3.7. Analysis of early culture marker expression

At day 2 and 4, cells are analysed for surface markers indicative of cellular differentiation. As cellular expression markers CD90 and CD105 are downregulated during differentiation into chondrocyte lineage[39], the presence of these markers is tested using flow cytometry.

First, all relevant surfaces are transferred to new wells. The used wells are checked with microscopy to identify potential populations of cells that have grown on the bottom of the plate instead of the treated surfaces, for example due to spilling of cells during the initial seeding process.

The transferred surfaces are placed into a 0.25% Trypsin-EDTA solution and are incubated at 37°C for 10 minutes. Trypsin was used as a more powerful alternative to TrypLE to reduce risk of cells being left on the surface. Although Trypsin has been shown to degrade expressed surface markers[287], short incubation times will cause only minor reductions in signal and this degradation was not considered a problem.

To reduce the risk of insufficient data points during each measurement, all original replicates are pooled, reducing the number of replicates to one but reducing the risk of the remaining measurement. The pooled volume is used for both standard and isotype measurements. Samples are centrifuged and washed in PBS, then split into two groups.

Samples were incubated in 1 mL of fluorescent antibody solution or equivalent Isotypes for 30 minutes, all at a concentration of 1 test per mL or equivalent Isotype concentration. PE-conjugated anti-CD105 and FITC-conjugated anti-CD90 were incubated simultaneously for stained groups. PE-conjugated Rabbit IgG Isotype and FITC-conjugated Rabbit IgG Isotype were incubated simultaneously for Isotype controls.

Following incubation, cells were analysed using a BD FACSCanto II Flow Cytometer, using the following measurement parameters: FSC=150V, SSC=150V, FITC=450V, and PE=450V. An FSC threshold of 2500 was applied to filter out debris from the measurements. Compensation for spectral overlap was calculated and used at 0.75% for PE to FITC and 23.5% for FITC to PE. All collected material was used for experiments to ensure maximum recovery of cells and event count for each sample. All cells were kept at 4-7°C and protected from all light between incubation with fluorescent markers and each sample's measurements.

Measured data was collected and prepared for analysis using FlowJo (FlowJo, LLC). Measured events were gated for cells using forward scatter and side scatter plots, using the same selection for all measurements. Insufficient events were acquired to further differentiate cells based on marker expression, and analysis was applied to the entirety of the selected cell populations. After cell populations were selected, further gating was used to remove any debris or air bubbles on a case-by-case basis by applying a gate on FITC fluorescence for the included events. Example plots of the implemented gating strategy may be found in Figure 60 in section 5.4.2.

For each selected sample population, geometric means are calculated for the fluorescence levels of FITC (CD90) and PE (CD105). Measured fluorescence values will be converted to MESF to estimate total fluorophores per cell using the fluorescence values of the MESF reference particles in the QuickCal conversion method offered by Bangs Laboratories, Inc. Event counts, as well as standard deviations of all measured values, are calculated but are not included in the initial analysis.

5.3.8. Analysis of late culture Collagen-II production

Production of Collagen-II was determined by measuring total fluorescence of samples after staining with primary and secondary antibodies on day 14 and day 21 of cell culture. Because of very low expected ECM deposition, the choice was made to expand analysis with additional isotype measurements. Planned replicates from the original experimental design are split into a marker group and an isotype group. Consequently, all measurements are performed as N=1 with no replicates.

Prior to measurements, the relevant surfaces are transferred to new 24-well plate wells and incubated for 30 minutes at 37°C with anti-Collagen-II Rabbit IgG or Rabbit

IgG isotype, both at 5 µg/mL and 1 mL per sample. The wells from the initial well plate are checked with optical microscopy to identify cells that have grown on the bottom of the plate, similar to the process used at 2 and 4 days.

After incubation, samples are washed in PBS, transferred to new wells and incubated for 30 minutes at 37°C with FITC-conjugated anti-rabbit IgG at 10 µg/mL and 1 mL per sample. Samples are washed with PBS, and fluorescence is measured with a FLUOStar Omega plate reader. Sample fluorescence is measured with both a gain of 1000V and 1500V.

5.3.9. Statistical analysis of measurement data

Collected data was analysed using Minitab 18 (Minitab Inc. USA). The data from the completed measurements is analysed as a two-level factorial model design with one center-point. Analysis will initially focus on the main and interaction effects of the patterning, growth factor concentration, and potential interaction. Further analysis includes Pareto analysis for the relative impact of various parameters, as well as the influence of immobilizing growth factors compared to using soluble growth factors.

Statistical significance for all statistical analyses is set at 5%, while stepwise modelling used α=0.15 for both adding and removing terms. Stepwise modelling keeps a hierarchical model at all steps.

5.4. Results

In this chapter the methods developed through chapters 2, 3 and 4 were combined to investigate the interaction of patterning and immobilization of TGF-β1 on the differentiation and ECM production of mesenchymal stem cells. Cell culture using the developed methods was performed and analysed, the results of which are presented below.

Five experimental groups could not be measured at day 21 as these became contaminated during cell culture. Discarded samples are: one well from 49.1µm pattern + 0.2 pMol/cm^2 TGF-β1, both wells from 49.1µm pattern + 0.02 pMol/cm^2 TGF-β1, and both wells from 1.93µm pattern + 0.2 pMol/cm^2 TGF-β1.

5.4.1. Metabolic activity during cell culture

Analysis of the data acquired using the Cedex showed a substantial loss of metabolic activity.

Glucose concentration at the time of measurement consistently increased as culture progressed, as shown in Figure 56. This indicates that consumption of glucose by cells in culture did not exceed the addition of Glucose through media changes or the increasing concentrations due to media evaporation. Glucose concentration increases to above 4500 mg/L (the starting media concentration) at later time points, indicating that media evaporation takes place over the time of culture.

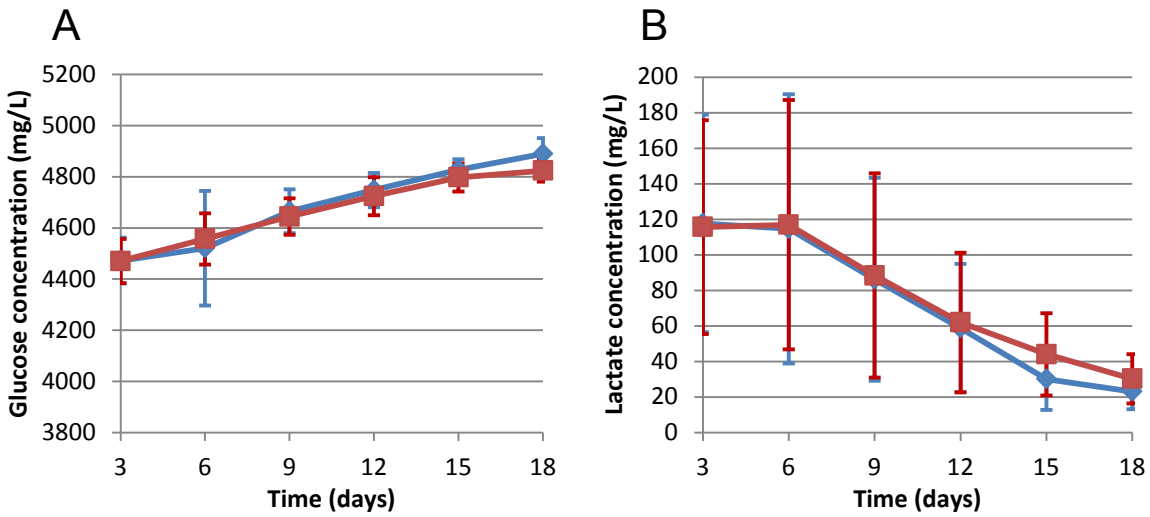

Figure 56: measured concentrations of Glucose (A) and Lactate (B) during culture, determined from spent media collected during media changes. Samples with immobilized TGF-β1 are shown in blue; samples with soluble TGF-β1 are shown in red. Results are shown as mean ± standard deviation for all samples regardless of surface type or TGF-β1 concentration.

Likewise, Lactate concentration sees a decline across all samples after the initial peak at day 3 and 6. As a portion of the produced Lactate is removed with each media change, this indicates that metabolic activity is maintained at most several days into culture with longer-term culture seeing no major metabolic activity or further proliferation of cells.

Three control samples, all flat surfaces with no added TGF-β1, showed noticeably higher metabolic activity across all time points with higher Glucose consumption (concentrations down to 4200-3500 mg/L) and Lactate production (concentrations up to 250-1000 mg/mL). However, this behaviour was not seen in any of the other samples cultured under these conditions, indicating that these differences may be caused by the initial seeding situation, such as an erroneously high seeding density

caused by insufficiently stirred cell suspension prior to seeding. These results are treated as outliers, and are not included during further data analysis.

Barring new production or consumption, both Glucose and Lactate will regress to the values of unused culture medium due to the partial media change. Total Glucose and Lactate changes over time can be calculated from the measured values, with the current activity calculated as $\Delta_{\text{Current}}(T) = \Delta_{\text{Total}}(T) - \Delta_{\text{Total}}(T-3) * \frac{2}{3}$ and total activity over cell culture calculated as $\Delta_{Cumulative} = \sum_{T=3}^{T=18} \Delta_{Current}(T)$. However, as Glucose concentration was already seen to increase due to (presumed) media evaporation over the culture period, Lactate will be used as the main indicator of metabolic activity, since changes over time will be proportionally larger to base value and total Lactate content does not change due to media changes as Glucose content does due to media changes.

As shown in Figure 57, cumulative Lactate production over time are largely determined by the first week of cell culture, with days 9 and later having an effectively negligible effect on the cumulative metabolic activity during culture.

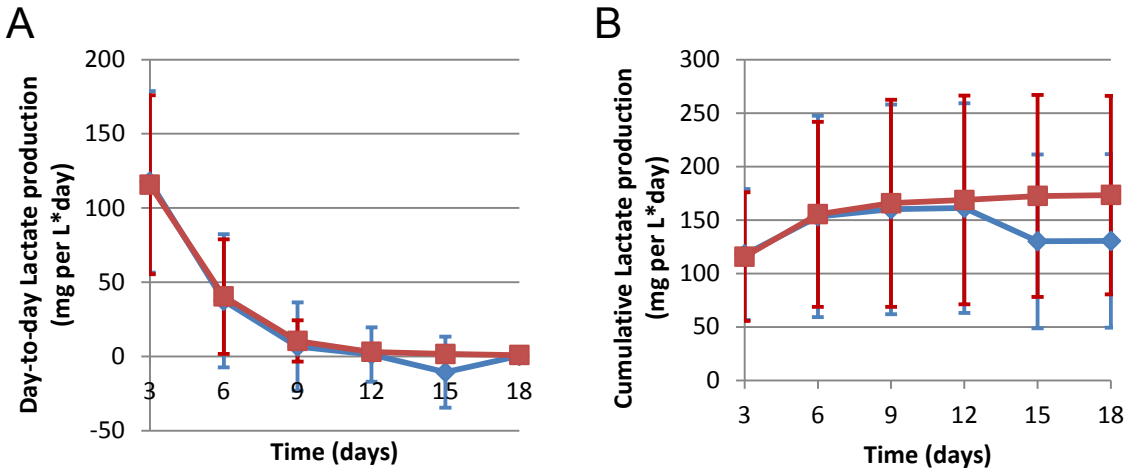

Figure 57: Calculated day-to-day (A) and cumulative Lactate production (B) during cell culture, determined from spent media collected during media changes. Samples with immobilized TGF-β1 are shown in blue; samples with soluble TGF-β1 are shown in red. Results are shown as mean ± standard deviation.

Together, these results indicate either a substantial loss of cells during culture, or a near-total cessation of metabolism in cultured cells. While a small drop in metabolic activity is expected due to cells differentiating from the initial hMSC phenotype to a chondrocyte phenotype, the reduction seen in these measurements is too great to be fully explained by this process. Proliferation will continue even in chondrocytes, and

any reduction in metabolic activity solely due to reduced proliferation would be expected to be accompanied by an increase in metabolic activity due to upregulated ECM production[288]. Consequently, the most likely explanation for the measured activity is a large-scale loss of cultured cells. It is not known if cells die during culture, be it through apoptosis or environmental factors, or if cells are lost due to other factors such as detachment from the surface.

Statistical analysis of the measured metabolic activity shows a number of important effects. The center-point samples used during the experiments showed substantially lower metabolic activity than all other samples in the immobilized TGF- β1 variants, and a substantially higher metabolic activity when used with soluble TGF- β1 as seen in Figure 58. As such, these points are considered outliers and will not be included for further analysis and interpretation of the measurement data.

Furthermore, samples using immobilized TGF- β1 on 49.1 µm diameter patterns showed a consistently higher metabolic activity than most other samples, and low concentrations of immobilized TGF- β1 showed increased metabolic activity compared to higher concentrations.

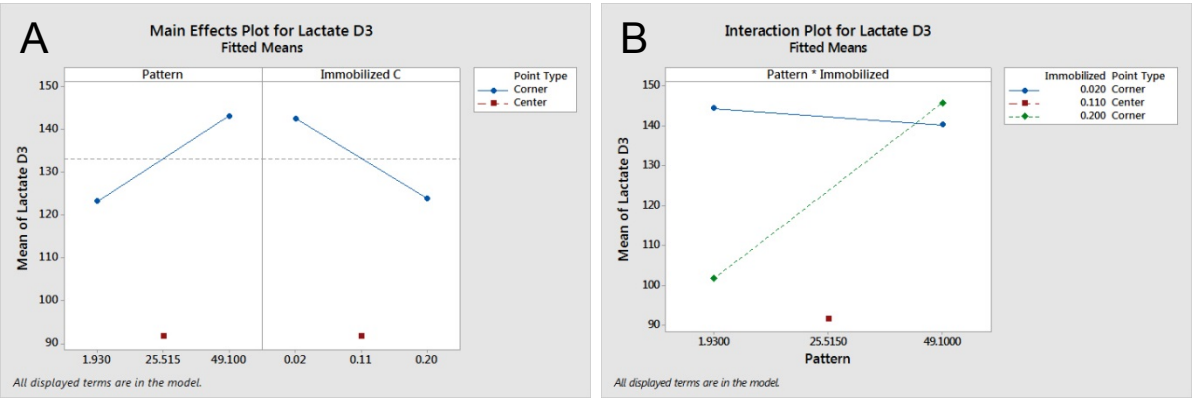

Figure 58: Main effects (A) and interaction plots (B) for measured Lactate levels at day 3 of cell culture using immobilized TGF-β1. Note the measured centre-point values at the bottom of the graphs.

However, the experiments with soluble TGF- β1 instead showed a negligible effect of pattern size and an advantage at high concentrations of TGF- β1 in solution, as seen in Figure 59.

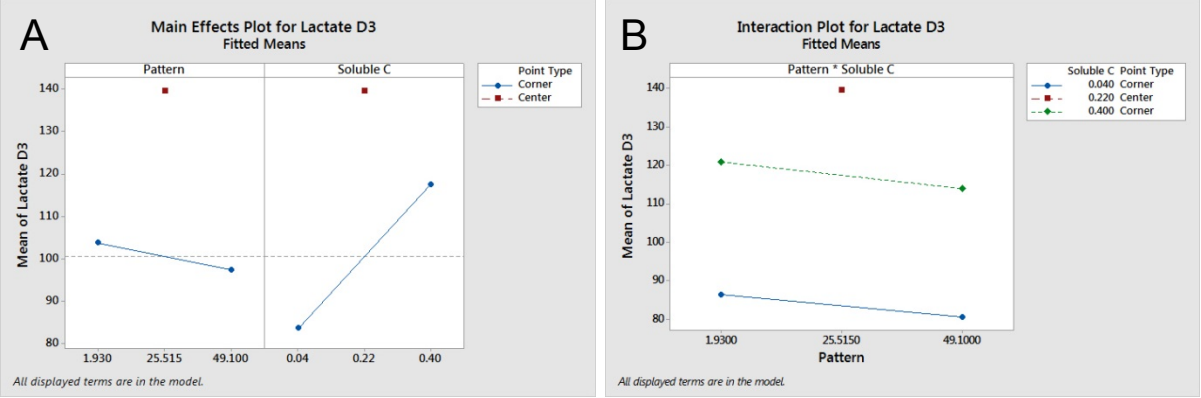

Figure 59: Main effects (A) and interaction plots (B) for measured Lactate levels at day 3 of cell culture using soluble TGF-β1. Note the measured centre-point values at the top of the graphs.

These stark contrasts, combined with the rapid loss of metabolic activity as cell culture progresses, suggest that the size and health of the initial cell population are the driving factor behind most of the changes seen in these measurements. That said, samples using immobilized TGF-β1 showed a higher metabolic activity than samples with soluble TGF-β1 (average Lactate concentrations of 130mg/L compared to 100mg/L, respectively), which may indicate a potential effect of immobilized proteins on initial cell attachment and survival. This interpretation is supported by results found in literature, though the complexity of the protein environment in cell culture makes direct comparison difficult[289–291].

Statistical analysis of the measurement data did not show statistically significant ($\sigma<0.05$) links between the patterning, TGF-β1 concentration, or combined effects for most time points. The only statistically significant effects were Patterning at day 6 and 12 on Glucose concentration for samples with immobilized TGF-β1, pattern + concentration combined (second-order effect) for Glucose concentration on day 12 for samples with soluble TGF-β1, and Pattern for Lactate concentration on day 12 for samples with immobilized TGF-β1. None of these effects were significant for these samples on different time points, nor for other experimental groups.

However, one notable difference between the experimental groups was found in the relative effects of the various environmental parameters. Although most time points did not show statistically significant effects, both immobilized and soluble TGF-β1-based samples showed clear trends. Samples with soluble TGF-β1 consistently showed a higher effect from TGF-β1 concentration on both measured Glucose and Lactate than patterning, shown in Figure 60. By contrast, the samples using

immobilized TGF-β1 consistently showed a greater effect from the patterning instead of the TGF-β1 concentration, as seen in Figure 61.

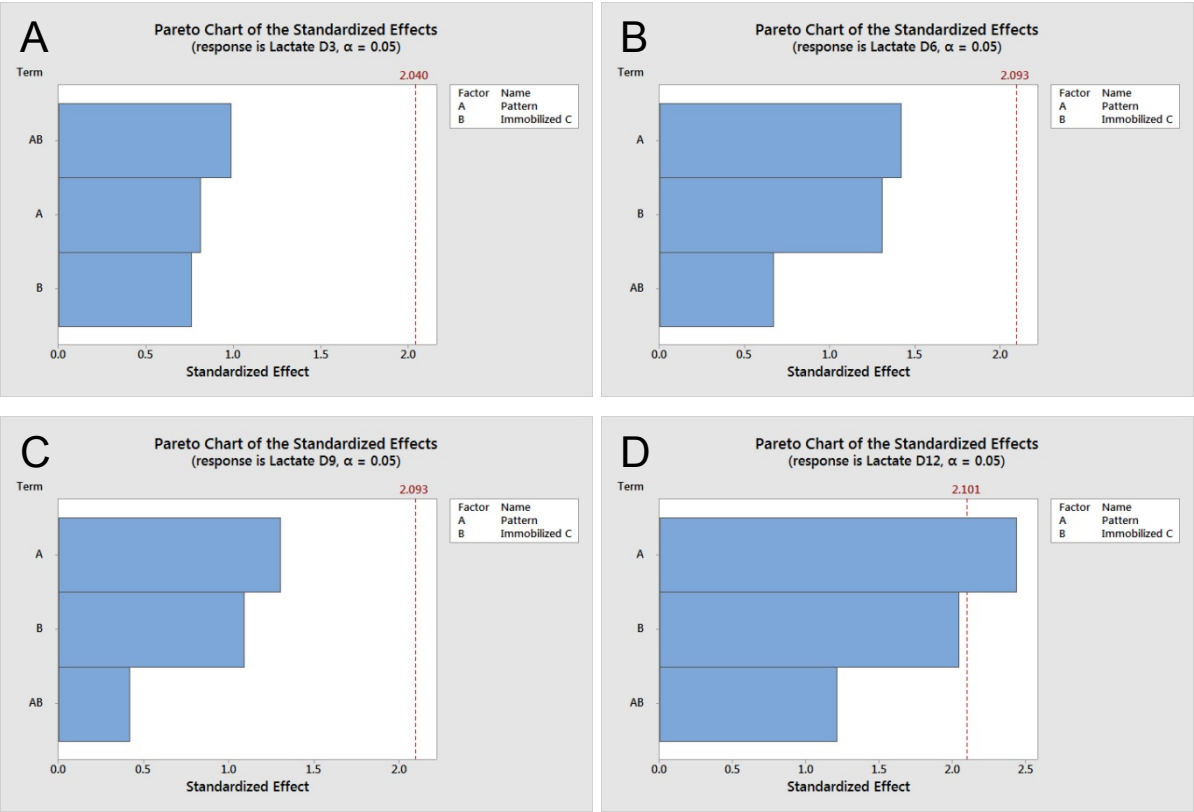

Figure 60: Pareto Charts of the contribution of pattern and growth factor concentration on metabolic activity (Lactate production) on days 3 (A), 6 (B), 9 (C) and 12 (D) for samples with immobilized TGF-β1.

This suggests that although none of these effects were statistically significant at each individual time point, there may nonetheless be a relevant effect. While influence from the second-order effects of patterning and immobilized concentration were not significant and in most case substantially smaller than first-order effects, the fact that immobilizing TGF-β1 appears to make patterning much more influential suggests an interaction between the surface pattern, the immobilized proteins and the cells in culture. This is further supported by Regression Modelling of the relation between Glucose or Lactate concentration and pattern size and soluble or immobilized concentrations of TGF-β1. Although R^2 values were low, Regression Modelling of a linear relationship as: $C_{\mathrm{Factor}} = A + B * Diam_{Pattern} + C * C_{TGF-\beta1}$ gave substantially higher values for B in samples with immobilized TGF-β1 (-0.3 to -14 for Glucose, +0.4 to +1.1 for Lactate) than for samples with soluble TGF-β1 (-0.6 to +0.5 for Glucose, -0.1 to +0.1 for E) from day 3 to day 12, as shown in Table 2. Insight into non-linear behaviour was impractical due to the unusual response seen in center

points, as shown in Figures 58 and 59, and is therefore not included. Samples from day 15 and 18 were not included so loss of samples would not skew results for later time points.

	$A_{Lactate}$	$B_{Lactate}$	$C_{Lactate}$	$A_{Glucose}$	$B_{Glucose}$	$C_{Glucose}$
T=3, Soluble	96.2	- 0.135	94.3	4513.0	- 0.551	- 124
T=6, Soluble	93.7	- 0.137	117	4585.1	0.27	- 161
T=9, Soluble	69.4	0.024	76.1	4627.2	0.502	5
T=12, Soluble	48.0	0.113	46.0	4736.6	- 0.122	-87
T=3, Immobilized	119.9	0.423	-103	4510.3	-0.333	-231
T=6, Immobilized	120.8	1.114	-269	4513	-4.28	976
T=9, Immobilized	85.7	0.814	-178	4465	-13.61	3222
T=12, Immobilized	61.8	0.762	-165.1	4757.2	-0.826	76

Table 2: Regression Model fits for relationships between measured Lactate and Glucose concentrations and the patterning and TGF-β1 concentrations used.

5.4.2. Early expression of cellular markers CD90 and CD105

Analysis of the Flow Cytometry measurements into the expression of CD90 and CD105 provided limited information. Event counts for all measurements were substantially lower than intended due to (suspected) cell loss during culture, supported by the findings of metabolic activity shown above. While surfaces were initially seeded with ≈ 20,000 cells, most measurements included only 600-800 events in total. Examples of the measured events and population gating used are shown in Figure 62.

To compensate for the low event counts seen during this analysis, all samples belonging to each corner point or center point are pooled prior to analysis so that individual measurements gain access to larger numbers of cells for analysis. While this ensures no replicates are available for these measurements, this change to the experimental design was considered a better option than risking further loss of data due to insufficient flow cytometry event counts.

Consequently, these results should not be extrapolated to predict behaviours of hMSCs in culture for more successful culture conditions. In addition to potential signalling effects of cell death during culture or continuing adverse influences from the environment, the remaining cells may represent only a sub-population of the initially seeded cells.

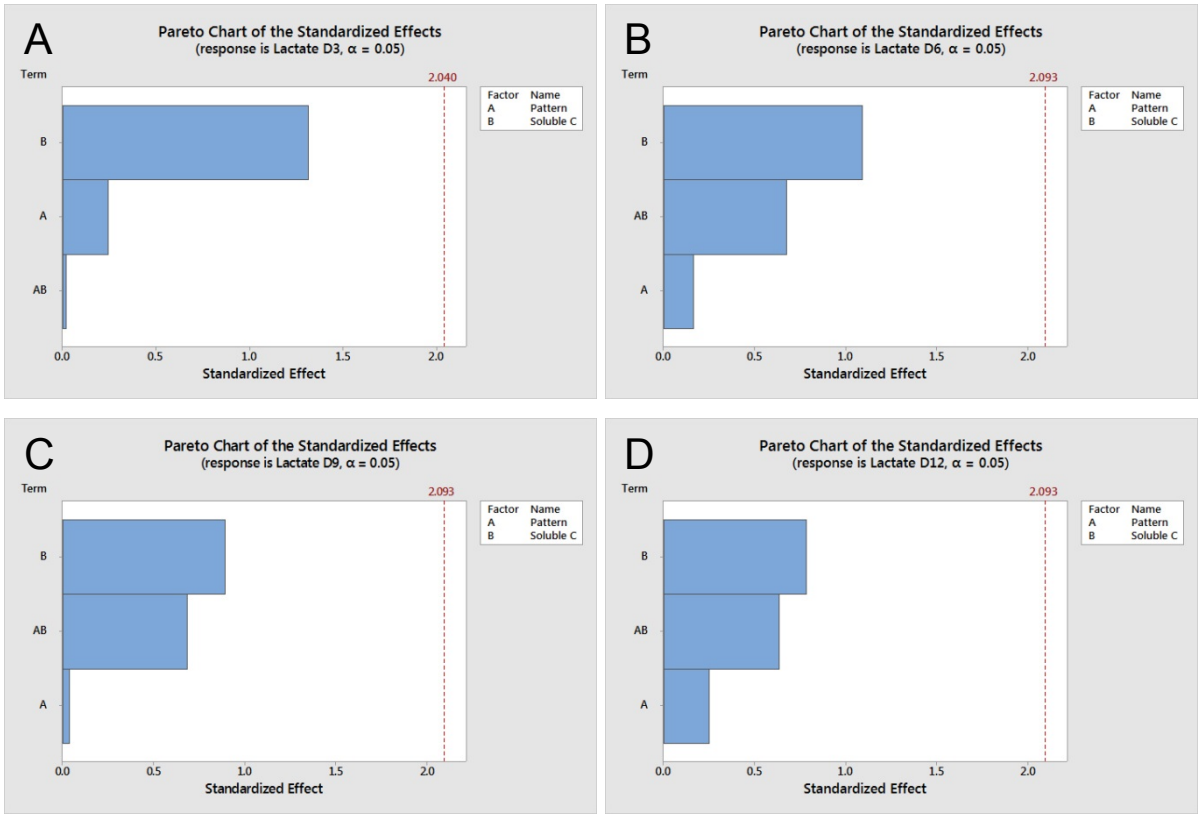

Figure 61: Pareto Charts of the contribution of pattern and growth factor concentration on metabolic activity (Lactate production) on days 3 (A), 6 (B), 9 (C) and 12 (D) for samples with soluble TGF-β1.

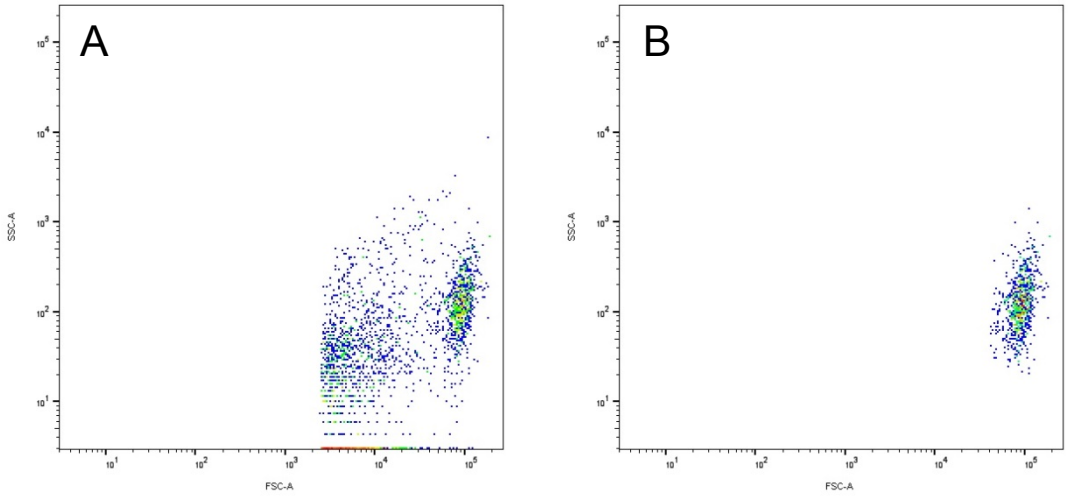

Figure 62: Example of measured events in the forward scatter – side scatter plots. The majority of measurements showed a large amount of debris, visible as extensive spread out events with low values of forward scatter on the total population (A). The gated cell population has very limited event counts (B).

Although the metabolic activity of the center points for immobilized TGF-β1 culture were unusually high, no major differences for CD90 or CD105 staining for these samples were found at Flow Cytometry analysis on day 4 as shown in Table 3. Likewise, the unusually low metabolic activity of the center points during soluble

Sample	T=2, CD90	T=2, CD90 Isotype	T=2, CD105	T=2, CD105 Isotype	T=4, CD90	T=4, CD90 Isotype	T=4, CD105	T=4, CD105 Isotype
49.1 µm, 0.2 pMol/cm^2	22084±25764	1497±904	3922±2540	4961±3616	27090±18934	1232±818	3866±2459	3804±2265
49.1 µm, 0.02 pMol/cm2	45185±31759	1767±1281	4807±3671	5517±4241	22403±21076	448±1705	5720±4739	916±5448
1.93 µm, 0.2 pMol/cm^2	47580±36850	1915±1462	5825±4298	6186±4560	16317±25159	2766±2076	5154±4274	8110±6268
1.93 µm, 0.02 pMol/cm^2	33319±29385	1534±809	4817±3617	4268±3030	29016±25059	335±1322	6007±3792	397±4864
18.8 µm, 0.1 pMol/cm^2 T=+0	24683±20309	1305±862	2003±2732	3324±3089	20986±51144	3149±1468	5499±2674	7530±3697
18.8 µm, 0.1 pMol/cm^2 T=+1	24683±20798	1228±1054	2721±2540	3431±3846	23820±31403	2482±2137	4619±4199	5833±4674
49.1, µm, 0.4 pmol/mL	36924±30876	1857±1076	5121±3344	6005±3820	23933±23319	1598±1587	3927±3394	4669±4201
49.1 µm, 0.04 pmol/mL	35048±33192	1376±811	4454±4187	4272±3057	25138±29533	1585±1348	3519±2175	4481±2613
1.93 µm, 0.4 pmol/mL	31706±20534	1710±954	4543±3020	5367±3487	13715±14716	271±1063	3803±2977	424±4935
1.93 µm, 0.04 pmol/mL	25862±14923	1343±753	3516±2661	4171±3065	13429±13004	1637±856	3439±1945	4825±2252
18.8 µm, 0.2 pmol/mL T=+0	19086±23727	1263±924	2633±2966	3738±2796	21001±14813	1334±916	3404±1818	3651±2715
18.8 µm, 0.2 pmol/mL T=+1	13465±33116	1658±880	4392±3500	5868±3592	19594±13121	1605±965	4043±2757	4749±3107
18.8 µm, TGF-β-free	22084±16869	1003±949	3071±2379	2285±3384	16892±12200	1504±924	3445±1883	4339±2921
Flat, TGF-β-free	45185±34831	1530±792	5940±3078	5308±2876	435±38810	2013±4035	234±4937	5279±3445
Flat, 0.1 pMol/cm^2	47580±36090	1451±1194	5470±4123	4437±3471	23996±26207	203±159	4890±3863	1500±7935
Flat, 0.2 pmol/mL	33319±46469	1747±821	4552±2884	6300±2955	19671±18905	1531±999	4360±2369	4229±3057

Table 3: Flow Cytometry measurements of cultured cells at T=2 days and T=4 days. A number of unusually low values, such as CD90 Isotype fluorescence for 49.1 µm, 0.02 pMol/cm2 were caused by very low numbers of cells and correspondingly higher influence of measurement artefacts.

TGF-β1 culture was not accompanied by similarly large differences in expression, although expression of CD105 was slightly elevated compared to standard

experimental groups. The observed higher metabolic activity seen in cell cultures on larger-scale patterning with immobilized TGF-β1 was not accompanied by higher expression of CD90 or CD105.

Together, these results suggest that metabolic activity and phenotype are not strongly linked in these experimental conditions.

Further differences between samples with soluble TGF-β1 and samples with immobilized TGF-β1 can be found in the measured expression of CD90 and CD105. While cells cultured with soluble TGF-β1 showed a consistently higher expression of both of these markers on large patterns, cells cultured on samples with immobilized TGF-β1 showed a lower expression on large patterns, especially on day 2, as shown in Figure 63. Unlike earlier results seen with regards to metabolic activity, neither pattern type nor concentration showed significant effects on measured marker expression or a clear hierarchy in terms of relative contributions.

Together, this further supports a potential interaction of immobilized proteins with the underlying pattern as suggested by the metabolic interaction, as further differences are found between these two groups despite the fact that factors within these groups do not themselves add any substantial effects.

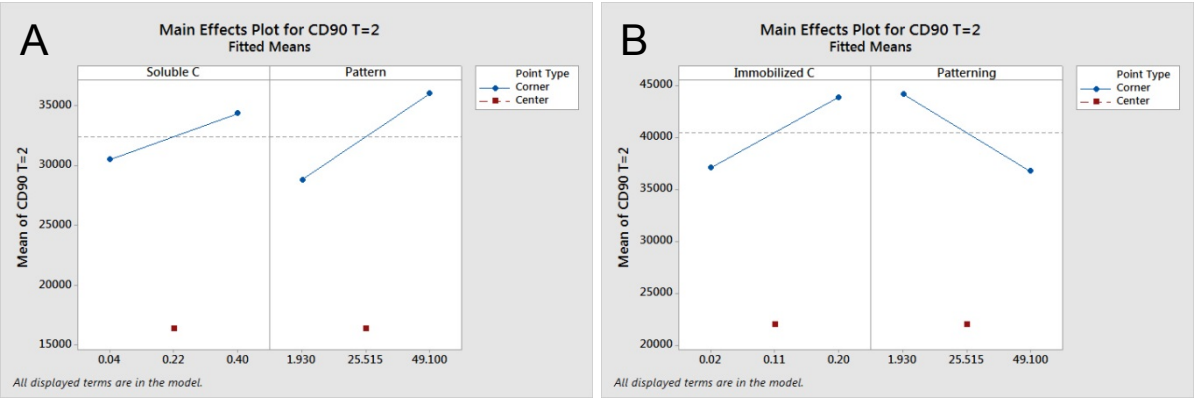

Figure 63: Main Effects Plots for CD90 expression after 2 days, for samples cultured with soluble TGF-β1 (A) or immobilized TGF-β1 (B). Note the shift from higher expression at large patterns with soluble TGF-β1 to lower expression when using large patterns with immobilized TGF-β1. Center-points were considered outliers as explained before.

5.4.3. Cumulative production and deposition of Collagen-II

Measured fluorescence intensities of the various samples showed a number of important things. Most importantly, numerous sample measurements showed a very high fluorescence when stained with Isotypes, as shown in Table 4. This includes

several samples that showed a higher fluorescence than the corresponding antibody-stained samples. It is unclear what caused this effect, and results should therefore be considered questionable unless consistent patterns are found across multiple samples.

Sample type	Antibody, T=14	Isotype, T=14	Antibody, T=21	Isotype, T=21
49.1 µm, 0.2 pmol/cm^2	184290	244687	174230	Sample lost
49.1 µm, 0.02 pmol/cm^2	175624	154960	Sample lost	Sample lost
1.93 µm, 0.2 pmol/cm^2	154279	124795	Sample lost	Sample lost
1.93 µm, 0.02 pmol/cm^2	106457	154525	99044	128534
18.8 µm, 0.1 pmol/cm^2 (standard)	120222	143519	140595	120928
18.8 µm, 0.1 pmol/cm^2 (offset)	109901	175600	179534	179168
49.1 µm, 0.4 pmol/mL	155486	212648	183133	156180
49.1 µm, 0.04 pmol/mL	255222	108872	170862	135290
1.93 µm, 0.4 pmol/mL	83472	185629	167388	146195
1.93 µm, 0.04 pmol/mL	140078	129944	120055	118281
18.8 µm, 0.2 pmol/mL (standard)	136132	114112	205386	177502
18.8 µm, 0.2 pmol/mL (offset)	185208	151676	241550	168162
18.8 µm, TGF-β1-free	133642	145082	144892	170256
Flat surface, TGF-β1-free	119621	128178	111498	101910
Flat surface, 0.1 pmol/cm^2	171258	140614	108931	116850
Flat surface, 0.2 pmol/mL	120377	122951	112116	94491

Table 4: measured fluorescence values of each sample type at day 14 and day 21. Five samples were lost due to contamination prior to measurements on day 21.

Though all samples showed fluorescence values around 150,000 units, results showed the highest values in samples with large-scale patterning (49.1 µm). These samples did not show substantially higher metabolic activity during culture, suggesting that the fluorescence intensity after staining for Collagen II is at least partially independent of overall cell activity in these samples. This indicates that extracellular matrix deposition occurred despite the low rates of proliferation and attachment seen during the experiment, and that higher matrix deposition was due to altered cell behaviour rather than an increased number of ECM-producing cells.

Regression Modelling of the gathered data indicated that a potential link exists between early metabolic activity (production of Lactate) and the measured fluorescence at day 14, with an R^2 of 21.82% and p-value of 0.007 for a linear correlation. However, the same correlation was not statistically significant at day 21, with an R^2 value of 9.69% and a p-value of 0.114. It is possible that the statistically

significant effect found for day 14 was due to chance, and that there is no true relation between these properties. Alternatively, while Collagen can dissolve into solution only under the correct circumstances (commonly requiring acidic pH), cell-produced Collagen monomers are water-soluble prior to crosslinking and forming the extracellular matrix network[292]. It is possible that without further cellular activity or ECM deposition, the created Collagen does not reach sufficient density and crosslinking to be fully bound to the surface. This would result in loss of ECM over time and weakening any statistical link between metabolism and measured fluorescence. However, as the measured fluorescences for the surfaces are of comparable values this was not considered a likely cause for this result.

After 14 days of cell culture, analysis of collagen deposition shows a continuation of the trends observed during the earlier analysis of metabolic activity and marker expression. Samples appear to provide the highest collagen deposition on large-scale patterns with both soluble and immobilized TGF-β1. Samples with soluble TGF-β1 appear to have the highest collagen deposition at lower concentrations of TGF-β1, while samples with immobilized TGF-β1 showed the highest fluorescence at high concentrations, as shown in Figure 64.
However, this difference no longer shows up at 21 days, with samples using soluble TGF-β1 now showing the highest collagen in high-concentration groups. Further analysis is complicated by the loss of a number of samples before measurements could begin on day 21, causing some of the planned data points to be unavailable (specifically for the immobilized TGF-β1 samples).

5.5. Discussion

A number of interesting trends could be seen in the cell culture experiments described in this chapter. Nonetheless, various problems were encountered with cell retention and proliferation during the experimental work.

Most importantly, the experiments saw a major loss of cell activity over the first week of culture. As culture prior to seeding on the experimental surfaces showed no problems, the most likely cause for this is a large-scale loss of cells, indicating a major incompatibility with the cell culture environment. The use of chemically

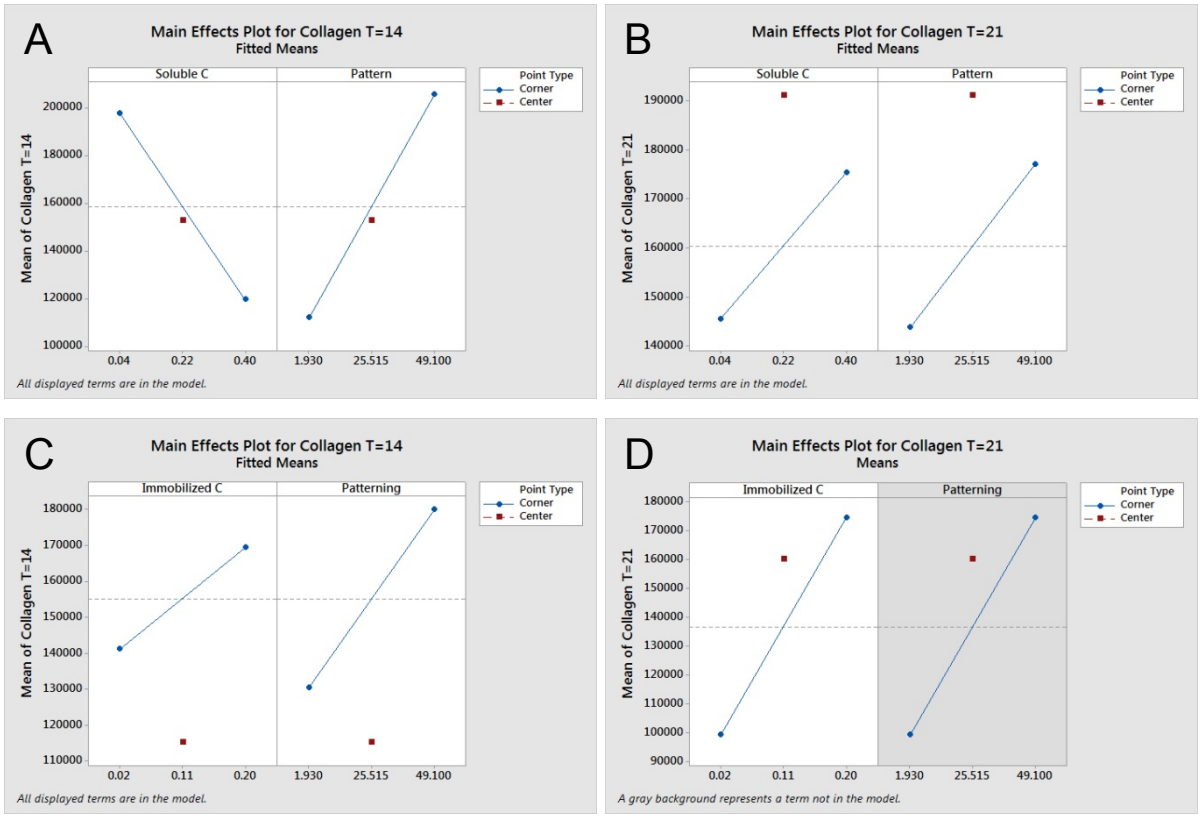

Figure 64: Main Effects on Collagen II deposition of the samples with soluble TGF-β1 (A, B) and immobilized TGF-β1 (C, D). Note the difference between sample types on day 14 (A, C) as well as the loss of data points for samples with immobilized TGF-β1 on day 21 (D).

modified Polycaprolactone was tested during chapter 4, which indicated that cells successfully attached after seeding, without substantial cell loss as seen here.

Furthermore, as microscopy analysis of the used well plates did not show any substantial cell attachment on the bottom of the plate, this suggests that cells were not 'washed off' the cell culture surface with the addition of the full medium after 3 hours. This is in line with other work that has shown that cells will attach onto surfaces in <3 hours on numerous different material types, with attachment times as low as <1 hour total showing good attachment[285,286,293]. Consequently, the effects seen during this experiment are considered to be due to cell behaviour following cell seeding and attachment (including responses to the culture environment such as surface material), rather than consequences of the seeding protocol itself.

However, one difference between the two situations was that the experiment in chapter 4 was not intended for further culture; cell seeding density was higher during the previous experiment since cells reaching confluence prior to measurements was not a consideration. The number of cells seeded during this experiment was only 10,000 cells per square centimetre of surface area, compared to the previously used

20,000 cells per square centimetre. Consequently, a potential cause for the losses in this experiment is the lower seeding density – though all cells were seeded in a single droplet, differences in initial cell density, spreading and cell-to-cell interaction may have negatively affected cells during the experiments described in this chapter.

Cell-to-cell signalling has been shown to have a substantial impact on both proliferation and differentiation of cells, with higher cell densities resulting in both increased paracrine signalling[294] and effects from direct cell-to-cell physical contact[295]. As mesenchymal stem cells have been shown to rapidly spread across stiff substrates after seeding[296], an insufficiently high initial seeding density may have resulted in cells spreading until a loss of necessary signalling effects occurs. This may also explain why the center-point samples had such unusual results – although cells were seeded onto surfaces using the same method regardless of sample type, it is possible that the initial cell suspension was not sufficiently mixed.

Consequently, these samples could then have been seeded with a lower concentration of cells, which may have further complicated attachment and survival beyond the effects seen with the rest of the experiment. Likewise, the outliers seen in the samples using TGF-β1-free flat surfaces may be caused by this process – if these samples were seeded with an above average number of cells, this may have been introduced additional signalling effects and partially prevented the cell loss seen in the other samples.

While the cellular environment was evidently unsuitable for the performed experiments, noticeable differences could be seen across the used values for both the patterning types and the concentrations of TGF-β1 used during these experiments. As such, further work with this type of environment may be able to use these parameters provided a solution is found for the cell loss seen during this experiment.

Despite the difficulties with acquiring suitably robust data, some interesting trends could be identified by looking at the gathered data. The increased cell survival and ECM production depending on patterning for samples with immobilized TGF-β1 compared to samples using soluble TGF-β1 suggest a relationship between immobilized growth factors, surface topology and cell response exists.

The immobilization of TGF- β1 showed an increased influence of pattern on cell behaviour across all samples using immobilized TGF-β1. This strongly suggests that the measured differences are due to a real effect; despite the fact each sample individually did not reach statistical significance. Regression modelling for showed $0.1 < p < 0.25$ for pattern and immobilized concentrations, with only Lactate on day 12 having $p=0.045$.

In particular, the topology of the cellular environment will have an impact on the cytoskeleton through both cell deformation and altered availability of focal adhesion sites[18,222]. The cytoskeleton has previously been shown to be involved in numerous cell processes, including differentiation of hMSCs[18,283]. Modifying the structure and behaviour of the cytoskeleton through altered cell deformation and attachment processes could therefore create both a direct influence on cell behaviour and modify responsiveness to other influences such as mechanical effects or exposure to growth factors[18,297] such as the TGF-β1 used during this project. Combined with the involvement of the cytoskeleton in chondrogenic differentiation[284], this presents a potential process through which the patterning and immobilized growth factors may interact as seen in these results.

Large-scale patterning showed the greatest advantage both in terms of early marker expression and total Collagen II expression. As the 49.1μm patterns are considerably larger than the cells themselves, this may have resulted in cells remaining in closer contact to each other within the confines of each ‘well’ in the pattern – a possibility which ties in closely with the potential impact of cell seeding density mentioned above. Smaller feature sizes may instead have a greater impact on cell deformation through sub-cellular topology.

While statistical analysis of these results was, by necessity, very limited due to both a limited number of samples and unexpected cell loss during culture, this still provides a tentative answer to the initial hypothesis suggested in chapter 1. The increased relevance of patterning when combined with immobilized proteins suggests this type of environment may form a useful tool for further improving cell culture processes. However, additional work will be needed to overcome the difficulties encountered during this chapter and ensure sufficiently robust data on this process.

Chapter 6: Discussion and conclusion

6.1. Discussion

Regenerative medicine provides a promising field for improving current methods and therapeutics in medical care. However, recent years have seen rapidly rising costs in healthcare services, driven by an aging population and an increased need for long-term care, making the cost-effectiveness of new treatments a major priority in medical research.

Regenerative medicine offers a potential avenue for the creation of long-lasting therapeutic results without the need for extensive follow-up or long-term care. However, the cost of regenerative medicine is comparatively high, owing to the need for high quality materials (including living tissues) and often lengthy processes to prepare such materials for the desired medical intervention. Consequently, improvements to cost-effectiveness, efficiency and overall level of control of the processes used for regenerative medicine treatments may greatly improve the effectiveness of these processes and allow them to meet society's current and future needs. In particular, the complexity of the cellular environment stem cells are found in in vivo is a major challenge to accurately recreate; with the shape and mechanical properties of surrounding tissue, level of exposure to numerous bioactive compounds, and direct cell-to-cell contact all combining to form a unique stem cell niche that is difficult to artificially replicate[15,16].

To tackle these challenges, the work described in this thesis focused on potential improvements to the efficiency and level of control over cell culture environments using a combination of topology and immobilized growth factors. Only a chondrocyte-based proof of concept was investigated, though similar methods may be applicable for other cell types, environments, or potential therapies as well.

The new insights gained from this experimental work should be suitable for modifying existing cell culture methods without the need for large-scale changes to implementation or the addition of costly resources or process steps. Ideally, any discovered improvements can be implemented during the preparation of the cell culture environment, adding appropriate surface topologies and/or immobilized proteins suitable for specific cell types without any changes to the cell culture process itself.

Initially, a review of published literature was used to determine suitable options for the work to be performed. Various options for creating micrometre-scale patterning, cell culture materials, chemical modification of such materials for the immobilization of proteins, as well as cell types and growth factors or growth factor combinations were identified. Based on both the project's needs and appropriate complexity and practical considerations, the available options were evaluated and a combination of mould-based patterning with chemically modified Poly (Ethylene Glycol) was chosen for the initial experiments.

First, experimental work focused on the creation of highly-defined micrometre scale patterning based on moulds formed using uniformly distributed microparticles.

Different patterns with feature sizes ranging from 1 to 50 μm diameter were successfully created by embedding microparticles in silicone, as seen in chapter 2. Following the creation of the initial patterns, surface topology was successfully transferred onto other materials for later cell culture, including Poly (Ethylene Glycol), Polystyrene and Polycaprolactone. Further improvements to this process were developed by adjusting the methods used during the copying process, including the use of specific concentrations of the polymer blend for Poly (Ethylene Glycol) to ensure the features are duplicated in detail, as seen in Figures 13-15. Furthermore, pattern transfer was notably improved by modifying the deposition process so that the initially created topology is transferred from the silicone mould under a vacuum when using Polystyrene and Polycaprolactone, as seen in Figures 12 and 21. The developed process allowed for large-scale creation of patterned surfaces suitable for later experiments without the need to repeat the lengthier process used to create new patterns from microparticles.

Further work focused on the immobilization of relevant proteins onto the surface of created materials. Numerous immobilization processes are described in literature, including the impact on cells cultured on modified adherent cell culture surfaces or three-dimensional hydrogel matrices. However, the wide spectrum of differing environments and processes used meant that comparison of published results is exceedingly difficult and immobilized concentrations were primarily useful only as guidelines for the current work. Therefore, experimental work was undertaken to verify and quantify the immobilization of selected proteins on cell culture materials.

The initial attempts to quantify immobilization of proteins onto functionalized surfaces using newly-created Poly (Ethylene Glycol) microparticles was not successful, as seen in chapter 3. Further work using flat Poly (Ethylene Glycol) surfaces showed further difficulties in reliably immobilizing proteins, and the decision was made to focus on different materials rather than fully investigate the cause of the immobilization problems.

Following further review of literature and the selection of alternate material choices, continued experimental work resulted in the creation of functionalized surfaces on newly created Polycaprolactone and Polystyrene samples. Surface treatment with Sodium Hydroxide solutions was used to create oxygen-rich functional groups. These groups were then used to further functionalize the surface using a Carbodiimide crosslinking process, creating covalent bonds between the oxygen groups on the material surface and exposed primary amines on TGF-β1 added to the surface in solution.

Using this process, these surfaces allowed for the immobilization of varying TGF-β1 concentrations up to 4 pMol/cm^2, with the exact values dependent on the TGF-β1 concentration used during the immobilization process.

Finally, the previously developed patterning methods and TGF-β1 immobilization process were combined to create surfaces for a larger scale cell culture experiment. hMSCs were cultured for three weeks on modified Polycaprolactone surfaces with highly regular patterns using feature sizes from 1.93 to 49.1 μm, using either soluble or immobilized TGF-β1 at concentrations of 0.04 to 0.04 pmol/mL or 0.02 to 0.2 pmol/cm^2.

Analysis of metabolic activity, expression of cellular markers CD90 and CD105 and the deposition of Collagen II showed noticeable differences between samples cultured with immobilized TGF-β1 and samples exposed to TGF-β1 in solution. Samples cultured on surfaces with immobilized TGF-β1 repeatedly showed a higher influence of pattern on cell behaviour with increased cell viability, reduced expression of CD90 and CD105 as well as increased Collagen-II deposition on samples with both large-scale patterns and immobilized TGF-β1. By contrast, surface patterning had a substantially smaller effect on samples cultured with soluble TGF-β1. These results suggest the existence of a link between the local topology of

the cell culture surface and the impact of immobilization on growth factors on such surfaces.

The completed experiments did not include any investigation into the underlying mechanisms due to practical limitations. Nonetheless, the greater impact of large-scale patterning on immobilized growth factor influence suggests that underlying mechanisms are more likely to involve larger scale processes such as cell deformation and cytoskeletal structure rather than effects on micrometre or smaller scales such as localized membrane deformation.

Few of the measured differences reached statistical significance at any single measurement point. Nonetheless, effects occurred in a large proportion of sample groups, suggesting these effects are real but the current experiment did not have enough statistical power to confirm them. Further work is required to both verify these results and, if appropriate, determine strategies to apply any gained insights for the improvement of current cell culture practices.

The initial expectations when starting this project underwent substantial changes as work progressed. Notably, early plans included more extensive cell culture tests including anisotropic and other non-spherical patterns. Instead, additional time was required to adjust the selected processes for the needs of the project. The differences compared to literature that were experienced when modifying Poly (ethylene glycol) and Polycaprolactone surfaces for cell culture highlights the need to verify published results and confirm if planned processes are suitable.

Consequently, the focus of this project shifted away from the minimum of surface modification and further cell culture work towards increased efforts on creating and modifying the necessary surfaces. Due to the increasing importance of verifying the used chemical modification processes, a number of choices that were made during the early parts of the project were, in retrospect, not the best options available.

Most importantly, the decision to quantify growth factor immobilization and accessibility in the selected PEG-based material before verifying the material's effects on cell culture resulted in a substantial amount of time and resources being spent on creating suitable PEG-based microparticles for analysis. Not only did these particles fail to provide the desired information in terms of protein immobilization, the

selected material itself ultimately proved to be unsuitable for the desired cell culture experiments, potentially due to the need for increased UV exposure compared to literature. Consequently, the experimental work described in chapter 3 did not result in a suitable strategy for further cell culture experiments. In contrast, PEG-based surfaces have been successfully used in published research[108,109,118,119,122,123,296,298], further highlighting the need to verify even comparatively basic assumptions used during cell culture work. Although similar, the changes made to the experimental process during this project were evidently too different from published work to ensure successful cell culture.

Likewise, Polycaprolactone has been used for (adherent) cell culture in published research and initial attachment tests were positive as seen in chapter 4, yet the experimental work in chapter 5 showed substantial difficulties with maintaining cell attachment and survival.

Polycaprolactone has been used for cell culture in various different forms, including fibrous scaffolds[299,300], porous scaffolds[301] as well as continuous surfaces[134,147]. Published work shows that chemical modification of the surface material can have substantial effects on cell attachment and viability. While culture using Polycaprolactone fibrous meshes functions with little changes to the polymer[299,300], inclusion of additional cell attachment proteins such as RGD is often required for effective implementation of solid surfaces[135]. Compared to the experiments completed during this project, the work by Drevelle and Marletta suggest that the chemical modification employed during this project may have resulted in a surface with too high hydrophilicity[134,135]. Consequently, the unexpected issues encountered with cell culture during the final experiment may be explained by this difference in surface chemistry. The inclusion of additional cell attachment proteins alongside the immobilized TGF-β1 may have been a suitable step to prevent this effect, but this was not tested. Likewise, using a different immobilization technique than the Sodium Hydroxide and Carbodiimide crosslinking technique used here may provide better results.

In addition, the work by Pok[147] indicates that the underlying nano-scale polymer structure of created Polycaprolactone surfaces may have an impact on cell behaviour for adherent culture. Although the oven-based process used here was not

considered in that publication, the fact that the initial method of creating the polymer surface itself may be a factor of interest suggests that different manufacturing techniques may yield better results.

Further work will have to solve these problems, either by further modification of the surfaces in question or by switching to a more reliable cell culture material (such as Polystyrene) at the cost of an increase in non-specific binding.

The experimental results were in line with published work in the context of TGF-β1 influence. Work during this project showed a higher Collagen II deposition in samples with higher concentrations of TGF-β1, matching results seen in literature both when used as a soluble component[50–52] and when immobilized onto the surface[20,56]. Still, further work on alternate immobilization techniques may be appropriate, as internalization or consumption of TGF-β1 was not verified during this experiment and this may have further effects on cultured cells[53,302].

6.2. Future work

The work completed during this project provided a number of important insights, but further improvements are required to verify the results and provide means to improve existing cell culture processes.

Most importantly, the concluding experiment could not provide robust data due to large-scale cell loss early in culture. Any future work should prioritize the creation of a more suitable cell culture environment to prevent such losses. It is unclear what the exact cause was for the cell loss seen during the experiments in chapter 5, though a number of potential improvements are nonetheless promising opportunities to pursue. First of all, this project focused substantially on the creation of a surface with a controlled, quantifiable amount of immobilized protein, not only in terms of immobilized TGF-β1 but also in terms of limiting the adsorption of other proteins out of solution. Despite the initial tests at the end of chapter 4, the used surface material, (chemically modified) Polycaprolactone, remains the most immediately likely cause of the problems encountered during the last experiments. Alternative materials or surface treatments may be preferable, and while these experiments could not be performed during this project, additional investigations into the use of other types of polymers may lead to substantial improvements.

Furthermore, testing the impact of non-specifically bound proteins adsorbed out of solution on the influence (or lack thereof) of specifically bound proteins such as growth factors may further increase the number of options available for surface materials. Treated Polystyrene was included in a number of tests as a 'back-up' option, but was not used for the final experiments due to its higher propensity for non-specific adsorption of proteins. Should future work indicate that non-specific adsorption of medium components do not have any adverse effects on immobilized proteins, the use of materials with higher adsorption such as Polystyrene might have a substantial beneficial impact on further cell culture.

Alternative material compositions may also solve some of the challenges encountered during the earlier work involving microparticle analysis. The lack of suitable filtering techniques for the particles created during this project severely limited the amount of potential processing and analysis methods that could be used for the project. For further work using particles for quantification of surface immobilization, establishing an effective collection process should be considered a priority. The use of modified particles may allow for additional collection strategies such as centrifugation (with suitable density differences), magnetic capture (with the inclusion of trace amounts of iron or other magnetic metals), or temperature- or solvent-based drying (provided immobilized proteins do not degrade during the process)[303]. Likewise, the use of filters or semi-permeable membranes may provide another way to remove excess suspension liquid[304].

The initial seeding density of the cells at the start of culture was also noted to be a potential factor in terms of cell survival and activity during the remainder of the culture period. Additional experiments focusing on the impact of different seeding densities should be used to verify if alternate seeding densities can serve to prevent the cell loss seen during the experimental work in chapter 5. In addition, the used drop-wise deposition method may be improved to allow for more equally distributed cell seeding, though this may depend in part on the use of different creation and functionalization processes available[133,134,305,306].

This project initially attempted to quantify the amount of immobilized protein that was accessible by cells during culture using flow cytometry, which was not successful. Later work estimated the immobilization of TGF-β1 by measuring fluorescent marker

binding using a plate reader, which provided the approximation of surface concentrations used during the experiments in chapter 5. The substantial level of variation in the measured results further supports the need for a more thorough understanding of the cellular environment, including potential effects of immobilized protein densities. Consequently, while a practical estimate was used during these experiments, gaining more accurate information on the level of exposure of cells to immobilized proteins in culture remains an important aspect of cell culture to consider.

Furthermore, only a very limited number of concentrations of TGF-β1 were used during this project due to practical considerations. Including additional growth factor concentrations in further work may provide additional insight into the effects of growth factor concentrations on cells during culture. Information on minimum concentrations of proteins and other chemical aspects required for specific responses, potential non-linear relationships between surface concentrations and cellular impact, and varying concentrations by location on the cell culture surfaces may all provide further means to improve current cell culture techniques [43,73,223,273,307,308].

Another limitation of this project is that only a single cell and tissue type were used for experiments. The increasing need for viable long-term treatments of damaged or poorly functional cartilage means that a greater degree of control over chondrocyte differentiation and extracellular matrix production is highly relevant. Nonetheless, a large number of other cell types and therapeutic purposes may benefit from further work using methods such as those developed during this project. Cells with a highly structured environment such as neurons, muscle cells and the cells constituting the tissues in arterial walls may show a larger impact of adjusting the local cellular environment, and further investigation of such cells and tissues may improve culturing techniques as well as short- and long-term biocompatibility of various medical devices such as stents[15,199,309,310]. Likewise, the relevant topology and growth factor presentation methods will almost certainly need adjustment to make them suitable for these different cell types.

Additionally, while the effectiveness of functionalized surfaces with specific topologies is likely substantially less effective in suspension-based cell culture,

functionalized particles are already used in other forms of cell culture for both short and long-term exposure[7,112]. Adapting this type of environment for the use of patterned particles might provide further insight into shorter-duration transient exposure on cells.

Another aspect of the recently completed experiments was the investigated variation during cell culture based on the patterning of the underlying cell culture surface. Initially, a larger number of different patterning scales were considered, but these options were not included in the final experiments due to practical limitations. Furthermore, the patterning types used during this project were exclusively spherical convex in shape, with no further variation in topology other than the scale of the constituent features. Both convex and anisotropic shapes were considered for inclusion, but were not included due to time constraints and practical limitations. As such, further work focusing on the most effective shape of the features making up the used patterns may provide additional methods to enhance the cell culture environment. Convex shapes may result in a higher effective cell density due to grouping of cells in each ‘well’ shape, as well as different biomechanical cues due to altered deformation of cells compared to concave shapes. Anisotropic shapes such as grooves and ridges may be of particular interest for the manipulation of cells normally found in highly anisotropic environments such as muscle cells and nerve cells. Likewise, different shapes may present varying curvature and ‘sharpness’ of features in contact with cells, which may present additional options to investigate potential effects of cell membrane deformation and cytoskeletal activity[216,223,224].

Finally, the use of different surface topology might allow for the inclusion of new gradients or other location-dependent exposure to immobilized growth factors. The use of rod-shaped features has been widespread in cell culture based research, predominantly in fields investigating the mechanical properties of cultured cells such as contractive force. However, such shapes also allow for the deposition of growth factors on only specific parts of the surface, creating a potential method for varying the growth factor exposure of cells along different stages of differentiation and morphology[89,215].

6.3. Conclusion

To conclude, the work performed during this project could not provide a definite answer to the initial research questions posed in chapter 1; the offered hypothesis remains unverified without additional, more robust experiments.

Nonetheless, the results from the experimental work shown in chapter 5 provided a number of important insights. While none of the measured effects reached statistical significance over the full experiment, trends across multiple measurements showed a noticeable effect of varying pattern feature sizes that only occurred on surfaces using immobilized TGF-β1. Most notably, the relative Pareto Effects of patterning and TGF-β1 concentration in the analysed samples show that pattern is consistently the more influential (though still non-significant) effect in all samples with immobilized TGF-β1, while the TGF-β1 concentration is consistently more important than patterning in samples using soluble TGF-β1. Immobilization of TGF-β1 non-significantly improved early differentiation as measured by expression of CD90 and CD105, as well as Collagen II deposition after two weeks of culture. Both of these effects were most pronounced on surfaces with patterning using large features (49.1µm diameter).

Together, these results suggest that immobilization of growth factors enhances the impact of a cell culture surface's topology on cells during culture. These results have not been confirmed and will require additional verification before these potential effects should be considered for implementation in clinical research, but they nonetheless provide preliminary evidence that the principle works as a proof-of-concept.

References

1. Lopreite, M. & Mauro, M. The effects of population ageing on health care expenditure : A Bayesian VAR analysis using data from Italy. *Health Policy (New. York).* **121,** 663–674 (2017).

2. Licchetta, M. & Stelmach, M. Fiscal sustainability analytical paper: Fiscal sustainability and public spending on health. 39 (2016). doi:10.1351/PAC-CON-09-10-22

3. Guzman-Castillo, M. *et al.* Forecasted trends in disability and life expectancy in England and Wales up to 2025: a modelling study. *Lancet Public Heal.* **2,** e307–e313 (2017).

4. *OECD/EU (2016), Health at a Glance: Europe 2016: State of Health in the EU Cycle, OECD Publishing, Paris, https://doi.org/10.1787/9789264265592-en*.

5. Chapel, J. M., Ritchey, M. D., Zhang, D. & Wang, G. Prevalence and Medical Costs of Chronic Diseases Among Adult Medicaid Beneficiaries. *Am. J. Prev. Med.* **53,** S143–S154 (2017).

6. Sampogna, G., Guraya, S. Y. & Forgione, A. Regenerative medicine: Historical roots and potential strategies in modern medicine. *J. Microsc. Ultrastruct.* **3,** 101–107 (2015).

7. Feyen, D. A. M., Gaetani, R., Doevendans, P. A. & Sluijter, J. P. G. Stem cell-based therapy: Improving myocardial cell delivery. *Adv. Drug Deliv. Rev.* **106,** 104–115 (2016).

8. Han, J., Park, J. & Kim, B. S. Integration of mesenchymal stem cells with nanobiomaterials for the repair of myocardial infarction. *Adv. Drug Deliv. Rev.* **95,** 15–28 (2015).

9. Aleksey Matveyenko, PhD1 and Adrian Vella, MD21Division of Physiology and Biomedical Engineering, Mayo Clinic, Rochester, MN2Division of Endocrinology & Metabolism, Mayo Clinic, Rochester, M. Regenerative Medicine in Diabetes. *HHS Public Access* **90,** 546–554 (2016).

10. Sepantafar, M. *et al.* Stem cells and injectable hydrogels: Synergistic therapeutics in myocardial repair. *Biotechnol. Adv.* **34,** 362–379 (2016).

11. Bitar, K. N. & Zakhem, E. Design Strategies of Biodegradable Scaffolds for Tissue Regeneration. *Biomed. Eng. Comput. Biol.* **6,** BECB.S10961 (2014).

12. Wei Teng, C., Foley, L., O'Neill, P. & Hicks, C. An analysis of supply chain strategies in the regenerative medicine industry - Implications for future development. *Int. J. Prod. Econ.* **149,** 211–225 (2014).

13. DeLong, J. M. & Bradley, J. P. The Current State of Stem Cell Therapies in Sports Medicine. *Oper. Tech. Orthop.* **26,** 124–134 (2016).

14. Mittra, J. *et al.* Identifying viable regulatory and innovation pathways for regenerative medicine: A case study of cultured red blood cells. *N. Biotechnol.* **32,** 180–190 (2015).

15. Liu, M., Liu, N., Zang, R., Li, Y. & Yang, S.-T. Engineering stem cell niches in bioreactors. *World J. Stem Cells* **5,** 124–35 (2013).

16. Lee, K., Silva, E. a & Mooney, D. J. Growth factor delivery-based tissue engineering: general approaches and a review of recent developments. *J. R. Soc. Interface* **8,** 153–70 (2011).

17. Stevens, M. M. Biomaterials for bone tissue engineering. *Mater. Today* **11,** 18–25 (2008).

18. Panadero, J. A., Lanceros-Mendez, S. & Ribelles, J. L. G. Differentiation of mesenchymal stem cells for cartilage tissue engineering: Individual and synergetic effects of three-dimensional environment and mechanical loading. *Acta Biomater.* **33,** 1–12 (2016).

19. Begam, H., Nandi, S. K., Kundu, B. & Chanda, A. Strategies for delivering bone morphogenetic protein for bone healing. *Mater. Sci. Eng. C* **70,** 856–869 (2016).

20. Mann, B. K., Schmedlen, R. H. & West, J. L. Tethered-TGF-β increases extracellular matrix production of vascular smooth muscle cells. *Biomaterials* **22,** 439–444 (2001).

21. Lee, Y. Bin *et al.* Polydopamine-mediated immobilization of multiple bioactive molecules for the development of functional vascular graft materials. *Biomaterials* **33,** 8343–8352 (2012).

22. Miller, E. D., Fisher, G. W., Weiss, L. E., Walker, L. M. & Campbell, P. G. Dose-dependent cell growth in response to concentration modulated patterns of FGF-2 printed on fibrin. *Biomaterials* **27,** 2213–2221 (2006).

23. Hume, P., He, J., Haskins, K. & Anseth, K. Strategies to reduce dendritic cell activation through functional biomaterial design. *Biomaterials* **33,** 3615–3625 (2012).

24. McCall, J. D., Luoma, J. E. & Anseth, K. S. Covalently tethered transforming growth factor beta in PEG hydrogels promotes chondrogenic differentiation of encapsulated human mesenchymal stem cells. *Drug Deliv. Transl. Res.* **2,** 305–312 (2012).

25. Hildebrandt, C., Büth, H. & Thielecke, H. Influence of cell culture media conditions on the osteogenic differentiation of cord blood-derived mesenchymal stem cells. *Ann. Anat.* **191,** 23–32 (2009).

26. Azarin, S. M. & Palecek, S. P. Development of scalable culture systems for human embryonic stem cells. *Biochem. Eng. J.* **48,** 378–384 (2010).

27. Chen, A. K. L., Chew, Y. K., Tan, H. Y., Reuveny, S. & Oh, S. K. W. Increasing efficiency of human mesenchymal stromal cell culture by optimization of microcarrier concentration and design of medium feed. *Cytotherapy* **17,** 163–173 (2015).

28. Wuchter, P. *et al.* Evaluation of GMP-compliant culture media for in vitro expansion of human bone marrow mesenchymal stromal cells. *Exp. Hematol.* **44,** 508–518 (2016).

29. Chen, K. G., Mallon, B. S., McKay, R. D. G. & Robey, P. G. Human pluripotent stem cell culture: Considerations for maintenance, expansion, and therapeutics. *Cell Stem Cell* **14,** 13–26 (2014).

30. Josh Miller, D. & Brophy, R. H. Microfracture and ability to return to sports after

cartilage surgery. *Oper. Tech. Orthop.* **24,** 240–245 (2014).

31. Solchaga, L. a., Penick, K. & Welter, J. F. *Chondrogenic Differentiation of Bone Marrow-Derived Mesenchymal Stem Cells: Tips and Tricks*. *Methods Mol Biol.* **2011,** (2006).

32. Anz, A. W., Bapat, A. & Murrell, W. D. Concepts in regenerative medicine: Past, present, and future in articular cartilage treatment. *J. Clin. Orthop. Trauma* **7,** 137–144 (2016).

33. Richardson, S. M. *et al.* Mesenchymal stem cells in regenerative medicine: Focus on articular cartilage and intervertebral disc regeneration. *Methods* **99,** 69–80 (2016).

34. Stevens, M. M. Exploring and Engineering the Cell Surface Interface. *Science (80-.).* **310,** 1135–1138 (2005).

35. Li, C., Vepari, C., Jin, H.-J., Kim, H. J. & Kaplan, D. L. Electrospun silk-BMP-2 scaffolds for bone tissue engineering. *Biomaterials* **27,** 3115–3124 (2006).

36. Lu, Z., Roohani-Esfahani, S.-I., Li, J. & Zreiqat, H. Synergistic effect of nanomaterials and BMP-2 signalling in inducing osteogenic differentiation of adipose tissue-derived mesenchymal stem cells. *Nanomedicine Nanotechnology, Biol. Med.* **11,** 219–228 (2015).

37. Kim, M. J. *et al.* BMP-2 peptide-functionalized nanopatterned substrates for enhanced osteogenic differentiation of human mesenchymal stem cells. *Biomaterials* **34,** 7236–7246 (2013).

38. Garza-Veloz, I. *et al.* Analyses of chondrogenic induction of adipose mesenchymal stem cells by combined co-stimulation mediated by adenoviral gene transfer. *Arthritis Res. Ther.* **15,** R80 (2013).

39. Lee, H., Choi, B., Min, B. & Park, S. Changes in surface markers of human mesenchymal stem cells during the chondrogenic differentiation and dedifferentiation processes in vitro. *Arthritis Rheum.* **60,** 2325–2332 (2009).

40. Koli, K., Ryynänen, M. J. & Keski-Oja, J. Latent TGF-beta binding proteins (LTBPs)-1 and -3 coordinate proliferation and osteogenic differentiation of

human mesenchymal stem cells. *Bone* **43,** 679–688 (2008).

41. Uccelli, A., Moretta, L. & Pistoia, V. Mesenchymal stem cells in health and disease. *Nat. Rev. Immunol.* **8,** 726–36 (2008).

42. Discher, D. E., Janmey, P. & Wang, Y. Tissue Cells Feel and Respond to the Stiffness of Their Substrate. *Mater. Biol.* **310,** 1139–1143 (2005).

43. Discher, D. E., Mooney, D. J. & Zandstra, P. W. Growth factors, matrices, and forces combine and control stem cells. *Science (80-.).* **324,** 1673–1677 (2009).

44. Fricke, S. *et al.* Allogeneic non-adherent bone marrow cells facilitate hematopoietic recovery but do not lead to allogeneic engraftment. *PLoS One* **4,** e6157 (2009).

45. Wan, C., He, Q., McCaigue, M., Marsh, D. & Li, G. Nonadherent cell population of human marrow culture is a complementary source of mesenchymal stem cells (MSCs). *J. Orthop. Res.* **24,** 21–28 (2006).

46. Zhang, Z. L. *et al.* Therapeutic potential of non-adherent BM-derived mesenchymal stem cells in tissue regeneration. *Bone Marrow Transplant.* **43,** 69–81 (2009).

47. Park, J. S. *et al.* The effect of matrix stiffness on the differentiation of mesenchymal stem cells in response to TGF-β. *Biomaterials* **32,** 3921–30 (2011).

48. Johnstone, B., Hering, T. M., Caplan, a I., Goldberg, V. M. & Yoo, J. U. In vitro chondrogenesis of bone marrow-derived mesenchymal progenitor cells. *Exp. Cell Res.* **238,** 265–272 (1998).

49. Li, L. *et al.* Fabrication of robust honeycomb polymer films : A facile photochemical cross-linking process. *J. Colloid Interface Sci.* **331,** 446–452 (2009).

50. Kim, Y. Il *et al.* Overexpression of TGF-β1 enhances chondrogenic differentiation and proliferation of human synovium-derived stem cells. *Biochem. Biophys. Res. Commun.* **450,** 1593–1599 (2014).

51. Jung, Y. *et al.* In situ chondrogenic differentiation of human adipose tissue-derived stem cells in a TGF-??1 loaded fibrin-poly(lactide-caprolactone) nanoparticulate complex. *Biomaterials* **30,** 4657–4664 (2009).

52. Cleary, M. A., Osch, G. J. V. M. van, Brama, P. A., Hellingman, C. A. & Narcisi, R. FGF, TGFb and Wnt crosstalk: embryonic to in vitro cartilage development frommesenchymal stemcells. *J Tissue Eng Regen Med* **9,** 332–342 (2015).

53. Huang, F. & Chen, Y.-G. Regulation of TGF-β receptor activity. *Cell Biosci.* **2,** 9 (2012).

54. Chou, C. H. *et al.* TGF-β1 immobilized tri-co-polymer for articular cartilage tissue engineering. *J. Biomed. Mater. Res. - Part B Appl. Biomater.* **77,** 338–348 (2006).

55. Penheiter, S. G. *et al.* Internalization-Dependent and -Independent Requirements for Transforming Growth Factor ␣ Receptor Signaling via the Smad Pathway. **22,** 4750–4759 (2002).

56. Zwaagstra, J. C., El-Alfyi, M. & O'Connor-McCourt, M. D. Transforming growth factor (TGF)-β1 internalization: Modulation by ligand interaction with TGF-β receptors types I and II and a mechanism that is distinct from clathrin-mediated endocytosis. *J. Biol. Chem.* **276,** 27237–27245 (2001).

57. Bianchi, G. *et al.* Ex vivo enrichment of mesenchymal cell progenitors by fibroblast growth factor 2. *Exp. Cell Res.* **287,** 98–105 (2003).

58. Buckley, C. T. & Kelly, D. J. Expansion in the presence of FGF-2 enhances the functional development of cartilaginous tissues engineered using infrapatellar fat pad derived MSCs. *J. Mech. Behav. Biomed. Mater.* **11,** 102–111 (2012).

59. Huang, Z., Ren, P. G., Ma, T., Smith, R. L. & Goodman, S. B. Modulating osteogenesis of mesenchymal stem cells by modifying growth factor availability. *Cytokine* **51,** 305–310 (2010).

60. Kabiri, A. *et al.* Effects of FGF-2 on human adipose tissue derived adult stem cells morphology and chondrogenesis enhancement in Transwell culture. *Biochem. Biophys. Res. Commun.* **424,** 234–8 (2012).

61. Khan, W. S., Tew, S. R., Adesida, A. B. & Hardingham, T. E. Human infrapatellar fat pad-derived stem cells express the pericyte marker 3G5 and show enhanced chondrogenesis after expansion in fibroblast growth factor-2. *Arthritis Res. Ther.* **10,** R74 (2008).

62. Mastrogiacomo, M., Cancedda, R. & Quarto, R. Effect of different growth factors on the chondrogenic potential of human bone marrow stromal cells. *Osteoarthr. Cartil.* **9,** 36–40 (2001).

63. Melrose, J., Shu, C., Whitelock, J. M. & Lord, M. S. The cartilage extracellular matrix as a transient developmental scaffold for growth plate maturation. *Matrix Biol.* **52–54,** 363–383 (2016).

64. Tiku, M. L. & Madhan, B. Preserving the longevity of long-lived type II collagen and its implication for cartilage therapeutics. *Ageing Res. Rev.* **28,** 62–71 (2016).

65. Martínez-Moreno, D., Jiménez, G., Gálvez-Martín, P., Rus, G. & Marchal, J. A. Cartilage biomechanics: A key factor for osteoarthritis regenerative medicine. *Biochim. Biophys. Acta - Mol. Basis Dis.* **1865,** 1067–1075 (2019).

66. Demoor, M. *et al.* Cartilage tissue engineering: Molecular control of chondrocyte differentiation for proper cartilage matrix reconstruction. *Biochim. Biophys. Acta - Gen. Subj.* **1840,** 2414–2440 (2014).

67. Sun, L. *et al.* In vitro biological characteristics of human cord blood-derived megakaryocytes. *Ann. Acad. Med.* **33,** 570–575 (2004).

68. Ronzoni, L. *et al.* Erythroid differentiation and maturation from peripheral CD34+ cells in liquid culture: cellular and molecular characterization. *Blood Cells. Mol. Dis.* **40,** 148–55 (2008).

69. Lai, A. & Kondo, M. T and B lymphocyte differentiation from hematopoietic stem cell. *Semin. Immunol.* **20,** 207–212 (2008).

70. Matsunaga, T. *et al.* Ex vivo large-scale generation of human platelets from cord blood CD34+ cells. *Stem Cells* **24,** 2877–2887 (2006).

71. Ema, H., Morita, Y. & Suda, T. Heterogeneity and hierarchy of hematopoietic

stem cells. *Exp. Hematol.* **42,** 74–82 (2014).

72. Babovic, S. & Eaves, C. J. Hierarchical organization of fetal and adult hematopoietic stem cells. *Exp. Cell Res.* 1–7 (2014). doi:10.1016/j.yexcr.2014.08.005

73. Cuchiara, M. L., Horter, K. L., Banda, O. a. & West, J. L. Covalent immobilization of stem cell factor and stromal derived factor 1α for in vitro culture of hematopoietic progenitor cells. *Acta Biomater.* **9,** 9258–9269 (2013).

74. Kishimoto, S. *et al.* Cytokine-immobilized microparticle-coated plates for culturing hematopoietic progenitor cells. *J. Control. Release* **133,** 185–190 (2009).

75. Bruno, S. *et al.* In vitro and in vivo megakaryocyte differentiation of fresh and ex-vivo expanded cord blood cells: rapid and transient megakaryocyte reconstitution. *J. Hematol.* **88,** 379–387 (2003).

76. Siddiqui, N. F. A., Shabrani, N. C., Kale, V. P. & Limaye, L. S. Enhanced generation of megakaryocytes from umbilical cord blood-derived CD34+ cells expanded in the presence of two nutraceuticals, docosahexanoic acid and arachidonic acid, as supplements to the cytokine-containing medium. *Cytotherapy* **13,** 114–128 (2011).

77. Kratz-Albers, K. *et al.* Effective ex vivo generation of megakaryocytic cells from mobilized peripheral blood CD34+ cells with stem cell factor and promegapoietin. *Exp. Hematol.* **28,** 335–346 (2000).

78. Dimitriou, H. *et al.* In vitro proliferative and differentiating characteristics of CD133+ and CD34+ cord blood cells in the presence of thrombopoietin (TPO) or erythropoietin (EPO): Potential implications for hematopoietic cell transplantation. *Leuk. Res.* **27,** 1143–1151 (2003).

79. Hatami, J. *et al.* Proliferation extent of CD34+ cells as a key parameter to maximize megakaryocytic differentiation of umbilical cord blood-derived hematopoietic stem/progenitor cells in a two-stage culture protocol. *Biotechnol. Reports* **4,** 50–55 (2014).

80. Schmetzer, O. *et al.* A novel method to generate and culture human mast cells: peripheral CD34+ stem cell-derived mast cells (PSCMCs). *J. Immunol. Methods* **413,** 62–8 (2014).

81. Boehm, D., Murphy, W. & Al-Rubeai, M. The potential of human peripheral blood derived CD34+ cells for ex vivo red blood cell production. *J. Biotechnol.* **144,** 127–134 (2009).

82. De Molfetta, G. *et al.* Role of NFKB2 on the early myeloid differentiation of CD34+ hematopoietic stem/progenitor cells. *Differentiation* **80,** 195–203 (2010).

83. Flores-Guzmán, P., Gutiérrez-Rodríguez, M. & Mayani, H. In vitro proliferation, expansion, and differentiation of a CD34+ cell-enriched hematopoietic cell population from human umbilical cord blood in response to recombinant cytokines. *Arch. Med. Res.* **33,** 107–114 (2002).

84. Qiu, C. *et al.* Differentiation of human embryonic stem cells into hematopoietic cells by coculture with human fetal liver cells recapitulates the globin switch that occurs early in development. *Exp. Hematol.* **33,** 1450–1458 (2005).

85. Wang, J. *et al.* In vitro hematopoietic differentiation of human embryonic stem cells induced by co-culture with human bone marrow stromal cells and low dose cytokines. *Cell Biol. Int.* **29,** 654–61 (2005).

86. Kuadkitkan, A., Wikan, N. & Smith, D. R. Induced pluripotent stem cells: A new addition to the virologists armamentarium. *J. Virol. Methods* **235,** 191–195 (2016).

87. De Vos, J., Bouckenheimer, J., Sansac, C., Lemaître, J. M. & Assou, S. Human induced pluripotent stem cells: A disruptive innovation. *Curr. Res. Transl. Med.* **64,** 91–96 (2016).

88. Youssef, A. A. *et al.* The Promise and Challenge of Induced Pluripotent Stem Cells for Cardiovascular Applications. *JACC Basic to Transl. Sci.* **1,** 510–523 (2016).

89. Oh, S. *et al.* Stem cell fate dictated solely by altered nanotube dimension. *Proc. Natl. Acad. Sci.* **106,** 2130–2135 (2009).

90. Puleo, D. a., Kissling, R. a. & Sheu, M. S. A technique to immobilize bioactive proteins, including bone morphogenetic protein-4 (BMP-4), on titanium alloy. *Biomaterials* **23,** 2079–2087 (2002).

91. Lavenus, S. *et al.* Behaviour of mesenchymal stem cells, fibroblasts and osteoblasts on smooth surfaces. *Acta Biomater.* **7,** 1525–34 (2011).

92. Kim, S. E. *et al.* Improving osteoblast functions and bone formation upon BMP-2 immobilization on titanium modified with heparin. *Carbohydr. Polym.* **114,** 123–132 (2014).

93. Krutty, J. D., Schmitt, S. K., Gopalan, P. & Murphy, W. L. Surface functionalization and dynamics of polymeric cell culture substrates. *Curr. Opin. Biotechnol.* **40,** 164–169 (2016).

94. Stratton, S., Shelke, N. B., Hoshino, K., Rudraiah, S. & Kumbar, S. G. Bioactive polymeric scaffolds for tissue engineering. *Bioact. Mater.* **1,** 93–108 (2016).

95. Hern, D. L. & Hubbell, J. a. Incorporation of adhesion peptides into nonadhesive hydrogels useful for tissue resurfacing. *J. Biomed. Mater. Res.* **39,** 266–276 (1998).

96. Kim, T. G. & Park, T. G. Biomimicking Extracellular Matrix : *Tissue Eng.* **12,** 221–233 (2006).

97. Yang, F. *et al.* The effect of incorporating RGD adhesive peptide in polyethylene glycol diacrylate hydrogel on osteogenesis of bone marrow stromal cells. *Biomaterials* **26,** 5991–5998 (2005).

98. Han, Y., Jin, J., Cui, J. & Jiang, W. Effect of hydrophilicity of end-grafted polymers on protein adsorption behavior: A Monte Carlo study. *Colloids Surfaces B Biointerfaces* **142,** 38–45 (2016).

99. Bačáková, L., Filova, E., Rypáček, F., Švorčík, V. & Starý, V. Cell adhesion on artificial materials for tissue engineering. *Physiol. Res.* **53,** S35–S45 (2004).

100. Budkowski, A. *et al.* Substrate-determined shape of free surface profiles in spin-cast polymer blend films. *Macromolecules* **36,** 4060–4067 (2003).

101. Beattie, D. *et al.* Honeycomb-structured porous films from polypyrrole-containing block copolymers prepared via RAFT polymerization as a scaffold for cell growth. *Biomacromolecules* **7,** 1072–1082 (2006).

102. Olivier, A., Meyer, F., Raquez, J. M., Damman, P. & Dubois, P. Surface-initiated controlled polymerization as a convenient method for designing functional polymer brushes: From self-assembled monolayers to patterned surfaces. *Prog. Polym. Sci.* **37,** 157–181 (2012).

103. Cheng, C., Tian, Y., Shi, Y., Tang, R. & Xi, F. Porous polymer films and honeycomb structures based on amphiphilic dendronized block copolymers. *Langmuir* **21,** 6576–6581 (2005).

104. Cui, G. *et al.* Perpendicular oriented cylinders via directional coalescence of spheres embedded in block copolymer films induced by solvent annealing. *Polymer (Guildf).* **55,** 1601–1608 (2014).

105. Li, B., Shi, Y., Zhu, W., Fu, Z. & Yang, W. Synthesis of Amphiphilic Polystyrene- b -Poly (acrylic acid) Diblock Copolymers by Iodide-Mediated Radical Polymerization. *Polym. J.* **38,** 387–394 (2006).

106. Kang, Y. & Taton, T. A. Core/Shell Gold Nanoparticles by Self-Assembly and Crosslinking of Micellar, Block-Copolymer Shells. *Angew. Chemie* **44,** 409–412 (2005).

107. Gong, F. *et al.* Biodegradable comb-dendritic tri-block copolymers consisting of poly (ethylene glycol) and poly (L-lactide): Synthesis , characterizations , and regulation of surface morphology and cell responses. *Polymer (Guildf).* **50,** 2775–2785 (2009).

108. Hudalla, G. a, Eng, T. S. & Murphy, W. L. An approach to modulate degradation and mesenchymal stem cell behavior in poly(ethylene glycol) networks. *Biomacromolecules* **9,** 842–9 (2008).

109. Kar, M., Shih, Y. V., Velez, D. O., Cabrales, P. & Varghese, S. Biomaterials Poly (ethylene glycol) hydrogels with cell cleavable groups for autonomous cell delivery. *Biomaterials* **77,** 186–197 (2016).

110. Xin, A., Gaydos, C. & Mao, J. In vitro degradation behavior of photopolymerized PEG hydrogels as tissue engineering scaffold. *Eng. Med. Biol. Soc.* 2091–2093 (2006). at <http://ieeexplore.ieee.org/xpls/abs_all.jsp?arnumber=4462199>

111. Gasparini, G., Holdich, R. G. & Kosvintsev, S. R. PLGA particle production for water-soluble drug encapsulation: Degradation and release behaviour. *Colloids Surfaces B Biointerfaces* **75,** 557–564 (2010).

112. Kumari, A., Yadav, S. K. & Yadav, S. C. Biodegradable polymeric nanoparticles based drug delivery systems. *Colloids Surfaces B Biointerfaces* **75,** 1–18 (2010).

113. Li, J. & Li, H. M. Functionalization of syndiotactic polystyrene with succinic anhydride in the presence of aluminum chloride. *Eur. Polym. J.* **41,** 823–829 (2005).

114. Niveleau, A. *et al.* Covalent linking of haptens, proteins and nucleic acids to a modified polystyrene support. *J. Immunol. Methods* **159,** 177–187 (1993).

115. Sasai, Y., Matsuzaki, N., Kondo, S. I. & Kuzuya, M. Introduction of carboxyl group onto polystyrene surface using plasma techniques. *Surf. Coatings Technol.* **202,** 5724–5727 (2008).

116. Wang, L. *et al.* Surface modification of polystyrene with atomic oxygen radical anions-dissolved solution. *Appl. Surf. Sci.* **254,** 4191–4200 (2008).

117. Yusilawati, a N. *et al.* Surface Modification of Polystyrene Beads by Ultraviolet / Ozone Treatment and its Effect on Gelatin Coating Department of Biotechnology Engineering , Faculty of Engineering , School of Arts and Science , Tunku Abdul Rahman College , Kuala Lumpur , Malays. *Am. J. Appl. Sci.* **7,** 724–731 (2010).

118. Francisco, A. T. *et al.* Photocrosslinkable laminin-functionalized polyethylene glycol hydrogel for intervertebral disc regeneration. *Acta Biomater.* **10,** 1102–1111 (2014).

119. Raic, A., Rödling, L., Kalbacher, H. & Lee-Thedieck, C. Biomimetic

macroporous PEG hydrogels as 3D scaffolds for the multiplication of human hematopoietic stem and progenitor cells. *Biomaterials* **35,** 929–940 (2014).

120. Mironi-Harpaz, I., Wang, D. Y., Venkatraman, S. & Seliktar, D. Photopolymerization of cell-encapsulating hydrogels: crosslinking efficiency versus cytotoxicity. *Acta Biomater.* **8,** 1838–48 (2012).

121. Phelps, E. *et al.* Maleimide cross-linked bioactive peg hydrogel exhibits improved reaction kinetics and cross-linking for cell encapsulation and in situ delivery. *Adv. Mater.* **24,** 1–12 (2012).

122. Smith, A. W. *et al.* Long-term culture of HL-1 cardiomyocytes in modular poly (ethylene glycol) microsphere-based scaffolds crosslinked in the phase-separated state. *Acta Biomater.* **8,** 31–40 (2012).

123. Li, Y. *et al.* Nanostructured PEG-based hydrogels with tunable physical properties for gene delivery to human mesenchymal stem cells. *Biomaterials* **33,** 6533–6541 (2012).

124. Castro, D., Conchouso, D., Fan, Y. & Foulds, I. Surface Treatments of Soft Molds for High Aspect Ratio Molding of Poly-PEGDA. *Proc. of MicroTAS* 1231–1233 (2012).

125. Starly, B., Chang, R. & Sun, W. UV-Photolithography fabrication of poly-ethylene glycol hydrogels encapsulated with hepatocytes. *Proc. 17th Annu. Solid Free. Fabr. Symp.* 102–110 (2006). at <http://edge.rit.edu/content/P10551/public/SFF/SFF 2006 Proceedings/Manuscripts/10-Starly.pdf>

126. Zhu, J., Beamish, J. A., Tang, C., Kottke-Marchant, K. & Marchant, R. E. Extracellular matrix-like cell-adhesive hydrogels from RGD-containing poly(ethylene glycol) diacrylate. *Macromolecules* **39,** 1305–1307 (2006).

127. Roberts, M. J., Bentley, M. D. & Harris, J. M. Chemistry for peptide and protein PEGylation. *Adv. Drug Deliv. Rev.* **64,** 116–127 (2012).

128. Salmaso, S. *et al.* Preparation and characterization of active site protected poly(ethylene glycol)-avidin bioconjugates. *Biochim. Biophys. Acta* **1726,** 57–

66 (2005).

129. Jiang, B., Waller, T. M., Larson, J. C., Appel, A. a & Brey, E. M. Fibrin-loaded porous poly(ethylene glycol) hydrogels as scaffold materials for vascularized tissue formation. *Tissue Eng. Part A* **19,** 224–34 (2013).

130. Salinas, C. N. & Anseth, K. S. The enhancement of chondrogenic differentiation of human mesenchymal stem cells by enzymatically regulated RGD functionalities. *Biomaterials* **29,** 2370–2377 (2008).

131. Tsiftsoglou, A., Bonovolias, I. & Tsiftsoglou, S. Multilevel targeting of hematopoietic stem cell self-renewal, differentiation and apoptosis for leukemia therapy. *Pharmacol. Ther.* **122,** 264–280 (2009).

132. Salinas, C. N. & Anseth, K. S. Decorin moieties tethered into PEG networks induce chondrogenesis of human mesenchymal stem cells. *J. Biomed. Mater. Res. - Part A* **90,** 456–464 (2009).

133. Zhu, J., Tang, C., Kottke-Marchant, K. & Marchant, R. E. Design and synthesis of biomimetic hydrogel scaffolds with controlled organization of cyclic RGD peptides. *Bioconjug. Chem.* **20,** 333–9 (2009).

134. Marletta, G. *et al.* Improved osteogenic differentiation of human marrow stromal cells cultured on ion-induced chemically structured poly-??-caprolactone. *Biomaterials* **28,** 1132–1140 (2007).

135. Drevelle, O. *et al.* Effect of functionalized polycaprolactone on the behaviour of murine preosteoblasts. *Biomaterials* **31,** 6468–6476 (2010).

136. Chouzouri, G. & Xanthos, M. In vitro bioactivity and degradation of polycaprolactone composites containing silicate fillers. *Acta Biomater.* **3,** 745–756 (2007).

137. Woodruff, M. A. & Hutmacher, D. W. The return of a forgotten polymer - Polycaprolactone in the 21st century. *Prog. Polym. Sci.* **35,** 1217–1256 (2010).

138. Shi, R. *et al.* Structure, physical properties, biocompatibility and in vitro/vivo degradation behavior of anti-infective polycaprolactone-based electrospun membranes for guided tissue/bone regeneration. *Polym. Degrad. Stab.* **109,**

293–306 (2014).

139. Lei, Y., Rai, B., Ho, K. H. & Teoh, S. H. In vitro degradation of novel bioactive polycaprolactone-20% tricalcium phosphate composite scaffolds for bone engineering. *Mater. Sci. Eng. C* **27,** 293–298 (2007).

140. Chen, M. *et al.* In-situ polymerisation of fully bioresorbable polycaprolactone/phosphate glass fibre composites: In vitro degradation and mechanical properties. *J. Mech. Behav. Biomed. Mater.* **59,** 78–89 (2016).

141. Guerra, A. J. & Ciurana, J. 3D-printed bioabsordable polycaprolactone stent: The effect of process parameters on its physical features. *Mater. Des.* **137,** 430–437 (2018).

142. Shao, Z. *et al.* Polycaprolactone electrospun mesh conjugated with an MSC affinity peptide for MSC homing in vivo. *Biomaterials* **33,** 3375–3387 (2012).

143. Sun, H. & Onneby, S. Facile Polyester surface functionalization via hydrolysis and cell-recognizing peptide attachment. *Polym. Int.* **55,** 1336–1340 (2006).

144. He, Y., Wildman, R. D., Tuck, C. J., Christie, S. D. R. & Edmondson, S. An Investigation of the Behavior of Solvent based Polycaprolactone ink for Material Jetting. *Sci. Rep.* **6,** 1–10 (2016).

145. Bahrami, S. H. & Gholipour Kanani, A. Effect of changing solvents on poly(ε-Caprolactone) nanofibrous webs morphology. *J. Nanomater.* **2011,** (2011).

146. Katsogiannis, K. A. G., Vladisavljević, G. T. & Georgiadou, S. Porous electrospun polycaprolactone (PCL) fibres by phase separation. *Eur. Polym. J.* **69,** 284–295 (2015).

147. Pok, S. W., Wallace, K. N. & Madihally, S. V. In vitro characterization of polycaprolactone matrices generated in aqueous media. *Acta Biomater.* **6,** 1061–1068 (2010).

148. Lee, S. H., Lee, J. H. & Cho, Y. S. Analysis of degradation rate for dimensionless surface area of well-interconnected PCL scaffold via in-vitro accelerated degradation experiment. *Tissue Eng. Regen. Med.* **11,** 446–452 (2014).

149. Willerth, S. M. & Sakiyama-elbert, S. E. in *StemBook* 1–18 (2008). doi:10.3824/stembook.1.1.1

150. Zhao, C., Tan, A., Pastorin, G. & Ho, H. K. Nanomaterial scaffolds for stem cell proliferation and differentiation in tissue engineering. *Biotechnol. Adv.* **31,** 654–668 (2013).

151. Sundelacruz, S. & Kaplan, D. L. Stem cell- and scaffold-based tissue engineering approaches to osteochondral regenerative medicine. *Semin. Cell Dev. Biol.* **20,** 646–655 (2009).

152. Tello, M. *et al.* Generating and characterizing the mechanical properties of cell-derived matrices using atomic force microscopy. *Methods* **94,** 85–100 (2016).

153. Lutolf, M. P. & Hubbell, J. a. Synthetic biomaterials as instructive extracellular microenvironments for morphogenesis in tissue engineering. *Nat. Biotechnol.* **23,** 47–55 (2005).

154. Ma, Z., Gao, C., Gong, Y. & Shen, J. Paraffin Spheres as Porogen to Fabricate Poly (L-Lactic Acid) Scaffolds with Improved Cytocompatibility for Cartilage Tissue Engineering. *J. Biomed. Mater. Res. - Part B Appl. Biomater.* **67,** 610–617 (2003).

155. Ellis, G. J. & Martin, M. C. Opportunities and challenges for polymer science using synchrotron-based infrared spectroscopy. *Eur. Polym. J.* **81,** 505–531 (2016).

156. Martinez, A. W., Caves, J. M., Ravi, S., Li, W. & Chaikof, E. L. Effects of crosslinking on the mechanical properties, drug release and cytocompatibility of protein polymers. *Acta Biomater.* **10,** 26–33 (2014).

157. Jin, C., Wang, Z., Volinsky, A. A., Sharfeddin, A. & Gallant, N. D. Mechanical characterization of crosslinking effect in polydimethylsiloxane using nanoindentation. *Polym. Test.* **56,** 329–336 (2016).

158. Zhou, T. *et al.* Surface functionalization of biomaterials by radical polymerization. *Prog. Mater. Sci.* **83,** 191–235 (2016).

159. Lin, C. C. & Anseth, K. S. Controlling affinity binding with peptide-

functionalized poly(ethylene glycol) hydrogels. *Adv. Funct. Mater.* **19,** 2325–2331 (2009).

160. Schüler, F. *et al.* Synthesis of Macroporous Polystyrene by the Polymerization of Foamed Emulsions. *Angew. Chemie* **51,** 2213–2217 (2012).

161. Dendukuri, D. *et al.* Modeling of oxygen-inhibited free radical photopolymerization in a PDMS microfluidic device. *Macromolecules* **41,** 8547–8556 (2008).

162. Douka, A., Vouyiouka, S., Papaspyridi, L. M. & Papaspyrides, C. D. A review on enzymatic polymerization to produce polycondensation polymers: The case of aliphatic polyesters, polyamides and polyesteramides. *Prog. Polym. Sci.* **79,** 1–25 (2018).

163. Gross, R. A., Ganesh, M. & Lu, W. Enzyme-catalysis breathes new life into polyester condensation polymerizations. *Trends Biotechnol.* **28,** 435–443 (2010).

164. Yokozawa, T. & Yokoyama, A. Chain-growth polycondensation: The living polymerization process in polycondensation. *Prog. Polym. Sci.* **32,** 147–172 (2007).

165. Moriyama, K., Minamihata, K., Wakabayashi, R., Goto, M. & Kamiya, N. Enzymatic preparation of streptavidin-immobilized hydrogel using a phenolated linear poly(ethylene glycol). *Biochem. Eng. J.* **76,** 37–42 (2013).

166. Ciofani, G. *et al.* A simple approach to covalent functionalization of boron nitride nanotubes. *J. Colloid Interface Sci.* **374,** 308–314 (2012).

167. Kopesky, P. W. *et al.* Controlled delivery of transforming growth factor β1 by self-assembling peptide hydrogels induces chondrogenesis of bone marrow stromal cells and modulates Smad2/3 signaling. *Tissue Eng. Part A* **17,** 83–92 (2011).

168. Sabino, M. A. Oxidation of polycaprolactone to induce compatibility with other degradable polyesters. *Polym. Degrad. Stab.* **92,** 986–996 (2007).

169. Perikamana, S. K. M. *et al.* Graded functionalization of biomaterial surfaces

using mussel-inspired adhesive coating of polydopamine. *Colloids Surfaces B Biointerfaces* **159,** 546–556 (2017).

170. Goreham, R. V. *et al.* A substrate independent approach for generation of surface gradients. *Thin Solid Films* **528,** 106–110 (2013).

171. Wang, P. Y., Clements, L. R., Thissend, H., Tsaia, W. B. & Voelckere, N. H. Screening rat mesenchymal stem cell attachment and differentiation on surface chemistries using plasma polymer gradients. *Acta Biomater.* **11,** 58–67 (2015).

172. Chu, P. K., Chen, J. Y., Wang, L. P. & Huang, N. Plasma-surface modification of biomaterials. *Mater. Sci. Eng.* **36,** 143–206 (2002).

173. Kim, M., Seo, K., Khang, G. & Lee, H. Preparation of a gradient biotinylated polyethylene surface to bind streptavidin-FITC. *Bioconjug. Chem.* **16,** 245–249 (2005).

174. Al-Bataineh, S. *et al.* Fabrication and Operation of a Microcavity Plasma Array Device for Microscale Surface Modification. *Plasma Process. Polym.* **9,** 638–646 (2012).

175. Langowski, B. A. & Uhrich, K. E. Microscale Plasma-Initiated Patterning (μPIP). *Langmuir* **21,** 10509–10514 (2005).

176. Terlingen, J. G., Gerritsen, H. F., Hoffman, A. S. & Feijfen, J. Introduction of functional groups on polyethylene surfaces by a carbon dioxide plasma treatment. *J. Appl. Polym. Sci.* **57,** 969–982 (1995).

177. Scaffaro, R. *et al.* Plasma modified PLA electrospun membranes for actinorhodin production intensification in Streptomyces coelicolor immobilized-cell cultivations. *Colloids Surfaces B Biointerfaces* **157,** 233–241 (2017).

178. Minati, L. *et al.* Plasma assisted surface treatments of biomaterials. *Biophys. Chem.* **229,** 151–164 (2017).

179. Daudt, N. F., Bram, M., Cysne Barbosa, A. P. & Alves, C. Surface modification of highly porous titanium by plasma treatment. *Mater. Lett.* **141,** 194–197 (2015).

180. Finbloom, J. A. & Francis, M. B. Supramolecular strategies for protein immobilization and modification. *Curr. Opin. Chem. Biol.* **46,** 91–98 (2018).

181. Awsiuk, K. *et al.* Immobilization of oligonucleotide probes on silicon surfaces using biotin–streptavidin system examined with microscopic and spectroscopic techniques. *Appl. Surf. Sci.* **290,** 199–206 (2014).

182. Min, E., Wong, K. H. & Stenzel, M. H. Microwells with Patterned Proteins by a Self-Assembly Process Using Honeycomb-Structured Porous Films. *Adv. Mater.* **20,** 3550–3556 (2008).

183. Balan, V. *et al.* Functionalized magnetic composites based on block copolymers poly (succinimide)-b-poly (ethylene glycol) with potential applications in blood detoxification. *Compos. Part B* **43,** 926–932 (2012).

184. Bauer, S., Schmuki, P., von der Mark, K. & Park, J. Engineering biocompatible implant surfaces: Part I: Materials and surfaces. *Prog. Mater. Sci.* **58,** 261–326 (2013).

185. Dhandayuthapani, B., Yoshida, Y., Maekawa, T. & Kumar, D. S. Polymeric Scaffolds in Tissue Engineering Application : A Review. **2011,** (2011).

186. Engel, E., Michiardi, A., Navarro, M., Lacroix, D. & Planell, J. A. Nanotechnology in regenerative medicine: the materials side. *Trends Biotechnol.* **26,** 39–47 (2008).

187. Floren, M. *et al.* Human mesenchymal stem cells cultured on silk hydrogels with variable stiffness and growth factor differentiate into mature smooth muscle cell phenotype. *Acta Biomater.* **31,** 156–166 (2016).

188. Camarero-Espinosa, S., Rothen-Rutishauser, B., Foster, E. J. & Weder, C. Articular cartilage: from formation to tissue engineering. *Biomater. Sci.* **4,** 734–767 (2016).

189. Zhao, F. *et al.* Preparation and histological evaluation of biomimetic three-dimensional hydroxyapatite/chitosan-gelatin network composite scaffolds. *Biomaterials* **23,** 3227–3234 (2002).

190. Cooperstein, I., Layani, M. & Magdassi, S. 3D printing of porous structures by

UV-curable O/W emulsion for fabrication of conductive objects. *J. Mater. Chem. C* **3,** 2040–2044 (2015).

191. Hua, F. J., Nam, J. Do & Lee, D. S. Preparation of a Macroporous Poly (l - lactide) Scaffold by Liquid-Liquid Phase Separation of a PLLA / 1 , 4- Dioxane / Water Ternary System in the Presence of NaCl. 1053–1057 (2001).

192. Liu, X., Ma, P. X., Iu, X. I. L. & Eter, P. X. M. A. Polymeric scaffolds for bone tissue engineering. *Ann. Biomed. Eng.* **32,** 477–486 (2004).

193. Chiu, Y., Larson, J., Isom, A. & Brey, E. M. Generation of porous poly (ethylene glycol) hydrogels by salt leaching. *Tissue Eng. Part C* **16,** 905–912 (2010).

194. Kim, T. G., Chung, H. J. & Park, T. G. Macroporous and nanofibrous hyaluronic acid/collagen hybrid scaffold fabricated by concurrent electrospinning and deposition/leaching of salt particles. *Acta Biomater.* **4,** 1611–1619 (2008).

195. Camarero-Espinosa, S. & Cooper-White, J. Tailoring Biomaterial Scaffolds for Osteochondral Repair. *Int. J. Pharm.* (2016). doi:10.1016/j.ijpharm.2016.10.035

196. Gupta, A. *et al.* Porous nylon-6 fibers via a novel salt-induced electrospinning method. *Macromolecules* **42,** 709–715 (2009).

197. Emmelmann, C., Scheinemann, P., Munsch, M. & Seyda, V. Laser Additive Manufacturing of Modified Implant Surfaces with Osseointegrative Characteristics. *Phys. Procedia* **12,** 375–384 (2011).

198. Lusquiños, F. *et al.* Bioceramic 3D Implants Produced by Laser Assisted Additive Manufacturing. *Phys. Procedia* **56,** 309–316 (2014).

199. Kucukgul, C., Ozler, B., Karakas, H. E., Gozuacik, D. & Koc, B. 3D hybrid bioprinting of macrovascular structures. *Procedia Eng.* **59,** 183–192 (2013).

200. Singh, J. P. & Pandey, P. M. Fitment study of porous polyamide scaffolds fabricated from selective laser sintering. *Procedia Eng.* **59,** 59–71 (2013).

201. Patrício, T., Domingos, M., Gloria, A. & Bártolo, P. Characterisation of PCL and PCL/PLA Scaffolds for Tissue Engineering. *Procedia CIRP* **5,** 110–114 (2013).

202. Bae, M., Divan, R., Suthar, K., Mancini, D. & Gemeinhart, R. Fabrication of poly (ethylene glycol) hydrogel structures for pharmaceutical applications using electron beam and optical lithography. *J. Vac. Sci. Technol. B. Microelectron. Nanometer Struct. Process. Meas. Phenom.* **28,** 1–17 (2010).

203. Khoda, A. K. M. B., Ozbolat, I. T. & Koc, B. Spatially multi-functional porous tissue scaffold. *Procedia Eng.* **59,** 174–182 (2013).

204. Rodriguez, G., Dias, J., D'Ávila, M. & Bártolo, P. Influence of Hydroxyapatite on Extruded 3D Scaffolds. *Procedia Eng.* **59,** 263–269 (2013).

205. Shishkovsky, I. & Scherbakov, V. Selective laser sintering of biopolymers with micro and nano ceramic additives for medicine. *Phys. Procedia* **39,** 491–499 (2012).

206. Gu, D. *et al.* Selective laser melting additive manufacturing of TiC / AlSi10Mg bulk-form nanocomposites with tailored microstructures and properties. *Phys. Procedia* **56,** 108–116 (2014).

207. Blau, A. Cell adhesion promotion strategies for signal transduction enhancement in microelectrode array in vitro electrophysiology : An introductory overview and critical discussion. *Curr. Opin. Colloid Interface Sci.* **18,** 481–492 (2013).

208. Ciurana, J. De, Serenóa, L. & Vallès, È. Selecting process parameters in RepRap additive manufacturing system for PLA scaffolds manufacture. *Procedia CIRP* **5,** 152–157 (2013).

209. Podshivalov, L. *et al.* Design , analysis and additive manufacturing of porous structures for biocompatible micro-scale scaffolds. *Procedia CIRP* **5,** 247–252 (2013).

210. Karageorgiou, V. & Kaplan, D. Porosity of 3D biomaterial scaffolds and osteogenesis. *Biomaterials* **26,** 5474–5491 (2005).

211. Escalé, P., Rubatat, L., Billon, L. & Save, M. Recent advances in honeycomb-structured porous polymer films prepared via breath figures. *Eur. Polym. J.* **48,** 1001–1025 (2012).

212. Munoz-Bonilla, A., Fernández-garcía, M. & Rodríguez-hernández, J. Towards hierarchically ordered functional porous polymeric surfaces prepared by the breath figures approach. *Prog. Polym. Sci.* **39,** 510–554 (2014).

213. Gao, J. *et al.* Well-defined monocarboxyl-terminated polystyrene with low molecular weight : A candidate for the fabrication of highly ordered microporous films and microspheres via a static breath-figure process. *Eur. Polym. J.* **59,** 171–179 (2014).

214. Lima, M. J., Correlo, V. M. & Reis, R. L. Micro / nano replication and 3D assembling techniques for scaffold fabrication. *Mater. Sci. Eng. C* **42,** 615–621 (2014).

215. Alapan, Y., Icoz, K. & Gurkan, U. A. Micro- and nanodevices integrated with biomolecular probes. *Biotechnol. Adv.* **33,** 1727–1743 (2015).

216. Prittinen, J. *et al.* Chondrocyte behavior on nanostructured micropillar polypropylene and polystyrene surfaces. *Mater. Sci. Eng. C* **43,** 424–431 (2014).

217. Ma, P. X. & Choi, J. Biodegradable Polymer Scaffolds with Well-Defined Interconnected Spherical Pore Network. *Tissue Eng.* **7,** 23–33 (2001).

218. Vaquette, C., Frochot, C., Rahouadj, R. & Wang, X. An Innovative Method to Obtain Porous PLLA Scaffolds With Highly Spherical and Interconnected Pores. *J. Biomed. Mater. Res. - Part B Appl. Biomater.* **86,** 9–17 (2007).

219. Yao, T. *et al.* Patterns of conducting polypyrrole with tunable morphologies. *Polymer (Guildf).* **50,** 3938–3942 (2009).

220. Santos, L. *et al.* Electrosynthesis of well-organized nanoporous poly(3,4-ethylenedioxythiophene) by nanosphere lithography. *Electrochem. commun.* **12,** 872–875 (2010).

221. Bettinger, C. J., Langer, R. & Borenstein, J. T. Engineering Substrate Micro-

and Nanotopography to Control Cell Function. *Angew Chem Int Ed Engl.* **48,** 5406–5415 (2010).

222. Diener, A. *et al.* Control of focal adhesion dynamics by material surface characteristics. *Biomaterials* **26,** 383–392 (2005).

223. Dalby, M. J. *et al.* The control of human mesenchymal cell differentiation using nanoscale symmetry and disorder. *Nat. Mater.* **6,** 997–1003 (2007).

224. Watari, S. *et al.* Modulation of osteogenic differentiation in hMSCs cells by submicron topographically-patterned ridges and grooves. *Biomaterials* **33,** 128–136 (2012).

225. Agarwal, S., Wendorff, J. H. & Greiner, A. Use of electrospinning technique for biomedical applications. *Polymer (Guildf).* **49,** 5603–5621 (2008).

226. Engelmayr, G. C. J. *et al.* Accordion-like Honeycombs for Tissue Engineering of Cardiac Anisotropy. *Nat. Mater.* **7,** 1003–1010 (2009).

227. Zink, C., Hall, H., Brunette, D. M. & Spencer, N. D. Biomaterials Orthogonal nanometer-micrometer roughness gradients probe morphological in fl uences on cell behavior. *Biomaterials* **33,** 8055–8061 (2012).

228. Vallés, G. *et al.* Topographical cues regulate the crosstalk between MSCs and macrophages. *Biomaterials* **37,** 124–133 (2015).

229. Nooeaid, P., Salih, V., Beier, J. P. & Boccaccini, A. R. Osteochondral tissue engineering: scaffolds, stem cells and applications. *J. Cell. Mol. Med.* **16,** 2247–2270 (2012).

230. Rutala, W. A. & David J. Weber. Guideline for Disinfection and Sterilization in Healthcare Facilities, 2008. *Center For Disease Control, U.S.A.* (2008).

231. Naing, M. W. & Williams, D. J. Three-dimensional culture and bioreactors for cellular therapies. *Cytotherapy* **13,** 391–399 (2011).

232. Shao, Y., Sang, J. & Fu, J. On human pluripotent stem cell control: The rise of 3D bioengineering and mechanobiology. *Biomaterials* **52,** 26–43 (2015).

233. Li, B. *et al.* Past, present, and future of microcarrier-based tissue engineering.

J. Orthop. Transl. **3,** 51–57 (2015).

234. Hlady, V., Buijs, J. & Jennissen, H. Methods for Studying Protein Adsorption. *Methods Enzymol.* **309,** 402–429 (1999).

235. Togashi, D. M., Ryder, A. G. & Heiss, G. Quantifying adsorbed protein on surfaces using confocal fluorescence microscopy. *Colloids Surfaces B Biointerfaces* **72,** 219–229 (2009).

236. Zhu, J., Beamish, A., Tang, C., Kottke-marchant, K. & Marchant, R. Extracellular Matrix-like Cell-adhesive Hydrogels from RGD-containing Poly(ethylene glycol) Diacrylate. *Macromolecules* **39,** 21–23 (2006).

237. Kim, J., Hefferan, T. E., Yaszemski, M. J. & Lu, L. Potential of hydrogels based on poly (ethylene glycol) and sebacic acid as orthopedic tissue engineering scaffolds. *Tissue Eng. Part A* **15,** 2299–2307 (2009).

238. Shin, H., Jo, S. & Mikos, A. G. Modulation of marrow stromal osteoblast adhesion on biomimetic oligo[poly(ethylene glycol) fumarate] hydrogels modified with Arg-Gly-Asp peptides and a poly(ethyleneglycol) spacer. *J. Biomed. Mater. Res.* **61,** 169–179 (2002).

239. Dendukuri, D. & Doyle, P. S. The synthesis and assembly of polymeric microparticles using microfluidics. *Adv. Mater.* **21,** 4071–4086 (2009).

240. Khan, I. U. *et al.* Microfluidic conceived drug loaded Janus particles in side-by-side capillaries device. *Int. J. Pharm.* **473,** 239–249 (2014).

241. Khan, I. U. *et al.* Microfluidic conceived pH sensitive core–shell particles for dual drug delivery. *Int. J. Pharm.* **478,** 78–87 (2015).

242. Vladisavljević, G. T. & Williams, R. a. Recent developments in manufacturing emulsions and particulate products using membranes. *Adv. Colloid Interface Sci.* **113,** 1–20 (2005).

243. Sun, X. T., Liu, M. & Xu, Z. R. Microfluidic fabrication of multifunctional particles and their analytical applications. *Talanta* **121,** 163–177 (2014).

244. Evans, S. M. *et al.* A microfluidic method to measure small molecule diffusion

in hydrogels. *Mater. Sci. Eng. C* **35,** 322–334 (2014).

245. Gokmen, M. T. & Du Prez, F. E. Porous polymer particles—A comprehensive guide to synthesis, characterization, functionalization and applications. *Prog. Polym. Sci.* **37,** 365–405 (2012).

246. Silverstein, M. S. PolyHIPEs: Recent advances in emulsion-templated porous polymers. *Prog. Polym. Sci.* **39,** 199–234 (2014).

247. Zhang, Z., Zhang, R., Chen, L., Tong, Q. & McClements, D. J. Designing hydrogel particles for controlled or targeted release of lipophilic bioactive agents in the gastrointestinal tract. *Eur. Polym. J.* (2015). doi:10.1016/j.eurpolymj.2015.01.013

248. Le Goff, G. C., Srinivas, R. L., Hill, W. A. & Doyle, P. S. Hydrogel microparticles for biosensing. *Eur. Polym. J.* (2015). doi:10.1016/j.eurpolymj.2015.02.022

249. Zhang, T. *et al.* The controllable preparation of porous PLGA microspheres by the oil/water emulsion method and its application in 3D culture of ovarian cancer cells. *Colloids Surfaces A Physicochem. Eng. Asp.* **452,** 115–124 (2014).

250. Gong, Y., Su, K., Lau, T. T., Zhou, R. & Wang, D.-A. Microcavitary hydrogel-mediating phase transfer cell culture for cartilage tissue engineering. *Tissue Eng. Part A* **16,** 3611–3622 (2010).

251. Fan, C. & Wang, D.-A. A biodegradable PEG-based micro-cavitary hydrogel as scaffold for cartilage tissue engineering. *Eur. Polym. J.* (2015). doi:10.1016/j.eurpolymj.2015.02.038

252. Dragosavac, M. M., Vladisavljević, G. T., Holdich, R. G. & Stillwell, M. T. Production of porous silica microparticles by membrane emulsification. *Langmuir* **28,** 134–143 (2012).

253. Dragosavac, M. M., Holdich, R. G., Vladisavljević, G. T. & Sovilj, M. N. Stirred cell membrane emulsification for multiple emulsions containing unrefined pumpkin seed oil with uniform droplet size. *J. Memb. Sci.* **392–393,** 122–129

(2012).

254. Hempel, E. A potential route to hydrogel multifunctionalization utilizing encapsulation of acrylate-conjugated streptavidin. (2006). at <http://dspace.mit.edu/handle/1721.1/36746>

255. Mitropoulos, V., Mütze, A. & Fischer, P. Mechanical properties of protein adsorption layers at the air/water and oil/water interface: A comparison in light of the thermodynamical stability of proteins. *Adv. Colloid Interface Sci.* **206,** 195–206 (2014).

256. Zhai, J. li, Day, L., Aguilar, M. I. & Wooster, T. J. Protein folding at emulsion oil/water interfaces. *Curr. Opin. Colloid Interface Sci.* **18,** 257–271 (2013).

257. Keerati-u-rai, M., Miriani, M., Iametti, S., Bonomi, F. & Corredig, M. Structural changes of soy proteins at the oil-water interface studied by fluorescence spectroscopy. *Colloids Surfaces B Biointerfaces* **93,** 41–48 (2012).

258. Kalogianni, E. P. *et al.* Effect of oleic acid on the properties of protein adsorbed layers at water/oil interfaces: An EPR study combined with dynamic interfacial tension measurements. *Colloids Surfaces B Biointerfaces* **158,** 498–506 (2017).

259. Patra, P. & Somasundaran, P. Evidence of conformational changes in oil molecules with protein aggregation and conformational changes at oil-'protein solution' interface. *Colloids Surfaces B Biointerfaces* **120,** 132–141 (2014).

260. Franco, C. L., Price, J. & West, J. L. Development and optimization of a dual-photoinitiator, emulsion-based technique for rapid generation of cell-laden hydrogel microspheres. *Acta Biomater.* **7,** 3267–3276 (2011).

261. Zhang, Q., Lin, B. & Qin, J. Synthesis of shape-controlled particles based on synergistic effect of geometry confinement, double emulsion template, and polymerization quenching. *Microfluid. Nanofluidics* **12,** 33–39 (2012).

262. Wallin, M., Altskär, A., Nordstierna, L. & Andersson, M. Meso-Ordered PEG-Based Particles. *Langmuir* **31,** 13–16 (2015).

263. Bax, D. V., McKenzie, D. R., Weiss, A. S. & Bilek, M. M. M. Linker-free

covalent attachment of the extracellular matrix protein tropoelastin to a polymer surface for directed cell spreading. *Acta Biomater.* **5,** 3371–3381 (2009).

264. Guo, B. *et al.* Plasma-treated polystyrene film that enhances binding efficiency for sensitive and label-free protein biosensing. *Appl. Surf. Sci.* **345,** 379–386 (2015).

265. Kumar, S., Chauhan, V. S. & Nahar, P. Preparation of biomolecule-ligated polystyrene cuvets and their applications in diagnostics. *Microchem. J.* **89,** 148–152 (2008).

266. Ma, Z., Gao, C., Ji, J. & Shen, J. Protein immobilization on the surface of poly-L-lactic acid films for improvement of cellular interactions. *Eur. Polym. J.* **38,** 2279–2284 (2002).

267. Schlichthaerle, T., Strauss, M. T., Schueder, F., Woehrstein, J. B. & Jungmann, R. DNA nanotechnology and fluorescence applications. *Curr. Opin. Biotechnol.* **39,** 41–47 (2016).

268. Li, H. *et al.* RNA as a stable polymer to build controllable and defined nanostructures for material and biomedical applications. *Nano Today* **10,** 631–655 (2015).

269. Paredes, E., Evans, M. & Das, S. R. RNA labeling, conjugation and ligation. *Methods* **54,** 251–259 (2011).

270. Ylikotila, J., Välimaa, L., Takalo, H. & Pettersson, K. Improved surface stability and biotin binding properties of streptavidin coating on polystyrene. *Colloids Surfaces B Biointerfaces* **70,** 271–277 (2009).

271. Zhu, J. Bioactive modification of poly(ethylene glycol) hydrogels for tissue engineering. *Biomaterials* **31,** 4639–4656 (2010).

272. Hwang, N. S. *et al.* Effects of three-dimensional culture and growth factors on the chondrogenic differentiation of murine embryonic stem cells. *Stem Cells* **24,** 284–291 (2006).

273. Ghaemi, S. R., Harding, F. J., Delalat, B., Gronthos, S. & Voelcker, N. H.

Exploring the mesenchymal stem cell niche using high throughput screening. *Biomaterials* **34,** 7601–15 (2013).

274. Hoffman, M. D., Van Hove, A. H. & Benoit, D. S. W. Degradable hydrogels for spatiotemporal control of mesenchymal stem cells localized at decellularized bone allografts. *Acta Biomater.* **10,** 3431–41 (2014).

275. Agata, H. *et al.* Feasibility and efficacy of bone tissue engineering using human bone marrow stromal cells cultivated in serum-free conditions. *Biochem. Biophys. Res. Commun.* **382,** 353–358 (2009).

276. Al-Saqi, S. H. *et al.* Defined serum-free media for in vitro expansion of adipose-derived mesenchymal stem cells. *Cytotherapy* **16,** 915–926 (2014).

277. Crapnell, K. *et al.* Growth, differentiation capacity, and function of mesenchymal stem cells expanded in serum-free medium developed via combinatorial screening. *Exp. Cell Res.* **319,** 1409–1418 (2013).

278. Hartmann, I. *et al.* Umbilical cord tissue-derived mesenchymal stem cells grow best under GMP-compliant culture conditions and maintain their phenotypic and functional properties. *J. Immunol. Methods* **363,** 80–89 (2010).

279. Jung, S., Sen, A., Rosenberg, L. & Behie, L. E. O. A. Identification of growth and attachment factors for the serum-free isolation and expansion of human mesenchymal stromal cells. *Cytotherapy* **12,** 637–657 (2010).

280. Yeo, A., Wong, W. J., Khoo, H. H. & Teoh, S. H. Surface modification of PCL-TCP scaffolds improve interfacial mechanical interlock and enhance early bone formation: An in vitro and in vivo characterization. *J. Biomed. Mater. Res. - Part A* **92,** 311–321 (2010).

281. Fischer, U. *et al.* Transforming growth factor β1 immobilized adsorptively on Ti6Al4V and collagen type I coated Ti6Al4V maintains its biological activity. *Biomaterials* **24,** 2631–2641 (2003).

282. Nuttelman, C. R. *et al.* Macromolecular monomers for the synthesis of hydrogel niches and their application in cell encapsulation and tissue engineering. *Prog. Polym. Sci.* **33,** 167–179 (2008).

283. Xu, Y. & Guan, J. Biomaterial property-controlled stem cell fates for cardiac regeneration. *Bioact. Mater.* **1,** 18–28 (2016).

284. Li, Y. Y., Choy, T. H., Ho, F. C. & Chan, P. B. Scaffold composition affects cytoskeleton organization, cell-matrix interaction and the cellular fate of human mesenchymal stem cells upon chondrogenic differentiation. *Biomaterials* **52,** 208–220 (2015).

285. Mobasseri, R., Tian, L., Soleimani, M., Ramakrishna, S. & Naderi-Manesh, H. Bio-active molecules modified surfaces enhanced mesenchymal stem cell adhesion and proliferation. *Biochem. Biophys. Res. Commun.* **483,** 312–317 (2017).

286. Rana, D. & Ramalingam, M. Enhanced proliferation of human bone marrow derived mesenchymal stem cells on tough hydrogel substrates. *Mater. Sci. Eng. C* **76,** 1057–1065 (2017).

287. Tsuji, K. *et al.* Effects of Different Cell-Detaching Methods on the Viability and Cell Surface Antigen Expression of Synovial Mesenchymal Stem Cells. *Cell Transplant.* **26,** 1089–1102 (2017).

288. Xu, J. *et al.* Chondrogenic Differentiation of Human Mesenchymal Stem Cells in Three-Dimensional Alginate Gels. *Tissue Eng. Part A* **14,** 667–680 (2008).

289. Lequoy, P., Murschel, F., Liberelle, B., Lerouge, S. & De Crescenzo, G. Controlled co-immobilization of EGF and VEGF to optimize vascular cell survival. *Acta Biomater.* **29,** 239–247 (2016).

290. Osorio, M. *et al.* Novel surface modification of three-dimensional bacterial nanocellulose with cell-derived adhesion proteins for soft tissue engineering. *Mater. Sci. Eng. C* **100,** 697–705 (2019).

291. Felgueiras, H. P., Antunes, J. C., Martins, M. C. L. & Barbosa, M. A. Fundamentals of protein and cell interactions in biomaterials. *Pept. Proteins as Biomater. Tissue Regen. Repair* **88,** 1–27 (2017).

292. Sherman, V. R., Yang, W. & Meyers, M. A. The materials science of collagen. *J. Mech. Behav. Biomed. Mater.* **52,** 22–50 (2015).

293. Haugh, M. G. *et al.* Investigating the interplay between substrate stiffness and ligand chemistry in directing mesenchymal stem cell differentiation within 3D macro-porous substrates. *Biomaterials* **171,** 23–33 (2018).

294. Koga, H. *et al.* Comparison of mesenchymal tissues-derived stem cells for in vivo chondrogenesis: Suitable conditions for cell therapy of cartilage defects in rabbit. *Cell Tissue Res.* **333,** 207–215 (2008).

295. Grassel, S. & Ahmed, N. Influence of cellular microenvronment and paracrine signals on chondrogenic differentiation. *Front. Biosci.* **12,** 4946–4956 (2007).

296. Chahal, A. S., Schweikle, M., Heyward, C. A. & Tiainen, H. Attachment and spatial organisation of human mesenchymal stem cells on poly(ethylene glycol) hydrogels. *J. Mech. Behav. Biomed. Mater.* **84,** 46–53 (2018).

297. Li, H. *et al.* TGF-β-mediated upregulation of Sox9 in fibroblast promotes renal fibrosis. *Biochim. Biophys. Acta - Mol. Basis Dis.* **1864,** 520–532 (2018).

298. Francisco, A. T. *et al.* Injectable laminin-functionalized hydrogel for nucleus pulposus regeneration. *Biomaterials* **34,** 7381–7388 (2013).

299. Marei, N. H., El-Sherbiny, I. M., Lotfy, A., El-Badawy, A. & El-Badri, N. Mesenchymal stem cells growth and proliferation enhancement using PLA vs PCL based nanofibrous scaffolds. *Int. J. Biol. Macromol.* **93,** 9–19 (2016).

300. Shafiei, S. S., Shavandi, M., Ahangari, G. & Shokrolahi, F. Electrospun layered double hydroxide/poly (??-caprolactone) nanocomposite scaffolds for adipogenic differentiation of adipose-derived mesenchymal stem cells. *Appl. Clay Sci.* **127–128,** 52–63 (2016).

301. Ferlin, K. M., Prendergast, M. E., Miller, M. L., Kaplan, D. S. & Fisher, J. P. Influence of 3D printed porous architecture on mesenchymal stem cell enrichment and differentiation. *Acta Biomater.* **32,** 161–169 (2016).

302. Chen, Y.-G. Endocytic regulation of TGF-beta signaling. *Cell Res.* **19,** 58–70 (2009).

303. Joye, I. J. & McClements, D. J. Biopolymer-based nanoparticles and microparticles: Fabrication, characterization, and application. *Curr. Opin.*

Colloid Interface Sci. **19,** 417–427 (2014).

304. Crucho, C. I. C. & Barros, M. T. Polymeric nanoparticles: A study on the preparation variables and characterization methods. *Mater. Sci. Eng. C* **80,** 771–784 (2017).

305. Hennessy, K. M. *et al.* The effect of collagen I mimetic peptides on mesenchymal stem cell adhesion and differentiation, and on bone formation at hydroxyapatite surfaces. *Biomaterials* **30,** 1898–1909 (2009).

306. Ventura Ferreira, M. S. *et al.* Cord blood-hematopoietic stem cell expansion in 3D fibrin scaffolds with stromal support. *Biomaterials* **33,** 6987–6997 (2012).

307. Clanchy, F. I. L. & Hamilton, J. a. The development of macrophages from human CD34+ haematopoietic stem cells in serum-free cultures is optimized by IL-3 and SCF. *Cytokine* **61,** 33–37 (2013).

308. Bryant, S. J., Arthur, J. a. & Anseth, K. S. Incorporation of tissue-specific molecules alters chondrocyte metabolism and gene expression in photocrosslinked hydrogels. *Acta Biomater.* **1,** 243–252 (2005).

309. Worley, K., Certo, A. & Wan, L. Q. Geometry–Force Control of Stem Cell Fate. *Bionanoscience* **3,** 43–51 (2012).

310. Mitchell, G. R. & Tojeira, A. Role of Anisotropy in Tissue Engineering. *Procedia Eng.* **59,** 117–125 (2013).